Synthesis of Model Cytochalasan Precursors and *In vitro* Studies of Their Activities

Von Der Naturwissenschaftlichen Fakultät der

Gottfried Wilhelm Leibniz Universität Hannover

zur Erlangung des Grades

Doktor der Naturwissenschaften (Dr. rer. nat.)

genehmigte Dissertation

von

Haili Zhang, Master (China)

2020

Referent: Prof. Dr. Russell J. Cox

Korreferent: Prof. Dr. Markus Kalesse

Tag der Promotion: 30 June 2020

Abstract

Cytochalasans are one type of PKS-NRPS secondary metabolites. The tailoring steps involved in cytochalasan biosynthesis are almost clear, but the formation of the isoindolone core is still mysterious. The ACE1 metabolite probably belongs to the cytochalasan family based on the biosynthetic gene cluster (BGC) analysis, even though the structure is not yet elucidated. Heterologous expression of *ace1* (PKS-NRPS) and *rap1* (*trans*-ER) in *A. oryzae* produced an unexpected alcohol, which is unlikely to undergo further Knoevenagel reaction. Therefore it is deduced to be a shunt metabolite during heterologous expression. To investigate the biosynthesis of the cytochalasan skeleton including reductive release, putative Knoevenagel condensation and Diels-Alder reaction, three model compounds mimicking the ACE1 metabolite precursor were designed, prepared and applied for *in vitro* assays.

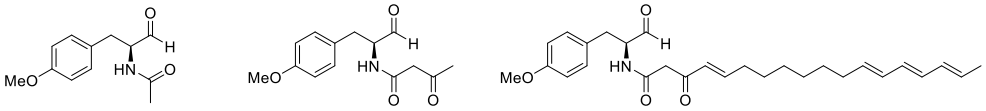

Model A was designed and synthesized for over-reduction investigation. *In vitro* assays confirmed that model A can be reduced to the corresponding primary alcohol by *A. oryzae* cell free extract. This indicates that the alcohol is a shunt metabolite and *A. oryzae* is not a suitable host for cytochalasan heterologous expression.

Model B was designed and prepared to study Knoevenagel condensation. *In vitro* assays with model B suggested model B can possibly form pyrrolinone spontaneously in buffer, while pyrrolinone was converted rapidly to alcohols. However, no enzyme activity was observed.

Besides, pyrrolinone tautomerism was further investigated by comparing tautomerized pyrrolinone and non-tautomerised pyrrolinone. From NMR and UV analysis, it is confirmed that pyrrolinones tautomerises and are no longer competitive for the following Diels-Alder reaction.

Model C was designed for both Knoevenagel condensation and Diels-Alder reaction tests. *In vitro* Assays showed that pyrrolinone was formed spontaneously, further confirming the Knoevenagel condensation is spontaneous. But its corresponding pyrrolinone also tautomerised and is no longer suitable for the following Diels-Alder reaction.

Key words: Cytochalasin; Biosynthesis; *In vitro* Assays.

Zusammenfassung

Cytochalasane sind eine Art von PKS-NRPS-Sekundärmetaboliten. Die einzelnen Schritte der Cytochalasan-Biosynthese sind nahezu klar, aber die Bildung des Isoindolon-Kerns ist immer noch rätselhaft. Basierend auf einer Analyse des biosynthetischen Genclusters (BGC) gehört der ACE1-Metabolit wahrscheinlich zur Cytochalasan-Familie, obwohl dessen Struktur noch nicht aufgeklärt wurde. Die heterologe Expression von *ace1* (PKS-NRPS) und *rap1* (trans-ER) in *A. oryzae* resultierte in der unerwarteten Produktion eines Alkohol, der wahrscheinlich keine weitere Knoevenagel-Reaktion eingeht. Daher wird davon ausgegangen, dass es sich um einen Shunt-Metaboliten handelt. Um die Biosynthese des Cytochalasan-Gerüsts einschließlich reduktiver Freisetzung, mutmaßlicher Knoevenagel-Kondensation und Diels-Alder-Reaktion zu untersuchen wurden drei Modellverbindungen, die den ACE1-Metabolitenvorläufer imitieren, entworfen, hergestellt und anschließend für *in-vitro* Tests verwendet.

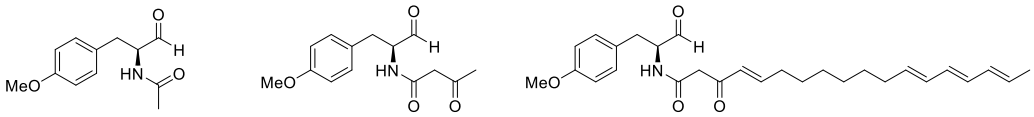

Modell A wurde für Untersuchungen zur Überreduktion entworfen und synthetisiert. *In-vitro* Tests bestätigten, dass Modell A durch zellfreien Extrakt von *A. oryzae* zu dem entsprechenden primären Alkohol reduziert werden kann. Dies zeigt, dass der Alkohol ein Shunt-Metabolit ist und *A. oryzae* kein geeigneter Wirt für die heterologe Produktion von Cytochalasanen ist.

Modell B wurde entwickelt und hergestellt, um die Knoevenagel-Kondensation zu untersuchen. *In-vitro* Tests mit Modell B deuteten darauf hin, dass Modell B möglicherweise spontan Pyrrolinon in Puffer bilden kann, welches schnell zu Alkoholen degradiert. Es wurde jedoch keine Enzymaktivität beobachtet.

Außerdem wurde die Pyrrolinon-Tautomerie weiter untersucht, indem tautomerisiertes Pyrrolinon und nicht-tautomerisiertes Pyrrolinon verglichen wurden. Aus der NMR- und UV-Analyse wurde bestätigt, dass Pyrrolinone tautomerisieren und für die folgende Diels-Alder-Reaktion nicht mehr geeignet sind.

Modell C wurde sowohl für Knoevenagel-Kondensationstests als auch für Diels-Alder-Reaktionstests entwickelt. *In-vitro* Tests zeigten, dass Pyrrolinon spontan gebildet wurde, was weiter bestätigt, dass die Knoevenagel-Kondensation spontan ist. Das entsprechende Pyrrolinon ist jedoch ebenfalls tautomerisiert und für die folgenden Diels-Alder Reaktion nicht mehr geeignet.

Schlüsselwörter: Cytochalasin; Biosynthese; *In-vitro*-Assays

Acknowledgements

I would like to express my first sincere thanks to Prof. Russell Cox for giving me this opportunity to work on this meaningful and challenging project especially when I was nearly in a desperate situation. I will always be grateful for his professional supervision and support during my study abroad.

Especially, I thank Prof. Markus Kalesse for your willingness to be the co–referee and the chair of the examination board of my PhD thesis. I also thank Prof. Jakob Franke for your time to be my examiner and I glad that I can be the first PhD student you are examined.

I thank the NMR department for the measurement of my unstable compounds, especially Monika Rettstadt, Jörg Fohrer and Dagmar Körtje. I thank the technicians, especially Katja Körner, who is always helpful and nice.

Next, I want to say many thanks to the past and current colleagues, especially Liz Skellam, who helped me when I was in need and comforted me when I was depressed. Steffen Friedrich, half-professional ping-pong player now, who always hold a neutral opinion about the world, accompanied me nearly during my whole study here, shares not only his professional chemistry knowledge, but also his life attitude and experiences with me. I will miss him whenever I think of this period of life in Germany. Francesco Trenti, the most charming Italian, shows me how colorful life should be. Your fair-sounding“Bocca di rosa” will be in my mind forever. The beautiful German girl Verena Hantke, my project collaborator, worked together with me and taught me how to run SDS gel. I also want to thank my student Franck Siakeu, who is a very nice guy and worked very hard during his master study. I also thank Pia Bruhnke for providing me shunt metabolite.

There are still so many other nice colleagues to thank, like Hao Yao, Eric Kuhnert, Oliver Piech, Lukas Kahlert, Carsten Schotte, but the space is too limited to mention all. I thank all for composing a nice group.

I would like to thank China Scholarship Council for the financial support.

At last, I want to thank my family including my parents, my sister. Without their love and encouragement, it would be impossible for me to keep going when I met troubles.

Abbreviations and Units

[α]	specific rotation
ACE	Avirulence Conferring Enzyme
AcOH	Acetic acid
ACP	acyl carrier protein
AT	acyl transferase
n-BuLi	*n*-butyl lithium
c	concentration in g/mL (optical rotation)
C	condensation domain
°C	Degrees Celsius
CFE	Cell free extract
CoA	Co-enzyme A
COSY	Correlation Spectroscopy
δ	chemical shift in ppm
d	doublet
DA	Diels-Alder
DAase	Diels-Alderase
DCC	*N,N'*-Dicyclohexylcarbodiimide
DH	dehydratase
DIPEA	*N, N*-diisopropylethylamine
DMAP	4-(dimethylamino)pyridine
DMF	Dimethylformamide
DMP	Dess-Martin periodinane
DMSO	dimethyl sulfoxide
EDC	1-ethyl-3-(3-dimethylaminopropyl)carbodiimide
e.g.	for example
ELSD	Evaporative Light Scattering Detector
eq.	equivalents
ER	enoyl reductase
ES	Electrospray
EtOAc	ethyl acetate
EtOH	ethanol
KS	ketosynthase
LCMS	Liquid chromatography–mass spectrometry
LDA	Lithium diisopropylamine
m	multiplet
M	molar
M^+	Molecular ion
m/z	mass to charge ratio
MAT	malonyl-CoA:ACP transacylase
Me	methyl
MeOH	methanol
min	minute
mM	millimolar
MS	Molecular sieve
MeT	methyltransferase domain
NADPH	*β*-nicotinamide adenine dinucleotide phosphate
NMR	nuclear magnetic resonance
NRPS	non-ribosomal peptide synthetase
ORF	open reading frame
p-TsOH	*p*-toluenesulfonic acid
PCC	Pyridinium chlorochromate
PDC	pyridinium dichromate
PKS	polyketide synthase
PKS-NRPS	polyketide synthase-non ribosomal peptide synthetase
PMB	*p*-Methoxybenzyl
ppm	parts per million
prep-LCMS	Preparative LCMS
q	quartet
R	reductase domain
R_f	Retention factor

$FADH_2$	flavin adenine dinucleotide (reduced)	RT	room temperature
FAS	fatty acid synthase	SAM	*S*-adenosylmethionine
FMO	FAD-dependent monooxygenase	sat.	Saturated
g	Grams	sp.	species
h	hour	T	thiolation domain
HMBC	Heteronuclear Multiple Bond Correlation	TBS	*tert*-butyldimethylsilyl
		TE	thiolesterase domain
HRMS	High Resolution Mass Sprectrometry	TF	transcription factor
HSQC	Heteronuclear Single Quantum Coherence	TFA	trifluoroacetic acid
	spectroscopy	THF	Tetrahydrofuran
HWE	Horner-Wadsworth Emmons	TLC	Thin layer chromatography
IR	infrared spectroscopy	µl	Microlitres
IMDA	Intramolecular Diels-Alder reaction	UV	Ultraviolet spectroscopy
J	coupling constant in Hertz	*v*	Wavenumber
KR	ketoreductase		

Table of Contents

1. Introduction

1.1 Cytochalasan Discoveries

Cytochalasans are large family of secondary metabolites produced by fungal polyketide synthase-non ribosomal peptide synthetase (PKS-NRPS) enzymes with a wide range of distinctive biological functions. In 1966, the first two cytochalasans, cytochalasin A **1** and B **2** were discovered by two research groups almost simultaneously and independently of each other by Tamm in Basel[1] and by the Aldridge *et al.*[2] in the research laboratories of ICI Ltd. in England from *Phoma* sp. S298 and *Helminthosporium dematioideum* respectively. Tamm named them as dehydrophomin and phomin respectively because of their origin, while Aldridge group named them cytochalasin A **1** and B **2** referring to their biological activities (cytos = cell, chalasis = relaxation).[2]

In 1969,[3] the structures of cytochalasin C **3** and D **4** were elucidated by the Aldridge group after their isolation in 1967[2] from *Metarrhizium anisopliae*. Then in 1968, Monato and co-workers[4] from Japan described a new antibiotic isolated from cultures of *Zygosporium masonii* and named it zygosporin A **4**. Soon afterwards, zygosporin A **4** was found to be identical with cytochalasin D **4**.[5]

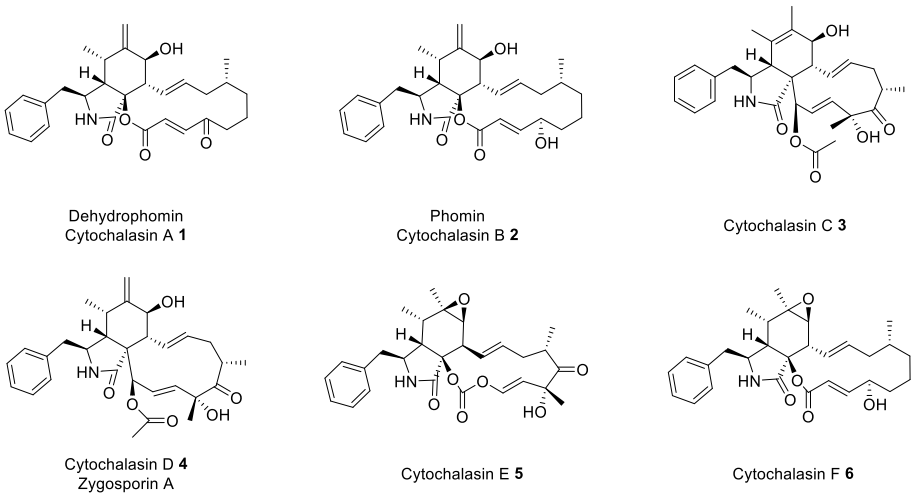

Figure 1.1 Chemical structures of some cytochalasans discovered during the 1970s.

In 1972, Aldridge[6] reported the final two cytochalasins at that time. Cytochalasin E **5**, a metabolic product of *Rosellinia necatrix*, is the first member of the cyclic carbonate group of cytochalasans. Cytochalasin F **6** was obtained from cultures of *Helminthosporium demafioideum*, which is a double-bond isomer of cytochalasin B **2** (Figure 1.1).

Later, other structurally intriguing cytochalasans have been isolated from various sources and characterized. Until now, it is estimated that around 400 cytochalasan analogues have been isolated.[7] They are widespread in fungi from different habitats including terrestrial, endophytic,[8] and insect-derived fungi,[9] as well as fungi from marine environments such as soft-coral,[10] deep-sea sediment[11] and even jelly-fish.[12]

1.2 Cytochalasan Structures and Bioactivities

The hallmark of cytochalasans includes a substituted octahydro isoindole-1-one scaffold fused to a macrocyclic ring derived from a highly reduced polyketide backbone and an amino acid. As for the amino acid moiety, tryptophan (*e.g.* chaetoglobosin A **7**)[13] and phenylalanine (*e.g.* cytochalasin E **5**)[14] are the most commonly observed. However, some other amino acids like tyrosine (*e.g.* phenochalasin A **8**),[15] leucine (*e.g.* periconiasin A **9**),[16] valine (*e.g.* trichalasin A **10**)[17] and alanine (*e.g.* alachalasin F **11**)[18] can also be incorporated into cytochalasans. With regard to the polyketide backbone, it can be a hexaketide (*e.g.* periconiasin G **12**),[16] a heptaketide (*e.g.* periconiasin A **9**), an octaketide (*e.g.* cytochalasin E **5**) or a nonaketide (*e.g.* chaetoglobosin A **7**). The macrocyle can be carbocyclic (*e.g.* chaetoglobosin A **7**), lactone-containing (*e.g.* trichalasin A **10**) or a carbonate (*e.g.* cytochalasin E **5**, Figure1.2). Cytochalasan structures can be further diversified during a set of tailoring steps including hydroxylation (*e.g.* chaetoglobosin A **7**), epoxidation (*e.g.* alachalasin F **11**) and Baeyer-Villiger oxidation (*e.g.* phenochalasin A **8**) among many other reactions.

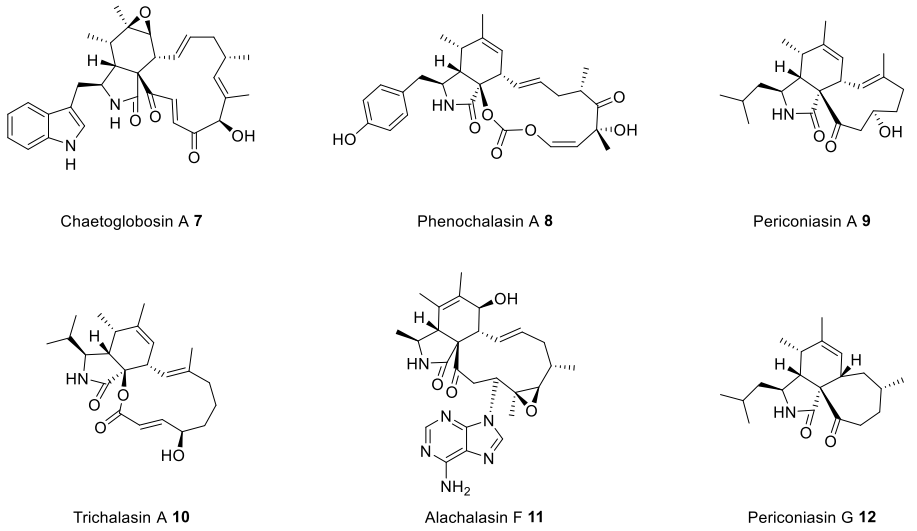

Figure 1.2 Structural diversity of cytochalasans.

Cytochalasans exhibit a wide range of biological activities such as cytotoxic, antimicrobial, antiviral and phytotoxic activities.[19] As was mentioned above, the most well-known bioactivity of cytochalasans is the ability to bind to actin filaments and block polymerization and the elongation of actin. After inhibition of actin polymerization, cytochalasans can change cellular morphology, inhibit cellular processes such as cell division, and even cause cells to undergo apoptosis.[20]

1.3 Cytochalasan Biosynthesis

Since the first discovery of cytochalasans, they have attracted great interests among scientists because of their structural complexity and strong bioactivity. For biologically oriented chemists, how nature biosynthesizes these complex secondary metabolites is an intriguing puzzle. However, the complete biosynthetic pathway has not yet been fully elucidated especially the assembly of the cytochalasan perhydroisoindole core despite the first discovery 50 years ago.

1.3.1 Isotope Labelling Experiments

During the 1970s isotope labelling studies were the main tools for investigating biosynthesis. Cytochalasin B **2**, cytochalasin D **4** and chaetoglobosin A **7** were well studied at that time by isotopic feeding experiments.

1.3.1.1 Cytochalasin B Isotope Labelling Experiments

The investigation of cytochalasan biosynthesis started from isotope labelling studies of cytochalasin B **2** in 1970 by Tamm and co-workers.[21] They fed a series of potential ^{14}C- and ^{3}H-labelled precursors to the growing culture of *Phoma* sp. (strain S298). After incubation for 12 days, the percentage incorporation into cytochalasin B **2** of the precursors was calculated and the obtained radioactive cytochalasin B **2** was investigated by chemical degradation experiments.

Feeding experiments with [1-^{14}C] acetate, [1-^{14}C] malonate and [2-^{14}C] malonate all showed alternating distribution of the radio-activity which suggested a polyketide-like biosynthetic pathway (Scheme 1.1). Moreover, compared with activities obtained in [2-^{14}C] malonate feeding experiments, the radioactivity measured for [1-^{14}C] malonate incorporation into cytochalasin B **2** was reduced to 50%, which is in accord with the decarboxylation of malonate at C-1 during polyketide chain elongation (Table 1.1).

Table 1.1 The precursors and percentages (absolute) incorporated into the cytochalasin B **2**.[22]

Precursor	Activity	Incorporation (absolute)%
[1-^{14}C]-*DL*-phenylalanine	0.1	4.9
[2-^{14}C]-*DL*-phenylalanine	0.1	6.7
[U^{14}C]-*L*-phenylalanine	0.1	10.4
[4'-^{3}H]-*L*-phenylalanine	1.0	10.4
[1-^{14}C]-Na propionate	0.1	0.29
[2-^{14}C]-Na propionate	0.1	0.4
[1-^{14}C]-Na malonate	0.1	0.33
[2-^{14}C]-Na malonate	0.1	1.04
[1-^{14}C]-Na acetate	1.0	0.123
[methyl-^{14}C]-*L*-methionine	0.1	1.96
[2-^{14}C]-mevalonate	0.25	0.007

In addition, [2-^{14}C]-propionate also caused an alternating distribution of radioactivity identical to that of [1-^{14}C] acetate and malonate, which is in accord with the well-known enzyme catalyzed oxidative fission of propionate to acetate (*a*-oxidation), which means propionate does not account for the methyl branches.

Instead, Tamm and co-workers found high absolute incorporation rates of [^{14}C-methyl]-methionine, revealing SAM is the methyl donor of the methyl branches in cytochalasan B (green in scheme 1.1).

Feeding experiments with racemic phenylalanine (^{14}C-labelled at C-1 or C-2) also showed high absolute rates of incorporation. Another feeding experiment with *L*-[*U*-^{14}C, 4-^{3}H] phenylalanine confirmed its intact incorporation into cytochalasin B **2** without the loss of the carboxyl group. These results demonstrate that the cytochalasan B backbone is composed of one unit of phenylalanine, nine units of acetate/malonate, and two methyl groups from methionine (Scheme 1.1).

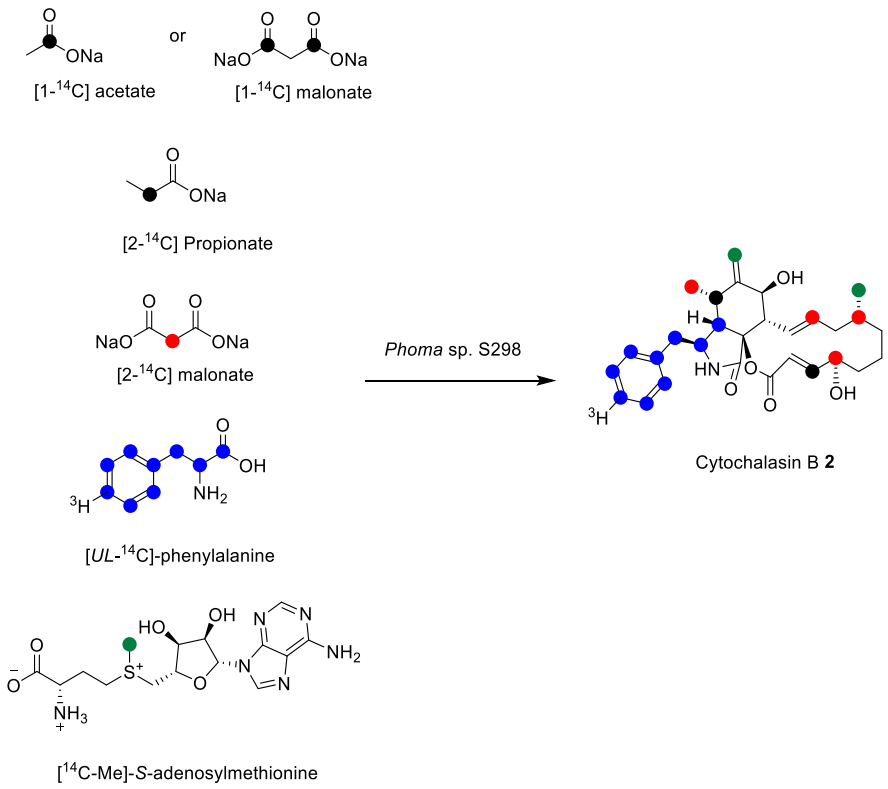

Scheme 1.1 Cytochalasin B **2** feeding experiments by Tamm *et al*.[21]

Although the position of incorporation of radioactive phenylalanine and methionine could be completely determined by degradation experiments, it is not accessible to detect all the position of [^{14}C]-acetate especially the carbons on the lactam ring. The detectable carbons are indicated with coloured dots in scheme 1.1. Therefore, in 1974,[23] Tamm and co-workers fed stable isotope precursors labelled with 2-^{13}C acetate to growing cultures of *Phoma* sp. S298 and detected the distribution of precursors with

^{13}C-NMR spectroscopy using sequential single frequency decoupling and partially relaxed Fourier transform (PRFT). By comparison of the mass spectra of labelled and unlabelled products, the absolute incorporation rate and the expected average enhancement of the ^{13}C NMR integral per labelled atom were determined. The results confirmed their previous proposals for the biosynthesis of cytochalasans and showed the C-1 and C-9 positions on the lactam ring are the terminus of a C_{18}-polyketide intermediate. The full isotope labelling pattern is shown in scheme 1.2.

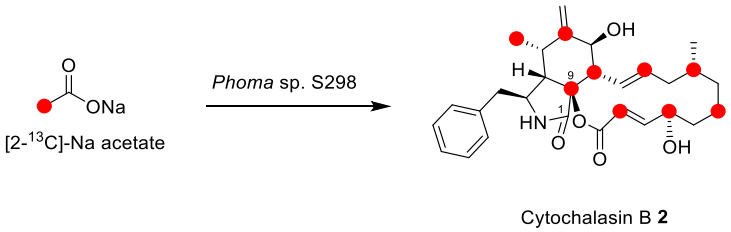

Scheme 1.2 Cytochalasin B **2** feeding experiments with ^{13}C-precursor.

In 1975, Tamm and co-workers[24] further proved that cytochalasin B **2** is a nonaketide by feeding radioactive deoxaphomin to *Phoma* sp. S298. Deoxaphomin **13**, is a possible cytochalasin B **2** precursor isolated from S298 culture, which has a 13-membered carbocyclic ring system.[25] Tamm and co-workers fed [4'-^{3}H, *U*-^{14}C]-*L*-phenylalanine to cultures of *Phoma* sp. to obtain radioactive deoxaphomin **13**. Subsequent feeding experiments demonstrated its intact incorporation into cytochalasin B **2**. This suggests that deoxaphomin **13** is the precursor for the biosynthesis of cytochalasin B **2** and an acetate unit is split as a result of an oxygen insertion (Scheme 1.3). This possible Baeyer-Villiger oxygenation in cytochalasin B **2** tailoring steps remains to be proven. However, the Tang group has recently proved the involvement of Baeyer-Villiger monooxygenase (BVMO) in cytochalasin E **5** biosynthesis for the carbonate formation.[26]

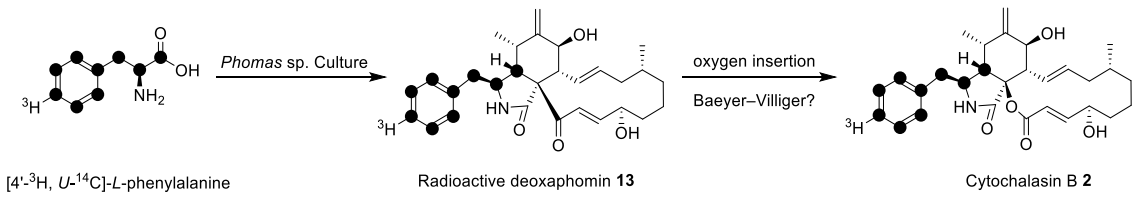

Scheme 1.3 Radioactive deoxaphomin **13** feeding experiments.

1.3.1.2 Cytochalasin D Isotope Labelling Experiments

An analogous situation exists with cytochalasin D **4**. By feeding experiments with potential ^{14}C- and ^{3}H-labellcd precursors to *Zygosporium masonii* and chemical degradation of [^{14}C]- and [^{3}H, ^{14}C]-cytochalasin D **4**, the distribution of the radioactivity was determined and the results demonstrated that cytochalasin D **4** is composed of 1 unit of phenylalanine, 3 units of methionine and acetate units (scheme 1.4).[27,28]

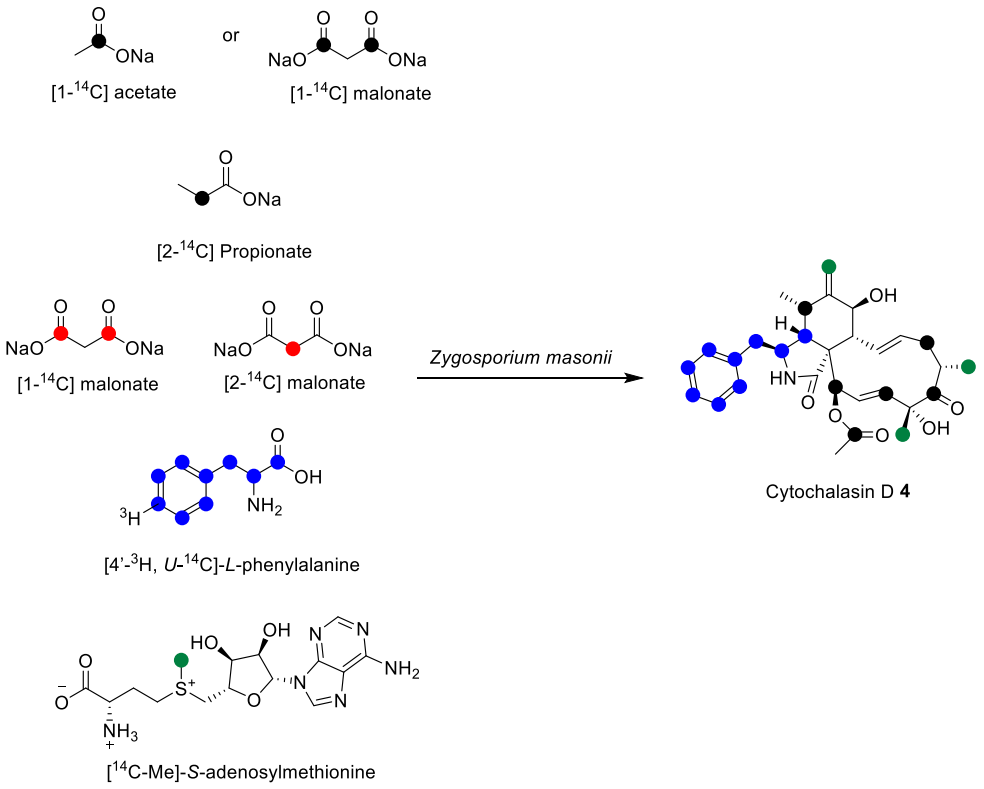

Scheme 1.4 Cytochalasin D **4** feeding experiments by Tamm *et al.*[27]

Almost at the same time, Tamm and co-workers[23] reported a feeding experiment using stable isotope labelling precursors with ^{13}C-sodium acetate (at C-1 or C-2) to growing cultures of *Zygosporium masonii* and detected the distribution of precursors with ^{13}C-NMR spectroscopy (scheme 1.5). Feeding experiment with [1-^{13}C]-sodium acetate shows the enhancement of ^{13}C atoms in an alternating distribution, as well as the carbonyl group on the *O*-acetyl group. Another feeding experiment with [2-^{13}C]-sodium acetate confirmed this result.

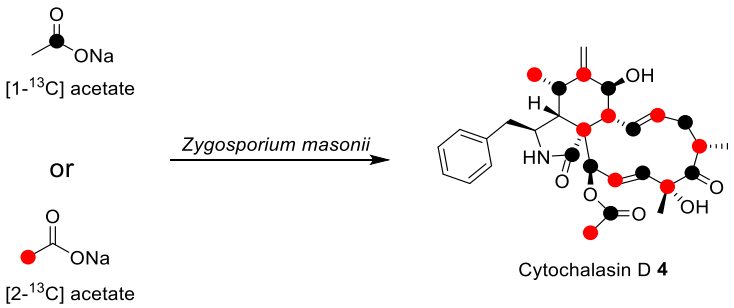

Scheme 1.5 Cytochalasin D **4** feeding experiments with ^{13}C-precursors.[23]

Further feeding experiments by Tamm and co-workers showed that both *DL*- and *L*-phenylalanine were equally well incorporated into cytochalasin D **4** due to a rapid equilibrium of *D*- and *L*-phenylalanines *via* phenylpyruvic acid. However, the *L*-enantiomer was shown to be the primary precursor.[29]

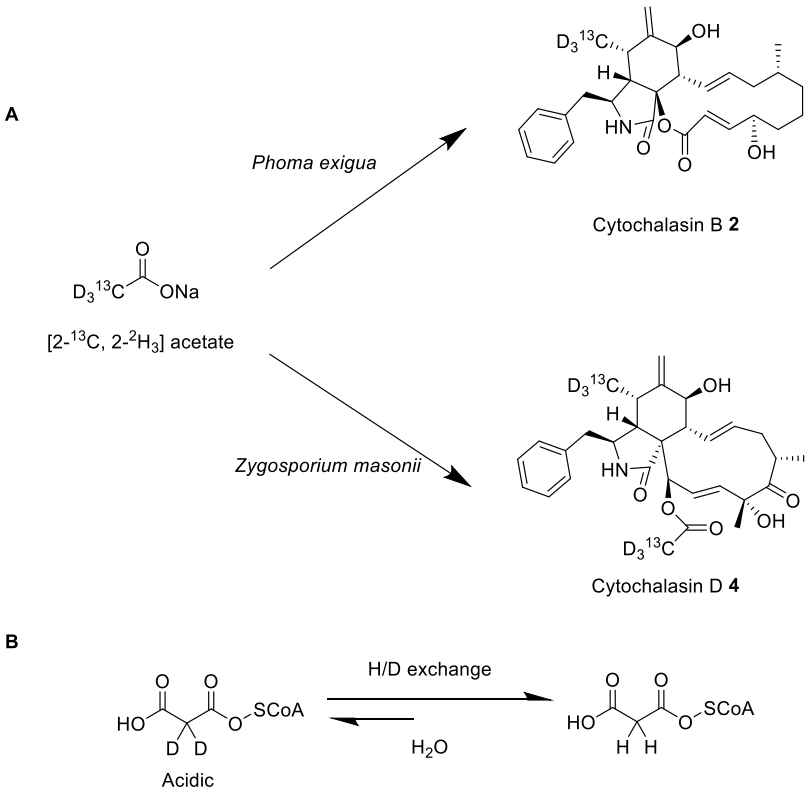

Scheme 1.6 A, feeding experiments with [2-^{13}C, 2-^{2}H$_3$] acetate to cytochalasin B **2** and D **4**; **B**, possible reason for substantial deuterium leakage.

Moreover, in 1980, Tamm performed another feeding experiment with sodium [2-^{13}C, 2-$^{2}H_3$] acetate into cytochalasin B **2** and D **4** by *Phoma exigua* and *Zygosporium masonii* respectively.[30] The metabolites were analyzed by ^{13}C NMR and ^{2}H NMR and the results showed that the deuterium was exclusively present at carbon atoms which are in polyketide chain-initiating units and *O*-acetyls that are introduced after the assembly of the cytochalasin D **4** core structure (scheme 1.6A). Apart from the one deuterium from acetate that is definitely lost during the incorporation into malonate, substantial deuterium leakage was observed, probably because of the non-stereoselective hydrogen exchange of acidic C-H at *a*-position at a post-malonate stage (Scheme 1.6B). This feeding experiment verifies acetate is the starter unit of the polyketide chain assembly.

1.3.1.3 Chaetoglobosin A Isotope Labelling Experiments

Chaetoglobosin A **7** together with 19-*O*-acetylchaetoglosobin A **13** were isolated in 1973 from *Chaetomlum globosum* in which a tryptophan rather than phenylalanine was introduced.[31] Therefore the investigation of its biosynthesis gained great interest. In 1981,[13] feeding experiments with radioactive isotope labelled [1-^{14}C] acetate, [2-^{14}C] acetate, [1-^{14}C] propionate, [^{14}C-CH_3]-*L*-methionine and [3-^{14}C]-*DL*-tryptophan to *Chaetomium globosum* showed high incorporation rates of acetate, methionine and tryptophan. This demonstrates that the origin of the chaetoglobosins from an acetate/malonate polyketide and from tryptophan with introduced methyl groups derived from methionine. The much lower incorporation of [1-^{14}C]-propionate indicates that it is incorporated indirectly as acetate after several biological transformations rather than as a chain elongation unit *via* methylmalonate.

After establishment of the basic biogenetic units, Tamm and co-workers also fed *Chaetomium globosum* with stable ^{13}C-labelled precursors to elucidate the labelling pattern. So [1-^{13}C], [2-^{13}C], [1,2-$^{13}C_2$]-acetate, [1-^{13}C]-propionate and [^{13}C-$^{2}H_3$-CH_3]-*L*-methionine were fed to *Chaetomium globosum* and the results demonstrated that the biosynthesis *via* a C_{18}-polyketide, which is obtained by head-to-tail condensation of nine intact acetate/malonate units, and a single acetate unit which is introduced as an *O*-acetyl function, probably at a later stage of the biosynthesis, and the three intact methyl groups are incorporated with retention of all three H-atoms (Scheme 1.7).

The starter unit of the polyketide was also identified to be sodium acetate by feeding experiment with [2-^{13}C, 2-$^{2}H_3$] acetate. Moreover, the intact incorporation of *L*-tryptophan into chaetoglobosin A **7** and 19-*O*-acetylchaetoglobosin A **14** was observed by feeding with various ^{14}C- and ^{3}H-labelled tryptophan samples and [2-^{2}H] and [2-^{15}N]-*L*-tryptophan with retention of both the *a*-H- and the *a*-N-atom (Scheme 1.7).

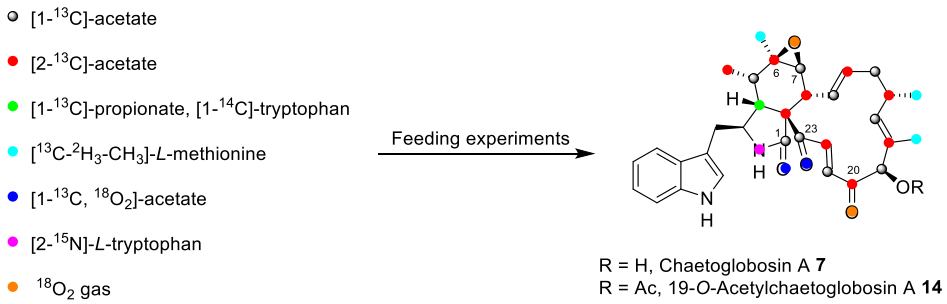

Scheme 1.7 Chaetoglobosin A **7** and 19-*O*-acetylchaetoglobosin A **14** isotope labelling patterns from *C. globosum*.

Apart from the origins of carbon skeleton and nitrogen atom as well as hydrogen atoms, the sources of oxygens were still mysterious. In 1992, Ichihara and co-workers[32] investigated the origins of oxygens in chaetoglobosin A **7** by feeding [l-^{13}C, $^{18}O_2$], [l-^{13}C, $^{2}H_3$] acetate and $^{18}O_2$ gas to *Chaetomium subaffine*. The results demonstrated that the carbonyl oxygens at C-1 and C-23 originate from acetate, while the epoxide and carbonyl oxygens at C-20 derive from oxygen gas (Scheme 1.7).

In conclusion, based on all these isotope labelling experiments, the biosynthesis of cytochalasans are clearly assembled from acetate as the starter unit and malonate as the elongation unit in a head to tail fashion *via* the polyketide pathway. Various amino acids are incorporated intact after assembly of the polyketide chain. Methionine is the methyl group donor for the alkyl branches in cytochalasans. Oxygen gas is also involved in the biosynthesis for the introduction of epoxide or hydroxyl moieties.

1.3.1.4 Primary Proposal for Cytochalasan Biosynthesis

Based on the great structural similarity of many cytochalasans and the isotope labelling investigations, in 1981, Tamm proposed a detailed biosynthesis of Chaetoglobosin A **7** (Scheme 1.8).[13]

The biosynthesis was proposed to start with the assembly of the C_{18}-polyketide **15** from acetyl-coenzyme A as the starter unit and eight malonates as enlongation units in a successive head-to-tail fashion. The *C*-methylation from methionine occurs before the stabilization of the polyketide, or before the release from the polyketide enzyme. Next, the amide linkage of *L*-tryptophan to the polyketide takes place and subsequent ring closure occurs to form the five-membered ring. After reductions, dehydrations and allylic oxidation, the tetramic acid derivative is converted to pyrrolinone **18**, which can undergo an intramolecular Diels-Alder (IMDA) reaction to form the tricyclic core structure **19**. After epoxidation, chaetoglobsin A is formed from chaetoglobosin J **19**.

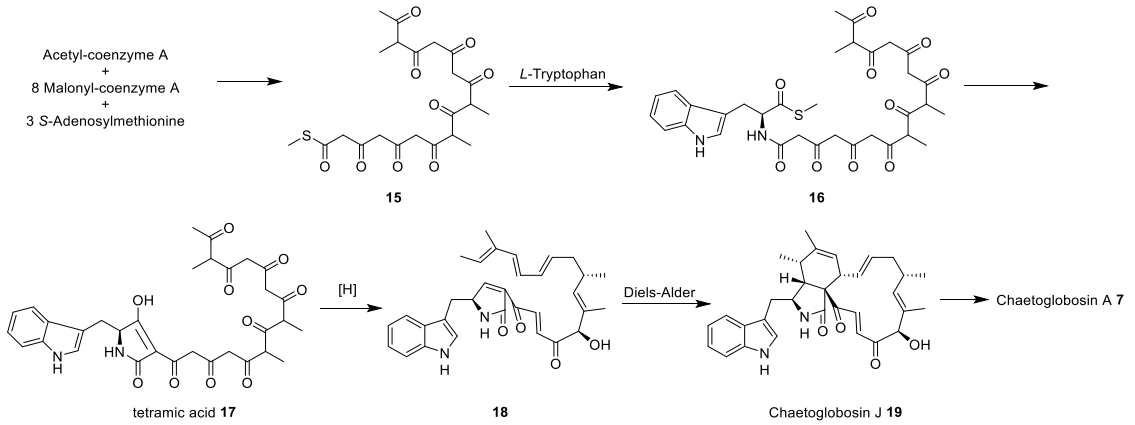

Scheme 1.8 Proposed Chaetoglobosin A **7** biosynthesis by Tamm.[13]

1.3.2 Molecular Basis of Cytochalasan Biosynthesis

According to the isotope labelling studies, the cytochalasans are composed of one molecule of an amino acid and a polyketide chain with different chain lengths. Since the amino acid is incorporated intact, the only conceivable scenario is through the polyketide synthase (PKS)-nonribosomal peptide synthetase (NRPS) hybrid.[19] The bacterial PKS-NRPS have been well studied for the biosynthesis of various of bacterial metabolites, such as bleomycin.[33] However, because of the lack of molecular tools for fungi, the fungal PKS-NRPS were unknown until the first PKS-NRPS discovery for fusarin C in 2004 by the Cox group.[34] Up to now, only a few cytochalasan biosynthetic gene clusters have been reported, including those for chaetoglobosin A **7**, cytochalasin E **5**, pyrichalasin H **20**[35] and two cryptic cytochalasan metabolites from *Pyricularia oryzae Guy11*,[36] in contrast to hundreds of cytochalasans reported (Figure 1.3).

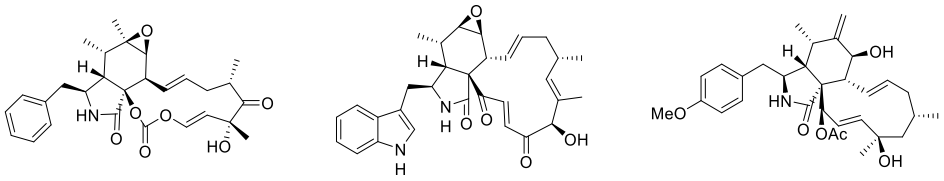

Cytochalasin E **5** Chaetoglobosin A **7** Pyrichalasin H **20**

Figure 1.3 Cytochalasans with known gene clusters.

1.3.2.1 Chaetoglobosin A Biosynthesis

The first discovery of a cytochalasan biosynthesis gene cluster was reported from the chaetoglobosin producer *Penicillium expansum* in 2007 by Hertweck and co-workers.[37] RNA silencing was applied to investigate a PKS-NRPS gene (*cheA*) which abolished the formation of chaetoglobosin A **7** and determined *cheA* was responsible for the biosynthesis of chaetoglobosin A **7**. However, their attempts to perform targeted gene knockout in *P. expansum* and heterologous expression of the entire or partial *che* cluster in *Aspergillus* were unsuccessful.[37] In 2015, the full genome sequences of three *Penicillium expansum* strains were reported but the *che* gene cluster was not identified.[38] There is no direct evidence that the *che* cluster is actually responsible for chaetoglobosin A biosynthesis and possibly it is only one similar PKS-NRPS gene.[39]

In 2013, Watanabe and co-workers[40] reported the correct gene cluster for chaetoglobosin A **7** biosynthesis from *Chaetomium globosum* using genome mining to identify the PKS-NRPS protein encoded by *CHGG_01239* (Scheme 1.9A). The cluster was confirmed by targeted gene deletion of *CHGG_01239* and the adjacent *trans*-ER gene (*CHGG_01240*), which abolished the production of chaetoglobosin A **7**. *CHGG_01239* encodes a PKS-NRPS hybrid synthetase. *CHGG_01240* encodes a *trans*-acting enoyl-reductase. The CHGG biosynthetic gene cluster also encodes two P450 oxygenases (CHGG_01242-1 and CHGG_01243), an FAD-dependent monooxygenase (CHGG_1242-2) and a transcription factor (CHGG_01237). Two additional genes, *CHGG_01241* and *CHGG_01244* were also identified. The first unknown protein encoded by CHGG_01241 has no significant similarity to characterized proteins, nor does it contain any conserved domains. While the second unknown gene CHGG_01244 encodes a protein with sequence similarity to α,β-hydrolases.[39]

Moreover, Watanabe and co-workers fully characterized the late tailoring steps in chaetoglobosin A **7** biosynthesis. The pathway from prochaetoglobosin I **22** to chaetoglobosin A **7** was elucidated by targeted gene deletion including *CHGG_01242-1*, *CHGG_01242-2*, *CHGG_01243*, which all encode redox enzymes for tailoring steps. Firstly, deteletion of all three genes resulted in the loss of chaetoglobosin A **7** and the accumulation of prochaetoglososin I **22**, which clarified that the oxygen at C-19 originated from molecular oxygen rather than part of the polyketide chain as previously proposed.[32,37,40] Next, to understand the function of single genes, a double mutant strain was created. To investigate the putative P450 function of CHGG_01242-1, disruption of *CHGG_01242-2* and *CHGG_01243* resulted in accumulation of **23** and a decrease of **22**. However, deletion of two P450s CHGG_01242-1 and CHGG_01243 showed no conversion of **22**, indicating that **22** is not the substrate for CHGG_01242-2. Disruption of *CHGG_01242-1* and *CHGG_01242-2* showed accumulation of **25** and a loss of **22**, suggesting CHGG_01243 is responsible for the conversion of **22** to **25** (Scheme 1.9B).

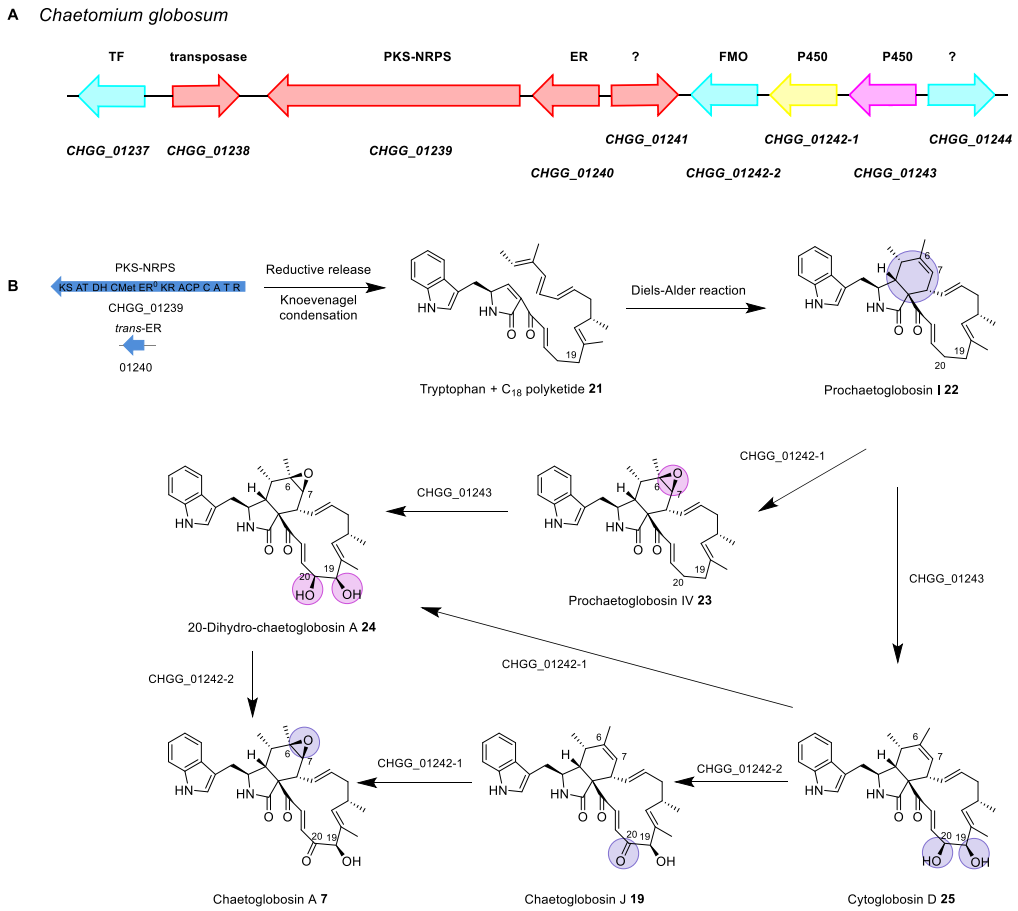

Scheme 1.9 A, revised chaetoglobosin A **7** CHGG biosynthetic gene clusters in *C. globosum*; **B**, the tailoring steps after assembly of chaetoglobosin A **7** backbone.

At last, to elucidate the whole biosynthetic pathway, a single mutant strain was created. Deletion of *CHGG_01242-1* showed accumulation of **25** and **19**, and loss of **22**, indicating **25** and **19** are substrates for CHGG_01242-1, which catalyses the epoxidation at C-6/C-7. Analysis of the CHGG_01242-2 strain showed that it accumulated **24** in exchange for the loss of **22**, demonstrating **24** is the substrate of the predicted FMO CHGG_01242-2, which catalyses the oxidation of the C-20 hydroxyl group into a ketone. Disruption of *CHGG_01243* accumulated **23** with a reduction of **22**, identifying that CHGG_01243 also accepts **23** as its substrate to perform dihydroxylation at C-19 and C-20.

Combining all of the results obtained from the mutant studies, the complete oxidative tailoring pathway was elucidated for the transformation of prochaetoglobosin I **22** to chaetoglobosin A **7** (Scheme 1.9B). The results reveal that the three redox enzymes possess a considerable substrate tolerance that leads to the formation of various intermediates and the post-PKS/NRPS modifications are not linear.[40]

1.3.2.2 Cytochalasin E Biosynthesis

Cytochalasin E **5**, a potent anti-angiogenic agent, is the first member of the cyclic carbonate group of cytochalasans. In 2011, Tang and co-workers[41] published the sequence of the gene cluster (*ccs*) responsible for the biosynthesis of cytochalasin E **5** in *Aspergillus clavatus* through genome mining (Scheme 1.10A). They deleted the central PKS-NRPS gene, *ccsA*, which abolished the production of cytochalasins E **5** and K **35**, confirming the association between the natural products and the gene cluster. Different from chaetoglobosin A **7**, cytochalasin E **5** has a unique vinyl carbonate moiety which is suggested to be introduced through the action of a Baeyer-Villiger monooxygenase (BVMO, CcsB). In addition, there is a typical *trans*-ER (CcsC), two P450 monooxygenases (CcsD and CcsG), a transcriptional regulator (CcsR) as well as two proteins with unknown functions (CcsE and CcsF). CcsE shows sequence similarity to an *α, β*-hydrolase and has 54% identity with CHGG_01244, while CcsF bears 51% sequence identity with the protein of unknown function CHGG_01241 from *C. globosum*. CcsF has been previously suggested to be involved in the IMDA cycloaddtion reaction,[41] although no evidence has been given.

With the gene cluster elucidated, Tang and co-workers also proposed the biosynthesis for cytochalasin E **5** guided by the chaetoglobosin A **7** biosynthesis

proposed by Hertweck[37] (Scheme 1.10B). Their proposal started with an ACP tethered highly reduced polyketide chain **26**, produced by the iterative incorporation of eight acetate moieties by CcsA, a PKS-NRPS hybrid enzyme. A phenylalanine residue is proposed to extend the acyl-bound chain to form the amide **27**. This amide was hypothesized to be reductively released by the terminal R-domain in an NAD(P)H dependent reaction to give aldehyde **28**. After reductive chain release, the *β*-keto amide is thought to react in a Knoevenagel condensation to produce pyrrolinone **29**, which is a dienophile for an IMDA reaction to give **30**. Then cytochalasin E **5** was proposed to be produced after some tailoring steps including double Baeyer-Villiger oxidation.

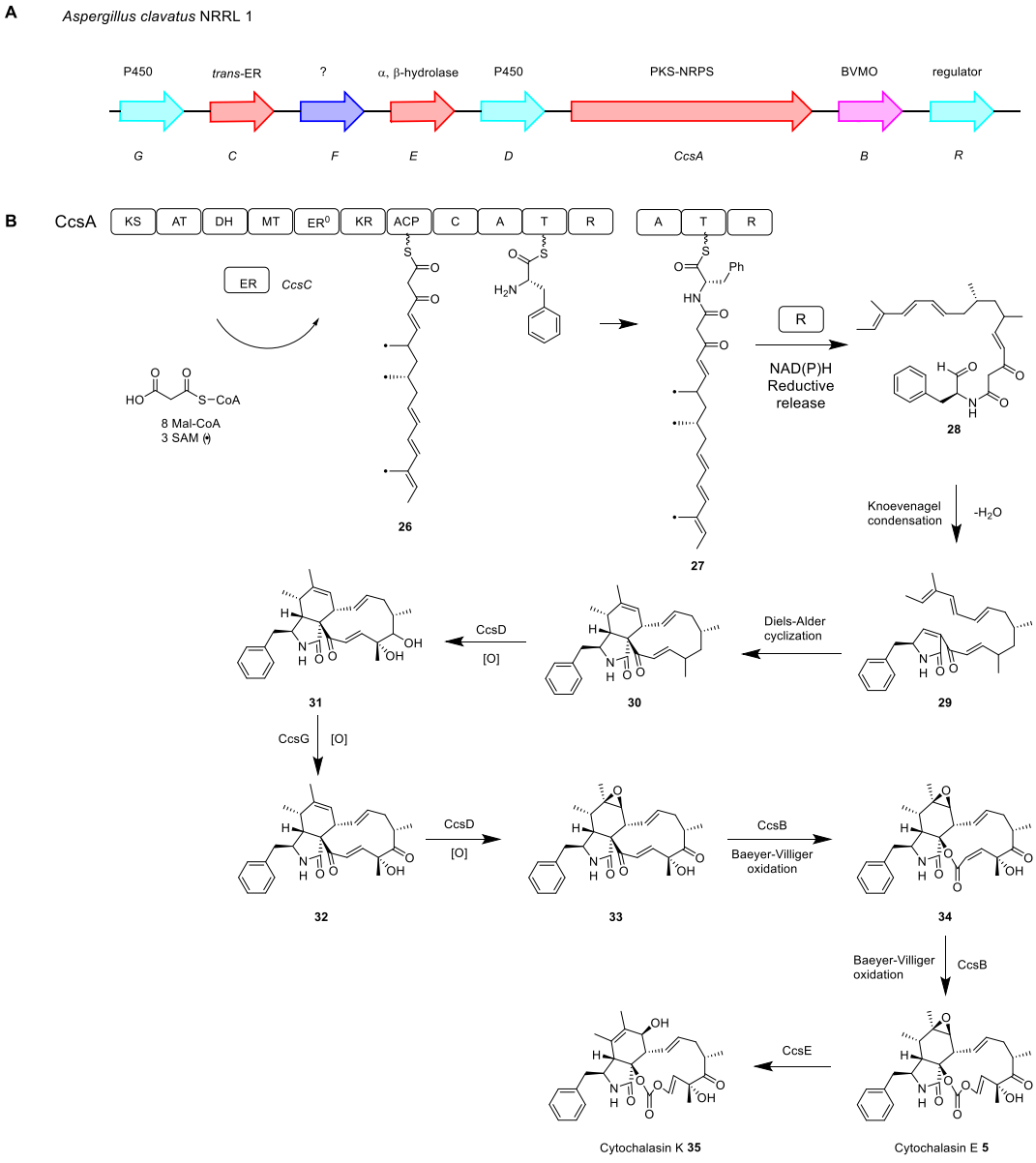

Scheme 1.10 A, cytochalasin E **5** biosynthetic gene clusters in *A. clavatus*; **B**, proposed biosynthesis for cytochalasin E **5** by the Tang group.

However, in 2013, heterologous co-expression of the cytochalasin E **5** PKS-NRPS *ccsA* and *trans*-ER *ccsC* from *A. clavatus* in *A. oryzae* by Oikawa and co-workers[42] produced metabolite **36**, an octaketide alcohol intermediate possessing the cytochalasin backbone, rather than the aldehyde or pyrrolinone or even DA adduct as proposed by Tang. Another unexpected feature was the loss of the olefin at C-4/C-5, which should be an alkene in cytochalasin E **5**, indicating possibly that a host enzyme in *A. oryzae* reduced the proposed cytochalasan aldehyde intermediate (Scheme 1.11A).[43] Apart from **36**, further investigation found a similar compound which was characterized to be **37**, a hydroxylated derivative of **36**, suggesting an oxidative enzyme within *A. oryzae* had also oxidised the backbone at C-16. But they suggested that the primary alcohol can be oxidized to an aldehyde for subsequent Knoevenagel condensation, which opens a door for the investigation of the IMDA reaction.

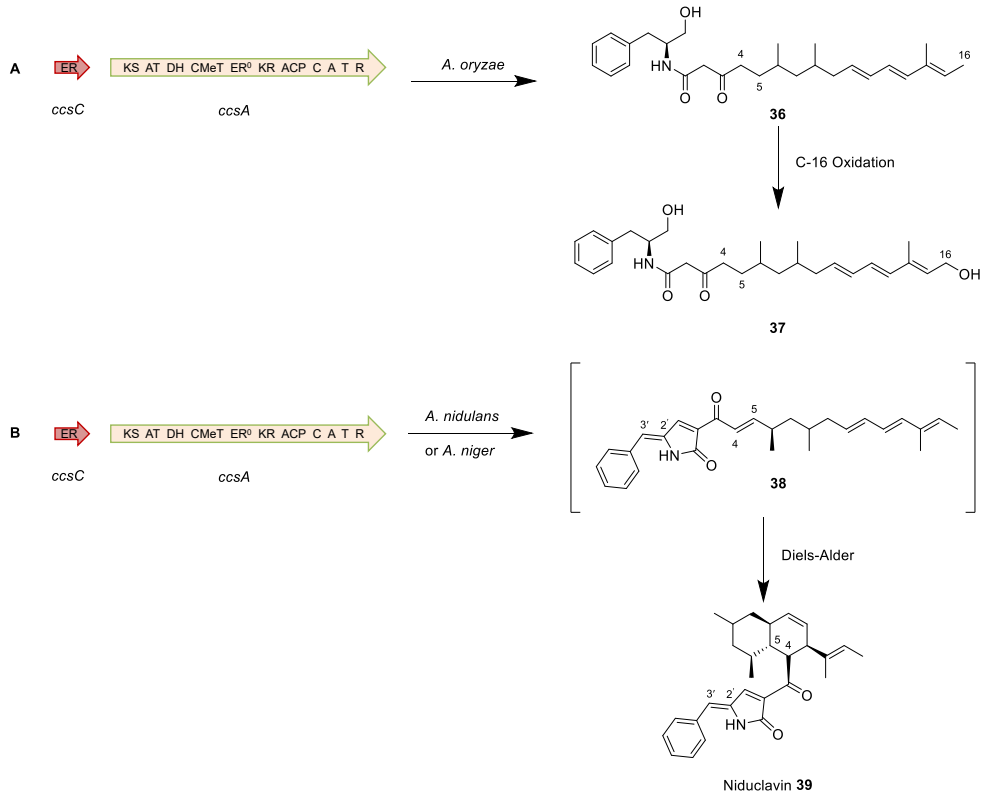

Scheme 1.11 A, heterologous co-expression of *ccsA* and *ccsC* in *A. oryzae*; **B**, heterologous co-expression of *ccsA* and *ccsC* in *A. nidulans* or *A. niger*.

In 2016, Larsen and co-workers[44] reported co-expression of *ccsA* and *ccsC* in the different expression hosts *A. nidulans* and *A. niger*. They found the *ccsC trans*-ER was necessary for the co-expression system, otherwise no secondary metabolites were

detectable. But the major metabolite produced in both *A. nidulans* and *A. niger* was niduclavin **39** with a decalin ring, which is a presumably spontaneous DA reaction product of **38** between olefin at C-4 / C-5 (Scheme 1.11B). Another unexpected feature is the olefin at C-2' / C-3' of the phenylalanine, which was speculated to be introduced from the native host oxidative enzyme. However, knockout of the possible gene responsible for formation of this olefin in the host did not affect the production of niduclavin **39**. These results show the potential problem with heterologous expression systems: the non-native host may not produce the identical metabolites as the native organism.

For the tailoring steps in the cytochalasin E **5** biosynthesis, the formation of the carbonate would be the most interesting as cytochalasin E **5** was a new group of cyclic carbonate cytochalasin and supposed to be introduced by double Baeyer-Villiger oxidation. In 2014, Tang and co-workers[26] reported their discovery about the carbonate-forming Baeyer-Villiger monooxygenase (BVMO) during cytochalasin E **5** biosynthesis (Scheme 1.12). Firstly the biosynthetic origin of the oxygen atoms in cytochalasin E **5** was investigated by feeding sodium [1-^{13}C, 1-$^{18}O_2$] acetate or $^{18}O_2$. Results showed that the carbonyl oxygen at C-21 of cytochalasin E **5** is derived from acetate during polyketide assembly, while both carbonate oxygen atoms attached to C-21 are derived from molecular oxygen, thereby pointing to an insertion pathway catalyzed by an oxygenase. Inactivation of the only possible BVMO, *ccsB,* abolished the production of cytochalasin E **5**, and accumulated ketocytochalasin **42**, revealing that CcsB participates earlier in the tailoring steps than previously proposed.[41] The function of CcsB was confirmed by *in vitro* assays with **42** in the presence of NADPH, FAD and an FMN reductase, showing that CcsB catalyses the conversion of **42** into **44** and **46** *via* two consecutive oxygen insertions. However, formation of **46** was beyond expectation and it was believed to be shunt product from the spontaneous isomerization. Feeding of **46** to *A. clavatus ccsB* deletion strain led to the restored production of **47**, along with a new product cytochalasin Z_{17} **48**, confirming the co-isolation of both **5** and **48** in all fungal producers.[45]

Although CcsB was proved to be responsible for the proposed Baeyer-Villiger oxidations to form carbonate **44**, the epoxidation of the C-6/C-7 olefin and the oxidative modifications at C-17 and C-18, as well as the conversion of cytochalasin E **5** to cytochalasin K **35** are still mysterious.

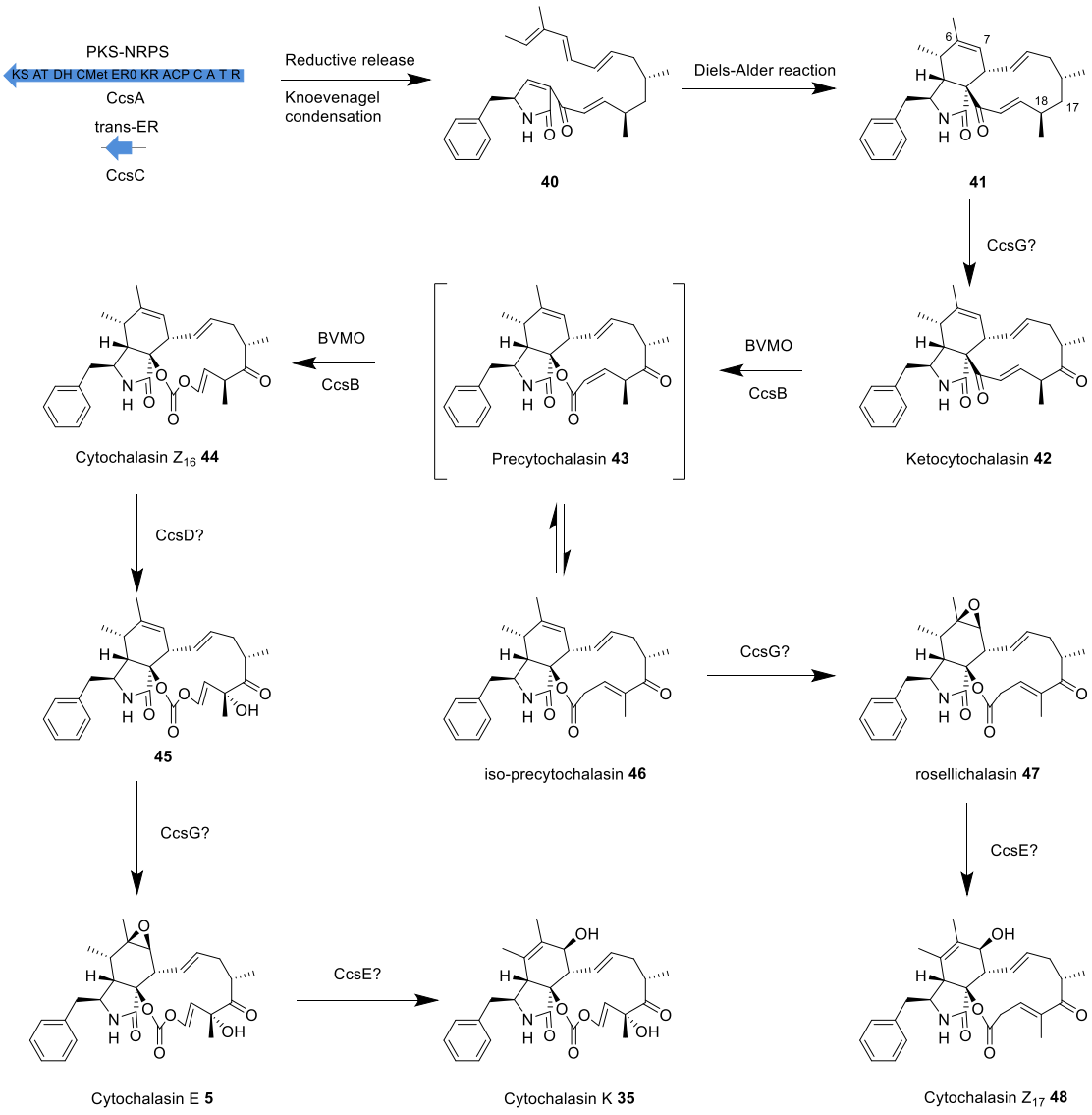

Scheme 1.12 Investigations of tailoring steps in cytochalasin E **5** biosynthesis by Tang and co-workers.

1.3.2.3 *ACE1* Metabolite Introduction and Biosynthesis

The rice blast fungus *Pyricularia oryzae* can cause significant reductions in rice yields which could annually feed 60 million people by estimate.[46] Researchers found that resistant rice strains carrying the *Pi33* gene are resistant to *avirulent P. oryzae* strains carrying the *ACE1* gene.[47] While all the other combinations of the pathogen and rice cultivar can cause blast disease (scheme 1.13).

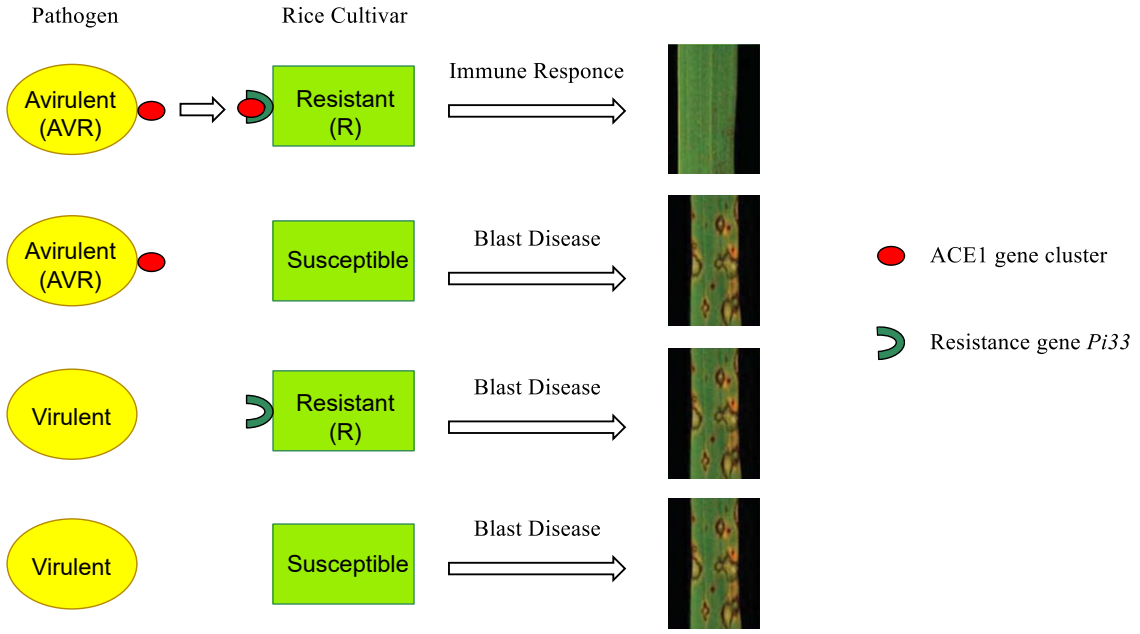

Scheme 1.13 Interactions between different pathogens and rice cultivars.

Molecular studies of *avirulent P. oryzae* strains showed that the *ACE1* biosynthetic gene cluster (BGC) encodes a biosynthetic enzyme (*avirulence* conferring enzyme 1), which is responsible for the production of a low molecular weight compound (Scheme 1.14). This *ACE1* metabolite is the likely effector that can be recognized by the *Pi33* plants to produce an effective defence response, killing or containing the fungus within the infected cells, preventing the infection to other cells and thereby conferring resistance to the plant. However the structure of the *ACE1* metabolite is still unknown.

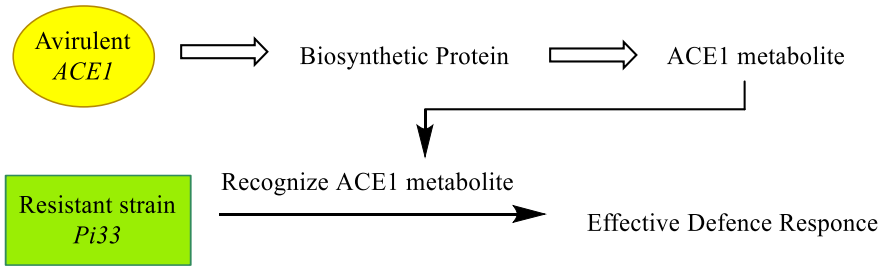

Scheme 1.14 Responce between *ACE1* biosynthetic genes and functions.

In order to identify the *ACE1* metabolite that might be quite useful in crop protection, the *ACE1* BGC was investigated. In 2007, Fudal and Lebrun *et al*. reported that the *ACE1* BGC is an infection specific secondary metabolite gene cluster which is exclusively expressed during appressorium-mediated penetration, but not at any other

stages of the *P. oryzae* life cycle.[48] Analysis of the *P. oryzae* genome revealed that the *ACE1* BGC is a cluster of 15 genes (Figure 1.4).[49] This 15-gene cluster encodes two PKS-NRPS (*ACE1* and *SYN2*), ten enzymes involved in polyketide tailoring modifications such as two enoyl reductases (*RAP1* and *RAP2*), a protein with unknown function (ORF3), an *α,β*-hydrolase (*ORFZ*), an MFS transporter (*MFS1*) and a putative transcription factor (*BC2*). Gene inactivation of *SYN2* and *RAP2* showed that they are not necessary for the production of the *avirulence* signalling compound.[49] *ACE1* itself is a 12.4 kb gene encoding an enzyme consisting of a fungal highly-reducing polyketide synthase (HR-PKS)[50] fused to a single module of a non-ribosomal peptide synthetase (NRPS) with a C-terminal R domain.[51]

Among the encoded tailoring enzymes, the *α,β*-hydrolase (ORFZ) has a 57% and 68% sequence identity to CcsE and CHGG_01244 respectively and the unknown protein (ORF3) has 44% and 64% sequence identity to the unknown proteins CHGG_01241 and CcsF respectively.[39] As CcsF is speculated to be DAase, ORF3 may be involved in the DA reaction. It has not yet been possible to identify or purify the *avirulence* compound from culture studies because *ACE1* is under very tight temporal and cell type specific control in *P. oryzae*.[47] Overall, cluster A of the *ACE1* BGC shows high similarity to the known cytochalasan BGC.

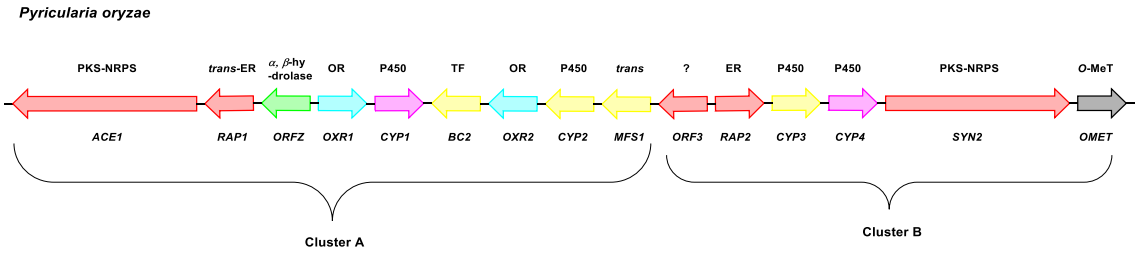

Figure 1.4 *ACE1* gene cluster from *P. oryzae*.

In 2015, the Cox group[47] reported the heterologous expression of the *avirulence* gene *ACE1* from *P. oryzae* in *A. oryzae* and *P. oryzae* itself using the multi-gene co-expression system devised and exploited by Cox group and co-workers. Expression of the *ACE1* gene alone produced a polyenyl pyrone, which was then regioselectively epoxidised and hydrolysed to give two different diols (compounds **49** and **50**) in the two host organisms (Scheme 1.15A). In contrast, co-expression of *ACE1* and *RAP1* in *A. oryzae* produced an amide **51** in low yield that is a nonaketide fused to tyrosine, similar to the PKS-NRPS derived backbone of the cytochalasans (Scheme 1.15B). But this

amide **51** is at the alcohol oxidation state, strikingly similar to the cytochalasin E **5** backbone **36** produced by co-expression of *ccsA* and *ccsC* in *A. oryzae* by Oikawa,[42] which cannot form the pyrrolinone by Knoevenagel condensation (scheme 1.11). But from the backbone we can speculate that the *ACE1* metabolite should be a member of cytochalasan family. Moreover, the biological tests showed that all of these three compounds had no bioactivities against rice blast disease. So these three compounds may be only intermediates or shunts from the real pathway which were probably reduced to an alcohol by an unknown enzyme in the host organism.

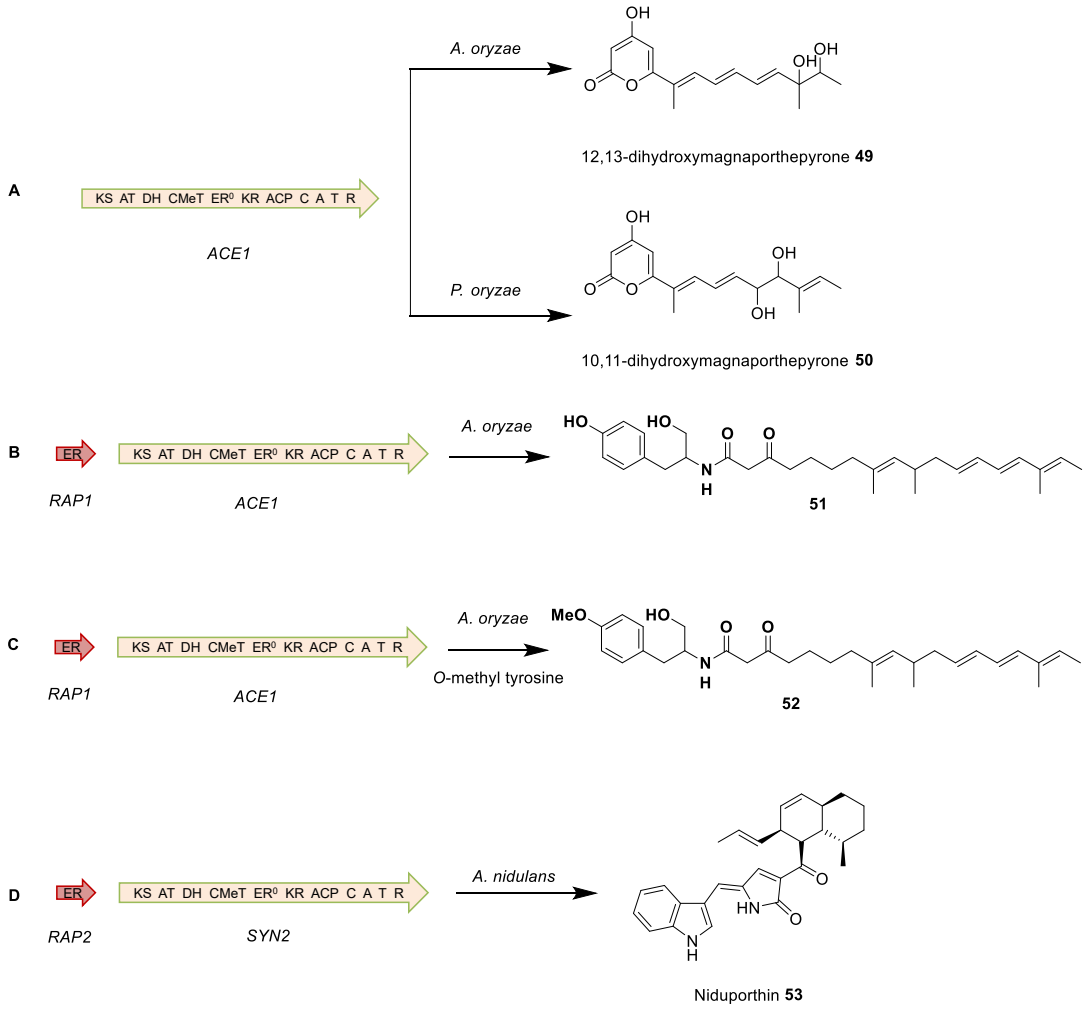

Scheme 1.15 A, expression of *ACE1* gene alone in *A. oryzae* or *P. oryzae*; **B**, heterologous co-expression of *ACE1* and *RAP1* in *A. oryzae*; **C**, *O*-methyl tyrosine was incorporated into ACE1 shunt metabolite by feeding experiment in *A. oryzae*; **D**, heterologous co-expression of *SYN2* and *RAP2* in *A. nidulans*.

Later in 2016, Larsen and co-workers[44] co-expressed the cryptic genes *SYN2* and *RAP2* present in the *ACE1* gene cluster from *P. oryzae* in *A. nidulans*, where *SYN2*

shares higher similarity with the *ccs* gene cluster than *ACE1*.[52] Again, co-expression of both *SYN2* and the *trans*-ER encoded by *RAP2* is necessary for the formation of detectable product. The produced metabolite was shown to be niduporthin **53**, with high similarity to niduclavin **39**, which is the product of *ccsA* gene expression (scheme 1.15D). Niduporthin **53** is also an octaketide with a decalin ring and pyrrole unit. But different from niduclavin **39**, niduporthin **53** incorporated tryptophan rather than phenylalanine, and introduced only a single methyl group.

In 2019, the Cox group reported that *O*-methyl tyrosine is the correct amino acid moiety incorporated into ACE1 metabolite.[36] They found that pyrichalasin H **20** BGC in *M. grisea* NI980 shares high sequence similarities with the *ACE1* BGC in *P. oryzae*. Therefore the biosynthetic pathway of pyrichalasin H **20** is highly similar to the ACE1 metabolite biosynthesis. By gene deletion of *pyiF* (putative Diels-Alderase) in *M. grisea* NI980, early biosynthetic intermediates were isolated which contained *O*-methyl tyrosine, suggesting that the methyl group is transferred to tyrosine at a very early stage. Disruption of *pyiA* (*O*-methyl transferase) abolished production of pyrichalasin H **20**, indicating *O*-methyl transferase is necessary for the production of cytochalasins. As an *O*-methyl transferase (56% amino acid identity to PyiA, encoded by *OMET*) is also present in the *ACE1* BGC, it is probable that *OMET* is important for efficient production of the ACE1 metabolite. Feeding experiments with *O*-methyl tyrosine into *A. oryzae* expressing with *ACE1*, *RAP1*, *ORF3* and *ORFZ* produced *O*-methyl tyrosine nonaketide **52** in higher titer (scheme 1.15C) and abolished the production of **51**, suggesting *O*-methyl tyrosine is the correct amino acid moiety incorporated into the ACE1 metabolite.

Based on the current knowledge about cytochalasan biosynthesis and the primary results, the Cox group proposed the biosynthetic pathway of the *ACE1* metabolite (Scheme 1.16). Similar to the proposals for chaetoglobosin A **7** and cytochalasin E **5** biosynthesis, ACE1 and RAP1 work together to catalyse the stepwise assembly of a nonaketide **54** from an acetyl-CoA starter unit and eight malonyl-CoA extenders to yield an enzyme-bound amide **55** (scheme 1.16). The co-expression of *ccsA* and *ccsC*, *ACE1* and *RAP1* produce the shunt metabolite **36** and **52** respectively in alcohol state rather than tetramic acid, suggesting the polyketide and amino acid hybrid was reductively released by the R domain to give an aldehyde.[42,47] However, the aldehyde **56** released from the R domain was reduced further to the observed hydroxyl group,

because of either the over-reduction by the R domain itself, or an unknown reductive enzyme in *A. oryzae*.

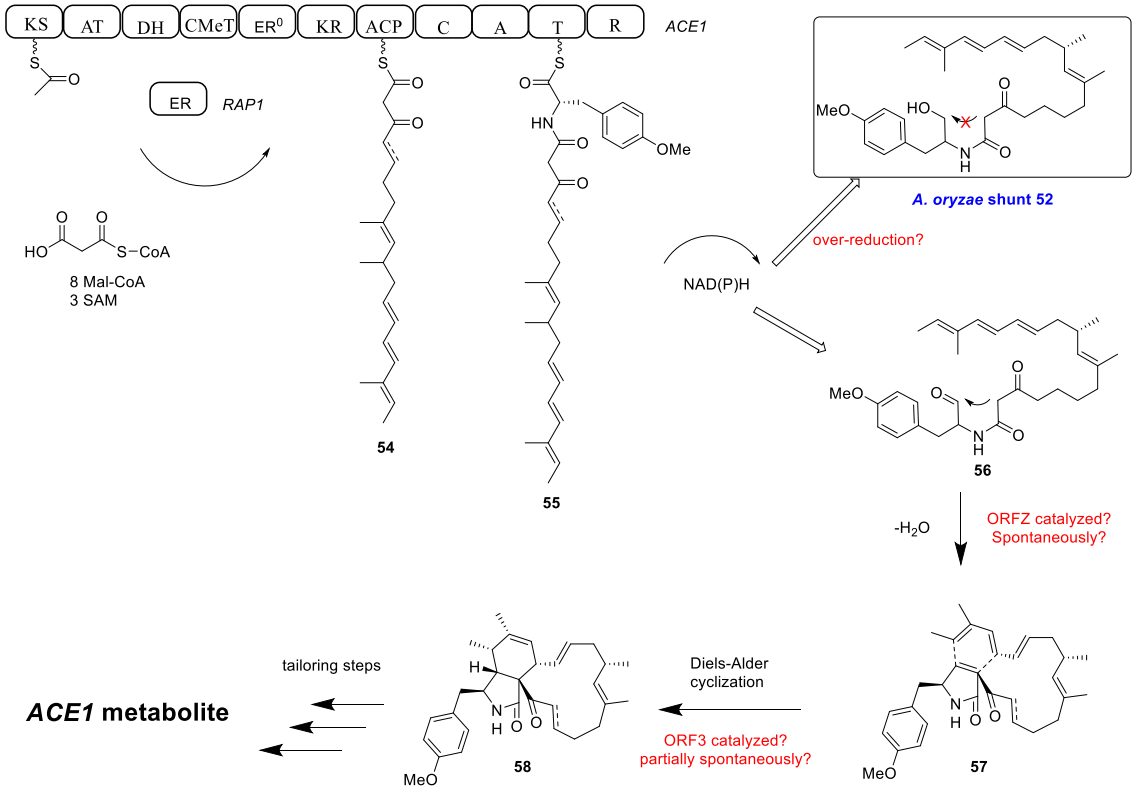

Scheme 1.16 Proposed biosynthetic pathway for *ACE1* metabolite by the Cox group.

Until now, there is no direct evidence to show how the formation of the shunt metabolite **52** is catalysed. If the aldehyde **56** was not over-reduced, it could undergo a Knoevenagel condensation to form pyrrolinone **57** catalysed by an enzyme or spontaneously. It is speculated that the commonly found α,β-hydrolase (*ORFZ* in the *ACE1* cluster, *CcsE* in the cytochalasin E **5** cluster) may be involved in the formation of pyrrolinone, but no evidence has so far been shown. Similarly, the function of proteins encoded by *ORF3* in the *ACE1* cluster and *ccsF* in cytochalasin E **5** as well as the *CHGG_01241* in chaetoglobosin A **7** are still unknown. These proteins are speculated to be the DAase for the ring formation. After the cytochalasan backbone **58** is formed, the tailoring steps that may occur include: epoxidations, hydroxylations and hydroxyl oxidations catalysed by various oxidative tailoring enzymes found in all clusters.

In conclusion, after the first discovery of cytochalasin 50 years ago, the biosynthesis of the cytochalasans is still not fully elucidated. Cytochalasin E **5**,

chaetoglobosin A **7** and *ACE1* gene clusters are reported and all cytochalasan biosynthetic gene clusters contain genes encoding a polyketide synthase/nonribosomal peptide synthetase (PKS-NRPS), a *trans*-enoyl reductase (ER), an α,β-hydrolase (HYD), and a putative Diels-Alderase (pDA). A *trans*-ER is required for the co-expression to form detectable product even though heterologous expression in other organisms proved to be problematic. But the shunt metabolites at the alcohol oxidation state suggests the aldehyde **56** is reductively released as opposed to tetramic acid formation by a Dieckman cyclization. The α,β-hydrolase is supposed to catalyze the Knoevenagel condensation, though it needs to be proven. The DA reaction is the most intriguing step in the biosynthesis and has been speculated to be catalyzed by DAase for a long time. However, until now only indirect evidence has been reported.[32]

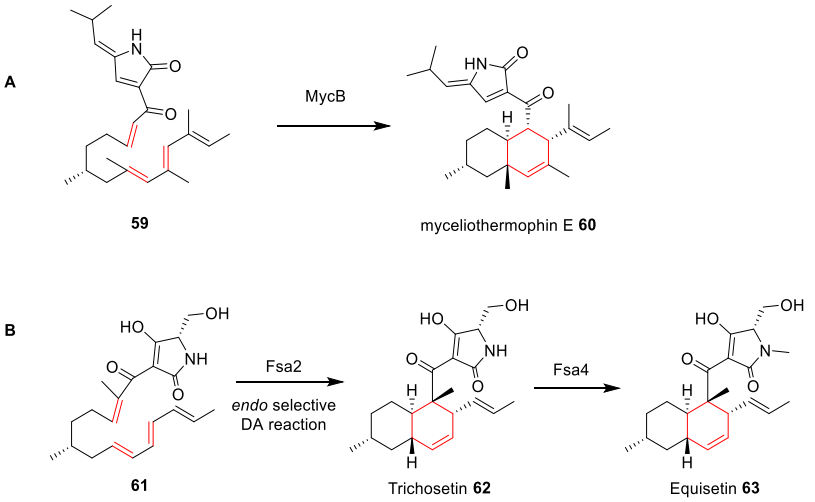

Scheme 1.17 Fungal DA reaction in the biosynthesis of myceliothermophin E **60** (**A**) and equisetin **63** (**B**).

In recent years, several fungal DAases have been characterized which catalyse *trans*-decalin ring formation, *e.g.* myceliothermophin **60**,[38] and equisetin **63**[53] (Scheme 1.17). Structural studies suggest that DAases show little homology to known proteins or functional motifs and there are also no conserved cofactor-binding domains. Like these characterized DAases, ORF3, CcsF, CHGG_01241 also have no significant similarity to characterized proteins, nor do they contain any conserved cofactor-binding domains.[39] The tailoring steps in chaetoglobosin A **7** biosynthesis have already been fully elucidated by gene knock-out experiments.[40] CcsB was proved to be the Baeyer-Villiger monooxygenase for the conversion of ketone to carbonate directly in the biosynthesis of cytochalasin E **5**.[26] However, the construction of the cytochalasan skeleton including

Knoevenagel condensation and DA reaction is of key importance and much more challenging than anticipated.

1.4 Cytochalasan Total Synthesis

As was mentioned above, cytochalasans display a wide range of biological properties, such as cytotoxic, antimicrobial, antiviral and phytotoxic activities.[19] Structurally cytochalasans are characterized by the presence of a highly substituted bicyclic octahydro isoindolone unit fused to a macrocyclic ring. The structural diversity and high biological activities of this family of secondary metabolites has attracted great interests for organic chemists in total synthesis. Among all the total syntheses of the isoindolone core, DA reaction is the most popular method. Since some cytochalasans are commercially available for biological test, relatively few members of the cytochalasans have been the targets for total synthesis.[19]

1.4.1 Total Synthesis of Cytochalasin B

In 1978, Stork and co-workers[54] reported the first total synthesis of cytochalasin B **2** in which an early intermolecular DA reaction was the key step (Scheme 1.18). The synthesis started with (+)-citrollenol acetate **68** and the acetate of the 1-ethyl ester of (+)-malic acid **70** in 8 steps including Kolbe coupling to synthesize intermediate **71**. The other component **67**, was derived from glycidaldehyde **66** after Wittig reaction, hydrolysis, protection, oxidation and reduction *etc*. The triene **72** was afforded by coupling of compound **67** and **71** through Horner-Wadsworth-Emmons reaction. The dienophile **65** for the [4+2] cycloaddition was prepared in 3 steps from methyl *L*-3-aminophenylbutyrate **64**. The intermolecular DA cyclization between **65** and **72** required harsh conditions (170 $^{\circ}$C, 4 d) and provided the isoindole compound **73** in moderate yields (40%, *endo*/*exo* 4 : 1). Various subsequent steps were needed to complete the total synthesis including the esterification in last step to form the macrocycle.[55] The formation of the isoindolone is biomimetic as the DA reaction reacts in the same way and gives the required stereoisomer.

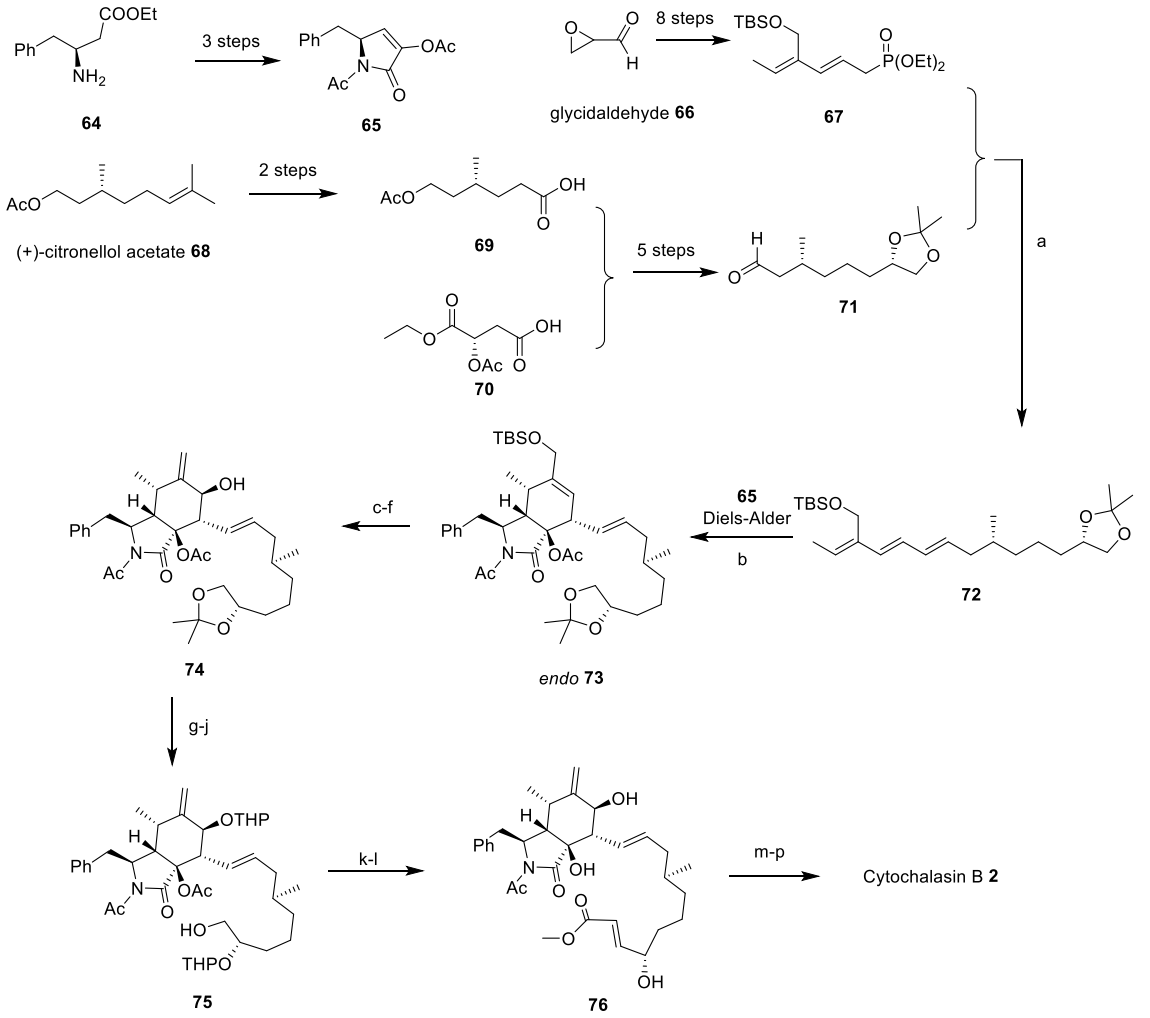

Scheme 1.18 Total synthesis of cytochalasin B **2** by Stork and co-workers by intermolecular DA reaction. Reagents and conditions: **a**, NaH, benzene, 0.25 equi. MeOH, 2 h, 55 °C, then **71**, 55 °C, overnight, 50%; **b**, xylene, 170 °C, 4 d, 40%, *endo*/*exo* ≥ 4; **c**, 3:1:1 AcOH-H_2O-THF, RT, overnight, then acetone-*p*-TsOH, 1.5 h, RT, 67%; **d**, *tert*-butyl hydroperoxide, $Mo(CO)_6$, 1.5 h reflux, benzene, 95%; **e**, carbon tetrabromide, triphenylphosphine, 4 h, RT; **f**, zinc dust/ NaI, acetone, 4 h reflux; **g**, aqueous AcOH-THF, 4 h, RT; **h**, *tert*-butyl dimethylsilyl ether, 74%; **i**, dihydropyran, 63%; **j**, TBAF; **k**, Collins oxidation; **l**, methyltriphenylphosphoranylidene acetate, 1.5 h, benzene, reflux, 68% from **75**; **m**, 1 N ethanolic NaOH, 60 °C, 1 h; **n**, diethyl phosphorochloridate, then thallium benzenethiolate; **o**, aqueous AcOH, then acetylation; **p**, Na_2HPO_4, $AgCF_3CO_2$, benzene, reflux, 2 h, argon atomosphere, 36%.

Later in 1983, Stork and co-workers[56] improved the total synthesis of cytochalasin B **2** through the simultaneous formation of the isoindolone core and the macrocyclic fused ring in a late-stage IMDA reaction (Scheme 1.19). After preparation of *N*-acetylhydroxypyrrolone **78** and triene **77** derived from (+)-citrollenol, different from their previous work, they firstly performed the esterification between **77** and **78** using

Mukaiyama's method to afford compound **79**. The conditions for the IMDA cyclization were also harsh (180-190 °C, 6 d) and the yield for macrocycle **80** was only moderate (30%, *endo*/*exo* 4:1). The harsh conditions required for synthetic DA reactions suggest that this reaction in biological systems probably needs enzyme catalysis. After subsequent steps for functional group conversions, cytochalasin B **2** was prepared in a simpler route. This route is also biomimetic and gives the required stereoisomer.

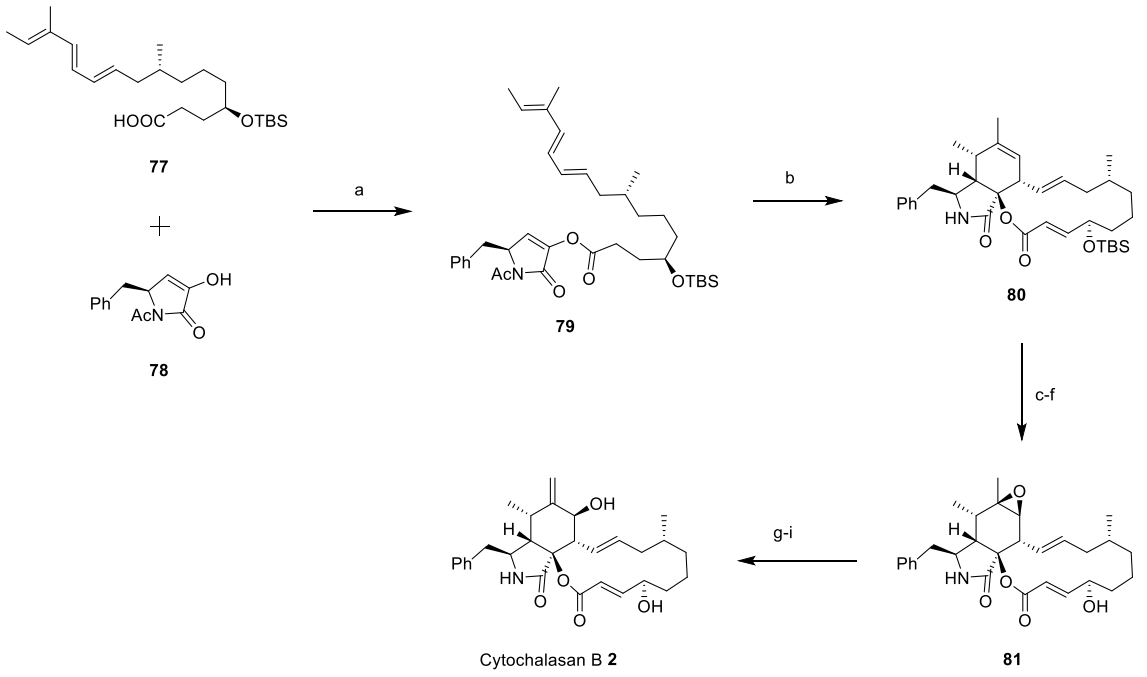

Scheme 1.19 Total synthesis of cytochalasin B **2** by Stork and co-workers. Reagents and conditions: **a**, 2-chloropyridine methiodide, 20 mol% DMAP, NEt_3, RT, CH_2Cl_2, 69%; **b**, 180-190 °C, 6 d, 30%; **c**, 3 equiv. LDA, -78 °C, THF; **d**, 3 equiv. PhSeCl, H_2O_2, pyridine, CH_2Cl_2, 76% *trans*-selective; **e**, Ac_2O, DMAP, NEt_3 88%; **f**, 1 equiv. *t*-BuOOH, 2.5 mol% $Mo(CO)_6$, 0.7 M in benzene, 75 °C, 1.5 h, 89%; **g**, $Al(OiPr)_3$, D, xylene, 8 h, 74%; **h**, K_2CO_3, MeOH, 86%; **i**, Bu_4NF, THF 75%.

Interestingly, in 2004, Haidle and Meyers[20] established a generally applicable synthetic platform for the preparation of cytochalasans with varying ring sizes and substitutions by using a common precursor **88**, derived from *N,N*-dibenzyl phenylalanal **82** in 9 steps (Scheme 1.20). Similar to other synthetic routes, they firstly prepared the isoindolone **86** by an IMDA cyclization, but a non-biomimetic method.

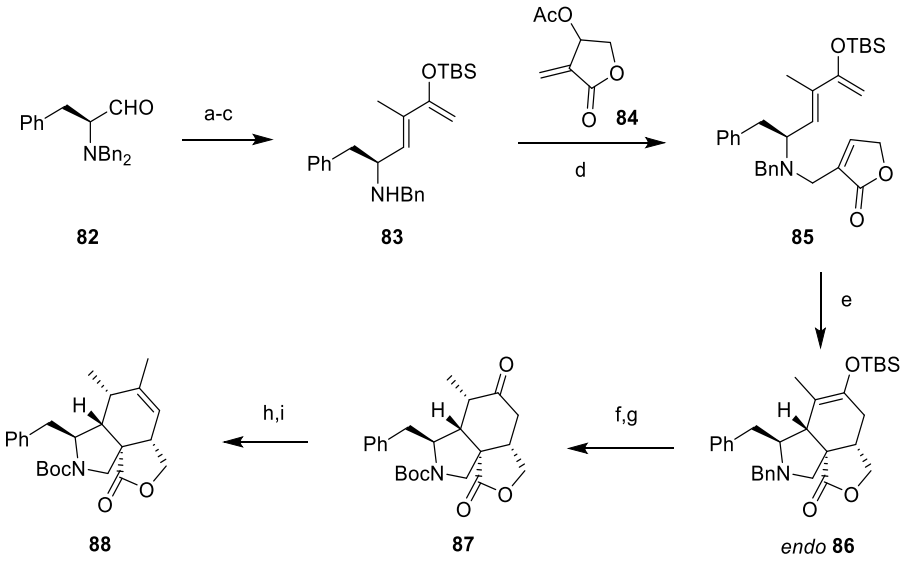

Scheme 1.20 Cytochalasan common precursor **88** synthesis (Meyers and Haidle). Reagents and conditions: **a**, Diethyl 3-oxo-2-butylphosphonate, $Ba(OH)_2$, THF-H_2O, RT, 87%; **b**, 2, 3-dichloro-5, 6-dicyanobenzoquinone, CH_2Cl_2, RT, 86%; **c**, *tert*-butyldimethylsilyl trifluoromethanesulfonate, 2, 6-lutidine, CH_2Cl_2, -78 °C / RT, 99%; **d**, MeOH, RT, 98%; **e**, *m*-xylene, 150 °C, 77%; **f**, H_2, 10% Pd/C, Boc_2O, Et_3N, EtOH, RT, 96%; **g**, TBAF, AcOH, THF, 0 °C; **h**, 1) KHMDS, THF, -78 °C; 2) 2-[*N*, *N*-bis(trifluoromethylsulfonyl)amino]-5-chloropyridine, 93% over 2 steps; **i**, Me_2CuLi, THF, -78 °C / 0 °C, 95%.

To test their strategy, 14-membered cytochalasin B **2** and the 11-membered cytochalasin *L*-696,474 were prepared from the common precursor **88**. For cytochalasin B **2** (scheme 1.21), after deformylation of the lactone ring and subsequent oxidation of the hydroxyl group, a complex aldehyde building block **89** was obtained from **88**. A fragment of the macrocyclic part of cytochalasin B **2**, derived from (1*R*, 2*R*)-pseudoephedrine, was coupled with **90** by means of Kocienski-Julia reaction to afford **91**, which was acylated with diethyl-phosphonoacetic acid in the next step. Ring closure was performed by an intramolecular Horner-Wadsworth-Emmons reaction to form **92**. Mild Mg(II)-induced rearrangement of the epoxide to the allylic alcohol completed the synthesis. As was mentioned above, this strategy was also applied to synthesize the 11-membered macrocarbocyclic cytochalasin *L*-696,474, and the authors proposed that this modular route is generally applicable to generate a large number of cytochalasin analogues by parallel synthesis.

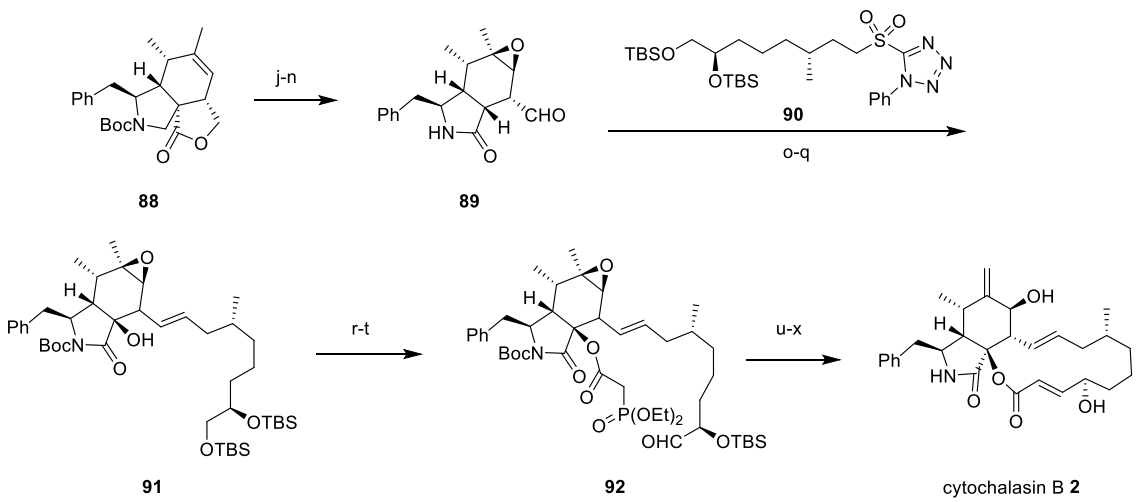

Scheme 1.21 Cytochalasin B **2** total synthesis from common precursor **88**. Reagents and conditions: **j**, Dimethyldioxirane, acetone, 23 °C, 100%; **k**, TFA, CH_2Cl_2, 0 °C; **l**, [Bis(trifluoroacetoxy)iodo]-benzene, 4 Å MS, CH_2Cl_2, 23 °C, 92% (two steps); **m**, Ethylenediamine, *tert*-amyl alcohol, 23 °C, 96%; **n**, DMP, $NaHCO_3$, CH_2Cl_2, RT; **o**, sulfone **90**, KHMDS, THF, -78 °C; aldehyde **89**, -100 °C / -40 °C, 60% over 2 steps; **p**, 1. lithium bis(trimethylsilyl)amide, THF, -78 °C; 2. Boc_2O, -78 °C / -40 °C, 80%; **q**, KHMDS, THF, -78 °C, *trans*-2-(phenylsulfonyl)-3-phenyloxaziridine, -100 °C to -78 °C, 85%; **r**, diethylphosphonoacetic acid, DCC, CH_2Cl_2, RT, 81%; **s**, HF-pyridine, THF, -20 °C, 69%; **t**, DMP, $NaHCO_3$, CH_2Cl_2, RT; **u**, $NaOCH_2CF_3$, CF_3CH_2OH, DME, RT, 65% over 2 steps; **v**, $Mg(OMe)_2$, MeOH, RT, 95%; **w**, TBAF, THF, RT, 96%; **x**, $MgSO_4$, benzene, 70 °C, 66%.

1.4.2 Total synthesis of cytochalasin D

Cytochalasin D **4** was first isolated from the microorganism *Metarrhizum anisopliae*, and its first total synthesis was published by Vedejs and Reid in 1984.[57] Before their total synthesis, they investigated the *N*-acylpyrrolinones for DA reactions in the cytochalasin area (Scheme 1.22).[58] According to the previous reports[59–61] and their own research,[58] the dienophile **94a** is not suitable for DA reaction because of the instability and tautomerisation to **96** or **97**.

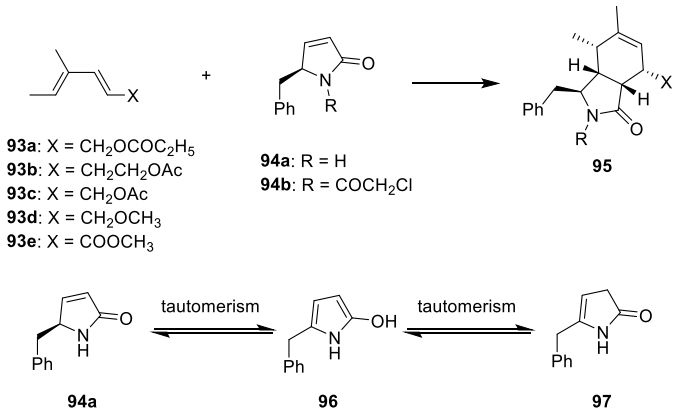

Scheme 1.22 *N*-acylpyrrolinones for intermolecular DA reactions and tautomerisation.

It is believed that hydroxypyrrole tautomer **96** is the crucial intermediate involved in the transformation.[58] To avoid formation of non-reactive tautomers from pyrrolinone dienophiles, it is desirable to introduce an electron-withdrawing *N* substituent, *e.g.* carbonyl group. Because the electron lone pair can be delocalized on the exocyclic carbonyl group (structure **98**), it is not favored to form hydroxypyrrole **99** which in fact is a 4-π-electron system and destabilizes the aromatic hydroxypyrrole intermediate.[62] Then the subsequent tautomerisation to **100** can be also blocked. So they found that *N*-chloroacetyl derivative **94b** was ideal for the purpose (Scheme 1.23).

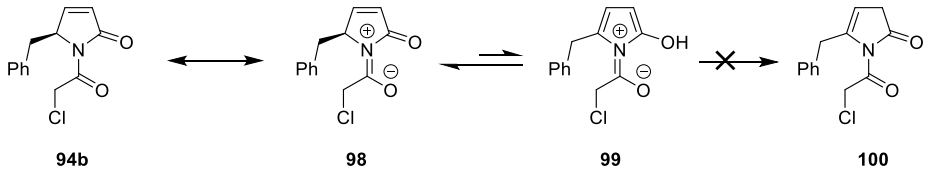

Scheme 1.23 The stabilizing effect of an electron withdrawing group on the pyrrolinone.

In 1990, the Thomas group[63] reported an another synthetic route to cytochalasin D **4** by an IMDA reaction using *N*-acylpyrrolinone. The simultaneous formation of the isoindolone core and the macrocyclic ring is shown in scheme 1.24. They started synthesis with methacrolein **101** and (*E*)-but-2-enyldiisopinocampheylborane **102** and the triene compound **108** was prepared after 7 steps. *N*-benzoylpyrrolidinone **109** was then introduced and the double bond was prepared by phenylselenenylation followed by oxidative elimination, which is a popular strategy for the synthesis of cytochalasans. The unstable compound **112** underwent an IMDA reaction to form the isoindolone core and macrocycle simultaneously in toluene at 80 °C with moderate yield.

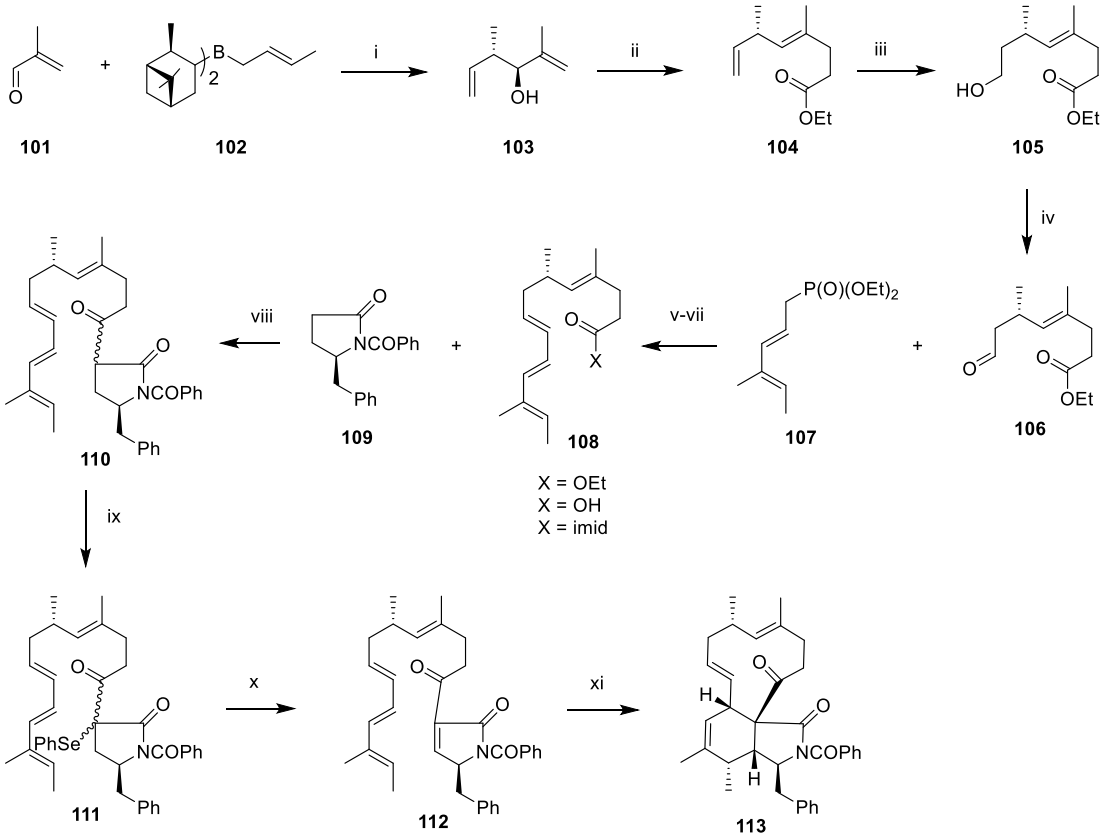

Scheme 1.24 Total synthesis of cytochalasin D **4** by the Thomas group. Reagents and conditions: **i**, -78 °C, 3 h, then H_2O_2; **ii**, $MeC(OEt)_3$, propanoic acid, 140-170 °C (48% from **101**); **iii**, 9-BBN then H_2O_2 (77%); **iv**, $(COCl)_2$, DMSO (77%); **v**, *n*-BuLi, **107**, THF, hexamethylphosphoramide (85%); **vi**, NaOH, EtOH; **vii**, CO(imidazole)$_2$, THF; **viii**, $LiN(SiMe_3)_2$, **109** (92% from **108**); **ix**, $LiN(SiMe_3)_2$, PhSeCl (100%); **x**, *m*-CPBA, H_2O_2, -50 °C to 0 °C; **xi**, toluene, 80 °C (25-30% from **111**).

1.5 Project Aims and Model Design

Since the first discovery of cytochalasans over 50 years ago, until now, the full biosynthesis of cytochalasans especially the formation of isoindolone core and the macrocyclic ring are still mysterious. It is speculated that the PKS-NRPS hybrid derived chain **55** is released reductively by the C-terminal NRPS R domain to give an aldehyde **56**, which could undergo an intramolecular Knoevenagel condensation to form pyrrolinone **57**. Afterwards, pyrrolinone **57** reacts with the diene through the putative DA reaction to afford the isoindolone core **58** (Scheme 1.25). However, the results from the literature synthetic studies suggest this is not a competent substrate for a DA reaction. In this project, we aim to verify these hypotheses with *in vitro* assays.

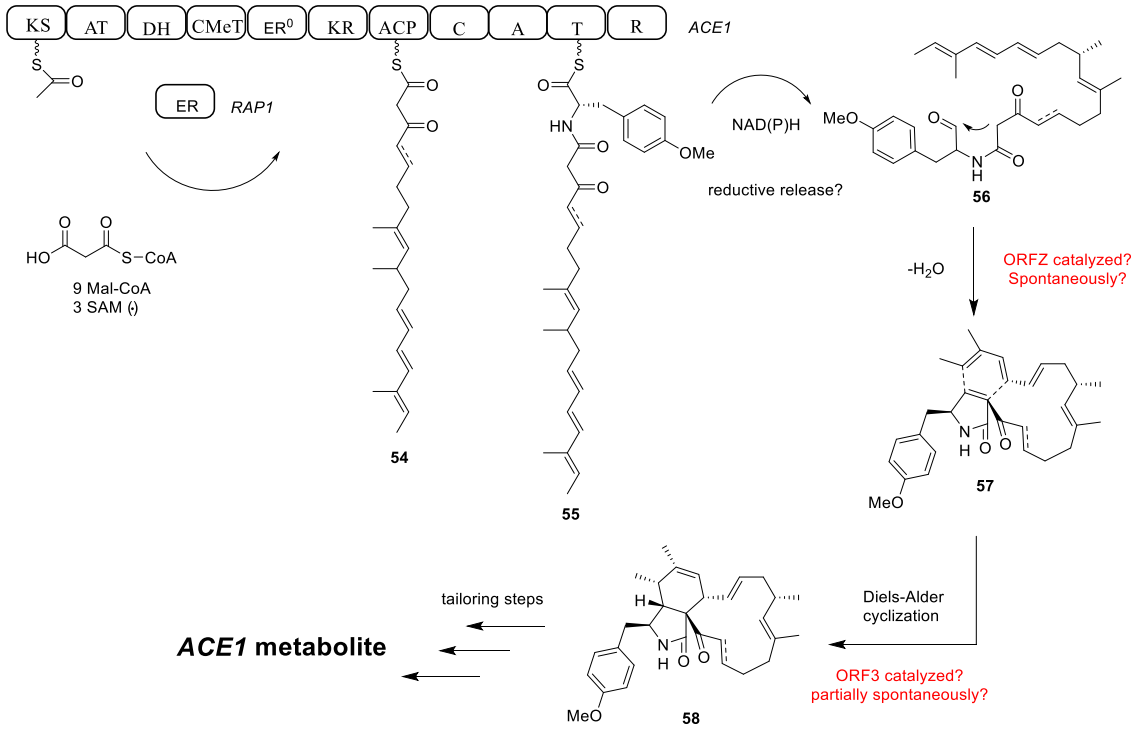

Scheme 1.25 Proposed *ACE1* metabolite biosynthesis.

However, heterologous expression of the cytochalasan gene clusters in *A. oryzae* (including *ACE1* and *RAP1*, *ccsC* and *ccsA* respectively) gave the alcohol state metabolites **36** and **52** rather than the corresponding aldehyde, which cannot undergo the Knovenagel condensation (Scheme 1.26). The product from *ACE1* and *RAP1* expression has no *avirulence* effect, suggesting that it should only be the intermediate or shunt rather than the final *ACE1* metabolite. Are they the shunt products of the cytochalasans precursors by over-reduction of the R domain or by unknown reductive enzyme in *A. oryzae*? This is the first question to investigate.

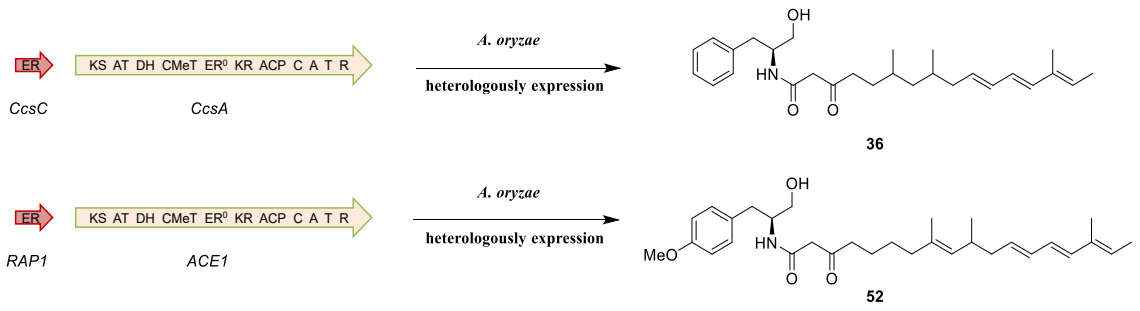

Scheme 1.26 Possible shunt metabolites from heterologous expressions in *A. oryzae*.

If the aldehyde rather than the alcohol is released, it could undergo an intramolecular Knoevenagel condensation to form pyrrolinone as proposed. According to Baldwin's rules, this reaction is 5-*exo*-*trig*, which is favored. So it is questionable whether this intramolecular Knoevanagel condensation is a spontaneous reaction or it needs enzyme catalysis. In fact, this reaction includes two steps: nucleophilic attack followed by elimination of water. If these are enzyme-catalysed steps, then which enzyme and which step is the enzyme involved in? This is the second question to answer. We also want to know which tautomer is formed.

After formation of the pyrrolinone, a putative DA reaction will occur according to the biosynthetic hypothesis. From the total synthesis we know, chemically, DA reaction needs harsh reaction conditions like high temperature and long reaction time. Moreover, the proposed pyrrolinone intermediate undergoes a rapid tautomerisation to a form unreactive for the DA reaction. Therefore it is likely that this DA reaction is an enzyme catalyzed reaction. But we need to provide sufficient evidence.

To answer these questions, *in vitro* assays can be performed to investigate. Instead of using the real intermediate, which is labor and time consuming to produce enough for *in vitro* assays, several tyrosine related model compounds are needed. For the first question, one possibility is that *A. oryzae* itself harbors a reductive enzyme and reduces the aldehyde before the formation of pyrrolinone. In this case, the reductive enzyme in *A. oryzae* may have low substrate selectivity. So a simple tyrosine related aldehyde with a biologically benign acetyl group (model A **114**) can be designed to perform *in vitro* assays with *A. oryzae* cell free extract (Figure 1.5).

In order to test the Knoevenagel condensation, a *β*-keto amide group is necessary. So model B **115** with the shortest possible chain length was designed (Figure 1.5). Since the model compound is not the real enzyme substrate, possibly there will be substrate selectivity. But at least we can know more information about the substrate properties *e.g.* stability, reactivity as well as the properties of the corresponding product pyrrolinone.

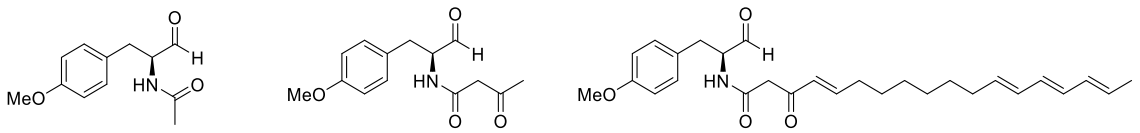

Figure 1.5 Structures of model compounds.

As for the putative DA reaction, a more complex model C **116** mimicking the shunt metabolite was designed (Figure 1.5). Model C **116** keeps not only the *β*-keto amide group, but also introduced the same alkyl chain length as the shunt metabolite with a triene at the end. The methyl groups on the shunt metabolite chain may be important for the DA reaction configuration, but for a primary test, model C **116** would be sufficient and relatively simple to make.

After all these primary assays, the results will be further tested with more realistic intermediates extracted from fungal fermentations. The shunt metabolite **52** is at the alcohol state, which has to be oxidized to an aldehyde by chemical methods. Another aim is therefore to find suitable oxidizing conditions to convert similar alcohols to aldehydes. All these aldehydes will be tested *in vitro* with corresponding enzymes including ORFZ and ORF3 or cell free extracts from *A. oryzae* provided by Verena Hantke. The process will be monitored by LCMS or NMR.

If possible, we can also feed the cytochalasan backbone to fungi to complete the biosynthesis of tailoring steps. After tailoring steps, hopefully we can discover the exact *ACE1* metabolite and have the fully characterized spectra including ^{1}H NMR, ^{13}C NMR, UV spectra, HRMS, and other necessary spectra. New compounds will be tested for *avirulence* properties by existing collaborators in France. In future, such compounds could be used in agriculture to switch on a plant's native resistance against fungal disease for protecting crops which is a new environmentally friendly strategy in crop protection.

2. Cytochalasan Shunt Metabolite Research, an Over-Reduction by *Aspergillus oryzae*.

2.1 Introduction

Heterologous expression is a common method in fungal secondary metabolite studies. The levels of expression of many genes in fungal hosts are often very low or even undetectable under typical cultivation conditions.[64] Among the heterologous hosts, the well-known fungus *Aspergillus oryzae* has proved to be an amenable host and has been used successfully for fungal secondary metabolite gene expression in cases including penicillin G **117**,[65] tenellin **118**,[66] aphidicolin **119**,[67] paxilline **120**,[68] citrinin **121**[69] and KK-1 **122**[70] among many others (Figure 2.1).

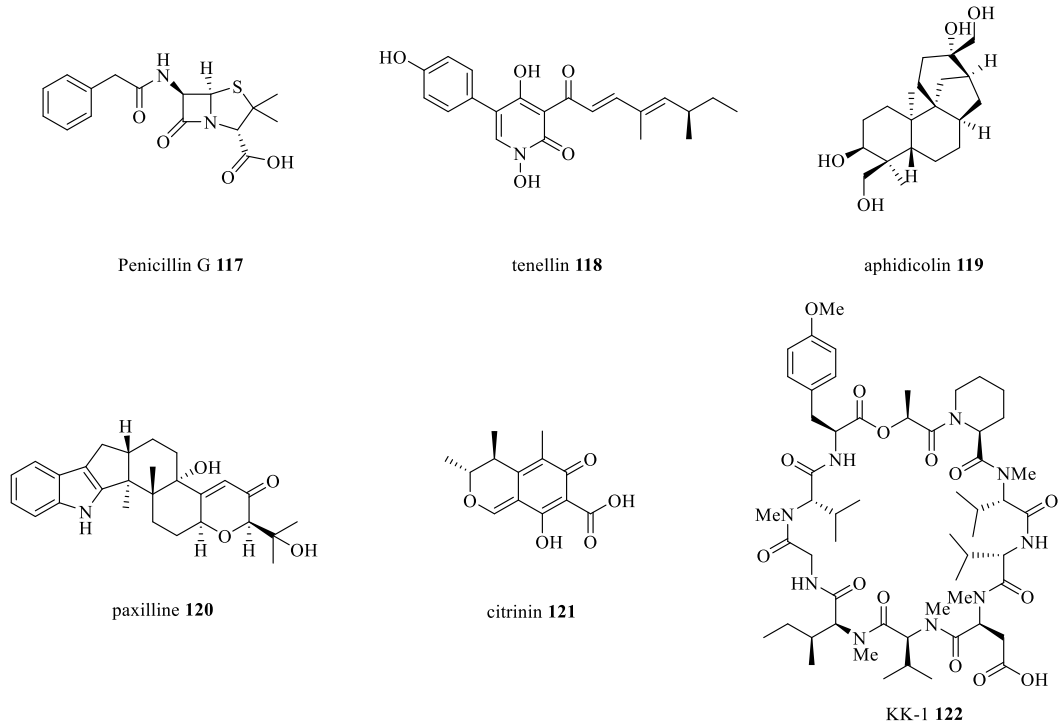

Figure 2.1 Examples of successful heterologous expression in *A. oryzae*.

However, heterologous co-expression of cytochalasin E **5** gene clusters (*ccsA* and *ccsC*) and ACE1 gene clusters (*ace1* and *rap1*) in *A. oryzae* has been problematic. The

ccsA R domain harbors an intact conserved NADPH binding motif GXSXXG and the catalytic triad Ser-Tyr-Lys shared among the short chain dehydrogenase reductase SDR superfamily proteins, so it is expected that the R domain should release aldehyde suitable for Knoevenagel condensation.

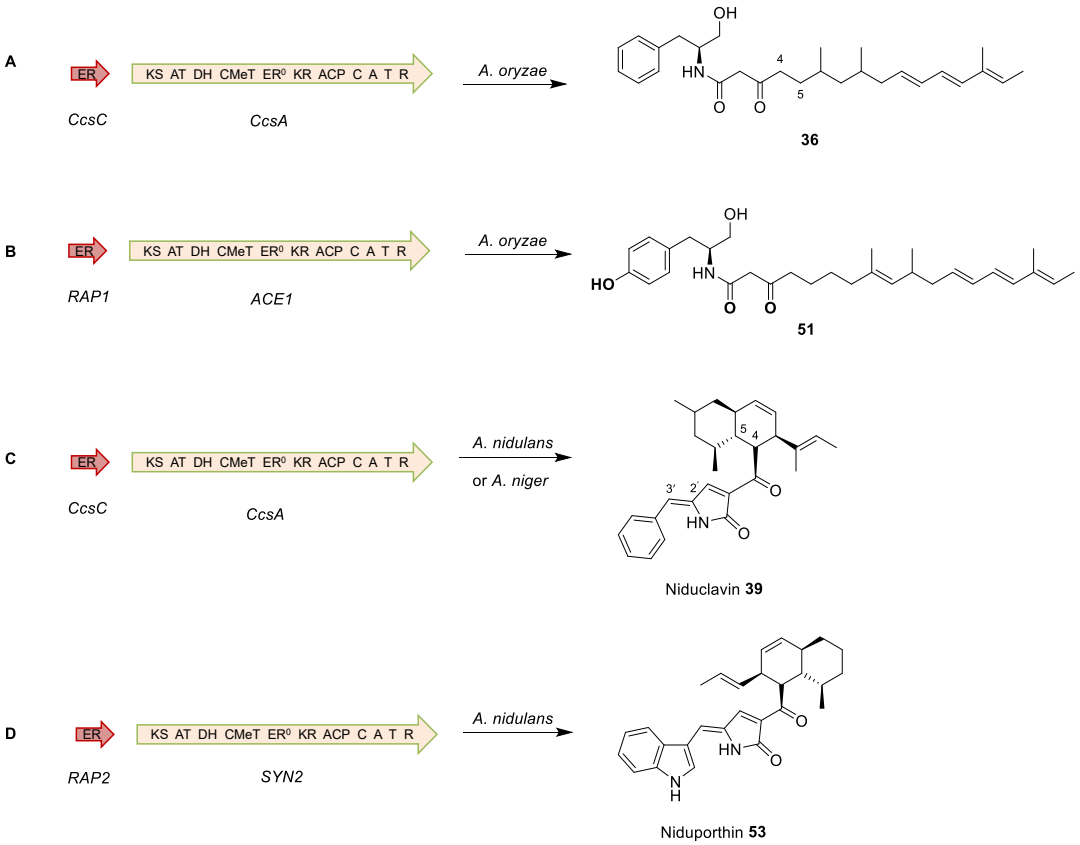

Scheme 2.1 Heterologous expressions in different fungal hosts.

But Alcohols **36** and **51** with linear PKS-NRPS backbones were produced after heterologous expression in *A. oryzae* (section 1.3.2.3). The observation of linear compounds suggests that the cytochalasan backbone is released in a reductive way to give an aldehyde. However, the aldehyde was then over-reduced to the alcohol in *A.oryzae* and no longer useful for Knoevenagel condensation. The alcohol could be formed in two possible ways: either over-reduction by the R domain; or correct reduction by the R domain to aldehyde followed by *A. oryzae* shunt reduction. Moreover, heterologous co-expressions of the cytochalasin E **5** gene clusters (*ccsC* and *ccsA*) and PKS-NRPS *SYN2* and *RAP2* in the alternative fungal host *Aspergillus nidulans* produced niduclavin **39** and niduporthin **53** which are not over-reduced.[44]

These observations suggest that *A. oryzae* may contain a shunt reductase which is not present in *A. nidulans* (scheme 2.1).

2.2 Aims

Heterologous expression in *A. oryzae* has been developed as a toolkit for fungal secondary metabolite pathway investigation.[71] But the potential problem caused by the possible presence of shunt enzymes in *A. oryzae* has not been well studied systematically, even though the unexpected over-reductions of aldehydes to alcohols have been observed and reported.[42,47,72] This project was designed to find out whether the shunt enzymes in *A. oryzae* have a strong influence in aldehyde reduction. If aldehydes are reduced to alcohols by an endogenous enzyme in *A. oryzae*, it is also necessary to find out the corresponding genes responsible for the reductase. Since possible over-reduced cytochalasin E and ACE1 metabolite precursors are not native in *A. oryzae*, the unknown enzyme in *A. oryzae* probably does not have strict substrate selectivity. In order to investigate this, model A **114** which is an *O*-methyl tyrosine derived aldehyde was designed and synthesized. Afterwards, the *A. oryzae* cell free extract will be tested for its ability to reduce model A **114** in *in vitro* assays. If reduction activity can be observed, then the enzyme could be purified and sequenced. In the longer term, we could knockout the gene and thereby engineer an *A. oryzae* expression host which cannot reduce the ACE1 metabolite precursor and potentially allow heterologous ACE1 metabolite production.

2.3 Results and Discussion

Work in this section was performed in collaboration with master student Franck Siakeu and with fellow Ph.D. student Verena Hantke. I was responsible for the synthetic and *in vitro* analytical work while Verena helped with the preparation of *A. oryzae* cell free extracts.

2.3.1 Model A Retrosynthetic Analysis

Model A **114** can be prepared from the oxidation of corresponding alcohol **128** which is an *N*-acetylated derivative of amino alcohol **127**. Compound **127** is a known compound derived from *L*-tyrosine **123** in 4 steps involving nucleophilic substitution, methylation, reduction and hydrolysis (Scheme 2.2).[73]

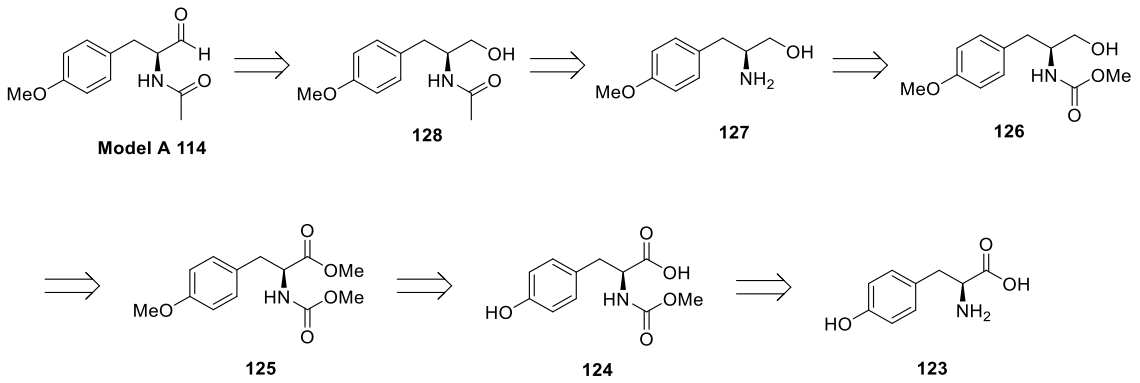

Scheme 2.2 Model A **114** retrysynthetic analysis.

2.3.2 Model A Synthesis

The synthesis of model A **114** started with amine protection of *L*-tyrosine **123** (scheme 2.3). Tyrosine has limited solubility in either organic solvent or water, so a mixture of THF and H_2O (1:1) were used to increase the solubility. After protection of the amino group, double methylation of both phenol and carboxylic acid was achieved by methyl iodide under basic conditions in good yield. Reduction of methyl ester **125** by $LiAlH_4$ afforded alcohol **126**, which was further deprotected with potassium hydroxide to free the amino group **127**.

After formation of the common intermediate **127**, we can choose to selectively acetylate the amino group, but there was always minor double acetylation product **128** formed. We therefore chose to acetylate both hydroxyl and amino groups with excess acetyl chloride in quantitive yield without purification and then hydrolyse the ester in MeOH with K_2CO_3 to afford compound **129**. A modified Moffat oxidation of the hydroxyl group was then applied to give model A **114**. The aldehyde is not very stable

over flash chromatography, but only milligram amounts of compound were needed for the bioassay, so preparative LCMS was used for the purification of model A **114**.

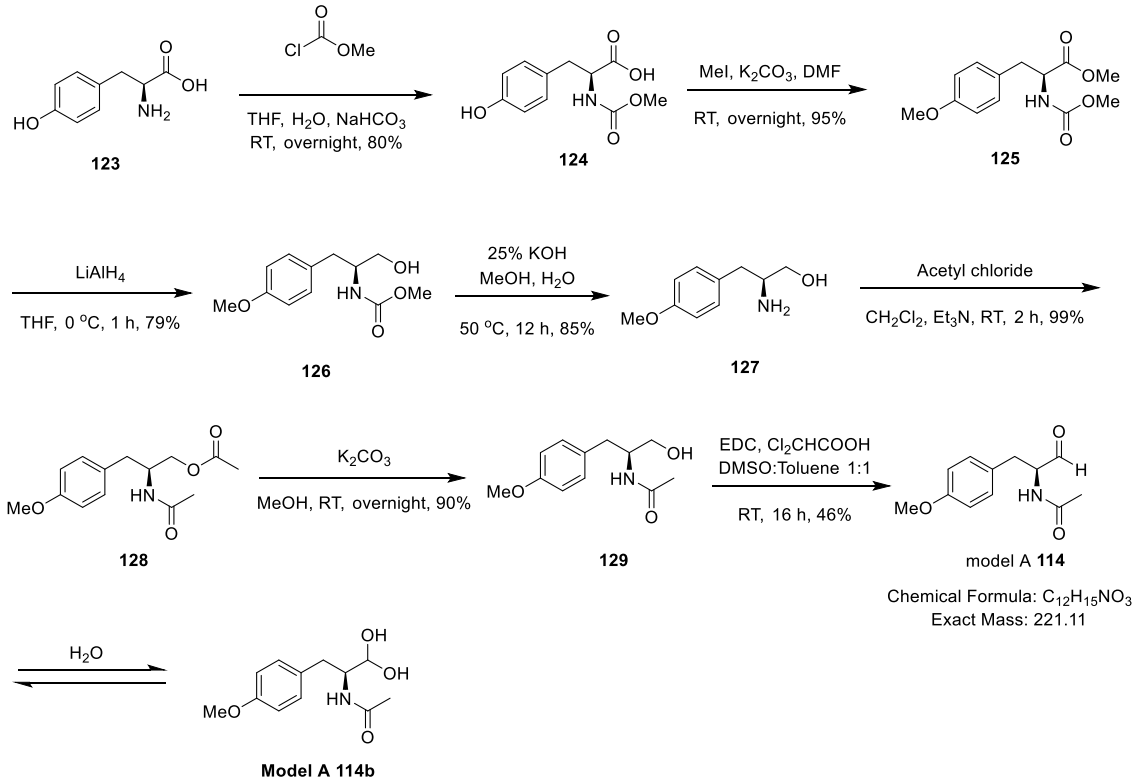

Scheme 2.3 Synthetic route to model A **114**.

The LCMS data of model A **114** is shown in Figure 2.2. The retention time is around 3.3 min tailing to 4.5 min because aldehydes are in equilibrium with its hydrate in the presence of water (scheme 2.3). The aldehyde hydrate **114b** is much more polar than aldehyde **114**, therefore it elutes earlier at 3.3 min. The aldehyde **114** which is the minor component of the equilibrium elutes at 4.5 min. The UV spectrum clearly shows the absorbance of the aromatic ring and the mass spectra ES^+ (222.1), ES^- (220.1) also fit the molecular weight (221.1). ES^- (266.1) is the molecule plus formic acid (46.0).

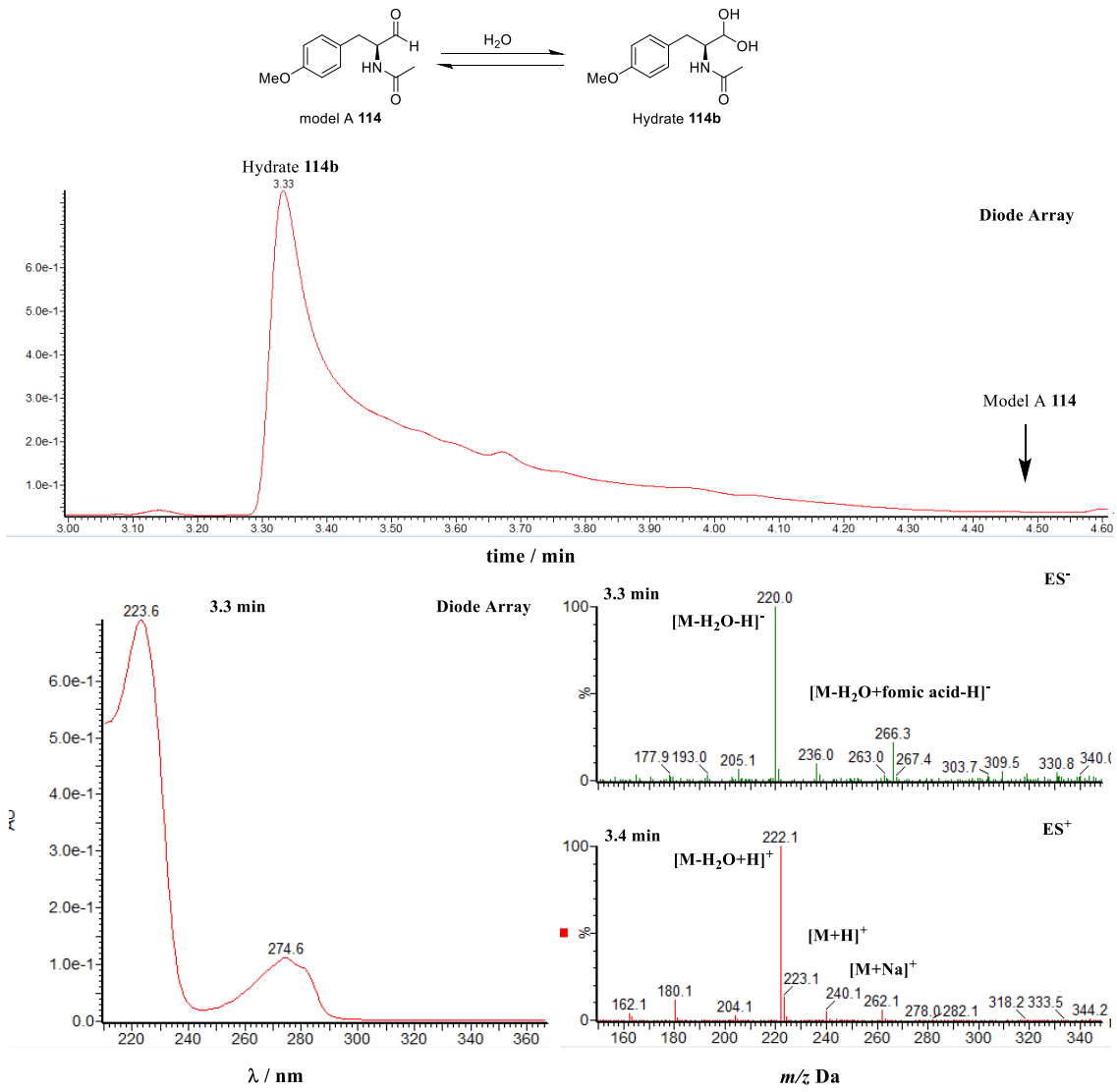

Figure 2.2 LCMS data of model A **114**.

The ^{1}H NMR of model A **114** in $CDCl_3$ clearly shows the characteristic protons including the aldehyde proton chemical shift at 9.67 ppm, α-proton at 4.72 ppm, two diastereotopic *β*-protons at 3.11 ppm. The aromatic protons and two methyl groups as well as the NH can be also found (Figure 2.3).

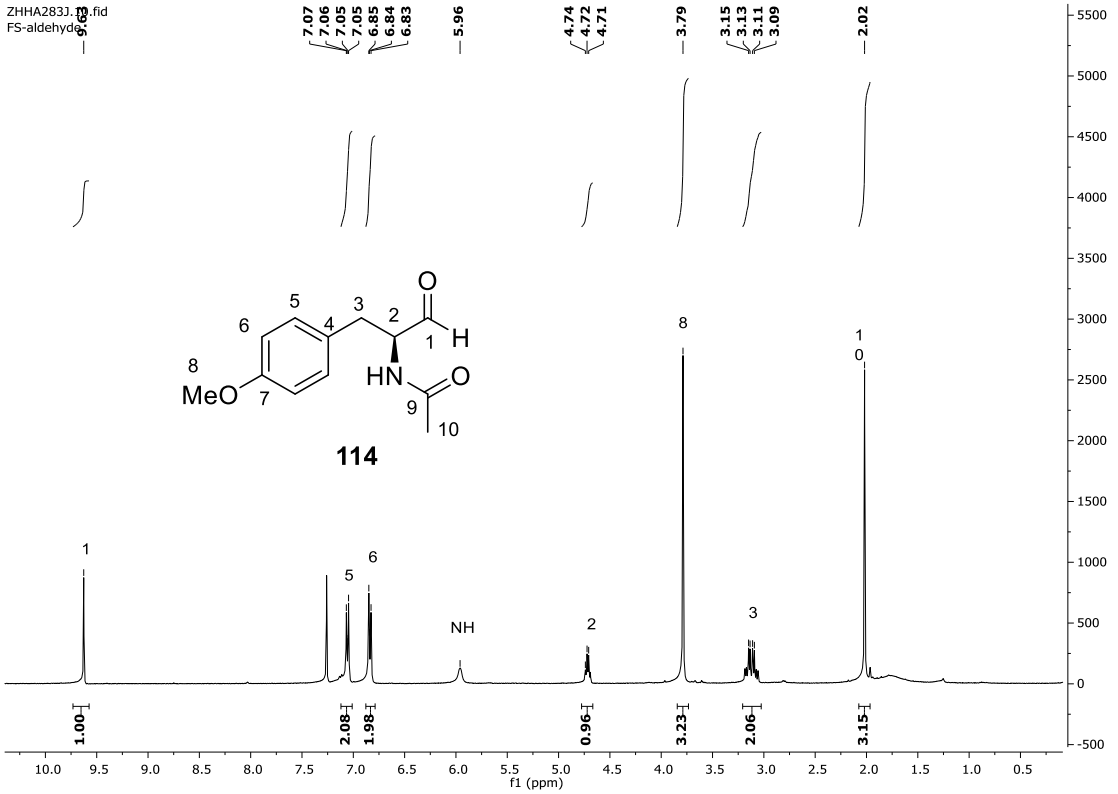

Figure 2.3 ^{1}H NMR of model A **114** in $CDCl_3$.

2.3.3 Model A Bioassays

2.3.3.1 Preparation of Cell Free Extract from *A. oryzae*

A. oryzae NSAR1 cells expressing *ACE1* and *RAP1* (2.0 g) were frozen in liquid nitrogen in a mortar and ground to a fine powder. Then 2 mL potassium phosphate buffer (pH 7.0, 50 mM) was added and mixed with the cell powder. After collection by centrifugation at 16000 × g for 30 min at 4 °C, the supernatant was collected and stored at -20 °C for further tests.

2.3.3.2 Model A Bioassays with Cell Free Extract

A suitable buffer system was developed for the *in vitro* assay. Since model A **114** is an aldehyde, any buffer containing an amino group, such as Tris, is not suitable because of likely imine formation. Therefore the common buffer potassium phosphate was first considered for the bioassay. To make sure potassium phosphate buffer has no influence

on model A **114**, the stabilities of model A **114** in H_2O and potassium phosphate buffer (pH 7.0, 50 mM) were tested at 28 °C over time.

Figure 2.4 shows the results of model A **114** in H_2O at 28 °C after 0 h, 1 h, 3 h and overnight. It clearly shows that model A **114** is stable in H_2O even after overnight incubation and there was no alcohol **129** formed.

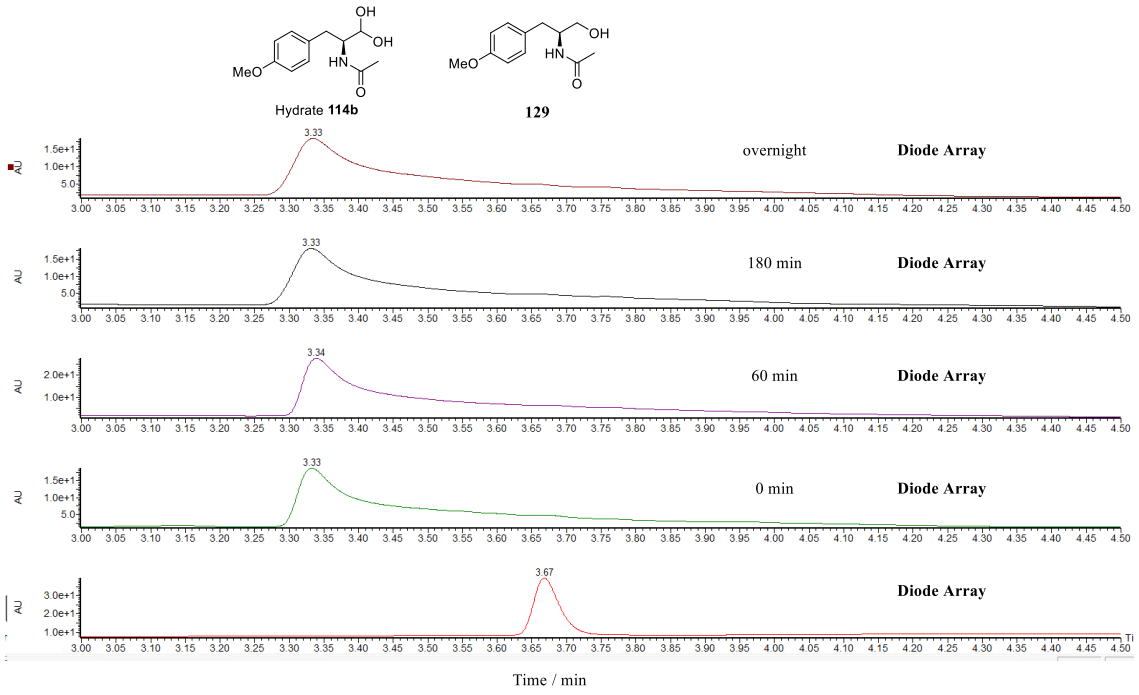

Figure 2.4 Model A **114** in H_2O over time at 28 °C.

Figure 2.5 shows the results of model A **114** in potassium phosphate buffer (pH 7.0, 50 mM) at 28 °C after 0 h, 1 h, 3 h and overnight. It shows that model A **114** is also stable in buffer over time and there was also tiny amount of alcohol **129** at 3.7 min, but this was from the incomplete oxidation of alcohol during the synthesis of the aldehyde. Therefore potassium phosphate buffer can be used for the bioassay with the CFE.

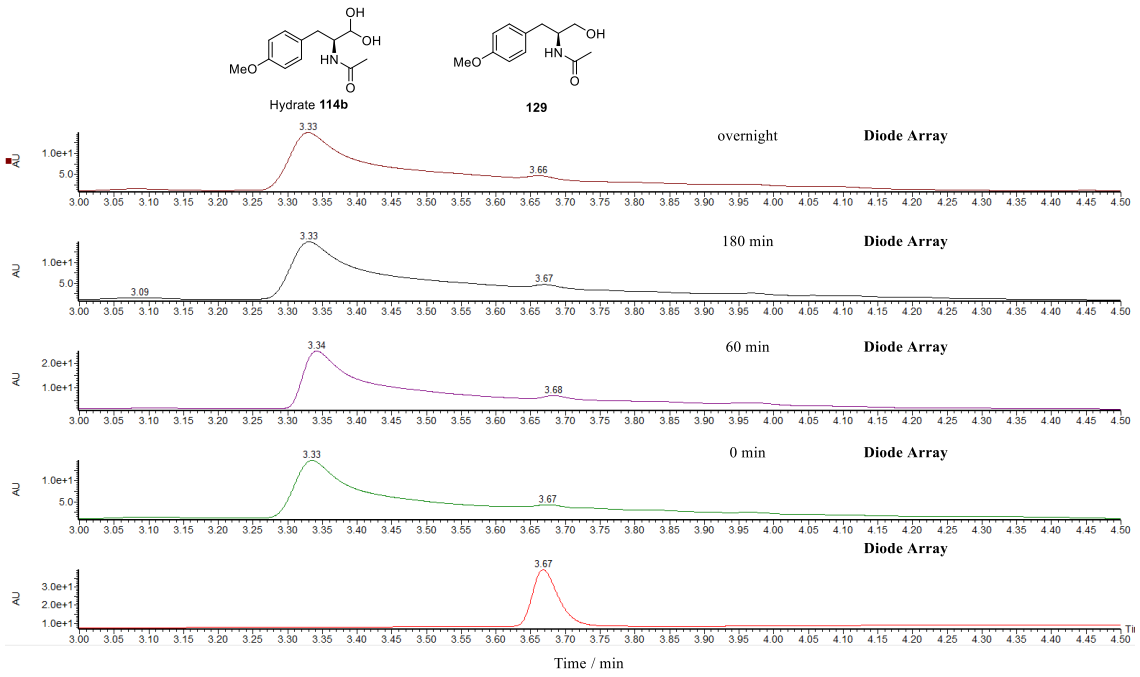

Figure 2.5 Model A **114** in potassium phosphate buffer (pH 7.0, 50 mM) over time (from bottom to top: alcohol **129**, 0 min, 60 min, 180 min and overnight) at 28 °C.

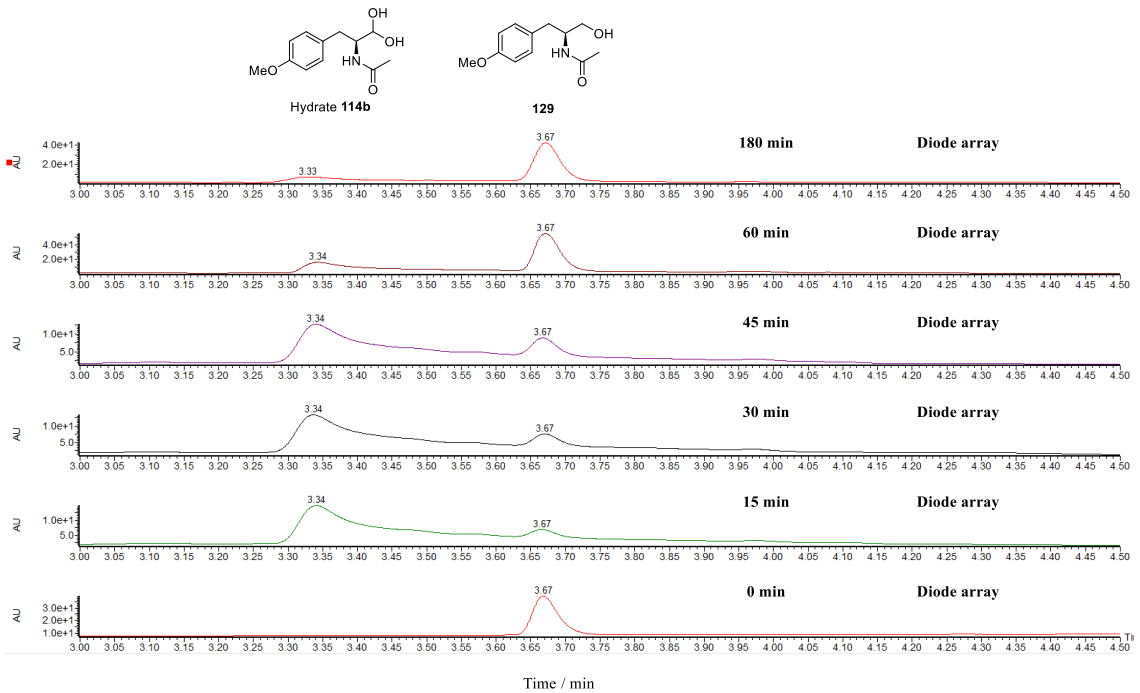

Figure 2.6 Model A **114** in potassium phosphate buffer (pH 7.0, 50 mM) with CFE over time (from bottom to top: 0 min, 15 min, 30 min, 45 min, 60 min and 180 min).

The model A **114** bioassay was performed with *A. oryzae* cell free extract (CFE) in potassium phosphate buffer (pH 7.0, 50 mM) with addition of NADPH at 28 °C over time and the sample without cell free extract was observed as a negative control. The result of the negative control is the same with the tests shown above in figure 2.5. While the CFE sample showed that after 15 min, some alcohol **129** was formed. After 1 h, almost all model A **114** was converted to alcohol **129** (Figure 2.6). Compared with the negative control, it is obvious that the aldehyde **114** was reduced to the corresponding alcohol **129** by an unknown protein in the CFE.

Moreover, the *N*-protected aldehyde **130**, prepared from oxidation of intermediate **126**, was also applied for the *A. oryzae* CFE assay and the aldehyde **130** was reduced to alcohol **126** as well in the presence of *A. oryzae* CFE. This further confirmed the exisistence of possible broadly selective aldehyde reductase in the *A. oryzae* CFE and indicated it has no strict substrate selectivity. Therefore it could also reduce the ACE1 metabolite precursor **56** to shunt alcohol **52**, even though it is not native metabolite in *A. oryzae*.

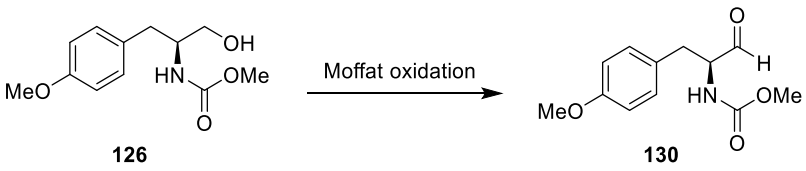

126 **130**

Scheme 2.4 Preparation of aldehyde **130** for the assay.

2.3.3.3 Protein Purification and Identification by ESI Q TOF

To find out the enzyme responsible for the reduction, proteins in the *A. oryzae* CFE were separated by size exclusion chromatography and the activities of different fractions were tested with model A **114** by Verena Hantke. The cofactor NADH or NADPH for the enzyme activity was tested by *in vitro* assays with the most effective fraction possessing enzyme activity. It showed that the enzyme of interest is NADPH-dependent.

Three fractions with enzyme activities were combined and the proteins inside were further separated by a strong anion exchange column. After further enzyme assays of different fractions, it turned out that the protein of interest was neutral or positively

charged at pH 7.0. Further protein sequence analysis by ESI Q TOF (Dr. Jennifer Senkler work group Prof. Braun, Institute of Plant Genetics, Leibniz University of Hannover) showed that the enzyme responsible for the reduction belongs to the family of NAD(P)H-dependent oxidoreductases. Malate dehydrogenase and alcohol dehydrogenase are two NADPH-dependent enzymes potentially involved in the reduction.

2.4 Conclusion and Outlook

Heterologous expression is a powerful tool in natural product biosynthesis investigation. However, heterologous expression of ACE1 gene cluster in *A. oryzae* was only partially successful. A native enzyme in *A. oryzae* was proposed to reduce the ACE1 metabolite precursor **56** to shunt alcohol **52** during the early biosynthetic step, thereby the full biosynthesis of ACE1 metabolite was not completed. The hypothesis was confirmed by *in vitro* assays with *A. oryzae* NSAR1 CFE. A synthetic model A **114** was reduced its corresponding alcohol **129** in the presence of CFE of *A. oryzae*. It proved the hypothesis that the ACE1 alcohol **52** is an over-reduction shunt metabolite, produced by a native enzyme in *A. oryzae*.

Further protein purification and sequence analysis showed that malate dehydrogenase and alcohol dehydrogenase in *A. oryzae* are two NADPH-dependent enzymes potentially involved in the reduction. Malate dehydrogenase is an enzyme in the citric acid cycle that catalyzes the reversible conversion of malate **131a** into oxaloacetate **131b** using the reduction of NAD^+ to NADH (scheme 2.5). As part of primary metabolism, it has specific and essential role. Therefore it might be not involved in the reduction of ACE1 metabolite precursor **56**.

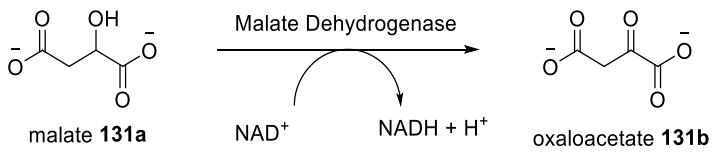

Scheme 2.5 Catalysed reaction by malate dehydrogenase.

Alcohol dehydrogenases exsist in many organisms and facilitate the interconversion between alcohols and aldehydes or ketones with the reduction of (NAD^+) to NADH (scheme 2.6). It is more likely that alcohol dehydrogenase is involved in the reduction of ACE1 aldehyde **56**.

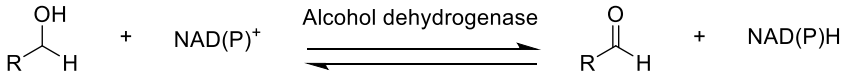

Scheme 2.6 Catalysed reaction by malate dehydrogenase.

Afterwards, the gene responsible for the alcohol dehydrogenase could be knocked out and *A. oryzae* after deletion of the reductase could be used for expression of cytochalasan BGC as well as some other secondary metabolites BGC where aldehydes are intermediates. Eventually it could be used for the investigation of α,β-hydrolase function and putative Diels-Alderase. It might also be possible to complete the full biosynthesis of ACE1 metabolite.

3. Investigation of Knoevenagel Reaction by *In Vitro* Assays with Model Compounds.

3.1 Introduction

3.1.1 Brief Introduction to the Knoevenagel Condensation

The Knoevenagel condensation is a modification of the aldol reaction named after Emil Knoevenagel (1865-1921).[74] It is a nucleophilic addition of an active hydrogen compound to a carbonyl group (usually an aldehyde) followed by a dehydration reaction to yield an α,β-unsaturated ketone, catalysed either by acid or by base.

Under basic conditions the dicarbonyl compound is deprotoned to form an enolate, which is ready to attack the aldehyde to form a new C-C bond. After protonation and elimination of H_2O through an E1cb mechanism, an α,β-unsaturated ketone is formed (scheme 3.1A). Under acidic conditions, an enol is formed which is nucleophilic and can attack the activated aldehyde to from a new C-C bond. Further elimination of H_2O under acidic condition then affords the α,β-unsaturated ketone (scheme 3.1B).

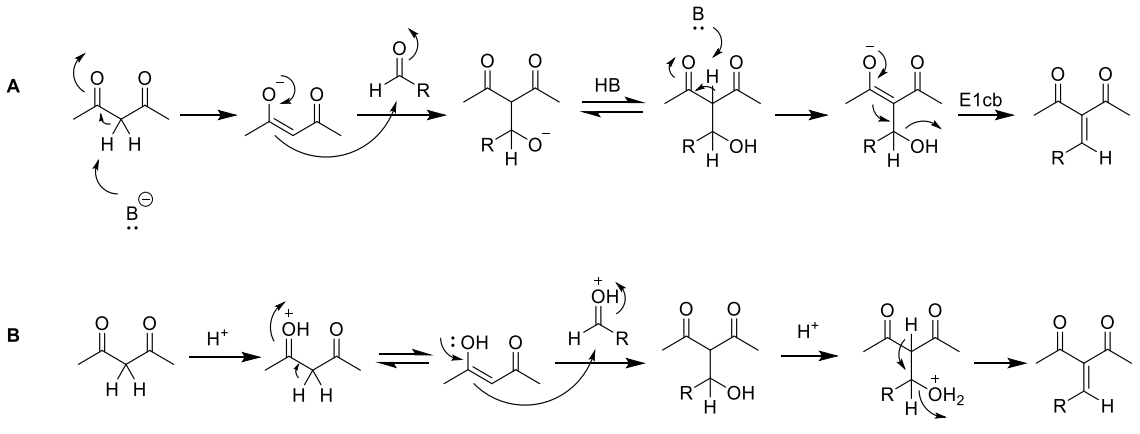

Scheme 3.1 Example of Knoevenagel condensation. **A**, mechanism catalyzed by base; **B**, mechanism catalyzed by acid.

The Knoevenagel condensation is a very useful reaction in organic synthesis. For example, in the synthesis of coumarin derivatives, which are natural products found in many plants with various bioactivities, the construction of the coumarin core can be achieved using a Knovenagel condensation in an efficient and environmentally friendly strategy.[75] An example is shown in scheme 3.2 for the synthesis of 3-acetyl-8-ethoxycoumarin **134**.[76] Here the initial Knoevenagel reaction is followed by an intramolecular transesterification to give the benzopyrone **134**.

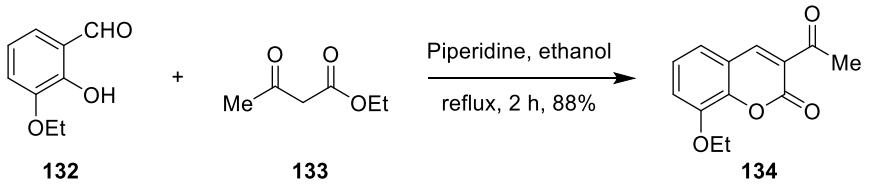

Scheme 3.2 Synthesis of 3-acetyl-8-ethoxycoumarin **134**.

3.1.2 Knovenagel Condensations Involved in Natural Product Biosynthesis

Knoevenagel condensations are hypothesized to be involved in many fungal natural product biosynthetic pathways, such as those for sorbicillin **137**,[77] oxaleimide A **142**,[78] fusarin C **146**[34] and UCS1025A **150**[79] among many others (scheme 3.3). The common feature for these proposed reactions in biosynthesis is that polyketide aldehydes are released by a reductive release (R) domain, followed by intramolecular Knoevenagel condensation, either spontaneously or catalyzed by as-yet uncharacterized enzymes to give a pyrrolinone.

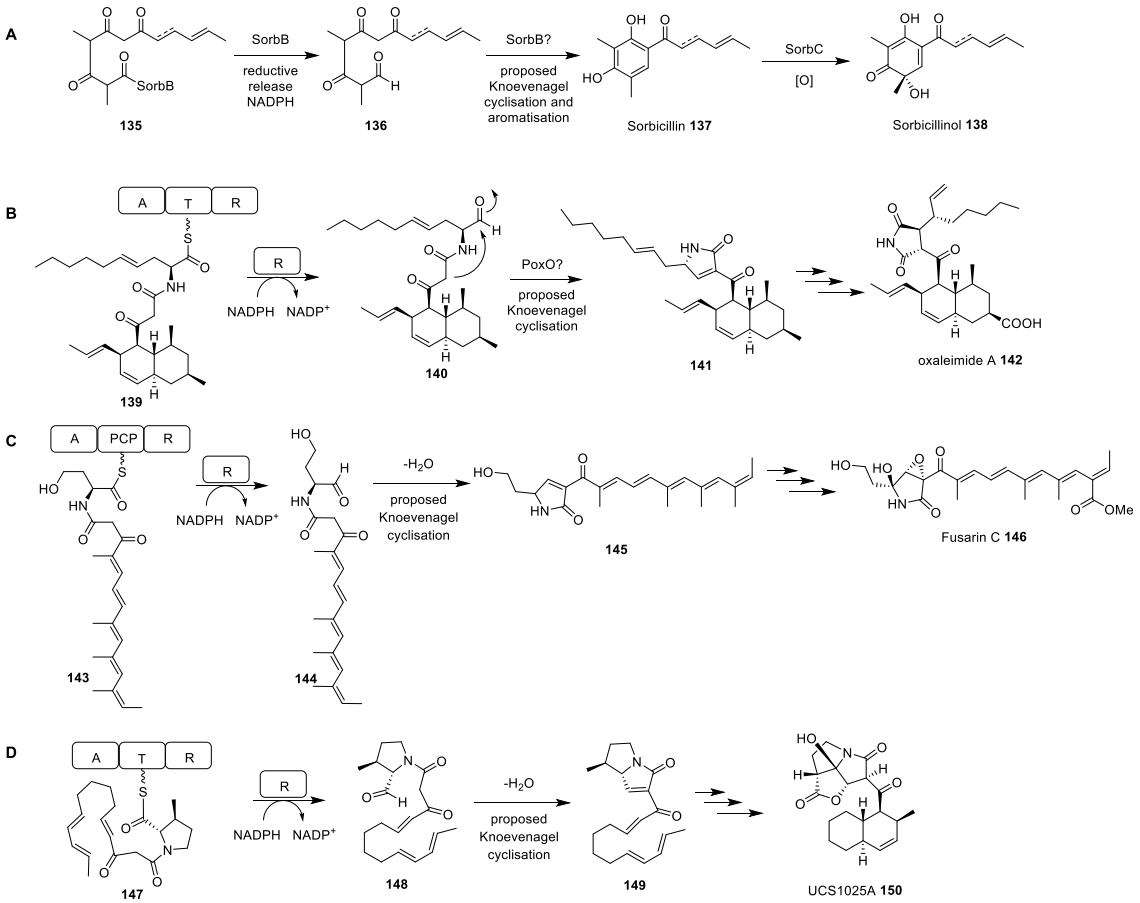

Scheme 3.3 Examples of fungal natural products biosynthesis potentially involving Knoevenagel condensations.

However, there is currently very little experimental support for the existence of Knoevenagel enzymes. One of the few examples is the biosynthesis of azaphilones. These are fungal pigments which exhibit a wide range of significant biological activities.[80] Targeted inactivation of the *mpp7* gene in *Monascus pilosus* resulted in the abolition of the main pigment components **152** and accumulation of **155**. Both **152** and **155** were Knoevenagel condensation products, but the regioselectivities were different. Therefore it was proposed that Mpp7 assists in regioselective Knoevenagel aldol condensation during pigment biosynthesis (scheme 3.4).[81]

But there is very little *in vitro* evidence for possible Knoevenagel enzymes, possibly because of competing facile chemical catalysis. This is especially likely to be possible in the cases of intramolecular Knoevenagel reactions.

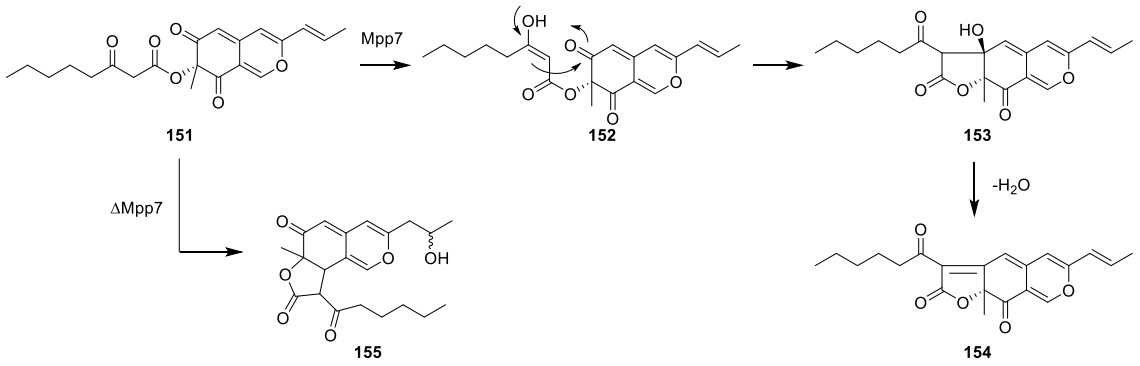

Scheme 3.4 Knock-out experiment of *mpp7* suggested its regioselective role in Knoevenagel condensation during azaphilone pigment biosynthetic pathway.

The skeleton of the cytochalasans has been also proposed to be formed *via* Knoevenagel condensation and subsequent Diels-Alder reaction for many years. For example, during cytochalasin E **5** biosynthesis, the PKS-NRPS backbone **27** is believed to be reductively released to an aldehyde **28** by the R domain (scheme 3.5). Aldehyde **28** could undergo a Knovenagel condensation to give pyrrolinone **29**, which could serve as a dienophile for a subsequent Diels-Alder reaction. However, it is still mysterious if this reaction is spontaneous or enzyme catalyzed. If enzyme catalysed, an α,β-hydrolase might be involved in this reaction. All known cytochalasan BGCs include an α,β-hydrolase encoding gene. But the precise role of this family of hydrolases is still unknown.

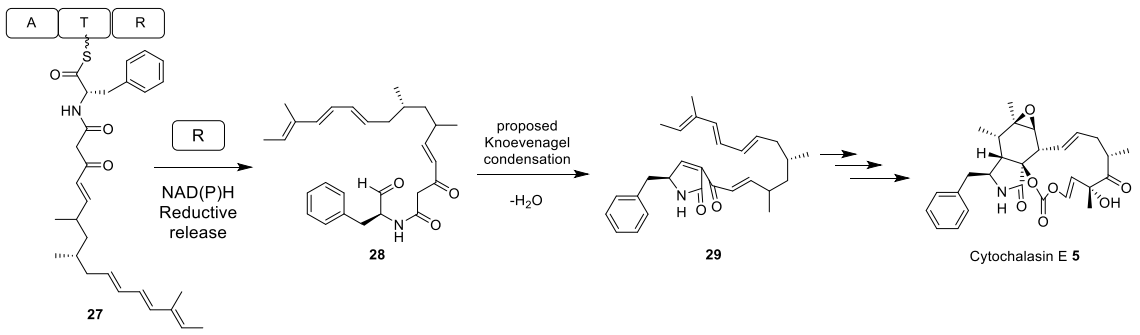

Scheme 3.5 Knoevenagel condensation is proposed to be involved in cytochalasin E **5** biosynthesis.

3.1.3 Synthesis of β-keto Amide Compounds

As shown in scheme 3.3, many natural products that are supposed to derive from a Knoevenagel condensation contain a β-keto amide or ester moiety. In fact, β-keto amides are versatile building blocks in the synthesis of different heterocycles, including pyrroles,[82] pyrans,[83] indoles,[84] tetrahydroquinolines,[85] dihydropyrimidones,[86] dihydrofuranodiones and succinimides.[87] Therefore, a variety of methods have been developed for the preparation of β-keto amides.

The most traditional methods for the introduction of β-keto amides involve reactions of amines with β-keto acids,[88] β-keto esters,[89] β-keto thiol esters,[90] *N*-hydroxysuccinimidylacetoacetate,[82] diketenes,[91] dioxinones[92] or acylated Meldrum's acids (Figure 3.1).[93] Among these methods, the straightforward coupling of amines and β-keto acids or aminolysis of β-keto esters are limited due to the instability of the keto-acid intermediates[93] and competing formation of enamines of the ketones. β-keto thiolester **158** and *N*-hydroxysuccinimidylacetoacetate **159** are effective reagents for introducing β-keto amides,[90] though they are restricted to certain structures. Diketene **160** is not stable and also limited to specific structural types.

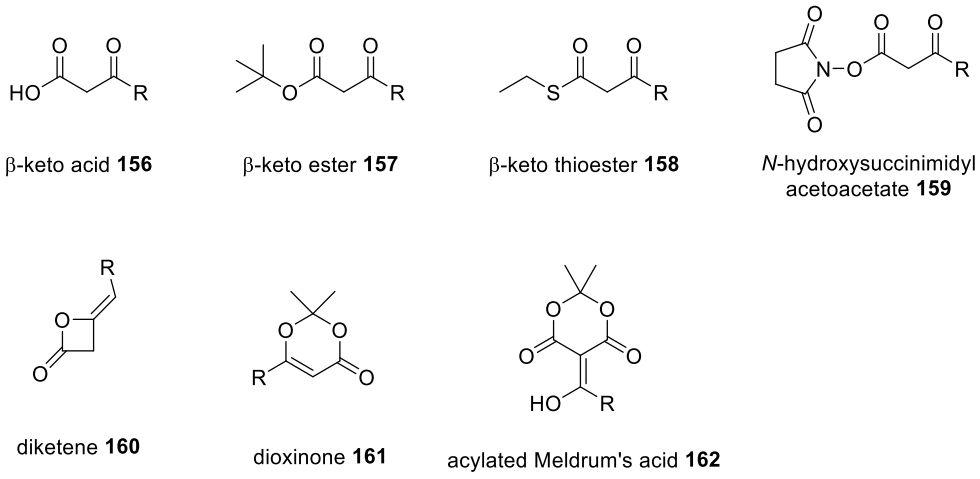

Figure 3.1 Reagents used for introducing β-keto amides.

Dioxinone **161** is also known as diketene acetone adduct, and is stable at room temperature. However, **161** releases acetylketene **163** when heated above 100 °C

(Scheme 3.6). Acetylketene **163** can efficiently acetoacetylate nucleophiles, *e.g.* aliphatic and aromatic alcohols, thiols, and amines in excellent yield.[92]

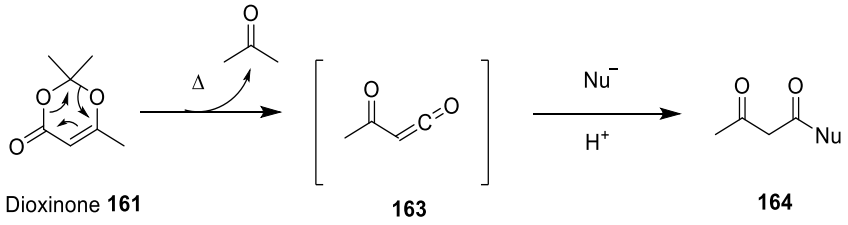

Scheme 3.6 Mechanism of dioxinone **161** theromolysis.

Dioxinones **161** can not only introduce β-keto amides, but also diverse functionalization of it is well studied. As shown in scheme 3.7, the dioxinone methyl group can be further functionalized with a carbonyl group[94] or phosphonate,[95] which are ready for a variety of chemical reactions, such as Wittig reaction, HWE reaction *etc*.

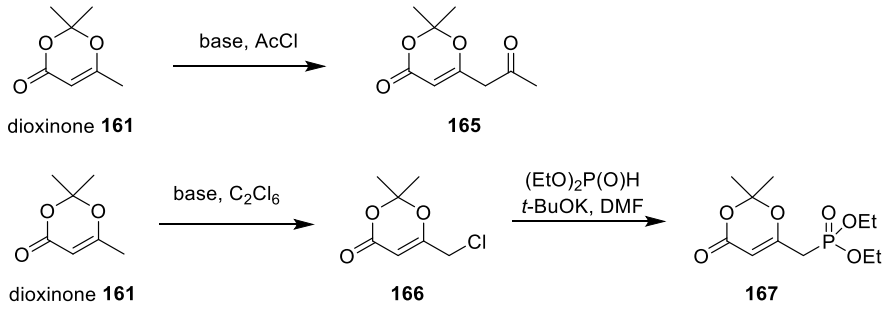

Scheme 3.7 Functionalization of the dioxinone **161**.

Dioxinone phosphonate **167** is widely used in natural product synthesis, especially for those compounds containing tetramic acids or pyrrolinones. Ikarugamycin **177** is an unusual pentacyclic tetramic acid antibiotic produced by *Streptomyces* sp.[96] The total synthesis of Ikarugamycin **177** was achieved by Napier and co-workers using dioxinone phosphonate **167** as an efficient way to construct the tetramic acid moiety (scheme 3.8).[97]

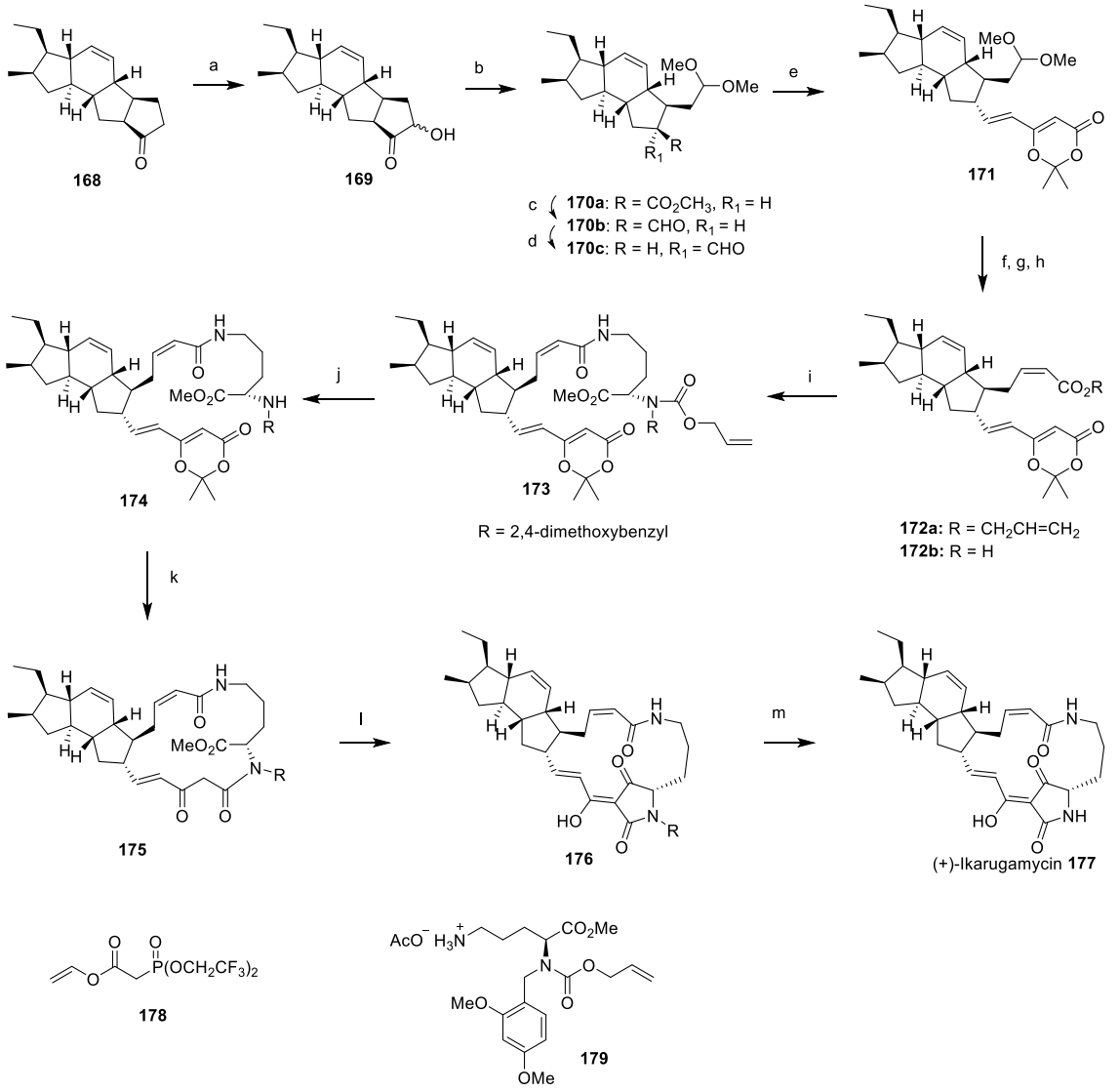

Scheme 3.8 (+)-Ikarugamycin **177** synthesis by Napier and co-workers. Reagents and conditions: **a**, $PhI(OAc)_2$ (1.2 eq.), KOH (2 eq.), MeOH, 25 °C, 8 h then Amberlyst-15, THF-H_2O (95:5 (*v*/*v*)), 25 °C, 24 h, 68%; **b**, $Pb(OAc)_4$ (1.05 eq.), MeOH-THF (1:1 (*v*/*v*)), 0 °C, 0.5 h then Amberlyst-15, 3Å molecular sieves, MeOH, 25 °C, 16 h, 62%; **c**, DiBAL-H (2 eq.), THF, 0 °C, 2 h; **d**, PDC (2 eq.), 3Å molecular sieves, CH_2Cl_2, 25 °C, 0.5 h, then DBU (cat.), CH_2Cl_2, 0 °C, 72-120 h; **e**, dioxinone phosphonate **167** (1.2 eq.), KHMDS (1.2 eq.), THF, 0 °C-25 °C, 4 h, 65%; **f**, Amberlyst-15, CH_3CN-H_2O (9:1 (*v*/*v*)), 25 °C, 12 h; **g**, **178** (1 eq.), K_2CO_3 (6 eq.), 18-C-6 (10 eq.), toluene, -20 °C-0 °C, 4 h; **h**, NH_4OAc (4 eq.), $Pd(PPh_3)_4$ (cat.), dioxane, 25 °C, 24 h, 78%; **i**, mesitylene sulfonyl chloride (1 eq.), Et_3N (1 eq.), THF, 25 °C, 10 min then **179** (2-3 eq.), DMAP (3-4 eq.), THF, 25 °C, 4 h, 60%-80%; **j**, HOAc, $Pd(PPh_3)_4$ (cat.), THF, 25 °C, 12 h, 96%; **k**, toluene, 105 °C, 8-10 h, 77%; **l**, *t*-BuOK (2 eq.), *t*-BuOH, 0 °C, 15 min, 75%; **m**, anhydrous TFA (0.01 M in substrate), 72 °C, 5 min, 55%.

The synthesis started from a previously reported intermediate **168**, which was constructed by an intramolecular Diels-Alder reaction.[98] Oxidation of **168** with $PhI(OAc)_2$ afforded a mixture of alcohol **169**. Subsequent oxidative cleavage of alcohol

169 with $Pb(OAc)_4$ and immediate protection of the resulting aldehyde provided acetal **170a**. After conversion of ester to aldehyde utilizing standard chemistry and epimerization of *cis*-aldehyde **170b** to a more stable *trans*-aldehyde **170c** in the presence of DBU, dioxinone phosphonate **167** was introduced by HWE reaction to give an exclusively *E* isomer **171**. After acetal deprotection, the required *Z* olefinic side chain was then elaborated *via* a *cis* selective Horner-Emmons reaction[99] with allyl *bis*-trifluoroethylphosphonoacetate **178**, providing the *Z* allyl ester **172a**. Deprotection of allyl ester **172a** afforded carboxylic acid **172b**, which was coupled with **178** to give amide **173**. Deblocking of **173** to secondary amine **174** and thermolysis of dioxinone moiety at 105 °C in a diluted solution yielded macrocyclic *bis*-amide **175** *via* an intramolecular trapping of the resulting highly electronphilic acyl ketene. The subsequent Dieckmann-type cyclization of the highly constrained *bis*-amide **176** was carried out to give the tetramic acid moiety, which was further deprotected to afford Ikarugamycin **177**.

Interestingly, dioxinone phosphonate **167** was also exploited for the construction of the isoindolinone core of muironolide A **194**, which is a tetrachlorinated marine metabolite isolated in minute quantities from a specimen of *Phorbas*.[100] Dioxinone **182** was affored in 3 steps including reduction of the ester **180** with *i*-Bu_2AlH, Swern oxidation and olefination with dioxinone phosphonate **167**. Amine **187** was prepared in three steps from propargyl alcohol **183**.[101] Copper-catalyzed methylmagnesation of propargyl alcohol **183** followed by the iodine quench afforded **184**. The synthesis was completed by the Kumada coupling with vinylmagnesiumbromide and a one-pot elaboration of the hydroxy group to PMB-protected amine **187**. Thermolysis of dioxinone **182** in the presence of amine **187** provided amide **188**, followed by site-selective cross-metathesis with methyl acrylate **189** to afford **190**. Heating of compound **190** in toluene at reflux resulted in intramolecular cycloaddition to isoindolinone core with correct stereochemistry. Triethylamine had no effect on the rate of the reaction, indicating that it cyclized through a pericyclic process rather than a stepwise anionic double Michael addition pathway.

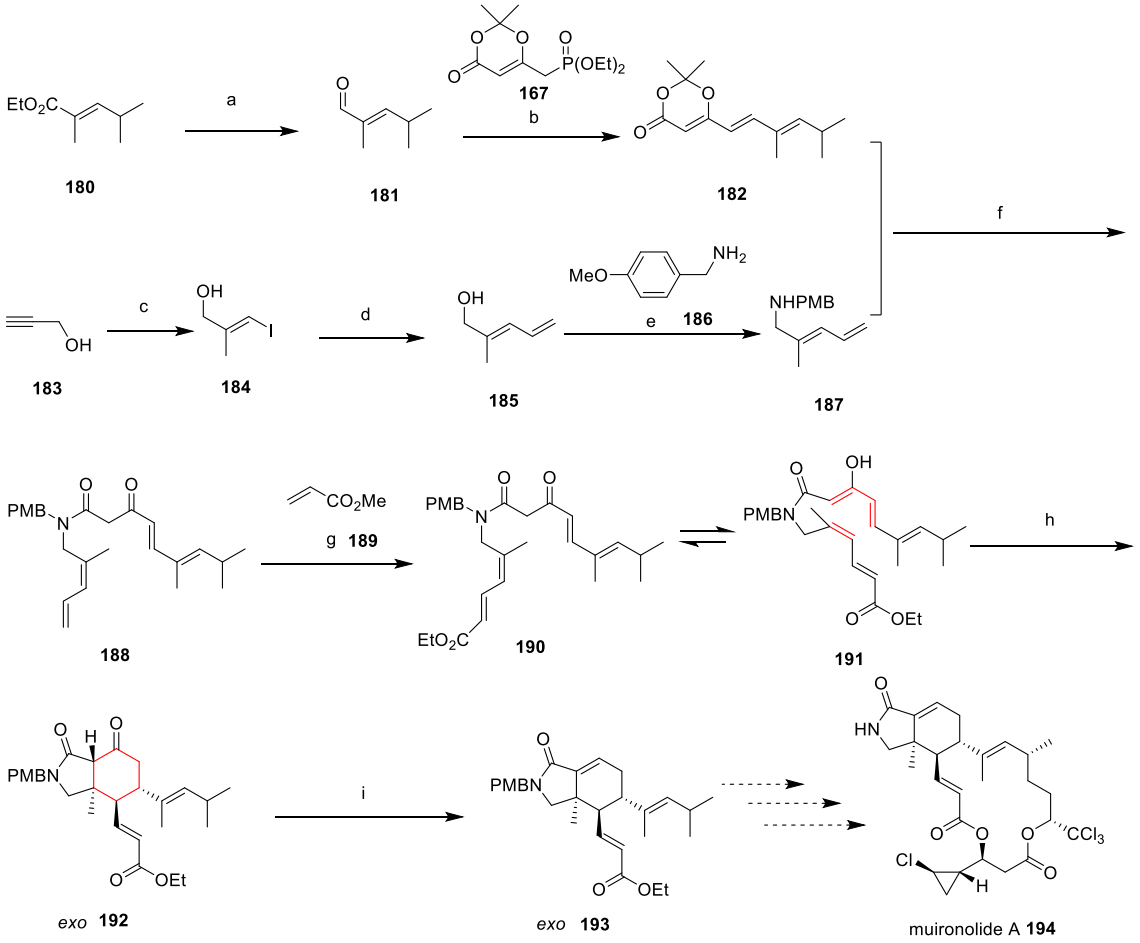

Scheme 3.9 Synthesis of muironolide A **194** isoindolinone core using dioxinone phosphonate **167**. Reagents and conditions: **a**, *i*-Bu_2AlH, CH_2Cl_2, then Swern oxidation, 40%; **b**, dioxinone phosphonate **167**, NaH, THF, 58%; **c**, MeMgBr, CuI (cat.), I_2; **d**, 5 mol% $Pd(PPh_3)_4$, CH_2=$CHMgBr$, toluene, 23 °C, 75%; **e**, NBS, PPh_3, THF, then *p*-methoxybenzylamine, 43%; **f**, PPTS, toluene, 110 °C, 3 h, 95%; **g**, 10 mol%, HGII catalyst, 81%; **h**, toluene, 110 °C, 60%, dr > 30:1; **i**, $NaBH_4$, $CeCl_3$, MeOH, CH_3SO_2Cl, Et_3N, CH_2Cl_2, 23 °C, DBU, toluene, 85 °C, 6 h, 64%.

Other approaches for introduction of β-keto amides have also been reported, *e.g.* condensation of isocyanates **196** with ketones,[102] activited carbamates[103] and condensation of amide enolates with acyl chlorides (scheme 3.10).[104] Enzymatic hydrolysis of nitriles is also an efficient way to provide β-keto amides (scheme 3.10D).[105]

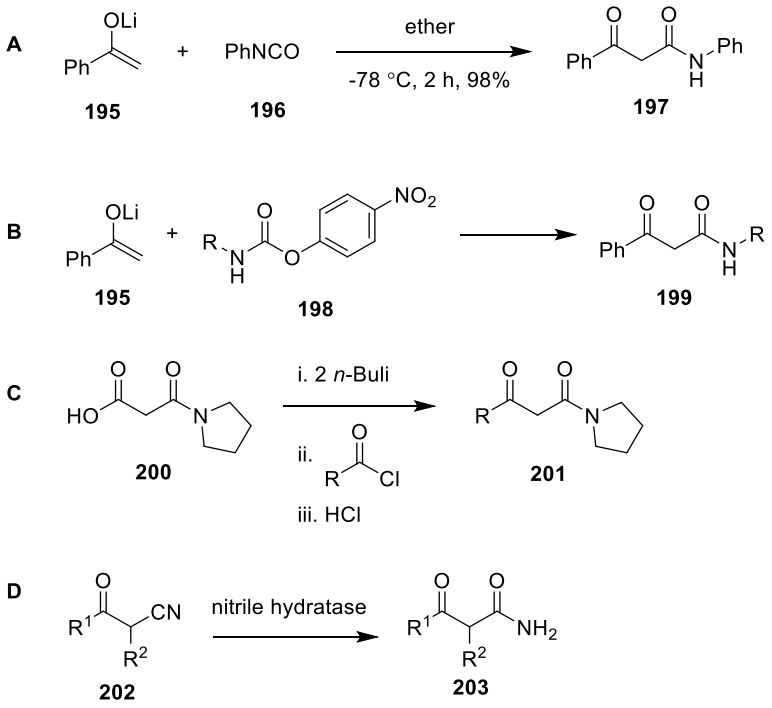

Scheme 3.10 Other approaches for introduction of β-keto amides.

3.2 Aims

Cytochalasans have been known for several decades and the late-stage tailoring steps including several oxidative reactions and Baeyer-Villiger rearrangements have been elucidated.[40,41] However, cytochalasan skeleton formation is still mysterious partially because of the lack of substrates for use in *in vitro* assays. It is proposed that Knoevenagel condensation and subsequent Diels-Alder reaction are likely to be responsible for the isoindolone core formation. In this project, we aim to investigate the proposed Knoevenagel reaction by *in vitro* assays.

For the cytochalasan substrate, we designed and synthesized model B **115** instead of the more complex and unavailable ACE1 nonaketide backbone for initial experiments. Model B **115** bears an aldehyde and a β-keto amide, which can be introduced by dioxinone **161**. For the enzyme, Verena Hantke expressed and partially purified ORFZ. Model B **115** will be firstly tested in H_2O and buffer to understand its properties. If it could form the corresponding pyrrolinone **204a** spontaneously, ORFZ would be tested to check if it can accelerate this reaction. If it is not spontaneous, *in vitro* assays would be performed with ORFZ to study its function in the proposed

Knoevenagel condensation (scheme 3.11). In addition the chemical stability of the proposed pyrrolinone product **204a** will also be investigated as this forms the required dienophile for the proposed later DA reaction. In addition, we wish to observe possible tautomer formation under biological reaction conditions.

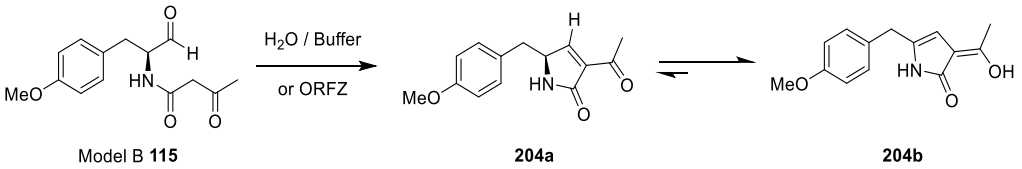

Scheme 3.11 Proposed *in vitro* assays with model B **115**.

3.3 Results and Discussion

3.3.1 Model B Retrosynthetic Analysis

Model B **115** is a new compound, but its phenylalanine analog **207** was reported by Tamm and Snider respectively using two different strategies.[106,107] Both of their β-keto amides were introduced using diketene **160** as shown in scheme 3.12. But the aldehyde group were preprared in two different ways: hydrolysis of a diethyl acetal **206** or oxidation of a primary alcohol **209**. Hydrolysis of diethyl acetal **206** with HCl in aqueous THF gave relatively pure aldehyde without further purification. But it needed more steps to prepare the somewhat inaccessible diethyl acetal **206**. Compound **209** was easily synthesized by acetoacetylation of the commercial available amino alcohol **208** using diketene **160**, even though some *bis*-ester amide also formed. But the unstable aldehyde had to be purified after oxidation of the primary alcohol.

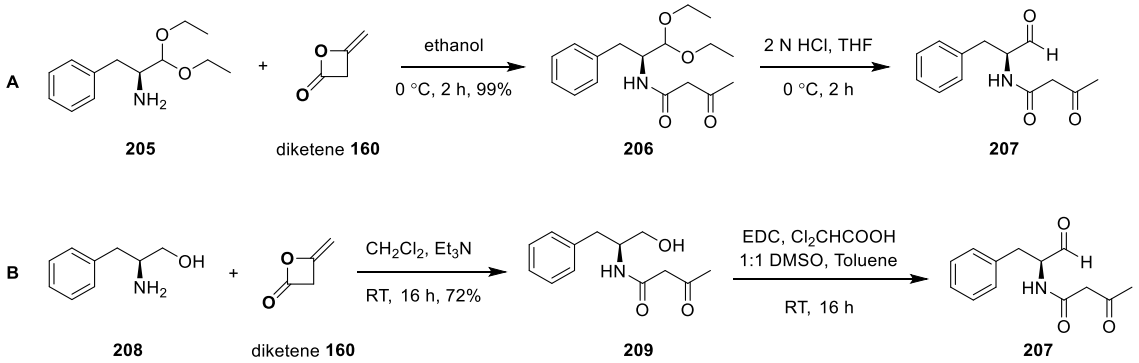

Scheme 3.12 Two methods reported for the synthesis of **207** by Tamm (**A**) and Snider (**B**).[106,107]

Model B **115** synthesis could be also achieved by the same strategies, *e.g.* oxidation of alcohol **210** or hydrolysis of diethyl acetal **213** (scheme 3.13). Alcohol **210** could be obtained by acetoacetylation of amino alcohol **127**, which was prepared previously in chapter 2. Diethyl acetal **213** could be derived from acetoacetylation of **212**. Since the dioxinone **161** is commercially available, we prefer to introduce *β*-keto amide by thermolysis of **161** instead of diketene **160**. This offers other advantages later since functionalization of **161** is also well-known.

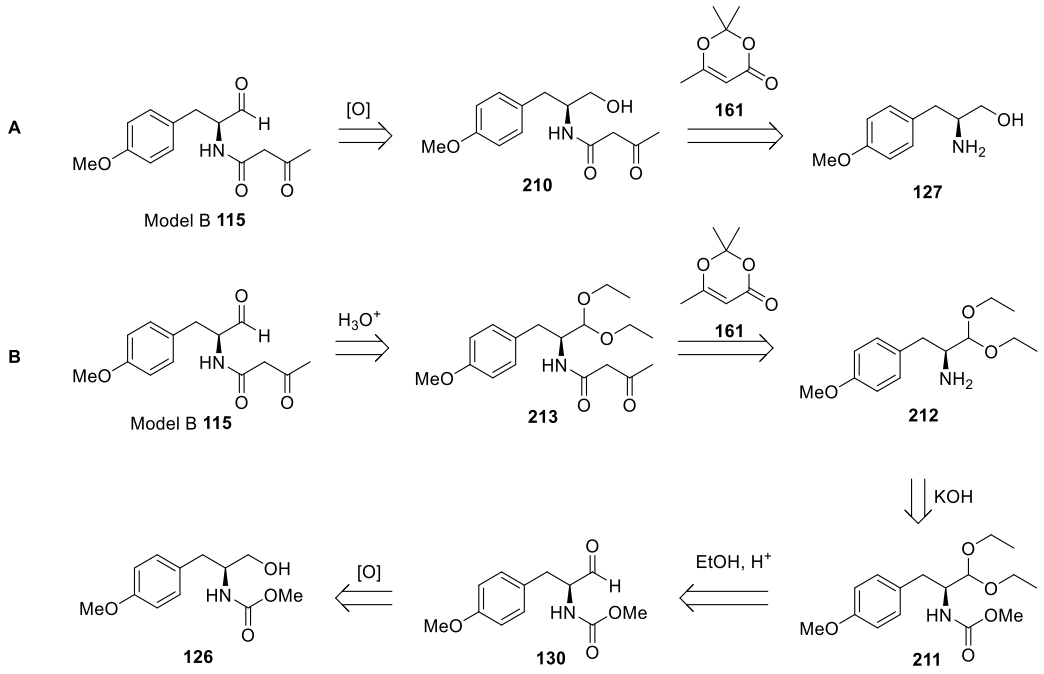

Scheme 3.13 Retrosynthetic analysis of model B **115**.

The intermediate 2**12** can be prepared from *N*-protected amino alcohol **126** *via* oxidation of hydroxyl group, protection of aldehyde and hydrolysis of carbamate (Scheme 3.13). The preparation of **126** was previously described in chapter 2.

3.3.2 Model B Synthesis

The model B **115** synthesis is shown in scheme 3.14. Amino alcohol **127** was prepared over 4 steps from *L*-tyrosine **123** as described in chapter 2. We introduced the dicarbonyl group with dioxinone **161** through thermolysis above 100 °C in toluene. When the ratio of the reagents is 1:1, there was some *bis*-ester amide formed. Use of

less dioxinone **161** resulted in relatively pure product and the excess amino alcohol **127** was recycled.

After synthesis of compound **210**, modified Moffat oxidation was applied to make model B **115**. Since **115** was not stable and underwent rapid degradation, **115** could not be purified by flash chromatography. But **115** was relatively stable in acetonitrile and water, so preparative LCMS was successfully applied for the milligram scale purification of model B **115**. In the presence of water, model B **115** is also in equilibrium with its hydrated form **115b**.

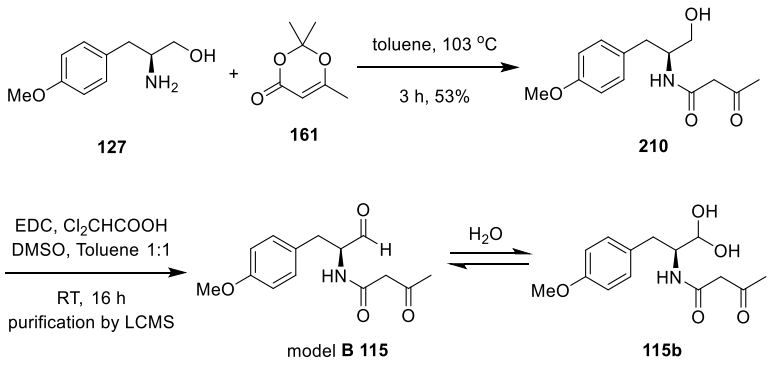

Scheme 3.14 Model B **115** synthesis *via* oxidation.

Model B **115** was also prepared *via* hydrolysis of diethyl acetal **213** (scheme 3.15). *N*-protected amino alcohol **126** was firstly oxidized to the aldehyde without purification, and then protected with triethyl orthoformate with a catalytic amount of *p*-TsOH at 50 °C overnight. The diethyl acetal group was stable in basic conditions, so the carbamate was hydrolysed with KOH in a mixture of H_2O and MeOH overnight at 50 °C to afford compound **212**. Reaction between compound **212** and dioxinone **161** in toluene above 100 °C for 2 h provided compound **213** in good yield, which was hydrolysed to give model B **115** in aqueous THF with HCl at 0 °C in 2 h. The reaction was monitored by LCMS over time to avoid formation of pyrrolinone **204a** after prolonged acidic conditions. After complete reaction, the mixture was neutralized with 1 M NaOH solution to pH 6 to reduce the solubility of aldehyde in acidic aqueous solution. This synthetic route provided relatively pure model B **115**.

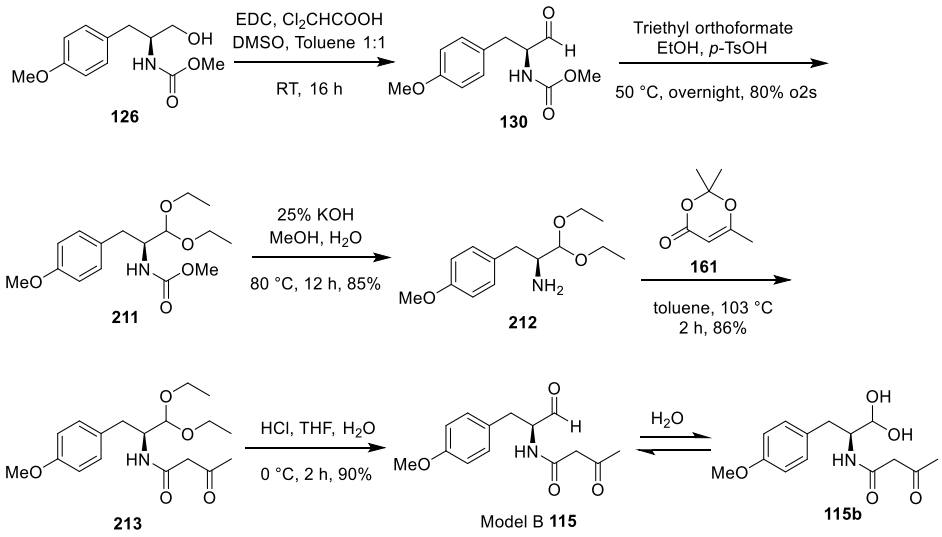

Scheme 3.15 Model B **115** synthesis *via* hydrolysis of diethyl acetal **213**.

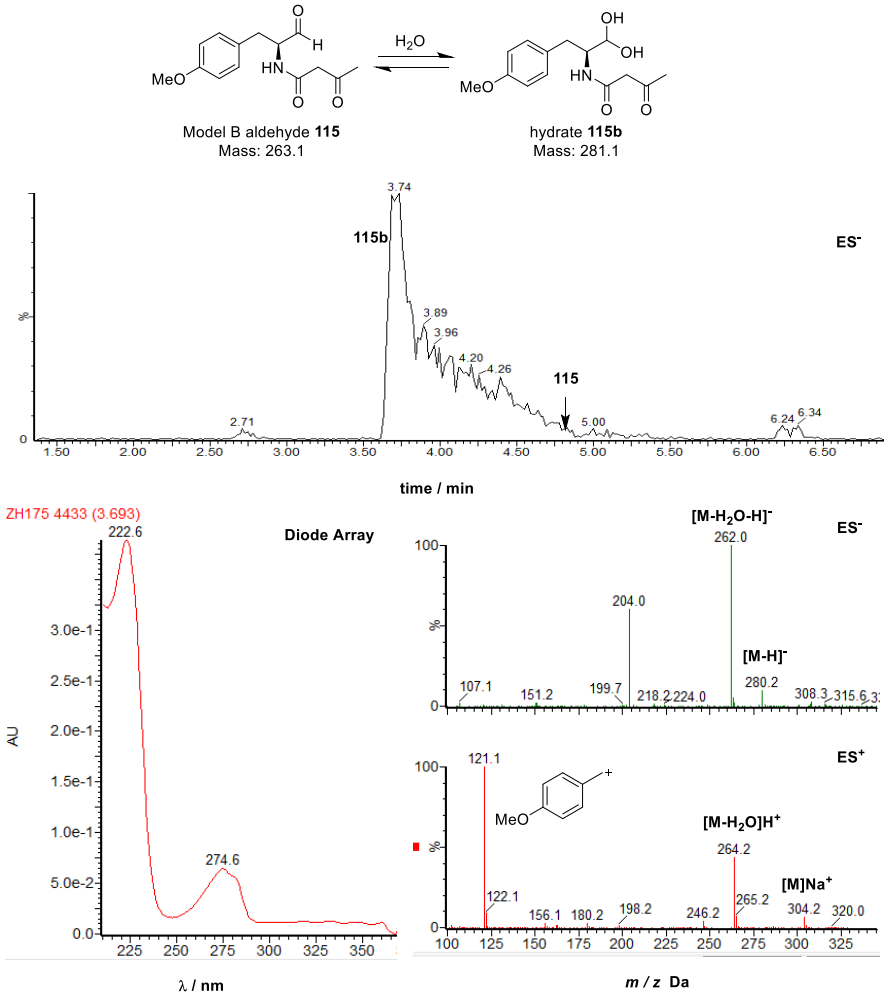

Figure 3.2 LCMS data of model B **115**.

The LCMS data of model B **115** after purification by preparative LCMS is shown in figure 3.2. It is tailing in the LCMS from 3.7 min to 4.8 min because aldehydes are in equilibrium with aldehyde hydrate in the presence of water. Hydrate **115b** elutes earlier at 3.7 min because it is much more polar. Aldehyde is minor in this equilibrium at 4.8 min. The UV spectrum clearly shows the aromatic ring absorbance at 223 nm and 274 nm. The mass spectra also fit the molecular weight (263.1).

^{1}H NMR data for model B **115** was not very clean, since after purification and lyophilisation model B **115** had already slightly degraded. But the characteristic chemical shifts can be found including the aldehyde proton (9.56 ppm), α-proton (4.47 ppm) as well as the diastereotopic benzylic protons (3.14 and 2.95 ppm, Figure 3.3).

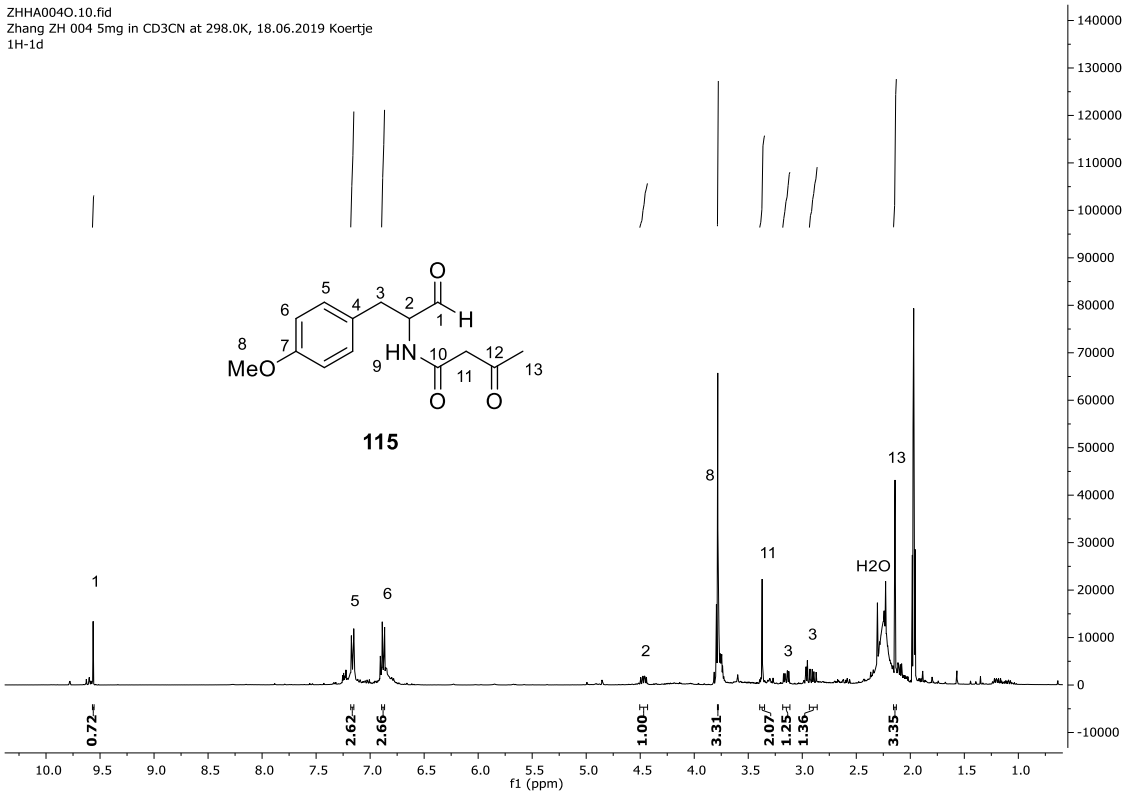

Figure 3.3 ^{1}H NMR of model B **115** in CD_3CN.

3.3.3 Tautomerism Investigations

3.3.3.1 Synthesis of Model B Pyrrolinone

Before we performed bioassays, we should firstly synthesize the pyrrolinone **204a** chemically to understand its properties. Model B **115** was treated with 1 M NaOH solution at 0 °C for 5 min, and extracted with EtOAc to afford pyrrolinone **204a**. By detection with LCMS, the clear conversion of model B **115** to the corresponding pyrrolinone can be observed (Figure 3.4). Different from model B **115**, the UV spectrum not only has the aromatic ring absorbance, but also has absorbance at 328 nm, which is the absorbance from the pyrrolinone ring. The molecular mass (245.1) also fit mass spectra with ES^+ and ES^-, as well as the aromatic carbon cation 121^+.

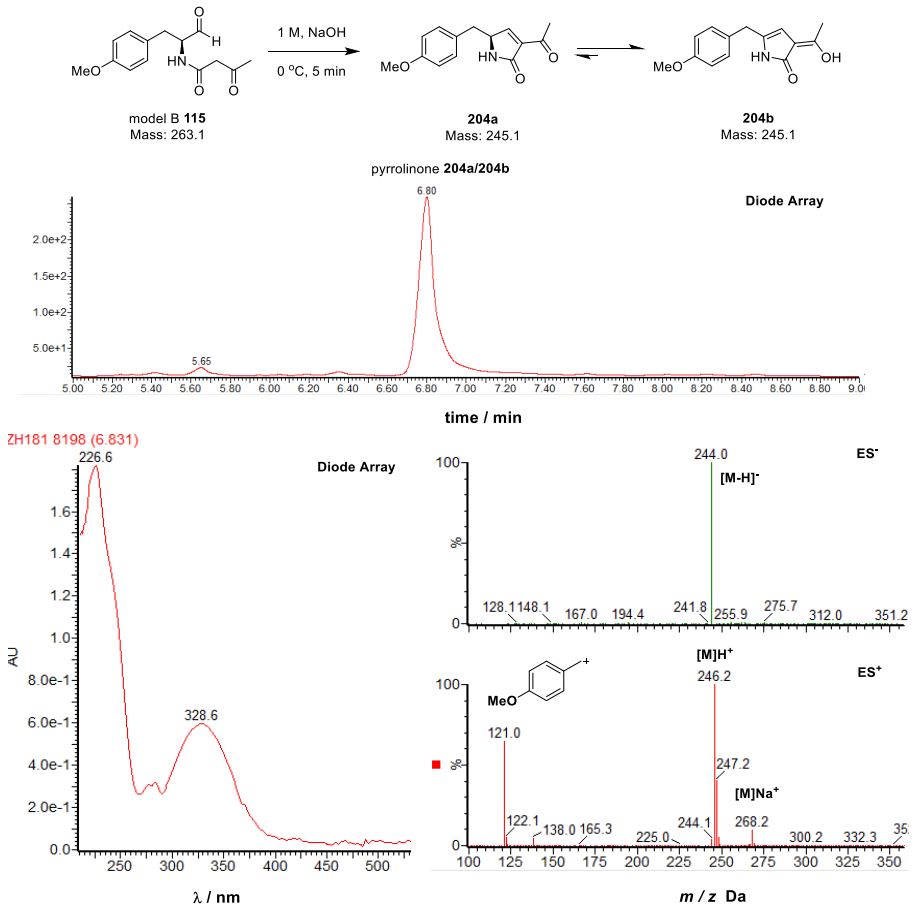

Figure 3.4 Conversion of model B **115** to pyrrolinone **204b** and its UV, mass spectra.

As mentioned in the cytochalasan total synthesis, pyrrolinone **204a** probably also undergoes a tautomerism to **204b**. To further confirm this, the pyrrolinone **204a** was

attempted to be characterized by NMR. However, *O*-methyl tyrosine pyrrolinone **204b** proved to be rather unstable and it was difficult to get good NMR data. Crude pyrrolinone **204b** from simple workup degrades even before the NMR measurement is finished. Purification by preparative LCMS following by evaporation at 35 °C afforded a different compound, rather than the *O*-methyl tyrosine pyrrolinone **204b** (Figure 3.5). The retention time of the new compound is around 4.4 min, which elutes earlier than pyrrolinone **204b** at 6.8 min, suggesting it is more polar. Moreover, UV absorbance beyond 300 nm disappeared, indicating the conversion occurred on the pyrrolinone ring. From the ES^+ and ES^-, we can deduce that water was added to the pyrrolinone ring.

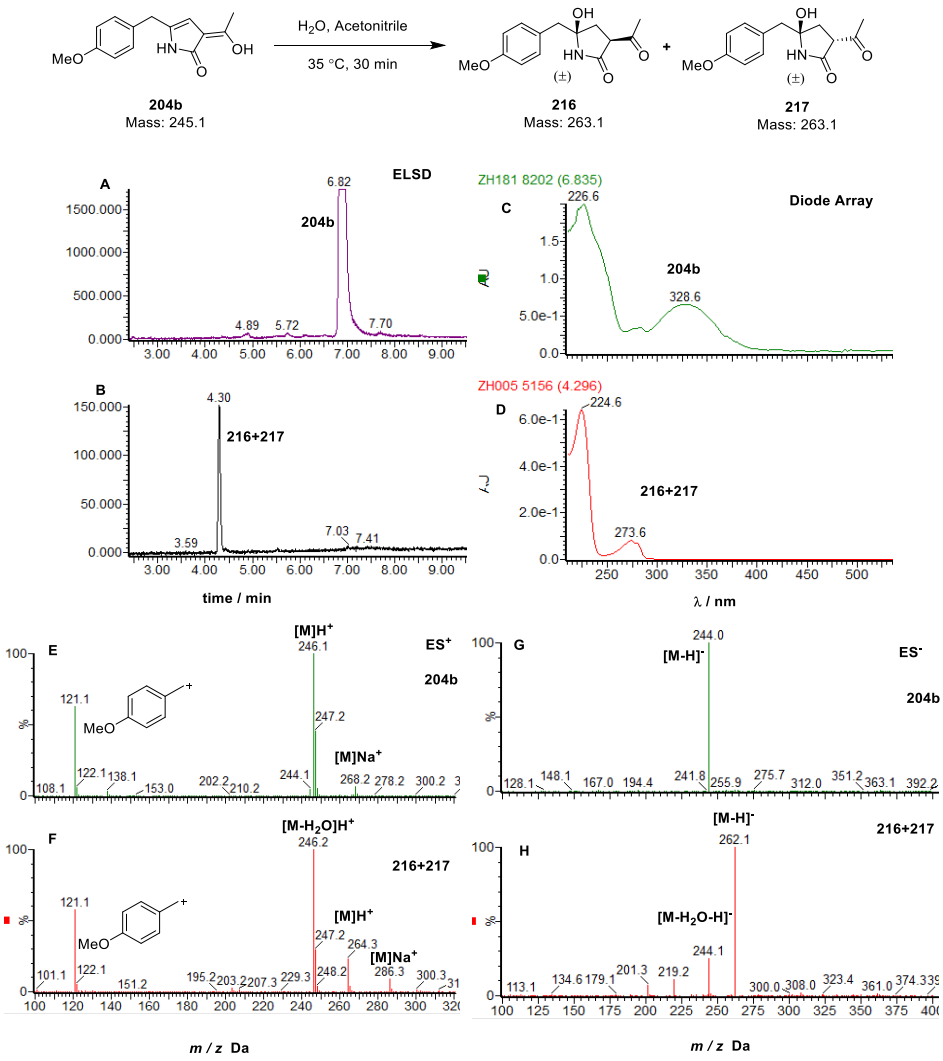

Figure 3.5 Retention time, UV, ES^+ and ES^- comparison of *O*-methyl tyrosine pyrrolinone **204b** and diastereomers **216/217** after purification. **A**, ELSD signal of pyrrolinone **204b**; **B**, ELSD signal of diasteromers after purification; **C**, UV absorption of pyrrolinone **204b**; **D**, UV absorption of diastereomers **216/217** after purifition; **E**, ES^+ of pyrrolinone **204b; F**, ES^+ of diastereomers **216/217** after purifition; **G**, ES^- of pyrrolinone **204b; F,** ES^- of diastereomers **216/217** after purifition.

Originally, we proposed that water was added to the pyrrolinone through Michael addition to form compound **219** (scheme 3.16). However, purification by preparative LCMS and characterization by NMR showed a different compound and a more complex reaction pathway.

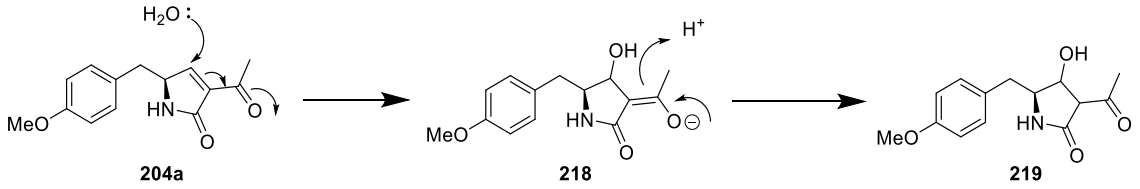

Scheme 3.16 Original proposal for the hydration of pyrrolionone **204a** through Michael addition.

The full NMR data of **216/217** is shown in figure 3.5. The ^{1}H NMR and ^{13}C NMR suggest it is a mixture of two diastereomers. The existance of more than two CH_2 groups in the HSQC spectrum ruled out the possibility of the original proposal that **219** is the compound.

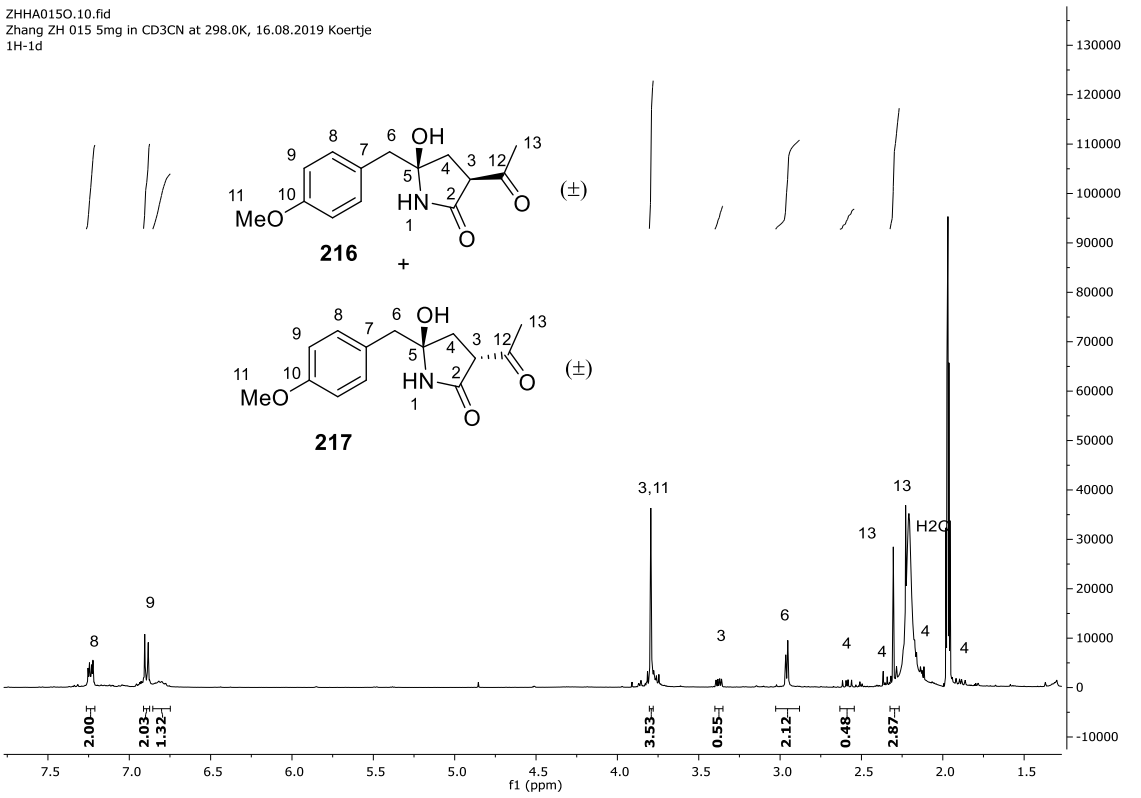

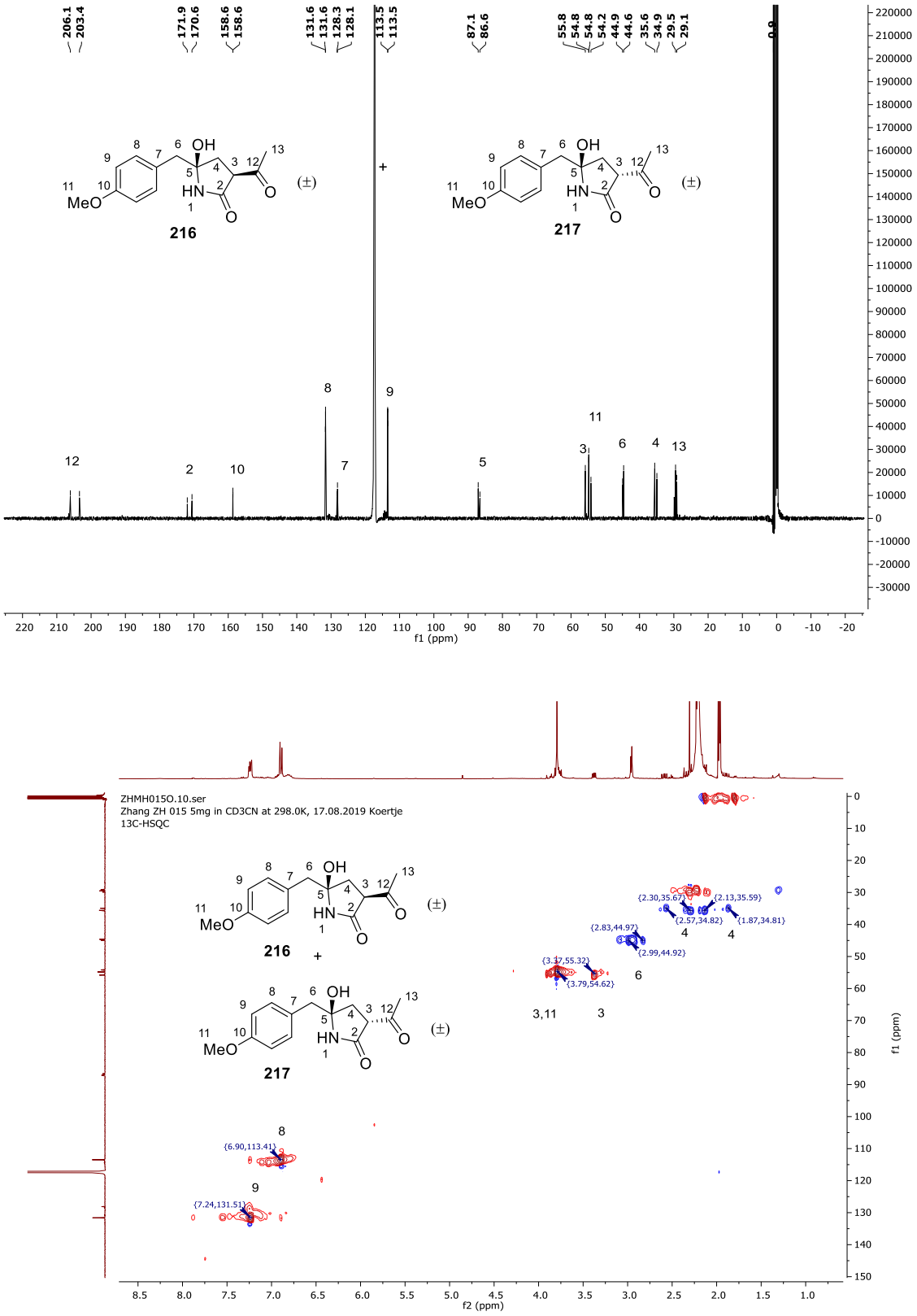

Figure 3.5 NMR data of diastereomers **216/217** in CD_3CN.

Table 3.1 NMR data of compounds **216/217**. Not all ^{1}H signals could be integrated due to overlap. Solvent: CD_3CN. (Two diastereomer assignments are based on nmrdb online H, C chemical shifts prediction).

Atom	δ_C (ppm)	δ_H (ppm)	Multiplicity (*J* / Hz)	COSY	HMBC	HSQC	Structure
2	170.6	--	--	--	--	--	
3	55.8	3.38	dd (4.5, 9.0)	4	2, 4, 12	CH	
4a	35.6	2.30	m	3	2, 3, 5, 6, 12	CH_2	
4b		2.12	m				
5	87.1	--	--	--	--	--	
6	44.9	2.94	m	--	4, 5, 7, 8	CH_2	
7	128.3	--	--	--	--	--	
8	131.6	7.24	d (8.6)	9	9, 10	CH	
9	113.5	6.90	d (8.6)	8	7, 10	CH	
10	158.6	--	--	--	--	--	
11	54.8	3.79	s	--	--	CH_3	
12	206.1	--	--	--	--	--	
13	29.5	2.30	s	--	3, 12	CH_3	

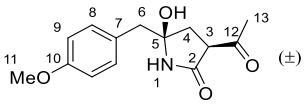

216
$C_{14}H_{17}NO_4$
MW: 263.1 g/mol

Atom	δ_C (ppm)	δ_H (ppm)	Multiplicity (*J* / Hz)	COSY	HMBC	HSQC	Structure
2	171.9	--	--	--	--	--	
3	54.2	3.77	m	4	2, 4, 12	CH	
4a	34.9	2.59	dd (8.6, 13.6)	3	2, 3, 5, 6, 12	CH_2	
4b		1.89	dd (8.6, 13.6)				
5	86.6	--	--	--	--	--	
6	44.6	2.96	m	--	4, 5, 7, 8	CH_2	
7	128.1	--	--	--	--	--	
8	131.6	7.24	d (8.6)	9	9, 10	CH	
9	113.5	6.90	d (8.6)	8	7, 10	CH	
10	158.6	--	--	--	--	--	
11	54.8	3.79	s	--	--	CH_3	
12	203.4	--	--	--	--	--	
13	29.1	2.23	s	--	3, 12	CH_3	

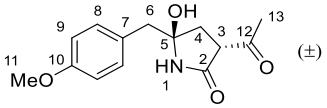

217
$C_{14}H_{17}NO_4$
MW: 263.1 g/mol

After analysis of full NMR, the new compounds were found to be a mixture of diastereomers **216**/**217**. The structures and possible mechanism of formation are shown in scheme 3.17.

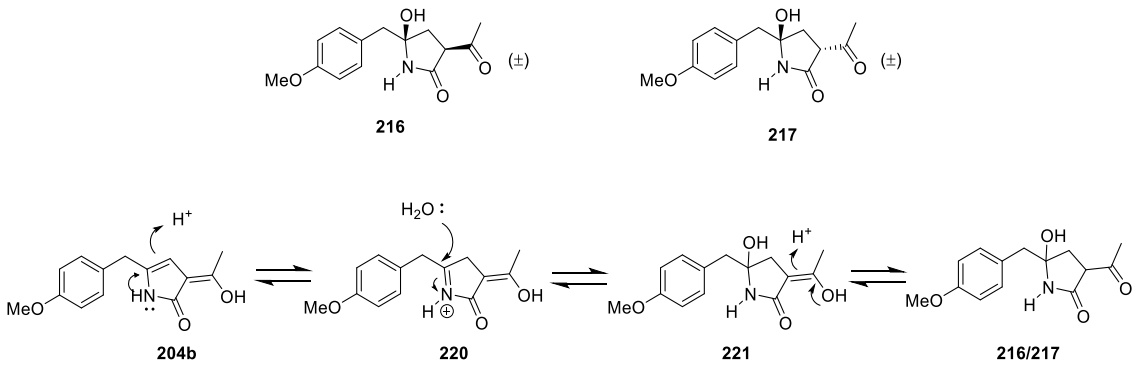

Scheme 3.17 Structures of new compounds and possible mechanism.

3.3.3.2 Synthesis of Phenylalanine Pyrrolinone

Since *O*-methyl tyrosine pyrrolinone **204b** is rather unstable to get NMR data, we decided to synthesize its analog phenylalanine pyrrolinone **222b** to investigate its properties. **222b** is reported to be relatively stable (scheme 3.18).[107] Theromolysis of dieketene acetone adduct **161** with commercially available phenylalanine derived amino alcohol **208** in toluene at 103 °C afforded **209**. Alcohol **209** was oxidized by Moffat oxidation to aldehyde **207**, following by cyclization with 1 M NaOH for 5 min. **222** was purified by prep-LCMS. ^{1}H NMR showed that it tautomerized to **222b**.

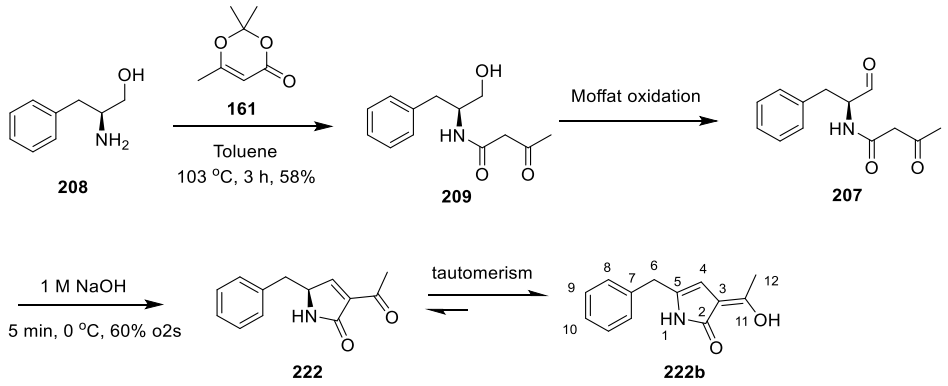

Scheme 3.18 Synthesis of known phenylalanine pyrrolinone **222b**.

The LCMS data of compound **222b** is shown in figure 3.6. From the UV we can see clearly the absorbance at 328 nm, arising from the unsaturated ring. This absorption was also observed for the *p*-methoxy analog **204b** (section 3.3.3.1). The ES^+ and ES^- also fit the molecular weight (215.1).

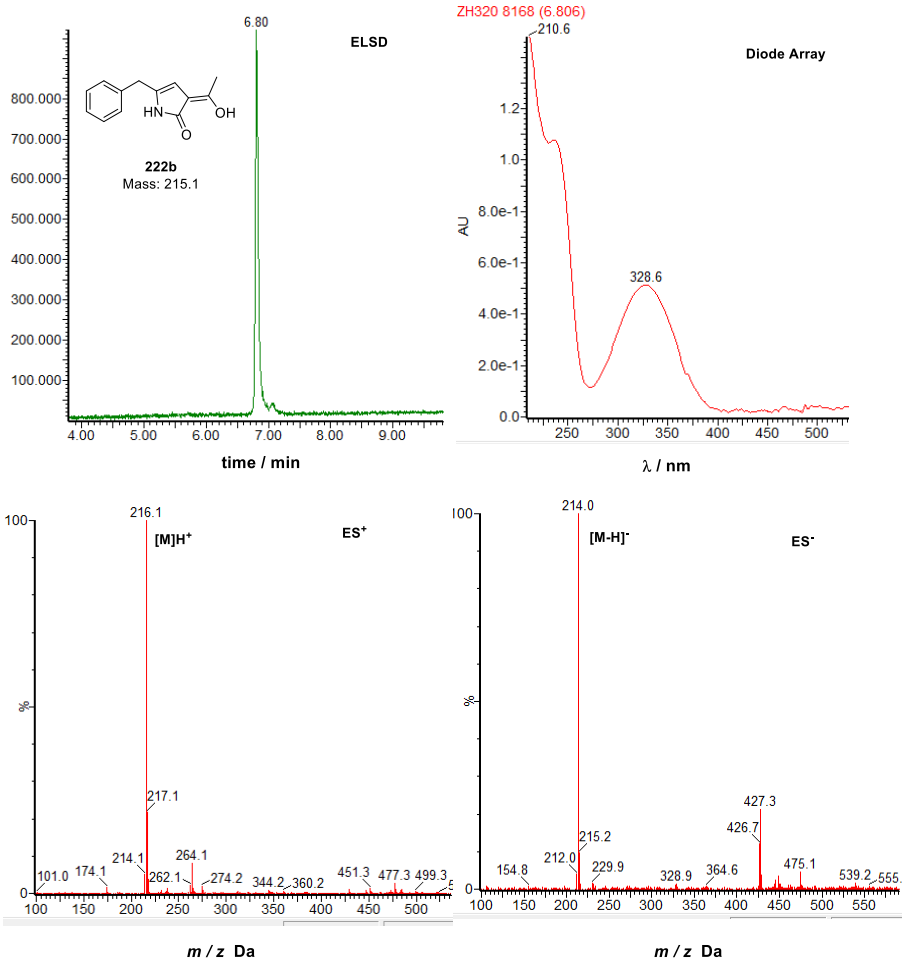

Figure 3.6 LCMS data of compound **222b**.

From the ^1H NMR (Figure 3.7), the chemical shift for proton 4 is a singlet at 5.56 ppm. This is consistent with the 6π aromatic structure of the ring, the downfield shift resulting from the aromatic ring current. The protons 6 now are no longer diastereotopic due to the loss of the stereocenter at the C-5. The optical rotations for compound **209** and **222b** were also measured. An optical rotation α of -20.6 was measured at 23 °C at 589 nm for compound **209**, while compound **222b** showed no rotation, consistent with the planar structure. The ^1H δ_H value for H-12 is consistent with C-11 being an enol rather than a ketone. Likewise the δ_C shift of C-11 at 172 ppm is also consistent with an enol rather than a ketone.

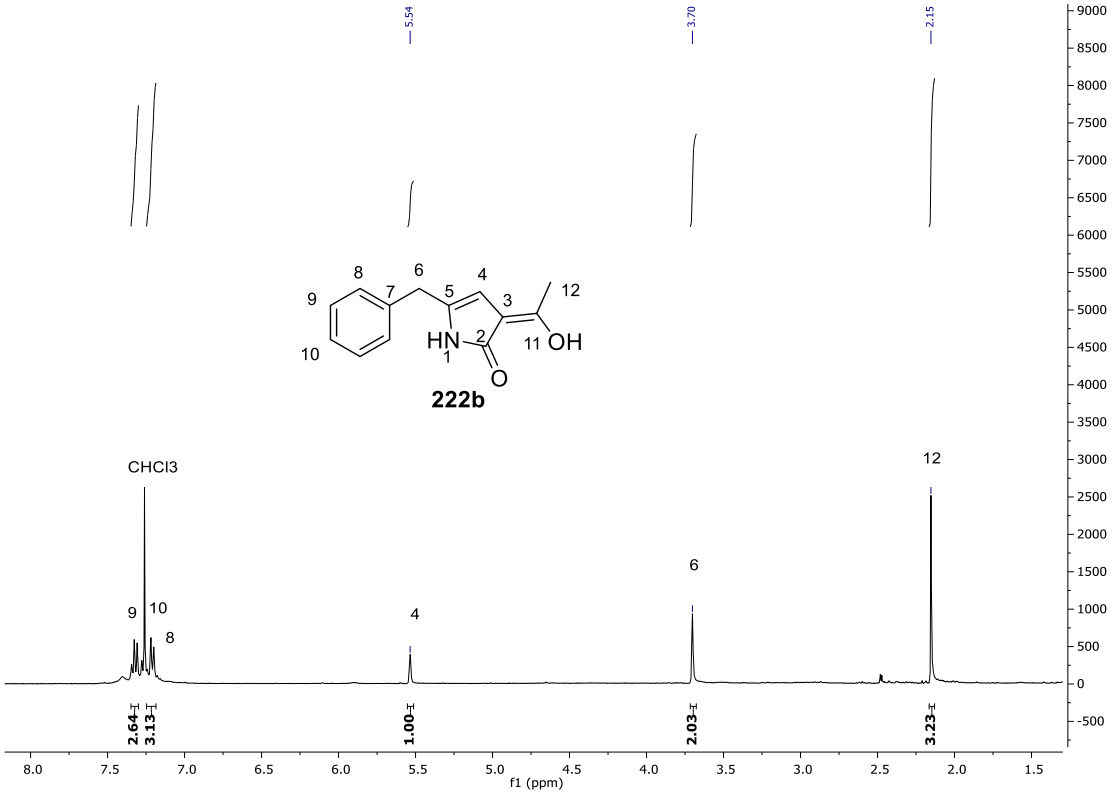

Figure 3.7 ^{1}H NMR of compound **222b** in $CDCl_3$.

Table 3.2 NMR data of compound **222b**. Solvent: $CDCl_3$.

Atom	δ_C (ppm)	δ_H (ppm)	Multiplicity (*J* / Hz)	COSY	HMBC	HSQC	Structure
2	170.5	--	--	--	--	--	
3	106.9	--	--	--	--	--	
4	98.9	5.54	s	6	2, 3, 5	CH	
5	131.7	--	--	--	--	--	
6	34.7	3.70	s	4, 8, 12	4, 5, 7, 8	CH_2	
7	136.8	--	--	--	--	--	
8	128.7	7.21	m	6, 9	6, 9, 10	CH	
9	128.8	7.33	m	8, 10	7, 8	CH	
10	127.0	7.28	m	9	8	CH	
11	172.3	--	--	--	--	--	
12	19.3	2.15	s	6	3, 11	CH_3	

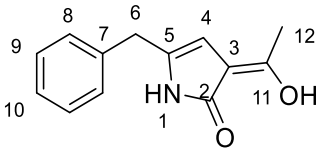

222b

MW: 215.1 g/mol

3.3.3.3 Retrosynthesis and Synthesis of α-methyl Pyrrolinone

Even though the pyrrolinone tautomerism was well studied from NMR, IR and theoretic calculations,[106,108] we still wanted to make a further investigation about tautomerism in a more straightforward way because it is of key importance for the following DA reaction. So we propose to block the tautomerism by introducing a methyl group at the alpha position to make a comparison between tautomerized pyrrolinone and non-tautomerized pyrrolinone.

The synthesis of α-methyl pyrrolinone **231** could mimic the model B **115** synthesis *via* dioxinone **161** theromolysis with amino alcohol **228** and oxidation of alcohol **226** following with cyclization. The synthesis of the key intermediate **228** was described by Heinrich *et al*[109] through a radical carbodiazenylation derived from *p*-anisidine **224** (Scheme 3.19).

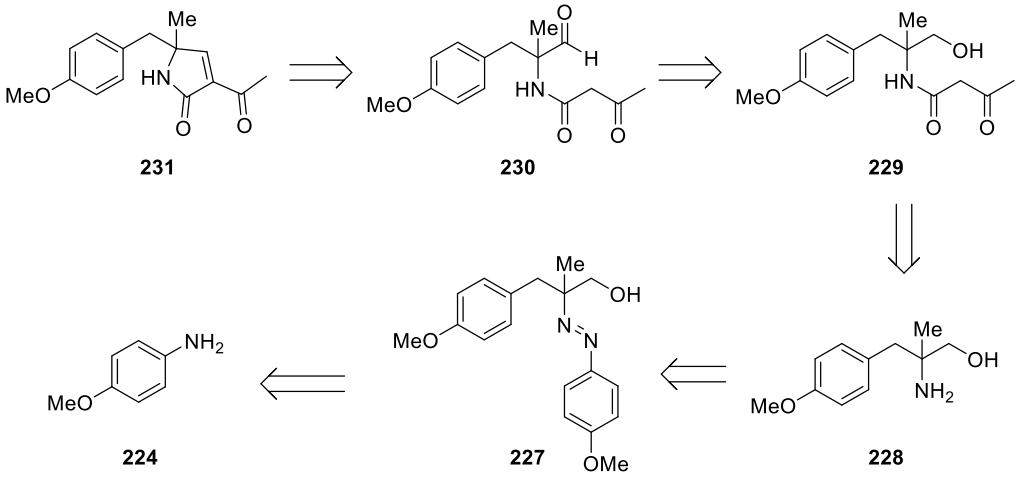

Scheme 3.19 Retrosynthetic analysis of α-methyl pyrrolinone **231**.

The synthesis of the α-methyl pyrrolinone started with the diazotization, by treatment of *p*-anisidine **224** with sodium nitrite and excess HBF_4 below 5 °C (scheme 3.20). The subsequent carbodiazenylation reaction was carried out at room temperature in a previously degassed mixture of DMSO and H_2O under an inert atmosphere, between diazonium salt **225** and methallyl alcohol **226** with iron(II)sulfate heptahydrate as reductant to afford compound **227** as a yellow oil.[109] After reduction of the diazo group with Zn/HCl, α-methyl amino alcohol **228** was obtained in high yield and reacted with dioxinone **161** at 103 °C for 2 h in toluene to afford compound **229**, which was

then oxidized by Moffat oxidation overnight to aldehyde **230**. Treatment of aldehyde **230** with 1 M NaOH solution at 0 °C for 5 min afforded α-methylated pyrrolinone **231**.

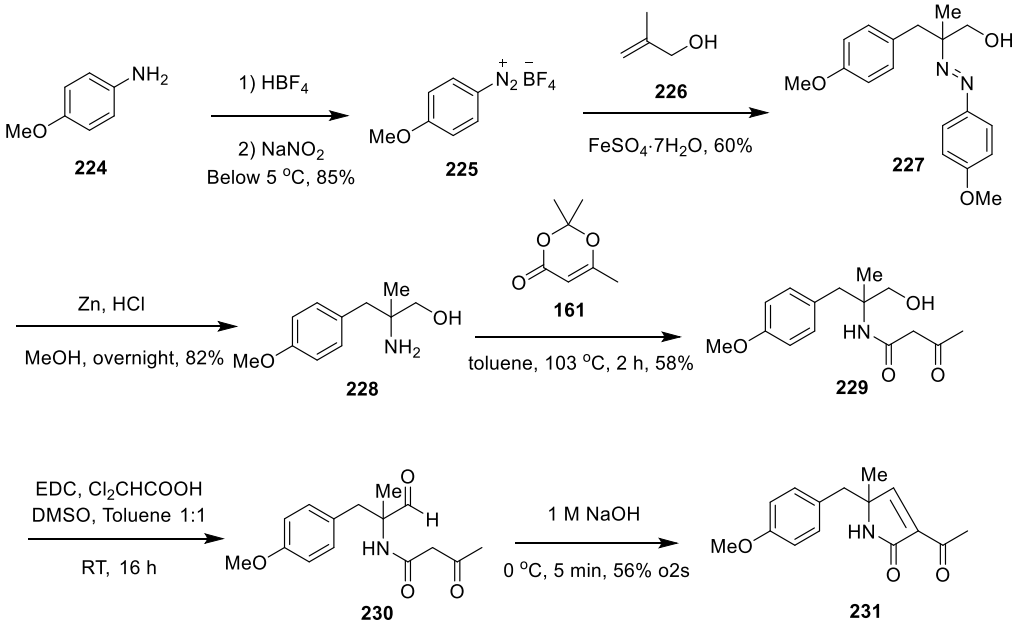

Scheme 3.20 Synthesis of α-methyl pyrrolinone **231**.

In contrast to the non-methylated pyrrolinones **204b** and **222b**, α-methyl pyrrolinone **231** has no UV absorbance beyond 300 nm, consistent with formation of a different tautomer as compared to the non-methylated pyrrolinones (Figure 3.8). The molecular weight (259.1) is also found in the ES^+ plus proton and sodium as well as the aromatic carbon cation (121.0). However, in contrast to pyrrolinone **222b** with a hydroxyl group which can form an anion, α-methyl pyrrolinone **231** cannot form anion well and only fragmentions are observed in the ES^- mass spectra.

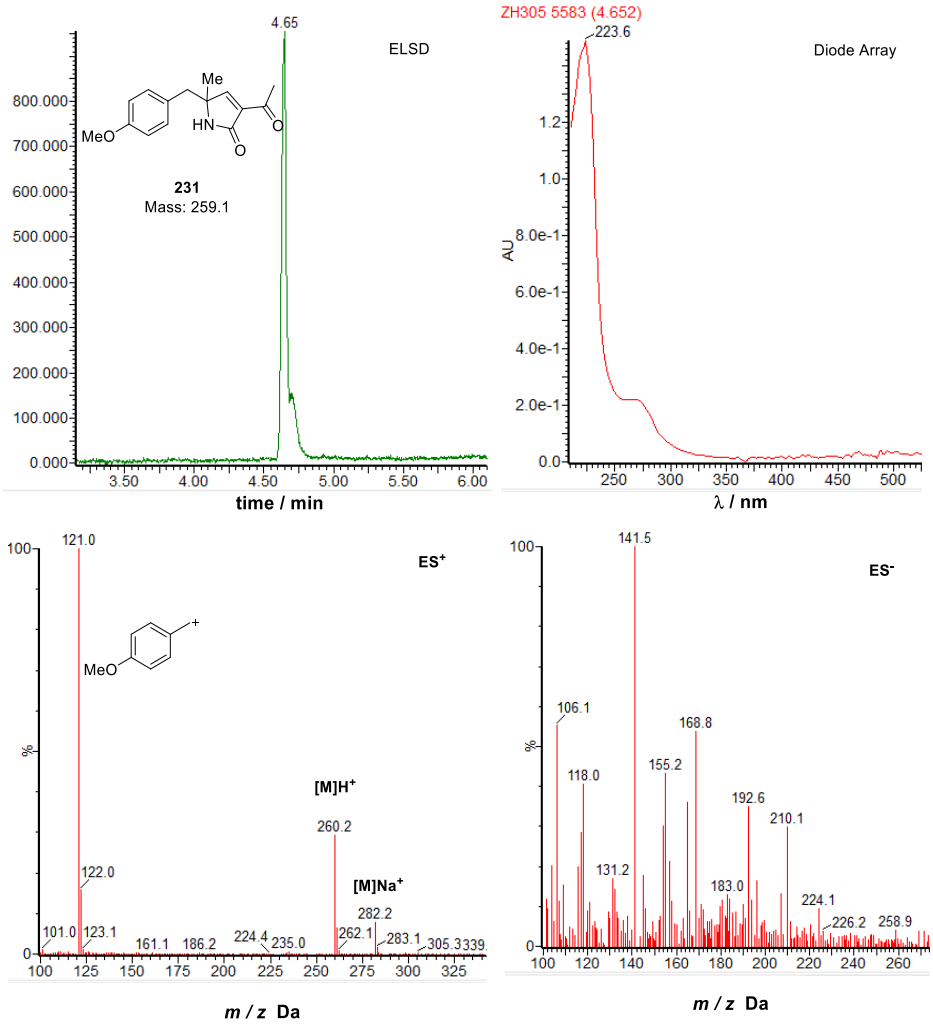

Figure 3.8 LCMS data of α-methyl pyrrolinone **231**.

From the ^{1}H NMR (Figure 3.9), benzylic proton 6 shows two doublets at 2.84 ppm, because the two protons are diastereotopic and split each other. The chemical shift for proton 4 is at 7.72 ppm because it is deshielded by eletron withdrawing groups. This compares to 5.7 ppm in compound **222b** which has a more aromatic character. Proton 13 resonates at 2.51 ppm, consistent with an acetyl group rather than the 1-hydroxy ethylidene observed in **222b** (2.2 ppm). Finally the δ_C value of 194 ppm for C-12 is consistent with it being a ketone.

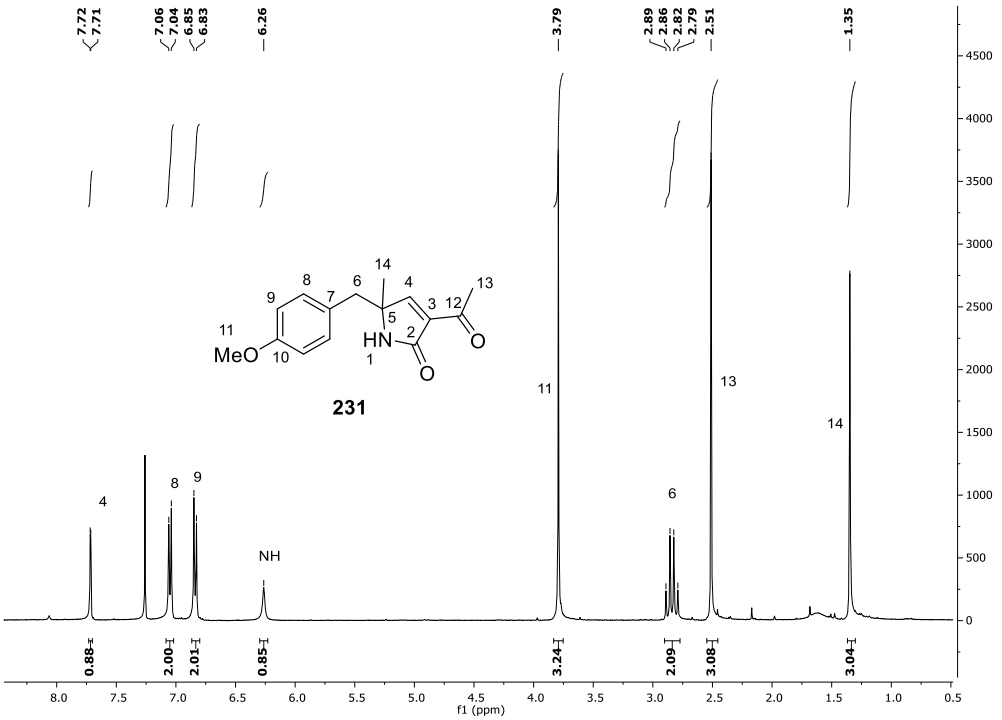

Figure 3.9 ^{1}H NMR of α-methyl pyrrolinone **231** in $CDCl_3$.

Table 3.3 NMR data of α-methyl pyrrolinone **231**. Solvent: $CDCl_3$.

Atom	δ_C (ppm)	δ_H (ppm)	Multiplicity (*J* / Hz)	COSY	HMBC	HSQC	Structure
1	--	6.26	s	4	--	--	
2	168.6	--	--	--	--	--	
3	135.2	--	--	--	--	--	
4	160.6	7.72	d (2.1)	1	2, 5, 12	CH	
5	61.7	--	--	--	--	--	
6a	44.1	2.87	d (^2J 13.6)	6b	4, 5, 7, 8, 14	CH_2	
6b		2.81	d (^2J 13.6)	6a			
7	126.9	--	--	--	--	--	
8	131.1	7.05	d (8.6)	9	6, 9, 10	CH	**231** MW: 259.1 g/mol
9	114.0	6.84	d (8.6)	8	7, 10	CH	
10	158.9	--	--	--	--	--	
11	55.3	3.79	s	--	10	CH_3	
12	194.3	--	--	--	--	--	
13	29.2	2.51	s	--	3, 12	CH_3	
14	23.0	1.35	s	--	4, 5, 6	CH_3	

From table 3.4, we can make a clear comparison about NMR chemical shifts between the tautomerised pyrrolinone **222b** and non-tautomerised pyrrolinone **231**. Tautomerism strongly influenced the carbon chemical shifts on the pyrrolinone rings as well as the proton chemical shift beyond the ring.

Table 3.4 NMR data comparison of phenylalanine pyrrolinone **222b** and α-methyl pyrrolinone **231**.

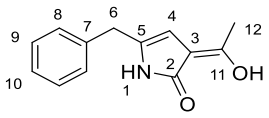 **222b**				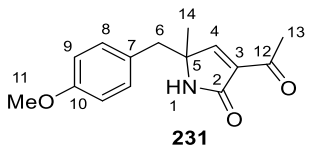 **231**			
Atom	δ_H / ppm	*J* / Hz	δ_C / ppm	Atom	δ_H / ppm	*J* / Hz	δ_C / ppm
2	--	--	170.5	2	--	--	168.6
3	--	--	106.9	3	--	--	135.2
4	5.54	--	98.9	4	7.72, d	2.1	160.6
5	--	--	136.8	5	--	--	61.7
6	3.70, s	--	34.7	6a	2.87, d	13.6	44.1
				6b	2.81, d	13.6	44.1
11	--	--	172.3	12	--	--	194.3
12	2.15	--	19.3	13	2.51, s	--	29.2

In compound **231**, H-4 is a normal alkene proton conjugated with eletron-withdrawing carbonyl group and amide group. Therefore the chemical shift is in lower field because of the lower electron density. C-12 is a normal carbonyl group with chemical shift at 194.3 ppm. H-6 are diastereotopic and hence two doublets are observed. However, in compound **222b**, H-4 is in an aromatic environment and shielded by the aromatic ring current, *i.e.* lone pair donation from nitrogen atom. Therefore the chemical shift of H-4 is in higher field. H-6 are no longer diastereotopic because of tautomerism and a singlet is observed, consistent with the planar structure. The carbon and proton chemical shifts at 12 shifted to high field significantly, suggesting the tautomerism occurred on the carbonyl group rather than on the amide to form an aromatic ring. This can be further confirmed by the fact that C-11 chemical shift goes to

higher field while C-2 chemical shift does not change so much. All these facts discussed above confirm the tautomerism occurs on the carbonyl rather than the amide group.

3.3.4 Model B Bioassays

3.3.4.1 Preparation of Proteins and Cell Free Extract

The ORFZ and ORF3 proteins were prepared and partially purified from *E. coli* expression by Verena Hantke. In addition, cell free extract was prepared from *A. oryzae* NSAR1 cells expressing the *ACE1*, *RAP1* and *ORFZ* genes from the *ACE1* gene cluster. The cells were frozen in liquid nitrogen in mortar and ground to an even powder. Then 2 mL potassium phosphate buffer (pH 7.0, 50 mM) was added and mixed with the cell powder. After collection by centrifugation at 16000 × g for 30 min at 4 °C, the supernatant was collected and stored for further tests.

3.3.4.2 Model B Assays in Water

Since model B **115** is not very stable, and there is a possibility that model B **115** can form the corresponding pyrrolinone **204b** spontaneously, it was first tested in water or buffers before enzyme assays to investigate the effects of the solvents.

Model B **115** was synthesized *via* oxidation of alcohol **210** or hydrolysis of diethyl acetal **213** and purified by prep-LCMS. After collection of model B **115** fractions, all the acetonitrile and most of the water were evaporated under reduced pressure to give a solution of model B **115** in water. The concentration was measured to be around 2 mM.

Model B **115** solution (50 µl) was further diluted with 150 µl distilled water and was incubated in a water bath at 28 °C over 1 h, 3 h and 17 h. After this time any reaction was observed by direct LCMS analysis of the aqueous solution. Figure 3.10 shows the results of model B **115** in H_2O at 28 °C over time. It is relatively stable in water after 3 h and only tiny amount of diastereotopic alcohols (**216/217** at 4.4 min) were formed after 17 h. The UV and mass spectra of the compound at 4.4 min is consistent with alcohols **216/217** (Figure 3.11). The peak at 4.0 min is the unoxidised alcohol **210** which is always present as a minor component of the aldehyde.

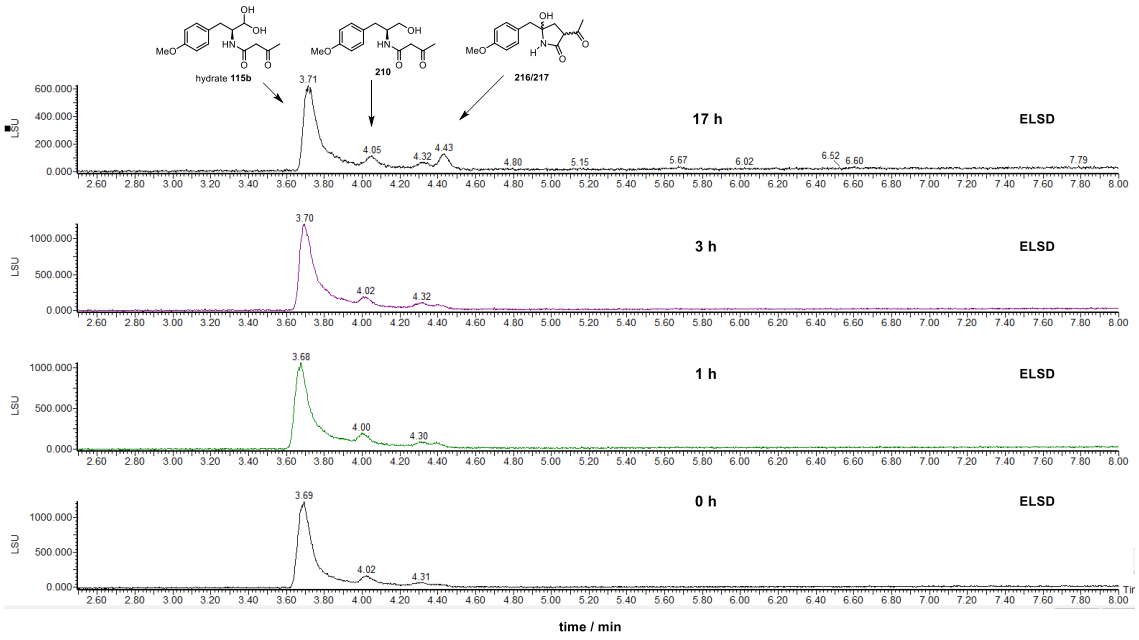

Figure 3.10 Model B **115** in H_2O at 28 °C over time.

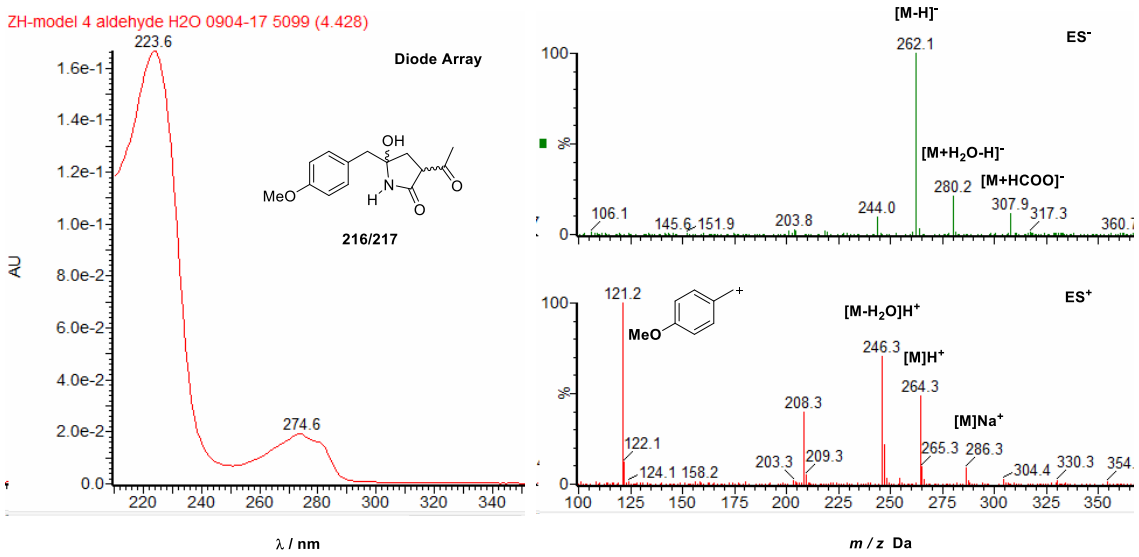

Figure 3.11 UV and Mass spectra of compound **216/217** at 4.4 min.

3.3.4.3 Model B Pyrrolinone Assays in Buffers

Since the pyrrolinone **204b** is not stable, it is necessary to understand its properties in buffers before further model B **115** assays. Therefore it was prepared and tested in phosphate buffer. The crude pyrrolinone **204b** was used directly for tests after workup

because of its instability. Pyrrolinone **204b** in potassium phosphate buffer (75 mM, pH 6.0, 7.0, 8.0) was incubated at 28 °C over time.

The results showed that after 2 hours, pyrrolinone **204b** was completely converted to a new peak at 5.7 min (Figure 3.12). The UV absorption at 273 nm and 224 nm indicates it contains tyrosine moiety, but the loss of the absorpotion around 328 nm means the the conversion occurred on the pyrrolinone ring. From mass spectral analysis, it is deduced to be a dimer **232** (Figure 3.13). The HRMS confirmed this since its calculated molecular fomular is $C_{28}H_{30}N_2O_8$.

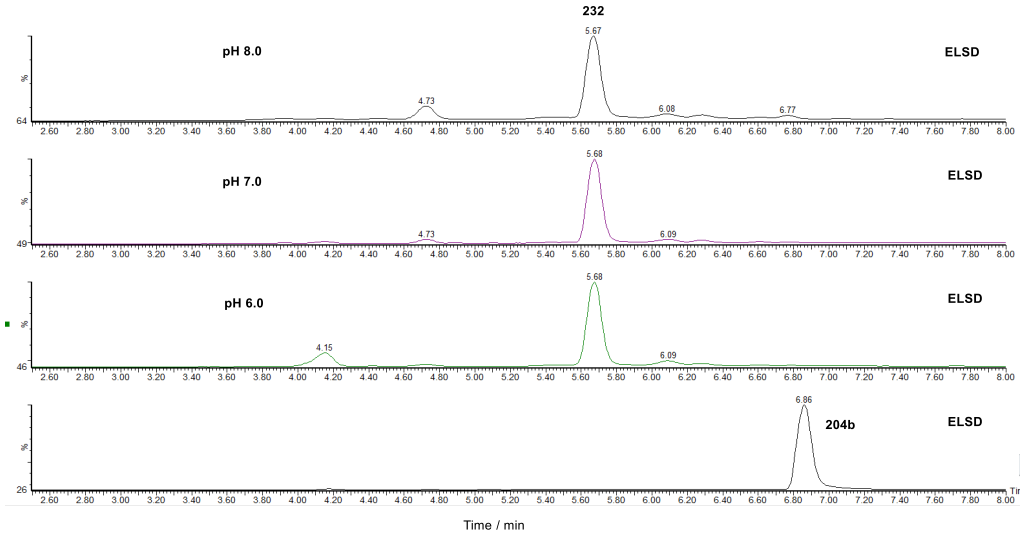

Figure 3.12 Pyrrolinone **204b** in potassium phosphate buffer (75 mM, pH 6.0, 7.0, 8.0) at 28 °C after 2 h.

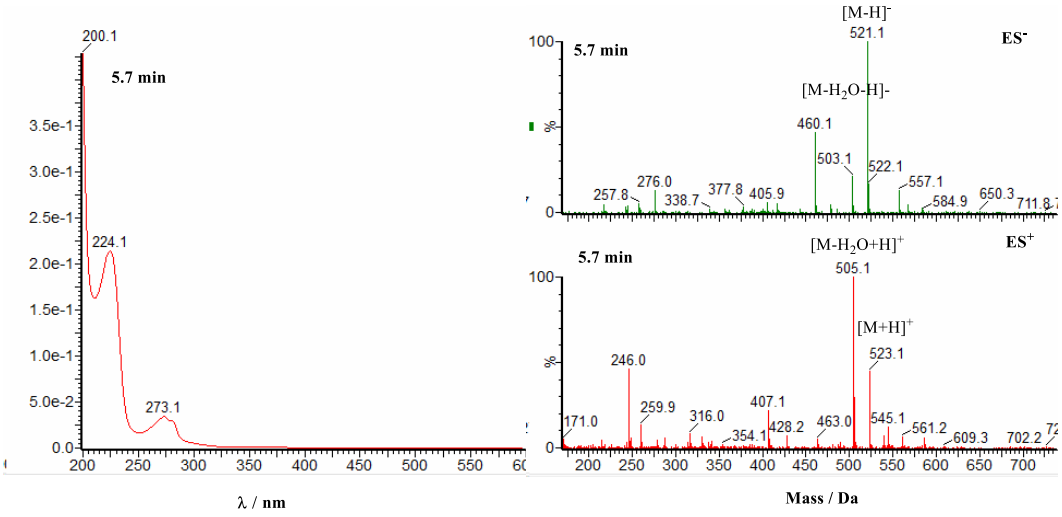

Figure 3.13 UV absorption and mass spectra of dimer **232** at 5.7 min.

Next, the new compound was prepared in large scale and purified by prep-LCMS. It was stable enough to get NMR data. From the ^{1}H NMR and ^{13}C NMR spectra, it is obvious this new compound is a dimer. Further analysis with 2D NMR shows its structure in table 3.5.

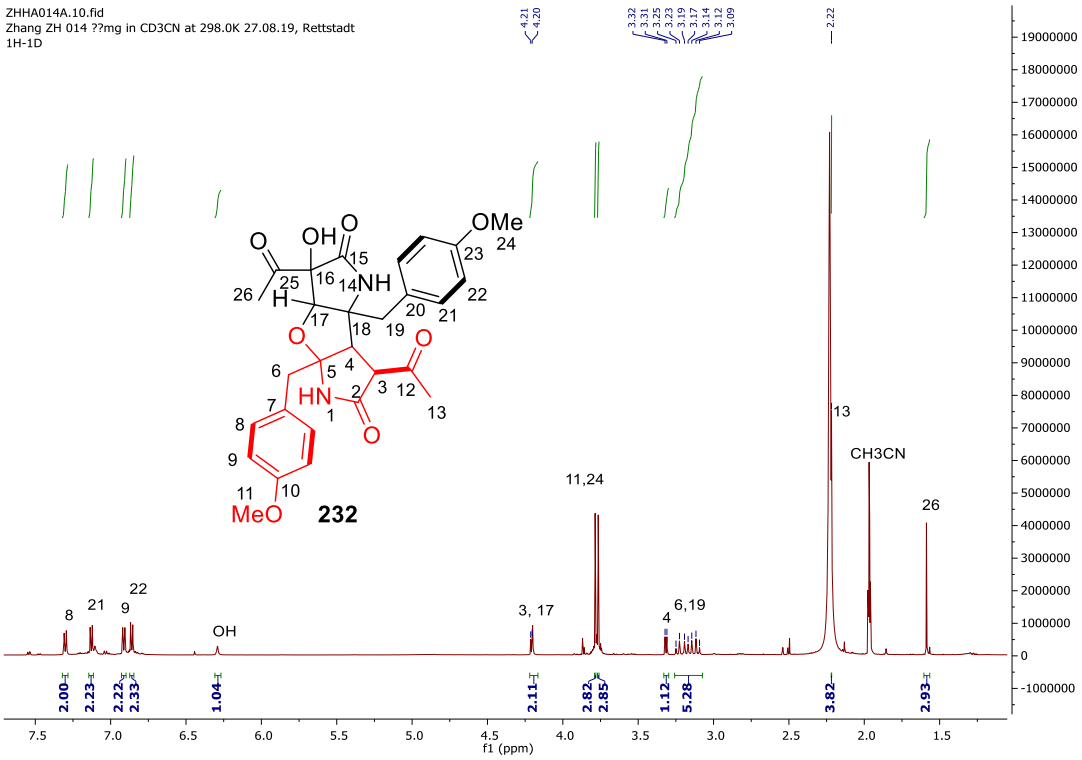

Figure 3.14 ^{1}H NMR of dimer **232** in CD_3CN.

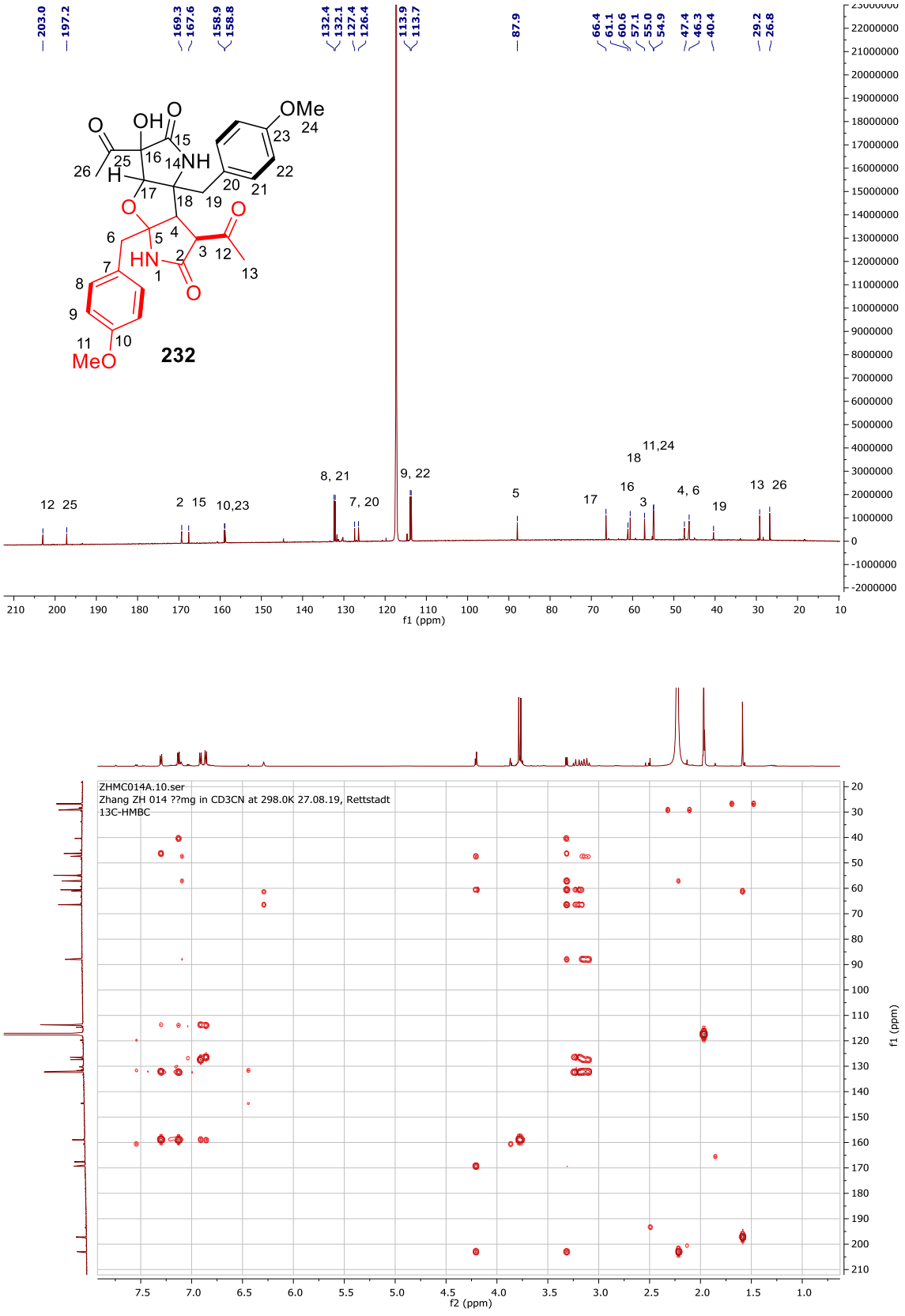

Figure 3.15 ^{13}C NMR and HMBC of dimer **232** in CD_3CN.

The mechanism of the dimer **232** formation is not very clear. It seems like model B **115** firstly forms pyrrolinone spontaneously, and then is converted to alcohols **216/217**. Alcohols **216/217** can react with pyrrolinone **204b** followed with oxidation to form the dimer **232**.

Table 3.5 NMR data of dimer **232** in CD_3CN.

Atom	δ_C (ppm)	δ_H (ppm)	Multiplicity (*J* / Hz)	COSY	HMBC	HSQC	Structure
2	169.3	--	--	--	--	--	
3	57.1	4.20	overlap	4	2, 4, 12	CH	
4	47.4	3.31	d (7.4)	3	2, 3, 5, 6, 12, 17, 18, 19,	CH	
5	87.9	-	--	--	--	--	
6	46.3	3.21	m	--	4, 5, 7, 8	CH_2	
7	127.4	--	--	--	--	--	
8	132.4	7.30	d (8.6)	9	6, 9, 10	CH	
9	113.9	6.91	d (8.6)	8	7, 10	CH	
10	158.9	--	--	--	--	--	
11	55.0	3.79	s	--	10	CH_3	
12	203.0	--	--	--	--	--	
13	29.2	2.22	s	--	3, 12	CH_3	
15	167.6	--	--	--	--	--	
16	61.1	--	--	--	--	--	
17	66.4	4.20	overlap	--	18	CH	
18	60.6	--	--	--	--	--	
19	40.4	3.13	m	--	17, 18, 20, 21	CH_2	
20	126.4	--	--	--	--	--	
21	132.1	7.13	d (8.6)	22	19, 22, 23	CH	
22	113.7	6.86	d (8.6)	21	20, 23	CH	
23	158.8	--	--	--	--	--	
24	54.9	3.76	s	--	23	CH_3	
25	197.2	--	--	--	--	--	
26	26.8	1.59	s	--	16, 25	CH_3	

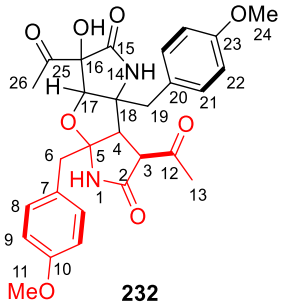

232

Chemical Formula: $C_{28}H_{30}N_2O_8$
Exact Mass: 522.2002

3.3.4.4 Model B Assays in Buffers without N_2 Protection

As model B **115** is an aldehyde, any buffer containing amino group, such as Tris, should be avoided. Therefore, potassium phosphate buffer is the first buffer to be considered. Model B **115** in 150 µl potassium phosphate buffer (pH 6.0, 7.0, 8.0, 75 mM) was incubated at 28 °C over 1 h, 4 h and 23 h without nitrogen protection.

At pH 6.0, model B **115** was relatively stable at 28 °C after 4 hours (Fig. 3.16). However, after 23 hours, some diastereotopic alcohols **216/217** formed and tiny amount of dimer **232** could be also observed.

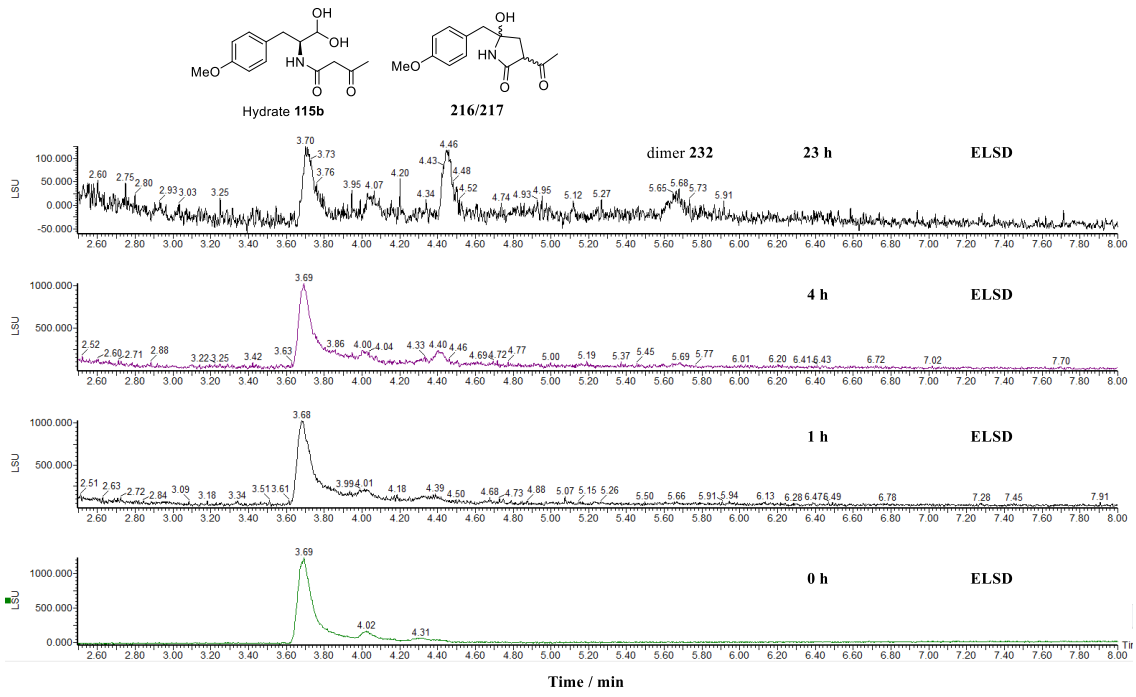

Figure 3.16 Model B **115** in potassium phosphate buffer (pH 6.0, 75 mM) at 28 °C without protection over time.

At pH 7.0, model B **115** in potassium phosphate buffer (75 mM) at 28 °C could form alcohols **216/217** in large amount after 4 hours (Fig. 3.17). After 23 hours, model B **115** disappeared and alcohols **216/217** and dimer **232** formed in a nearly equal amount.

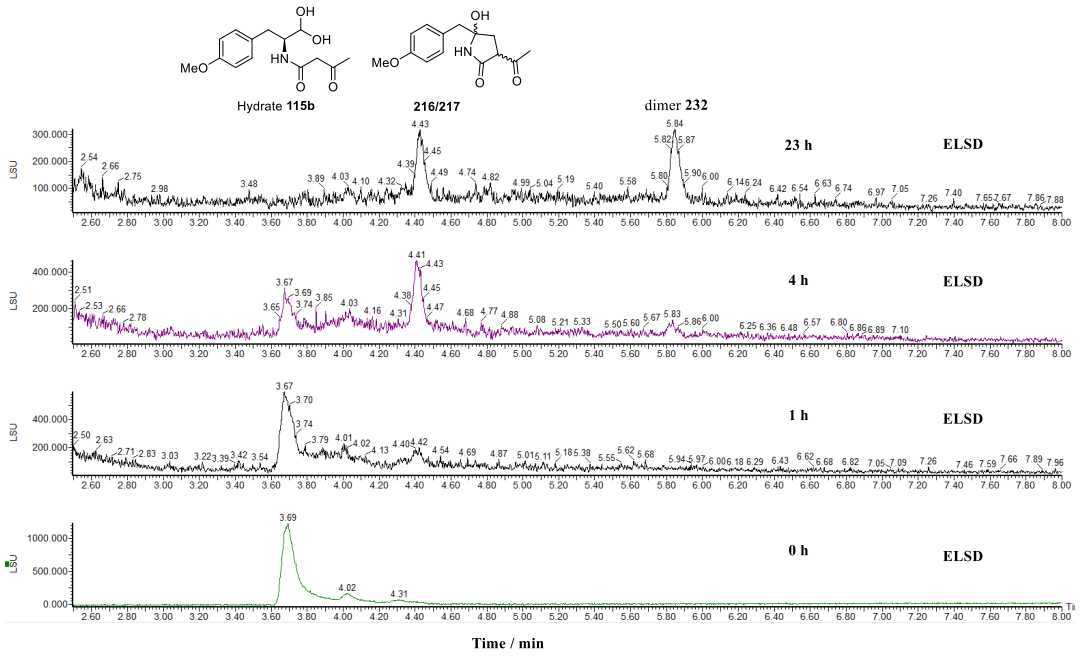

Figure 3.17 Model B **115** in potassium phosphate buffer (pH 7.0, 75 mM) at 28 °C without protection over time.

At pH 8.0, model B **115** in potassium phosphate buffer (75 mM) at 28 °C was stable in 1 hour. After 4 hours, model B **115** disappeared and only tiny amount of alcohols **216/217** left, while dimer **232** formed in large amount (Fig. 3.18). After 23 hours, only dimer **232** was detectable.

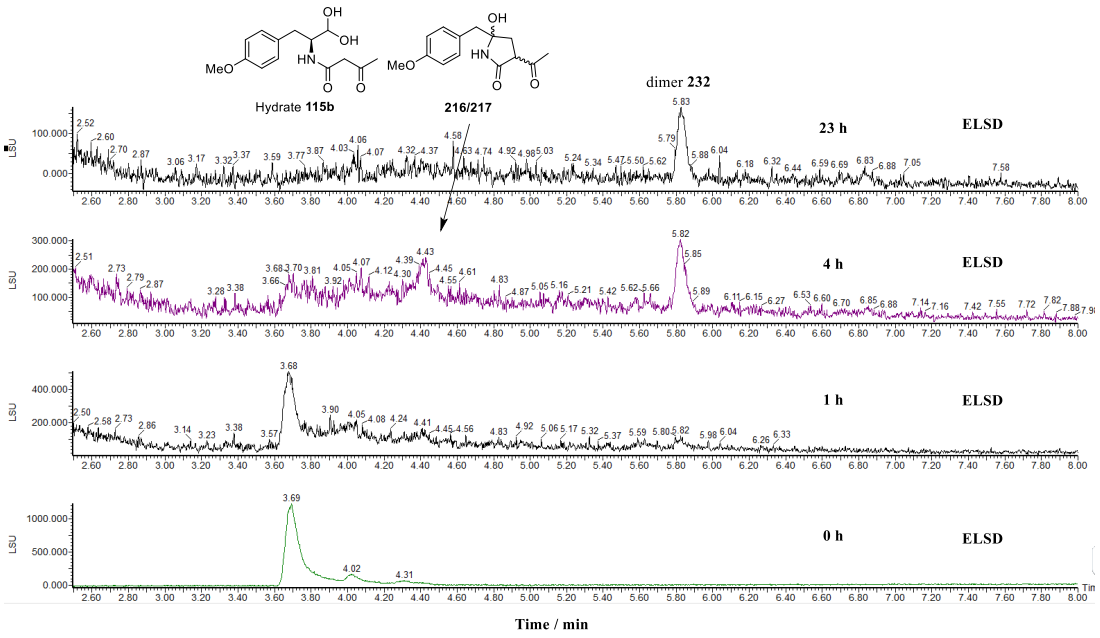

Figure 3.18 Model B **115** in potassium phosphate buffer (pH 8.0, 75 mM) at 28 °C without protection over time.

3.3.4.5 Model B Assays in Buffers with N_2 Protection

The formation of the dimer **232** is an oxidation, so it is better to perform assays under an inert atmosphere. Therefore model B **115** in potassium phosphate buffer (pH 6.5, 7.0, 7.5, 8.0, 37.5 mM) were incubated in water bath at 28 °C over 2 h, 6 h and 23 h under nitrogen protection.

At pH 6.5, model B **115** was relatively stable after 6 h at 28 °C (Figure 3.19). But after 23 h, some alcohols **216/217** were formed. The formation of **216/217** appeared faster in phosphate buffer (pH 6.5, 37.5 mM) than that in water.

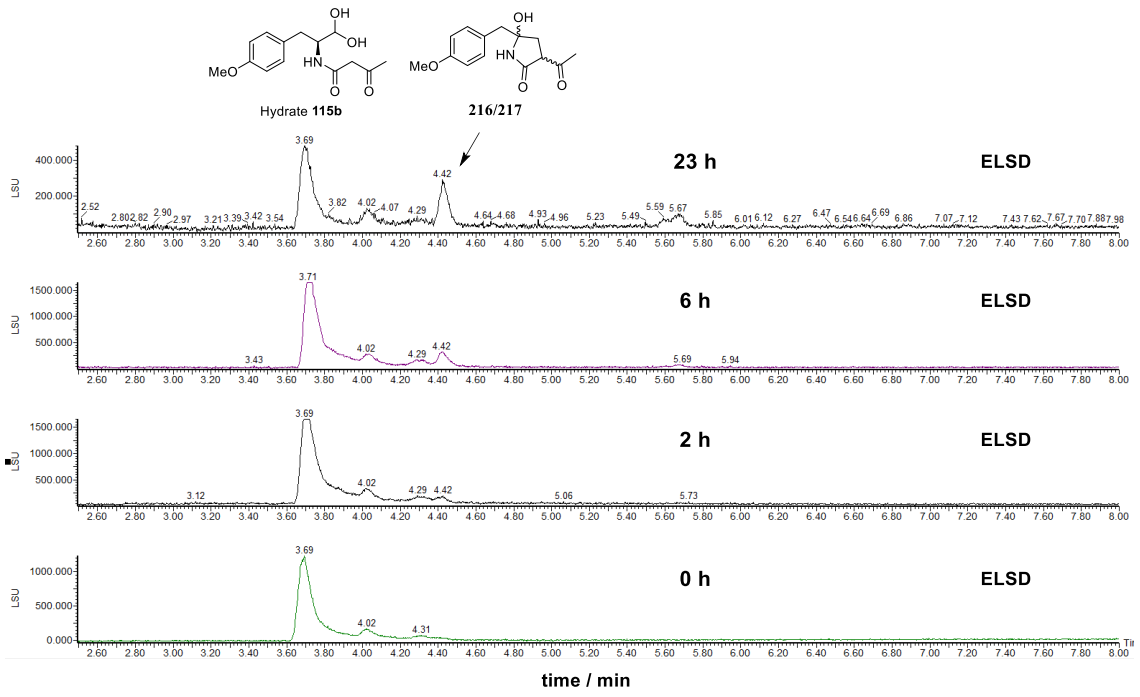

Figure 3.19 Model B **115** in potassium phosphate buffer (pH 6.5, 37.5 mM) at 28 °C.

When the buffer pH was raised to 7.0, model B **115** was observed to be less stable. After 23 h at 28 °C, large amount of alcohols **216/217** were formed (Figure 3.20).

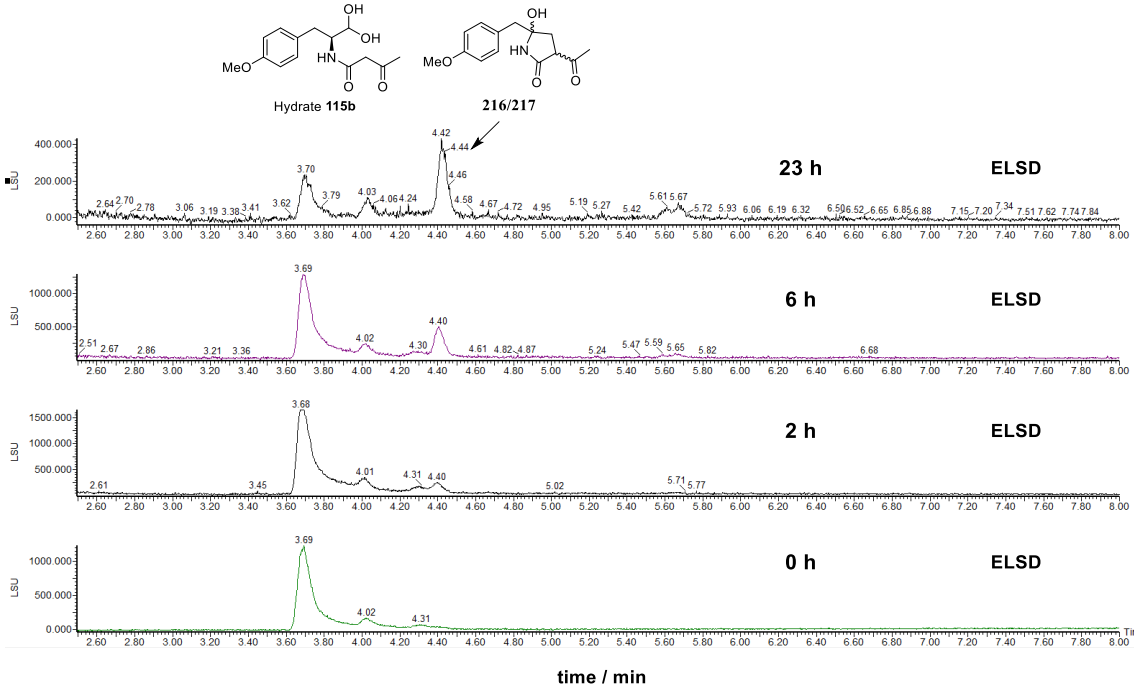

Figure 3.20 Model B **115** in potassium phosphate buffer (pH 7.0, 37.5 mM) at 28 °C.

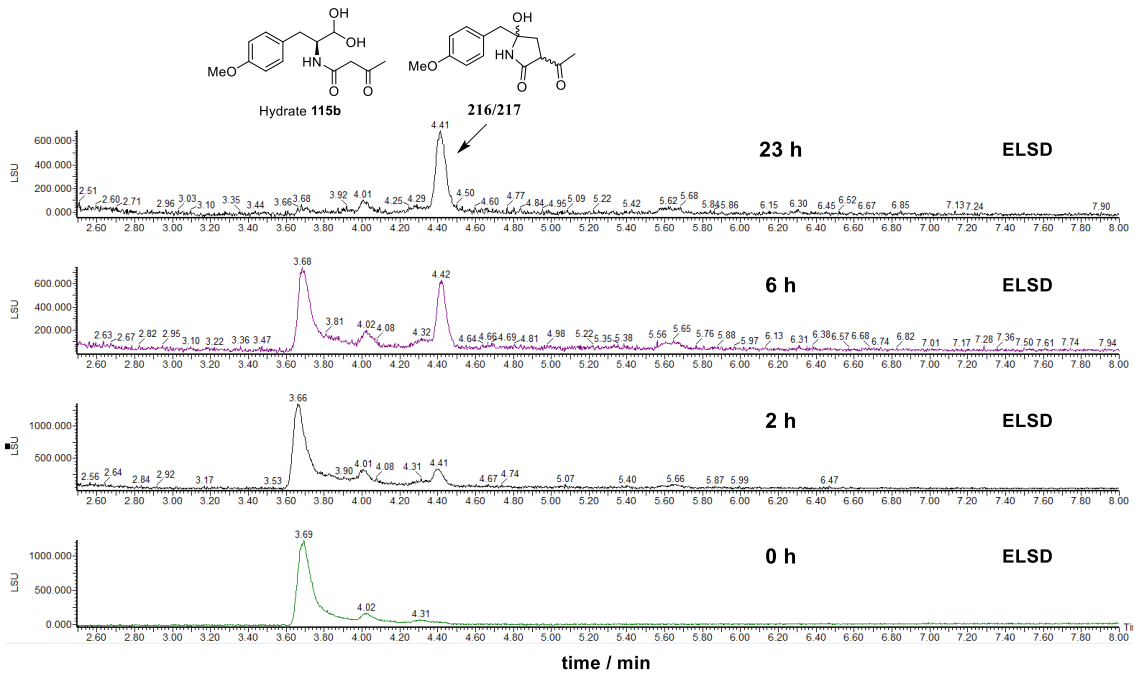

Figure 3.21 Model B **115** in potassium phosphate buffer (pH 7.5, 37.5 mM) at 28 °C.

The results of model B **115** in potassium phosphate buffer pH 7.5 and pH 8.0 were very similar and shown in figure 3.21 and figure 3.22 respectively. They showed that model B **115** formed alcohols **216/217** in a much faster rate in weakly basic conditions

than in slightly acidic or neutral conditions. After 23 hours, model B **115** was converted to alcohols completely and quantitatively, with no formation of the dimer **232**.

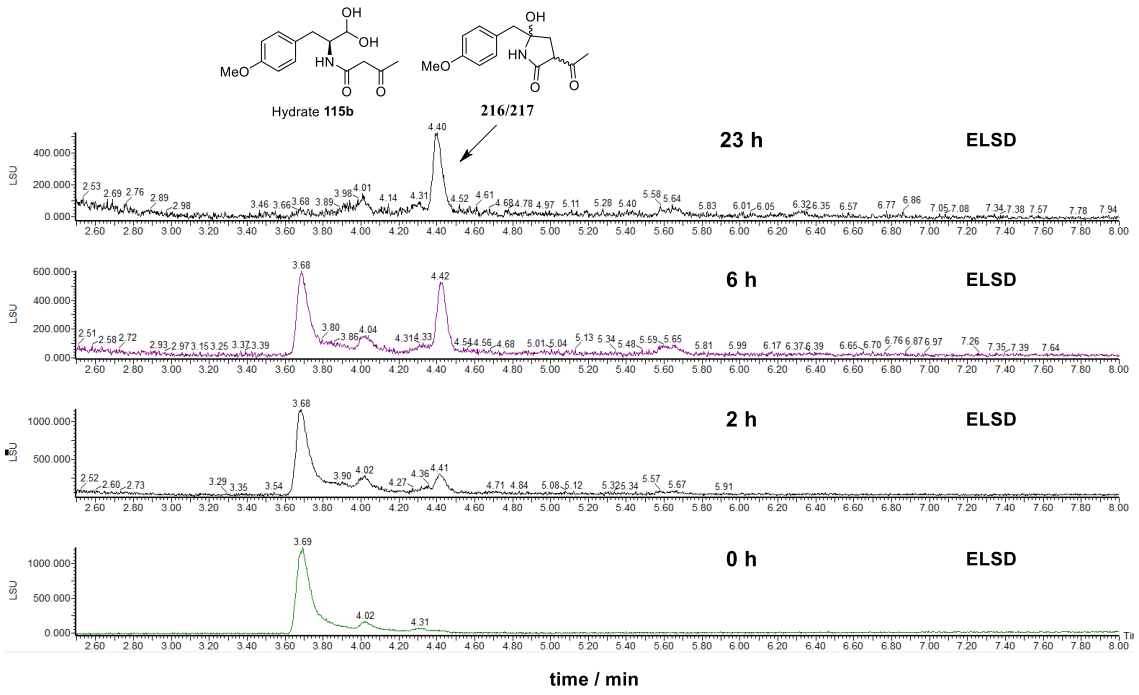

Figure 3.22 Model B **115** in potassium phosphate buffer (pH 8.0, 37.5 mM) at 28 °C.

The model B **115** in potassium phosphate buffer tests suggest that it is sensitive to pH values in phosphate buffer. Compared to that in water, it seems potassium phosphate also has influence on model B **115** stability. To further confirm this, model B **115** in potassium phosphate buffers (pH 8.0) with different concentrations at 28 °C over time were performed.

It showed that when the concentration of the phosphate buffer was higher, the more alcohols **216/217** were formed (Figure 3.23). The peak at 6.1 min has no UV absorbance and the mass is not relevant to model B **115**. Therefore it may be impurity inside, but it did not affect the tests.

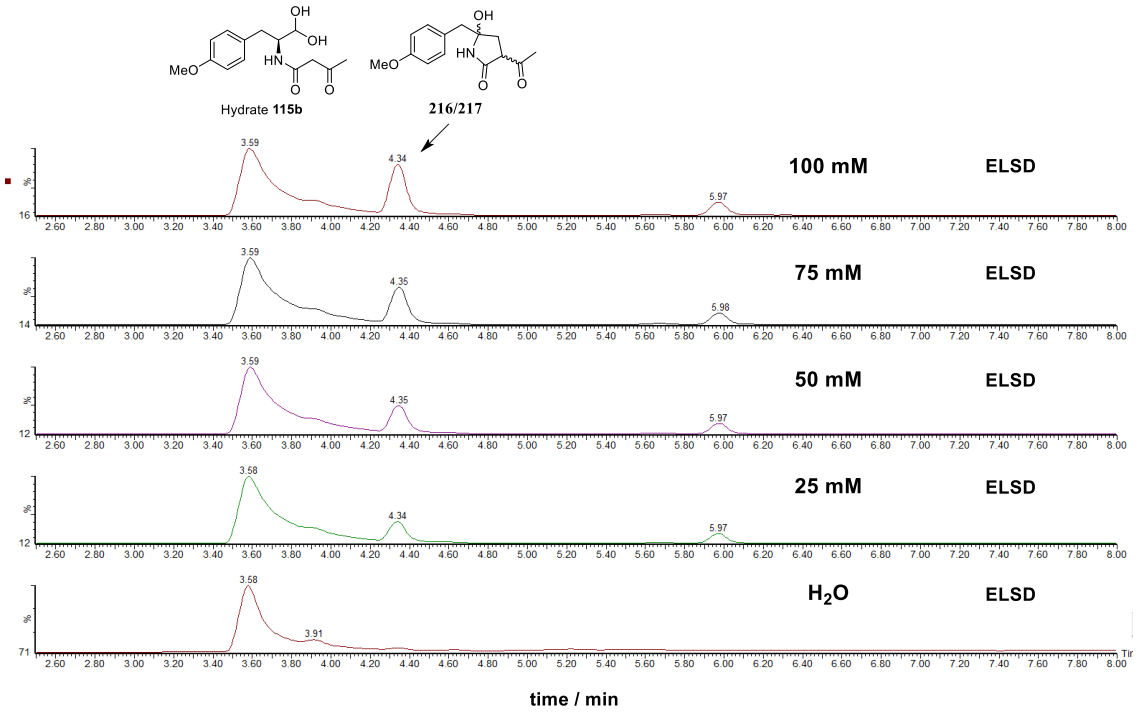

Figure 3.23 Model B **115** in potassium phosphate buffer (pH 8.0) after 2 h at 28 °C.

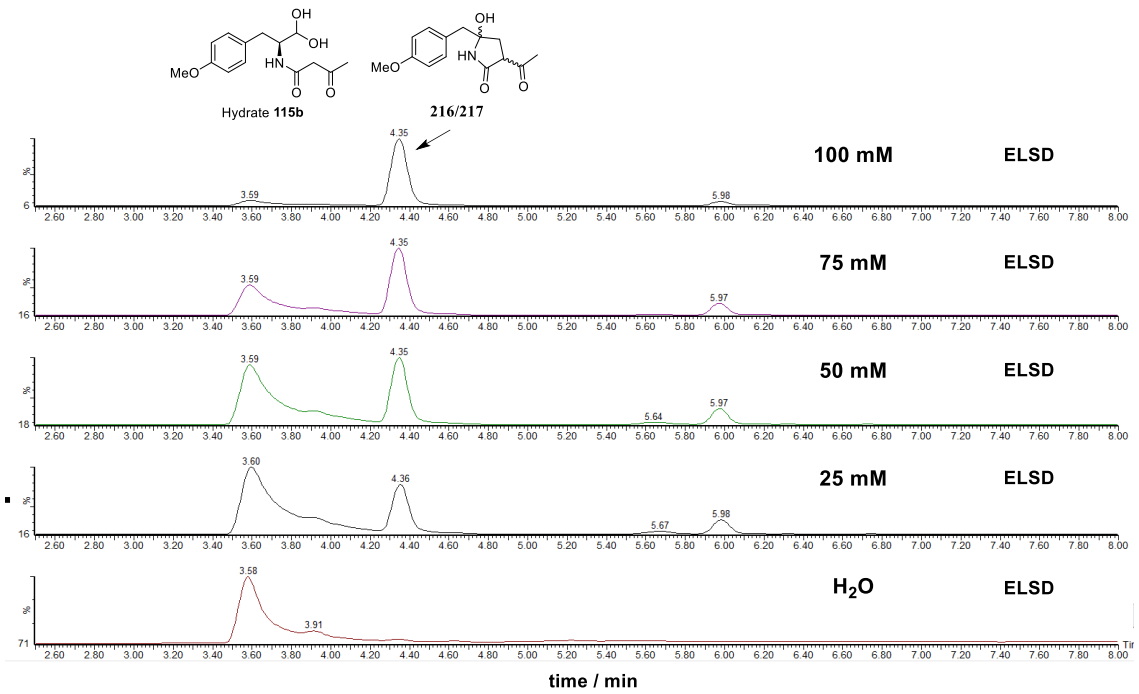

Figure 3.24 Model B **115** in potassium phosphate buffer (pH 8.0) after 8 h at 28 °C.

After 8 hours, model B **115** was almost all converted to alcohols **216/217** when the buffer concentration was 100 mM (Figure 3.24). However, only a little of alcohols

216/217 was formed when the buffer concentration was 25 mM. It clearly shows the potassium phosphate strongly influenced the stability of model B **115**.

Next, model B **115** stability in HEPES buffer (pH 7.5, 50 mM) was tested at 37 °C over time. Compared to that in potassium phosphate buffer, model B **115** is much more stable in HEPES even in slightly basic condition. After 5 h, only a tiny amount of alcohols **216/217** were formed. So it can be used for bioassays with enzymes (Figure 3.25).

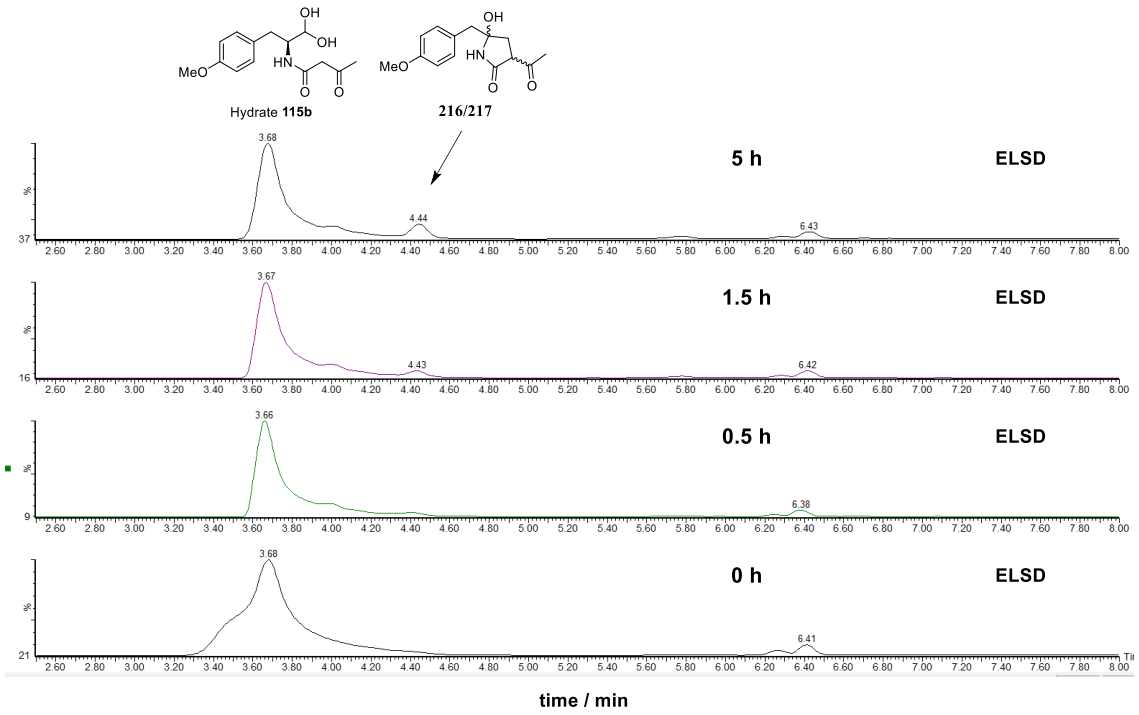

Figure 3.25 Model B **115** in HEPES buffer (pH 7.5, 50 mM) at 37 °C.

3.3.4.6 Model B Bioassays with Enzymes

ORFZ was expressed and partially purified from *E. coli* by Verena Hantke. The bioactivity was tested with model B **115** in water firstly to see if it was active in water. Model B **115** in H_2O and with boiled enzyme are two negative controls. ORFZ and ORF3 together were also tested to see if ORF3 was needed. The bioassays were performed in 200 µl scale at 30 °C over time.

After 30 min and 90 min, the reaction mixtures were monitored by LCMS respectively (figure 3.26 and figure 3.27). Apparently there are no significant differences between enzyme and negative controls even after 90 min. Model B **115** was stable in this condition and the enzyme did not appear to catalyze Knoevenagel condensation possibly because the enzyme was not active in H_2O.

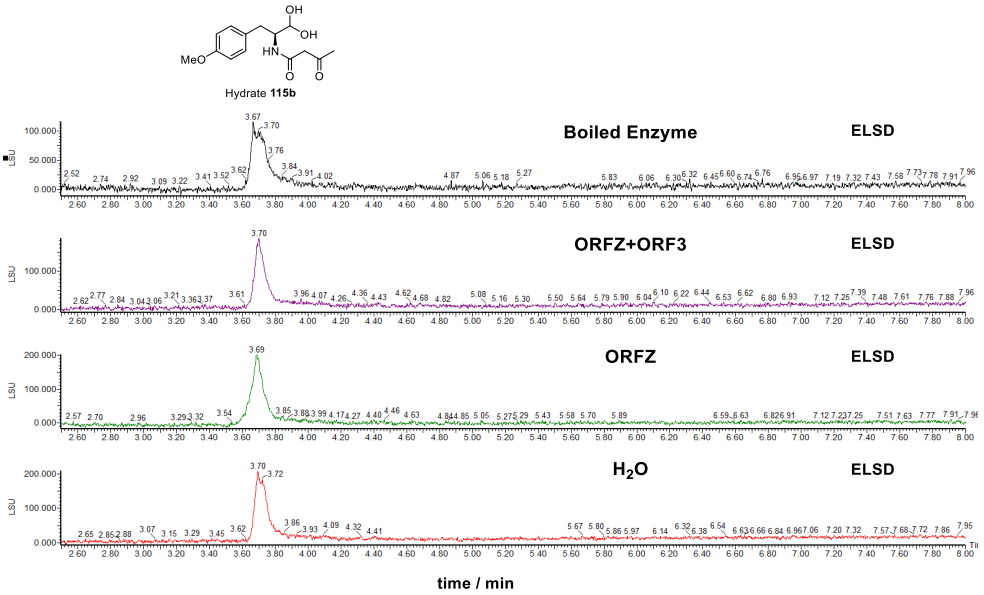

Figure 3.26 Model B **115** in H_2O with enzymes after 30 min at 30 °C.

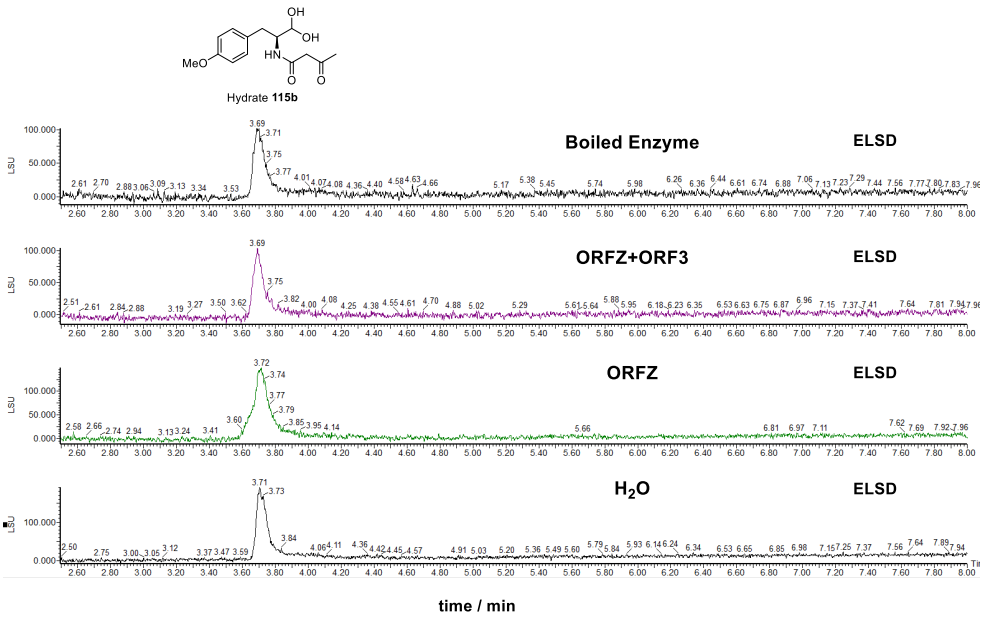

Figure 3.27 Model B **115** in H_2O with enzymes after 90 min at 30 °C.

Next, ORFZ activity was tested in HEPES buffer (pH 7.5, 50 mM) with model B **115** at 35 °C over time. As usual, model B **115** in HEPES and with boiled enzyme were two negative controls. After 30 min, the reaction mixtures were analyzed by LCMS (Figure 3.28). Compared with negative controls, no obvious conversion was observed after 30 min.

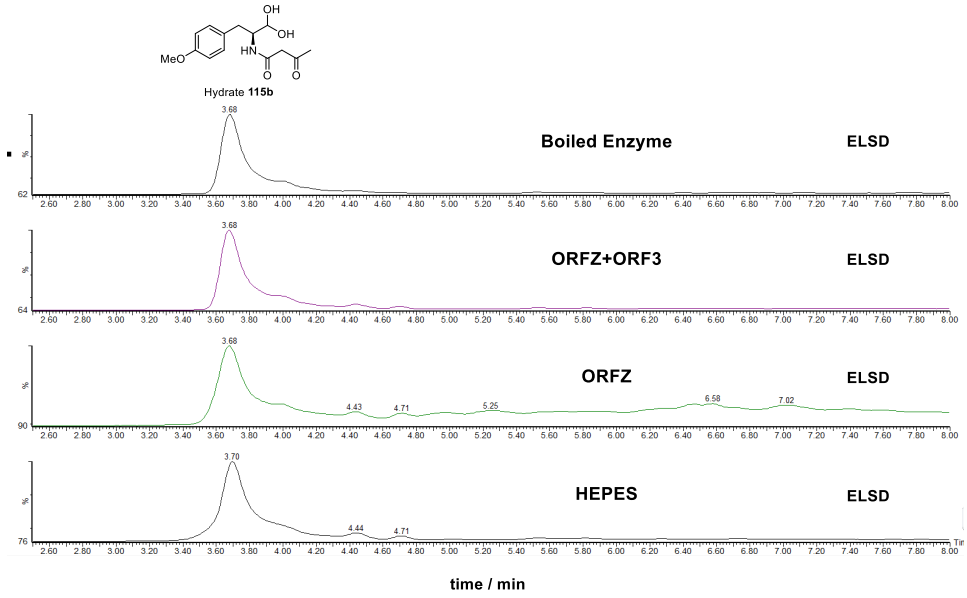

Figure 3.28 Model B **115** in HEPES (pH 7.5) with enzymes after 30 min at 35 °C.

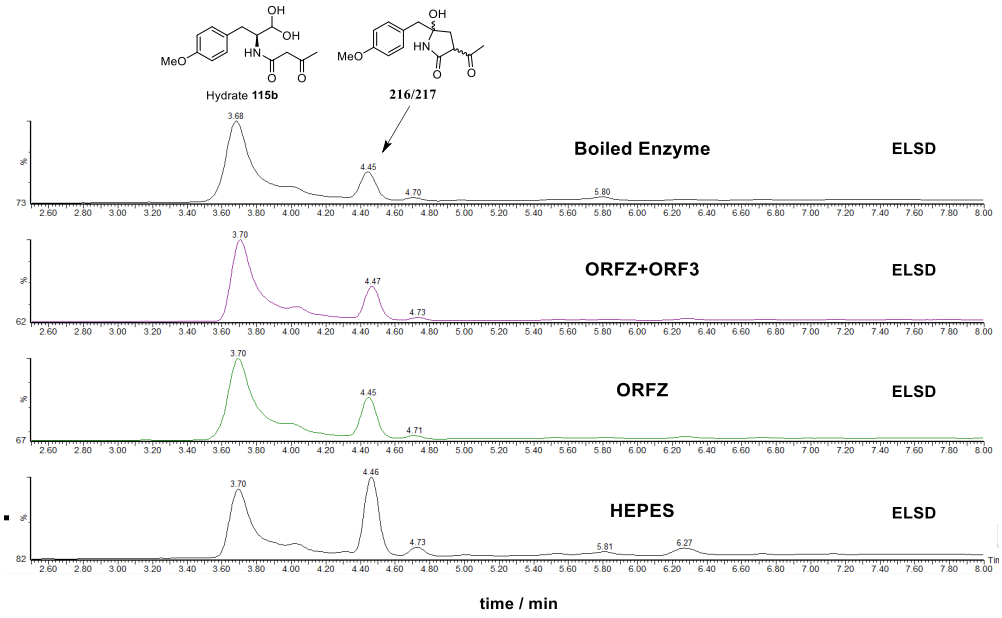

Figure 3.29 Model B **115** in HEPES (pH 7.5) with enzymes after 90 min at 35 °C.

After 90 min, some alcohols **216/217** were formed in all negative and positive controls possibly because of the HEPES buffer rather than the enzyme activity (Figure 3.29).

3.4 Discussion and Conclusion

3.4.1 Pyrrolinone Tautomerism

In this project, three pyrrolinones were prepared (Fig. 3.30). Compared with α-methyl pyrrolinone **231**, both *O*-methyl pyrrolinone **204b** and phenylalanine pyrrolinone **222b** tautomerize and have a characteristic UV absorbance at 328 nm indicative of the aromatic tautomers. The stabilities between *O*-methyl pyrrolinone **204b** and phenylalanine pyrrolinone **222b** are very different. Phenylalanine pyrrolinone **222b** can be purified by prep-LCMS and characterized by NMR. However, *O*-methyl pyrrolinone **204b** is much less stable and converted to alcohols **216/217** after prep-LCMS purification. Oxygen atom can make the aromatic ring more electron rich and influence the stability, but the detailed mechanism is still uncertain because the aromatic ring is isolated from the pyrrolinone.

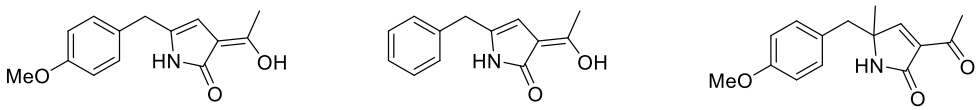

Figure 3.30 Pyrrolinones prepared.

As discussed in cytochalasan total synthesis (section 1.4), synthetic chemists have proved that tautomerised pyrrolinones are not suitable for DA reaction. However, if an acyl group is introduced on the nitrogen atom, the pyrrolinone will not tautomerise and hence can be applied for DA reaction (scheme 3.21).[110] When the dienophile **235** is doubly activated, the DA reactions tend to be highly selective and efficient. Moreover, unsymmetrical 1,3,5-trienes react preferentially at the most substituted 1,3-diene unit and this was applied for successful total synthesis of cytochalasin D **4** by the Thomas group.[63]

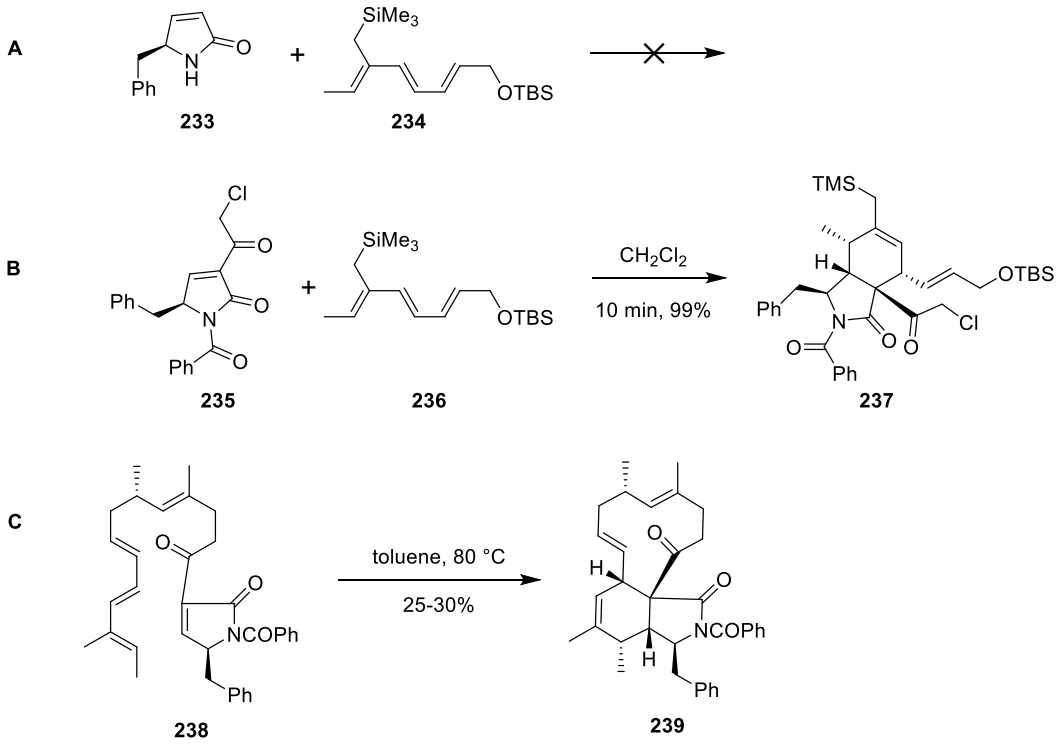

Scheme 3.21 Failed attempt of DA reaction and successful DA reaction with *N*-acyl pyrrolinone.

However, in nature, cytochalasan precursors do not contain an electron-withdrawing group on the nitrogen atom of the pyrrolinone ring. Therefore the pyrrolinones during cytochalasan biosynthesis are not competent for the following DA reaction. The putative DA reaction in cytochalasan biosynthesis is thus not spontaneous and needs a DAase. The enzyme can affect the reaction possibly in two ways, either by catalysis of the reaction in a much faster rate before pyrrolinone tautomerism, or speeding up the equilibrium between the tautomerised and non-tautomerised pyrrolinone.

3.4.2 Pyrrolinone Conversion

O-Methyl pyrrolinone **204b** is converted spontaneously to alcohols **216**/**217**. This modification is observed in a class of fungal natural products, including pyrrocidines B **240**,[111] pyrrospirones **241**[112] and hirsutellones **242** (Fig. 3.31).[113]

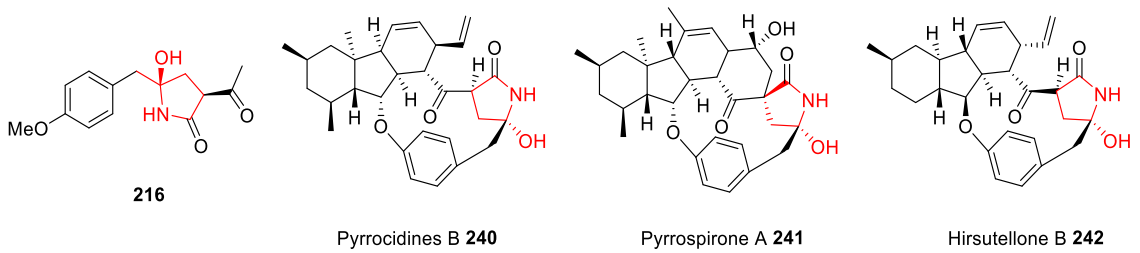

Figure 3.31 Fungal natural products containing alcohols **216/217** framework.

However, pyrrolinone **243** was also proposed to be oxidized either spontaneously or enzyme catalyzed to a similar hydroxylation pattern with intact olefin **244** (scheme 3.22).[78]

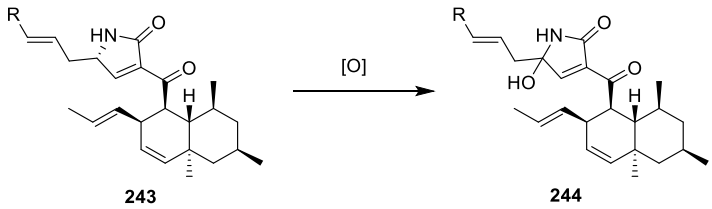

Scheme 3.22 Proposed hydroxylation biosynthesis pathway.

This modification is more common in fungal natural products, such as myceliothermophin A **245**,[108] oteromycin **246**,[114] quinolactacins **247**[115] and pyrrocidines A **248** (Figure 3.32).[111]

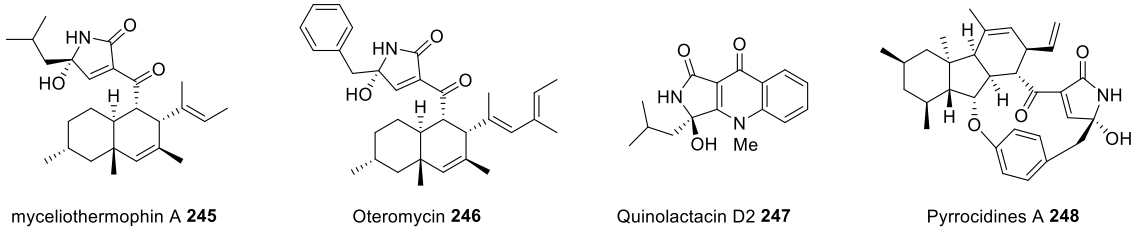

Figure 3.32 Fungal natural products containing similar hydroxylation pattern.

3.4.3 Enzyme Assays

After performing bioassays in different buffers with different pH values, no enzyme activity was observed. There are so many possibilities accounting for this. Firstly, the α,β-hydrolase (ORFZ) may have strict substrate selectivity since the model compound is

not the real cytochalasin precursor. Moreover, the pyrrolinone might be converted too fast to be monitored.

However, there is high probability that Knoevenagel condensation is spontaneous. Firstly, model B **115** can form alcohols **216/217** in different buffers spontaneously after several hours. While model B pyrrolinone **204b** can be also converted to alcohols **216/217** in less than 30 min. From model B **115** to **216/217**, a five-membered ring was formed probably by Knoevenagel condensation. If Knoevenagel condensation is the rate-determining step, so pyrrolinone **204b** cannot be observed in the assays (Scheme 3.23).

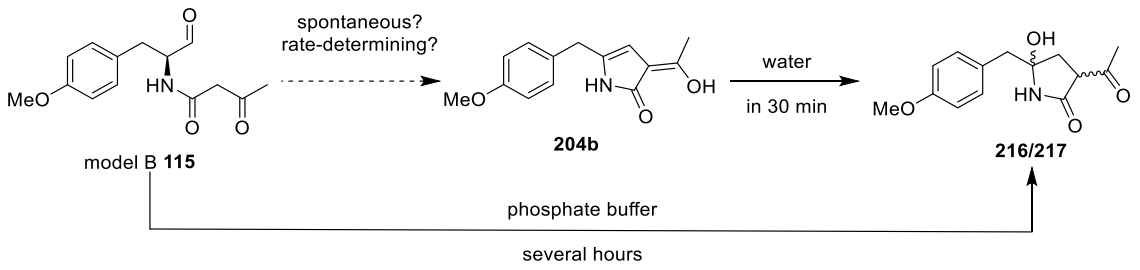

Scheme 3.23 Formation of alcohols **216/217** probably *via* Knovenagel condensation.

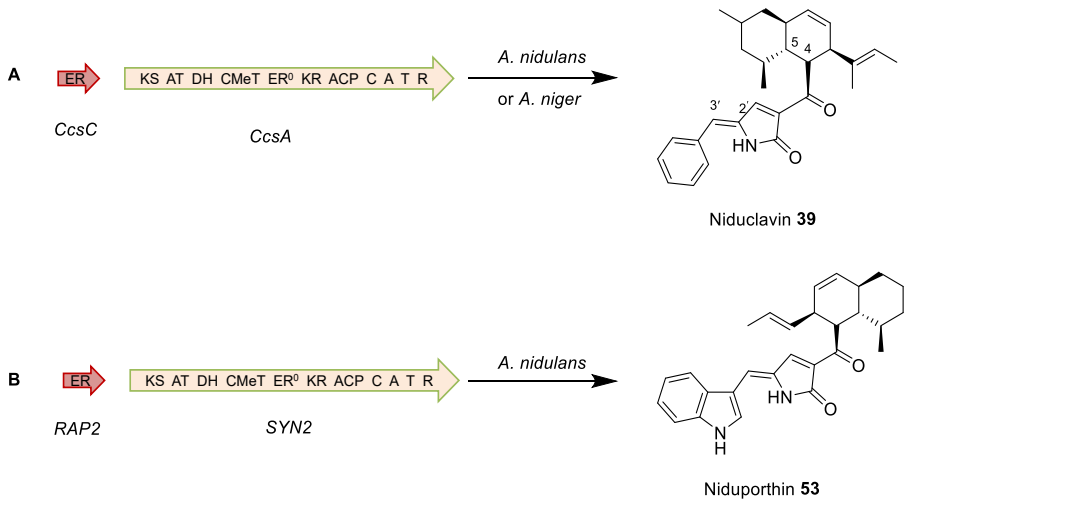

Scheme 3.24 Heterologous expression of cytochalasin E **5** genes (*ccsC* and *ccsA*) and PKS-NRPS genes (*SYN2* and *RAP2*) in *A. nidulans*.

Moreover, heterologous expression of cytochalasin E genes (*ccsC* and *ccsA*) and PKS-NRPS genes (*SYN2* and *RAP2*) in *A. nidulans* produced niduclavin **39** and niduporthin **53** respectively. In this heterologous expression, Knoevenagel condensation

must be spontaneous because *ccsF* or *orfz* were not expressed. The olefin at 2‘ and 3‘ was possibly introduced by a shunt oxidation in *A. nidulans*, or by an air oxidation reported by Tang group (Scheme 3.24).[108]

The proposal for the biosynthesis of niduporthin **53** is shown in scheme 3.25. Polyketide aldehyde **249** is reductively released from the PKS-NRPS by its R domain, which undergoes spontaneous Knoevenagel condensation to form pyrrolinone **250**. Pyrrolinone **250** tautomerises to **251**, that is not suitable for both two possible DA reactions any more, *e.g.* isoindolone core formation and decalin ring formation.[108] The tautomerised pyrrolinone **251** cannot undergo DA reaction to form decalin possibly because the hydroxyl group cannot make dienophile as electron poor as a carbonyl group. But tautomerised pyrrolinone **251** can be oxidized in air automatically to compound **252**,[108] which is ready for DA reaction. But this air oxidation was not observed during model B **115** assays. The decalin formation is possibly spontaneous through a [4+2] DA reaction between the terminal diene and the dienophile present within the polyketide chain.

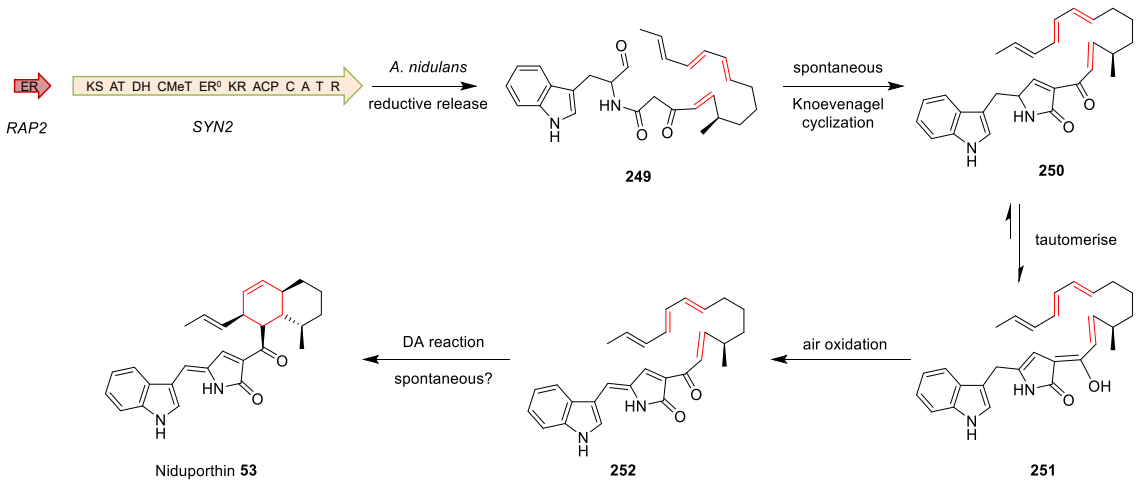

Scheme 3.25 Proposal for niduporthin **53** biosynthesis in *A. nidulans*.

From the observations discussed above, Knoevenagel condensation is deduced to be probably spontaneous. However, fast tautomerization produces an aromatic intermediate which is not competent for the expected subsequent DA reaction.

4. Investigation of Diels-Alder Reaction by *In Vitro* Assays with Model Compounds.

4.1 Introduction

4.1.1 General Description of the Diels-Alder Reaction.

The Diels-Alder reaction is named after Professor Otto Diels and his student Kurt Alder, who were awarded the Nobel Prize for the discovery of this reaction.[116] Diels-Alder reactions are [4+2] cycloadditions between a conjugated diene and an alkene (usually called the dienophile) to afford a six-membered ring with up to four contiguous stereocenters in a stereospecific and highly stereoselective manner. In a Diels-Alder reaction, the conjugated diene can be linear or cyclic with different substituents, but it has to be in the s-*cis* conformation. Diels-Alder Reactions can be further divided into normal electron demand and inverse electron demand Diels-Alder reactions based on the conjugated substituents.

4.1.1.1 Normal Electron Demand and Inverse Electron Demand Diels-Alder Reactions.

When the diene is electron-rich and dienophile is electron-deficient, two new bonds are formed between the highest occupied molecular orbitals (HOMO) of the diene and lowest unoccupied molecular orbital (LUMO) of dienophile (scheme 4.1A). Electron-donating group raises the HOMO of the diene and electron-withdrawing group lowers the LUMO of the dienophile, thus the Diel-Alder reaction occurs smoothly. This is the most common type of Diels-Alder reaction, which is also called normal electron demand Diels-Alder reaction.

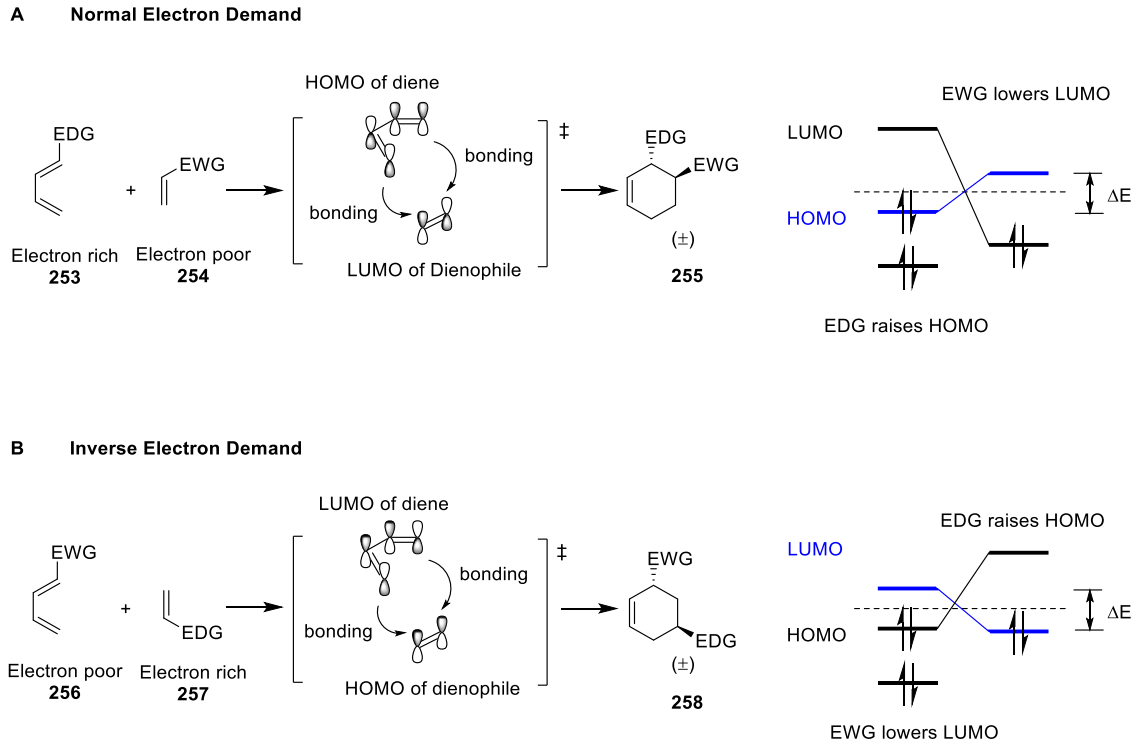

Scheme 4.1 A, Normal electron demand Diels-Alder reaction; **B**, Inverse electron-demand Diels-Alder reaction.

However, in contrast to a normal electron demand Diels-Alder reaction, when the diene is electron-deficient and dienophile is electron-rich, the LUMO of diene and HOMO of dienophile are close in energy, thus they interact strongly and result in bond formation. This is called inverse electron-demand Diels-Alder reaction (iEDDA) which was discovered by Bachmann and Deno in 1949.[117] Since inverse electron demand Diels-Alder reactions often involve hetero atoms, it is particularly useful in the synthesis of compounds containing heterocycles.

Scheme 4.2A shows a general inverse electron demand Diels-Alder reaction between tetrazines **259** and olefins **260**. This reaction proceeds rapidly in aqueous media in high yield without need for catalysis and tolerates a broad range of functionality. It has already been developed to be a potential click reaction by both the Fox and Hilderbrand groups.[118,119] Now it is widely used in bioorthogonal chemistry for labeling of proteins,[120] cell surface,[121] nucleic acids,[122] and cancer cells.[123]

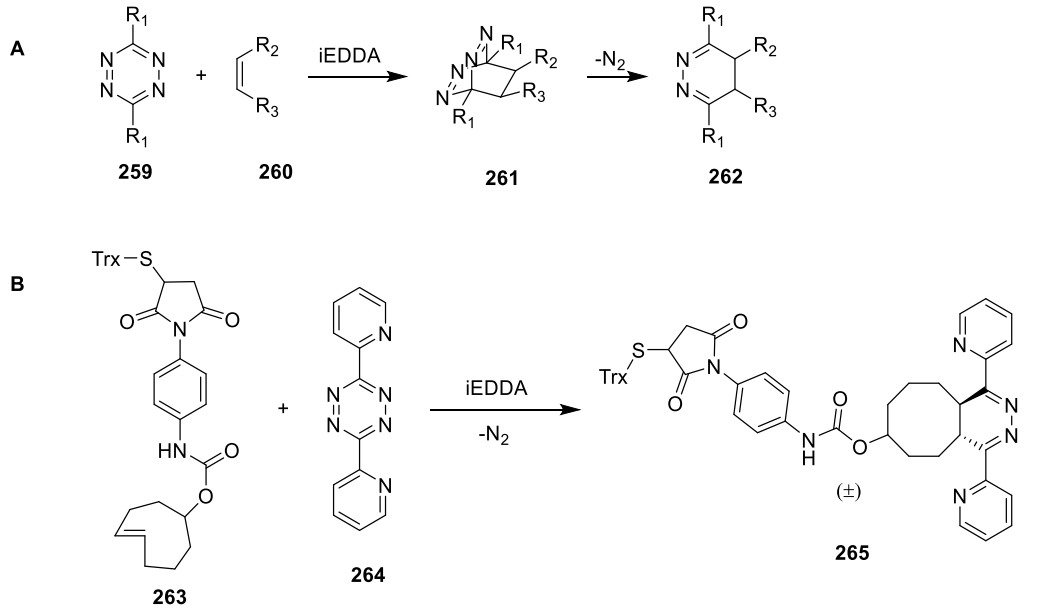

Scheme 4.2 A, general scheme of inverse electron demand Diels-Alder reaction between tetrazines **259** and olefins **260**; **B**, Testing the reaction as a bioorthogonal biolabelling method with a functionalized thioredoxin by Fox and co-workers.[119] Trx = thioredoxin.

4.1.1.2 Stereospecificity and Stereoselectivity

The Diels-Alder reaction is a *syn* addition with respect to both the dienophile and the diene, thus it is stereospecific. When the substituents are on the same side of the dienophile, they will be *cis* on the newly formed ring, and *vice versa* (scheme 4.3).

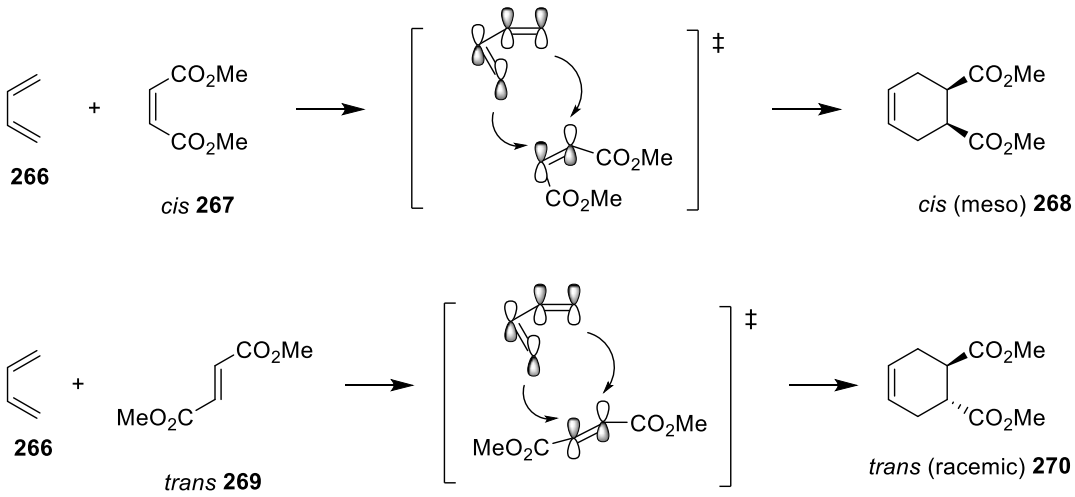

Scheme 4.3 The Diels-Alder reaction *via syn* addition.

The substituents on the diene can be *cis*,*cis*, *cis*,*trans* and *trans*,*trans*. Both *cis*,*cis*- and *trans*,*trans*-disubstitued dienes give rise to *cis* product whereas *cis*,*trans*-disubstituted dienes give *trans* product (scheme 4.4).

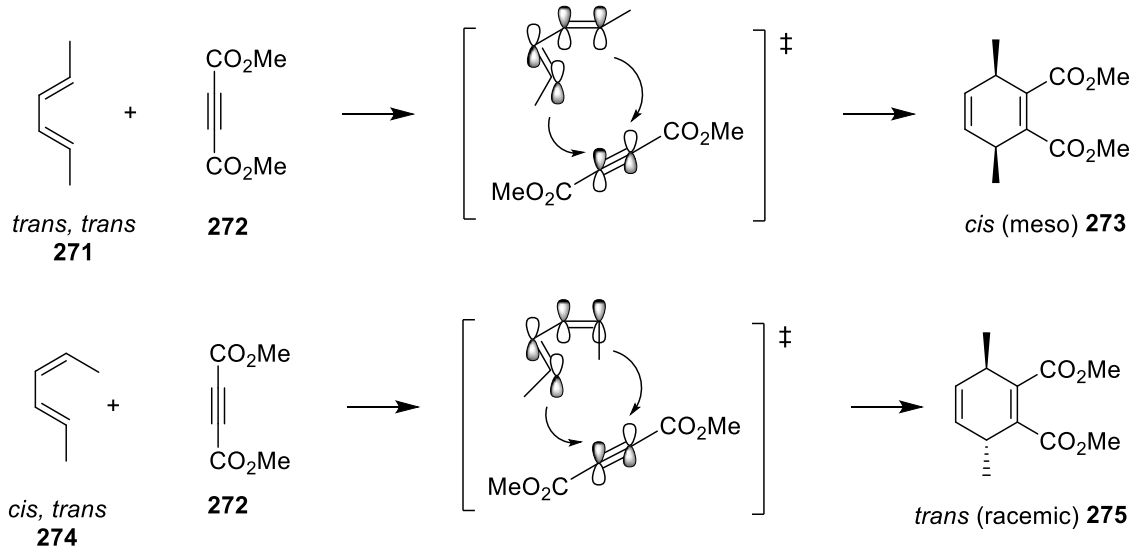

Scheme 4.4 The Diels-Alder reaction *via syn* addition.

The Diels-Alder reaction is stereoselective and follows *endo* rule when it is irreversible and the dienophile has a π bond in its electron-withdrawing group. Though the *endo* product is more sterically hindered, it is kinetically favorable because in the *endo* transition state, p orbitals of the electron-withdrawing group on the dienophile with the p orbitals of the diene overlap to stabilize the transition state, even though no bonds are formed (scheme 4.5).

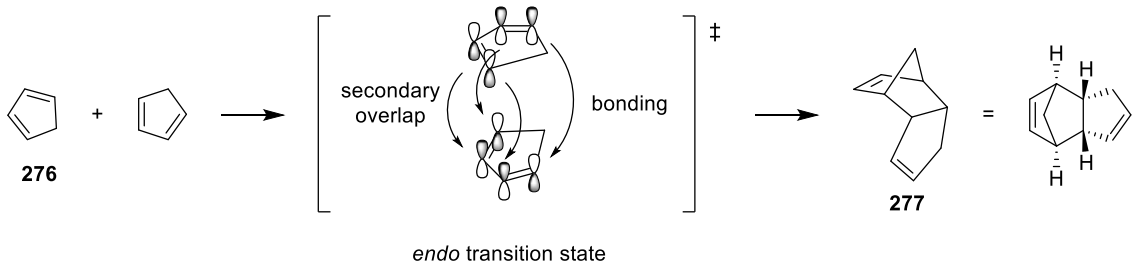

Scheme 4.5 *Endo* product formation due to secondary orbital overlap.

However, secondary orbital effects are not strong bonding interactions. When dienes are highly substituted and dienophiles are bulky, or it is a reversible reaction, the secondary orbital effect only plays a minor role and the *exo* isomer will be favored due

to steric effects. In an intramolecular Diels-Alder reaction (IMDA), dienophile and diene are held together, thus bonding interactions across space are also not so important and the *exo* product is also often preferred.

4.1.2 Diels-Alder Reactions in Total Synthesis

The Diels-Alder reaction is one of the most powerful tools in synthetic organic chemistry, especially in complex natural product synthesis, such as for terpenes, sesquiterpenes, and even alkaloids. Indeed, it has been applied to the synthesis of complex pharmaceutical and biologically active compounds,[124] such as equisetin **63**,[125] betaenone C **282**,[126] reserpine **286**,[127] and diaporthichalasin **290** (Scheme 4.6).[128,129]

Equisetin **63** and betaenone C **282** are two decalin-containing natural products with biological activities.[126,130] Both of their decalin formations were achieved using the intramolecular Diels-Alder reaction where new stereocenters were formed stereoselectively (Scheme 4.6A and 4.6B). Reserpine **286** is an indole alkaloid isolated in 1952 with remarkable physiological properties.[131] The first total synthesis of reserpine **286** was carries out by Woodward using an intermolecular Diels-Alder reaction in the first step to afford three new stereocenters stereoselectively (Scheme 4.6C).[127]

Diaporthichalasin **290** is an isoindolone and decalin-containing secondary metabolite isolated from the filamentous fungus *Diaporthe* sp. Bkk3.[132] It is suspected to be biosynthesized in a cytochalasin-type pathway.[129] The total synthesis of diaporthichalasin **290** was accomplished using two intramolecular Diels-Alder reactions to give decalin ring and isoindolone core (scheme 4.6D). It is notable that the hydroxyl group on the pyrrolinone ring blocks the tautomerism, thus making pyrrolinone possible for the following Diels-Alder reaction. The dehydrated compound **291** was also produced, either before or after the Diels-Alder reaction.

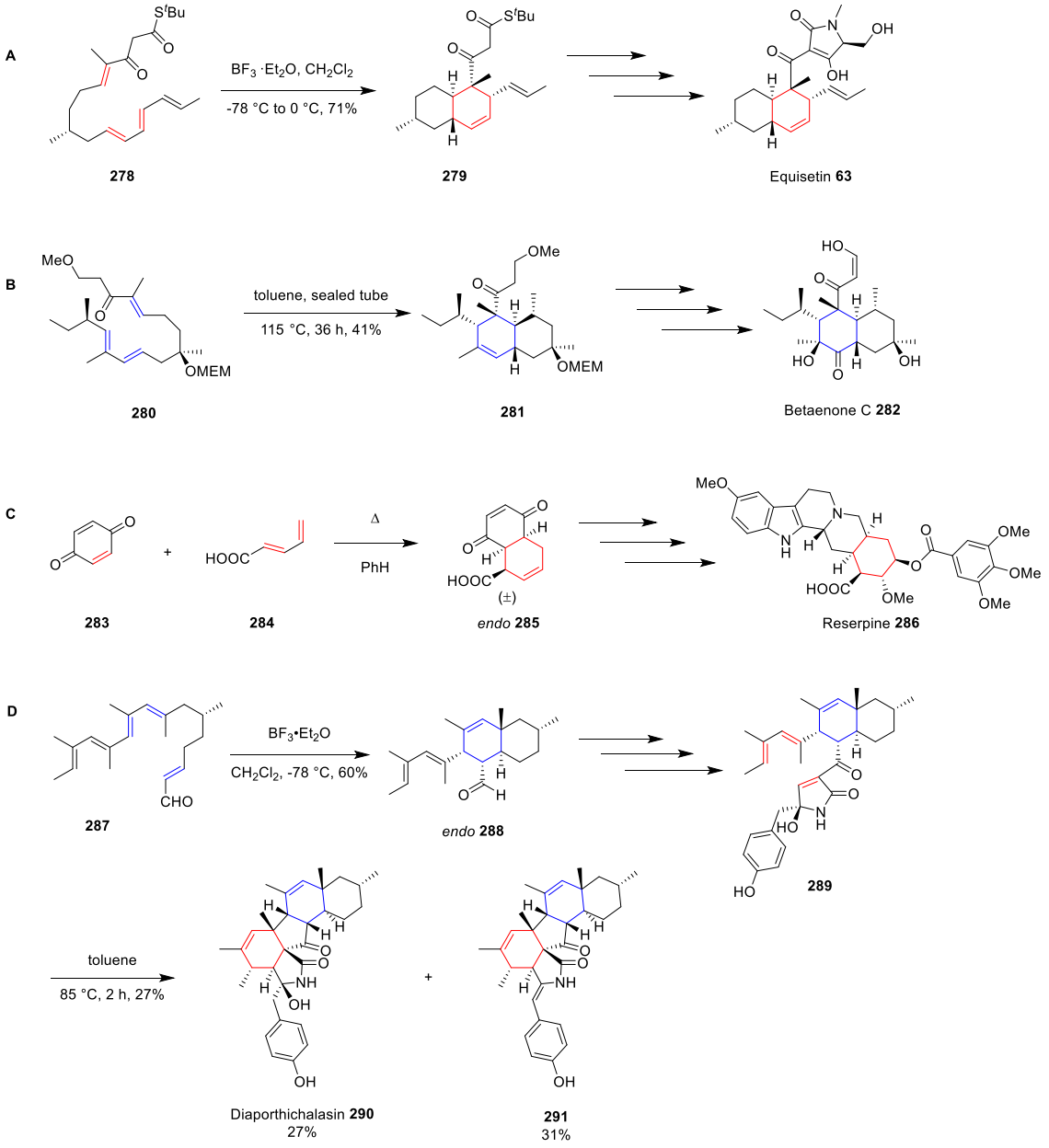

Scheme 4.6 Diels-Alder steps in natural product total synthesis.

The DA reaction has been also applied to the synthesis of cytochalasans. The simultaneous formation of the isoindolone core and macrocyclic ring using IMDA reaction is an efficient stragety for the construction of cytochalasan skeleton. In chapter one, we have already described the total synthesis of cytochalasin B **2** and cytochalasin D **4** in detail *via* DA reactions. Another good example of cytochalasin H **303** total synthesis is shown in scheme 4.7 using this strategy.[133]

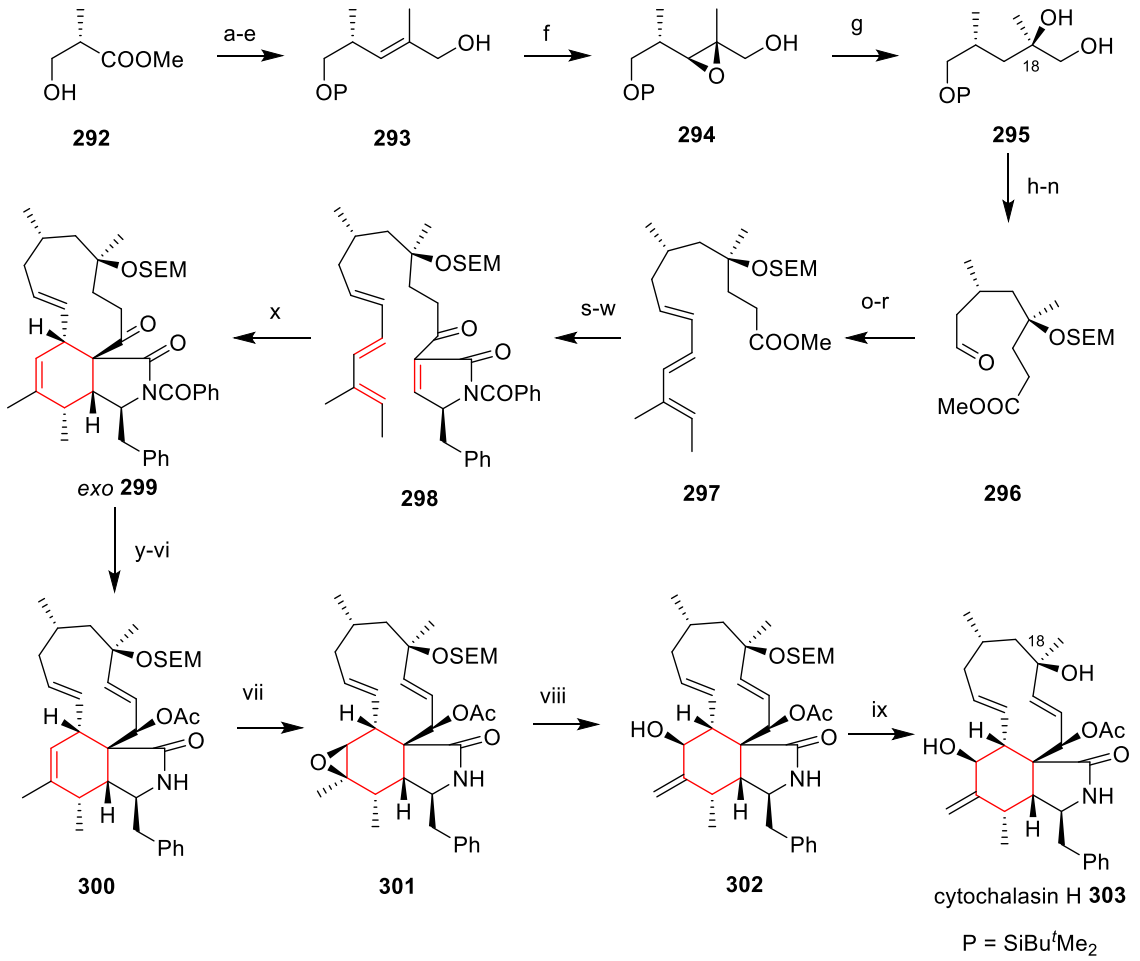

Scheme 4.7 Syntheis of cytochalasin H **303** *via* IMDA reaction. Reagents and conditions: **a**, imidazole, TBDMSCl, DMF, RT, 12 h, 98%; **b**, DIBAL-H, toluene, -78 °C, 2 h, RT, 2 h, 87.5%; **c**, DMSO, oxalyl chloride, CH_2Cl_2, -60 °C, NEt_3, 95%; **d**, $Ph_3P{=}CHCO_2Et$, bezene, 70 °C, 5 h, 71%; **e**, $LiAlH_4$, ether, 0 °C, 2 h, 88%; **f**, *m*-CPBA, $CHCl_3$, -20 °C, 2 h, 96%; **g**, $LiAlH_4$, THF, 0 °C, 2 h, 69%; **h**, Dimethyl sulphide, *N*-chlorosuccinimide, toluene, -20 °C, 30 min, then 2 h, triethylamine, 75%; **i**, $Ph_3P{=}CHCO_2Me$, bezene, 80 °C, 6 h, 63%; **j**, Dowex 50W-X8, MeOH, RT, 3 h, 98%; **k**, Diisopropylamine, $ClCH_2OCH_2CH_2SiMe_3$, reflux, 2 h, 86%; **l**, Dowex 50W-X8, MeOH, RT, 3 h, 70%; **m**, Pd-C, H_2, 4 h, 95%; **n**, DMSO, oxalyl chloride, CH_2Cl_2, -60 °C, NEt_3, 95%; **o**, *n*-BuLi, methyl triphenylphosphonium bromide, THF, 0 °C, 3 h; **p**, 9-Bicycloboranonane, THF, reflux, 4 h, 0 °C, NaOH, H_2O_2, 30 min, 78%; **q**, DMSO, oxalyl chloride, CH_2Cl_2, -60 °C, NEt_3, 85%; **r**, *n*-BuLi, dienylphosphonate, THF, -78 °C, 2 h, 87%; **s**, NaOH, MeOH, H_2O, RT, 3 h, 98%; **t**, 1,1'-Carbonyldi-imidazol, THF, 12 h, 95%; **u**, LiHMDS, THF-hexane, 1-benzoylpyrrolidinone, -78 °C, 7 h, 87%; **v**, LiHMDS, THF-hexane, PhSeCl, -78 °C, 2 h, 95%; **w**, *m*-CPBA, $CHCl_3$, -50 °C, then H_2O_2; **x**, toluene, 100 °C, 5 h, 37%; **y**, NaOH, MeOH, H_2O, 0 °C, 2 h, 98%; **z**, LDA,TMSCl, THF, -78 °C, 1 h, 98%; **ii**, PhSeCl, THF, TBAF, 0 °C, 2 h, 78%; **iii**, pyridine, H_2O_2, RT, 12 h, 68%; **iv**, $NaBH_4$, EtOH, 0 °C, 72%; **vi**, pyridine, 4-DMAP, Ac_2O, RT, 2 h, 94%; **vii**, *m*-CPBA, CH_2Cl_2, -20 °C, 1 h, 65%; **viii**, Aluminium isopropoxide, *o*-xylene, 125 °C, 8 h, 51%; **ix**, HF, ACN, RT, 3 h, 40%.

The synthesis started with chiral hydroxyl ester **292** and introduced another chiral center at C-18 by stereoselective peracid epoxidation, followed by reduction of the epoxide **294** using lithium aluminum hydride to give diol **295**. The diol **295** was further converted to the long-chain aldehyde ester **296** using conventional chemistry including alcohol protection, deprotection, oxidation and Wittig reaction *etc*. The conjugated triene **297** was constructed by Horner-Wadsworth-Emmons reaction to afford mainly the *EEE*-isomer. The introduction of *N*-benzoyl pyrrolinone moiety to **298** was achieved by substitution and phenylselenation-oxidation elimination. The benzoyl group delocalizes the electron lone pair on the nitrogen to increase the antiaromatic character of the pyrrolinone to keep it reactive for DA reaction. Intramolecular Diels-Alder reaction was performed in toluene at 100 °C for 5 h to give desired *exo* adduct **299** with high stereoselectivity. After construction of the cytochalasan skeleton, modifications were carried out on the tricyclic core including hydrolysis, phenylselenation-oxidation elimination, reduction, epoxidation and rearrangement *etc* to provide cytochalasin H **303**.

4.1.3 Diels-Alderase during Natural Product Biosynthesis

The importance of the Diels-Alder reaction also gained intense interests among biochemists. Frequent occurrence of apparent [4+2] cycloaddition adducts in secondary metabolites such as lovastatin **304**,[134] cytochalasin B **2**,[2] solanapyrone **305**,[135] and spirotetronates (*e.g.* Maklamicin **306**)[136] among others, and the feasibility of biomimetic total synthesis of complex natural products using Diels-Alder reactions as the key steps suggest that nature may also make use of this valuable reaction (Figure 4.1).[124] Extensive survey of these possible [4+2] adducts demonstrated more than 400 natural products are potentially biosynthesized using a DA reaction.[137]

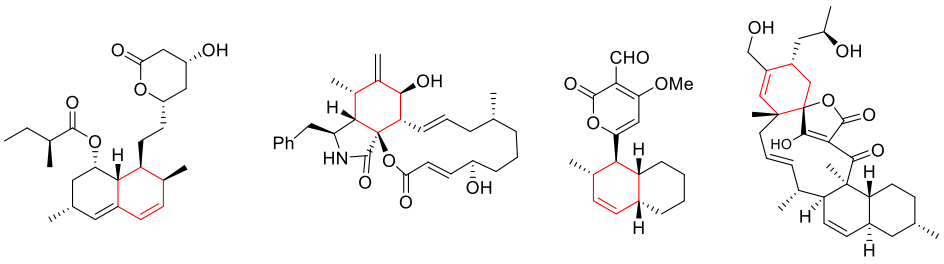

Figure 4.1 Examples of natural products containing apparent [4+2] cycloaddition adducts.

However, even though many proposals for the involvement of Diels-Alderase in natural products biosynthesis and numerous efforts have been made, relatively few Diels-Alderases were reported during late 1990s to early 2000s. These include solanapyrone synthase (Sol5)[135] and lovastatin nonaketide synthase (LovB).[134]

Solanapyrone **305** is a decalin-containing phytotoxin produced by the pathogenic fungus, *Alternaria solani*. After the first suggestion of a biological Diels-Alder reaction by labelling experiments,[138] enzyme activity was confirmed by *in vitro* assays with crude enzyme from *A. solani* (scheme 4.8). Incubation of prosolanapyrone III **308** with denatured enzyme for 10 min at 30 °C resulted in 10% conversion of the substrate to give the decalin product **309** and **310** in an *exo:endo* ratio of 3:97, consistent with the *endo* rule. Incubation with crude enzyme increased the conversion of the substrate to 25% and the *exo*/*endo* ratio to 53:47. These results show that the net enzymatic consumption of the substrate is 15% and *exo*/*endo* ratio for the enzymatic reaction is 87:13. Moreover, the enzyme is also responsible for the oxidation of alcohol **307** to aldehyde **308**.

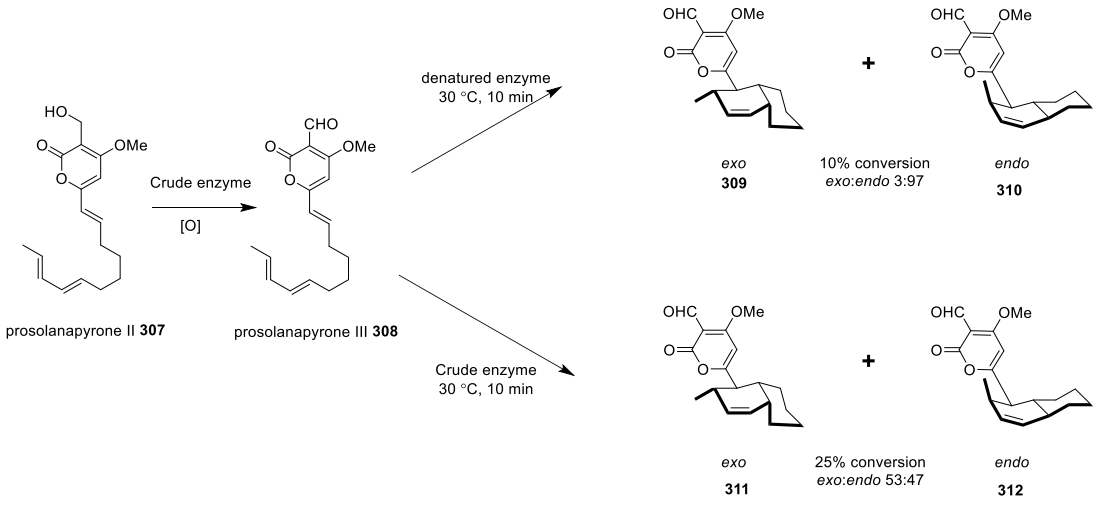

Scheme 4.8 *In vitro* assays of solanapyrone **305** Diels-Alderase (Sol5).

Lovastatin **304** is a decalin-containing cholesterol-lowering drug isolated from *Aspergillus terreus*. Its biosynthesis has been long proposed to require a Diels-Alder reaction. Its biosynthesis has been extensively investigated by Vederas and co-workers.[139] The exsistence of Diels-Alder catalysis during lovastatin biosynthesis was confirmed by *in vitro* assays in 2000.[134] Because the dienophile moiety in lovastatin **304** does not contain an electron-withdrawing group, the Diels-Alder reaction is proposed to occur at the hexaketide stage before the termination of chain extension.

Hexaketide **313** can undergo a spontaneous Diels-Alder reaction with denatured lovastatin nonaketide synthase (LNKS) to give a 1:1 ratio of the decalins **314**b and **314**c. However, incubation with active LNKS without co-factor afforded three products **314**a, **314**b and **314**c in a ratio of 1:15:15, in which **314**a has the same configuration with lovastatin **304**. Compared with the negative control, LNKS catalyzed Diels-Alder reaction to form the lovastatin decalin ring (scheme 4.9).

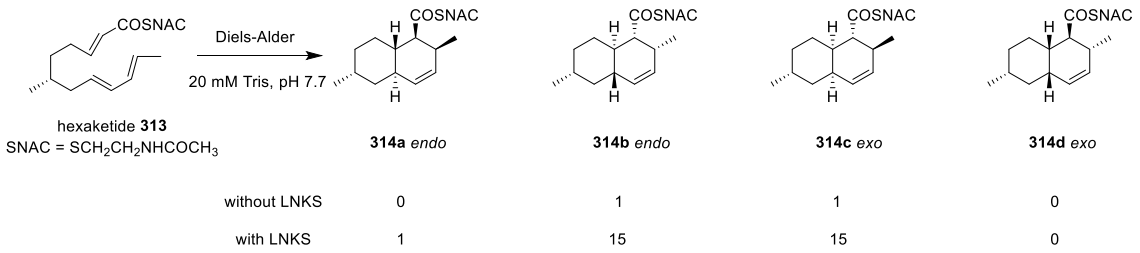

Scheme 4.9 *In vitro* assays of lovastatin nonaketide synthase (LNKS).

As the whole-genome sequencing and searching tools of biosynthetic gene clusters of the secondary metabolites develop, the identification and characterization of plausible Diels-Alderases become more convenient and faster. In recent years, investigation of Diels-Alder reaction involved in natural product biosynthesis has become a hot topic and more than ten Diels-Alderases have been identified during the biosynthesis of PKS-NRPS metabolites, such as spinosyn A **317**,[140] myceliothermophin E **60**,[108] equisetin **63**,[53] varicidin A **320**[141] and pyrroindomycin A **324**[142] (scheme 4.10).

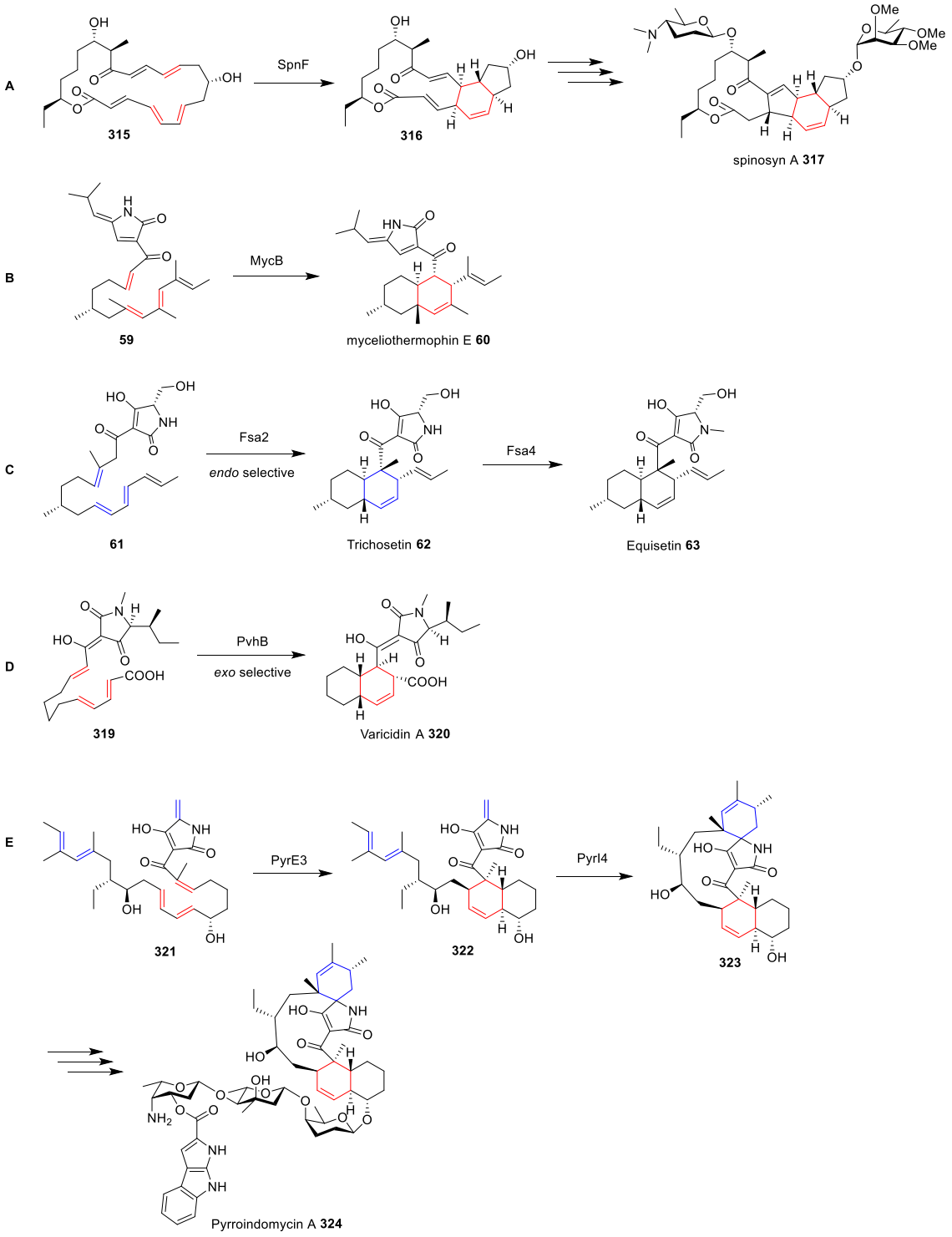

Scheme 4.10 Diels-Alderases identified in recent years involved in the biosynthesis of decalins and cyclohexenes.

4.1.4 Putative Diels-Alderase Involved in Cytochalasan Skeleton Biosynthesis

Many of the known Diels-Alderases which have been identified catalyze decalin formation. The biogenetic formation of the octahydro-isoindolone core of the cytochalasan skeleton has not been reported yet since the first cytochalasan discovery 50 years ago.

4.1.4.1 Indirect Evidences of Involvement of a Diels-Alder Reaction

The involvement of a Diels-Alder reaction during cytochalasan biosynthesis was implied by the occurance of proxiphomin **325**[143] and P450 inhibition experiments.[144] Proxiphomin **325** was isolated from *Phoma* sp. S298 culture (Figure 4.2). It possesses the same stereochemistry as cytochalasin B **2**. It is believed to be an adduct of the intramolecular [4+2] cyclization, a biogenetic precursor of cytochalasin B **2**. Treatment of *Chaetomium subaffine* with cytochrome P-450 inhibitors caused accumulation of various less-oxidized intermediates, including prochaetoglobosin I **22**, which is suggested to be the chaetoglobosin A **7** intermediate directly after the IMDA reaction. The great structure similarity of potential cytochalasin precursors after putative IMDA reaction also implies cytochalasan isoindolone formation shares the same biosynthetic pathway.[145]

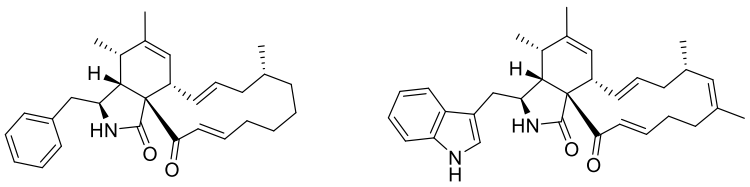

Proxiphomin **325** Prochaetoglobosin I **22**

Figure 4.2 Strucures of potential cytochalsan precursors after IMDA reaction.

4.1.4.2 Indirect Chemical Evidences of a Putative Diels-Alderase

It has been long speculated that a putative Diels-Alderase is involved during the isoindolone formation,[13] which is supported indirectly by several observations. Chemically, low stereoselectivity (*endo* : *exo* = 52 : 48) was observed during biomimetic synthesis of proxiphomin **325** *via* IMDA reaction (scheme 4.11A),[146]

indicating that a DAase is needed to control the steroselectivity. Moreover, the harsh chemical conditions (high temperature and long reaction time) required for the IMDA reactions to construct the isoindolone core during cytochalasan total synthesis also suggest the involvement of an enzyme *in vivo* (scheme 4.11).

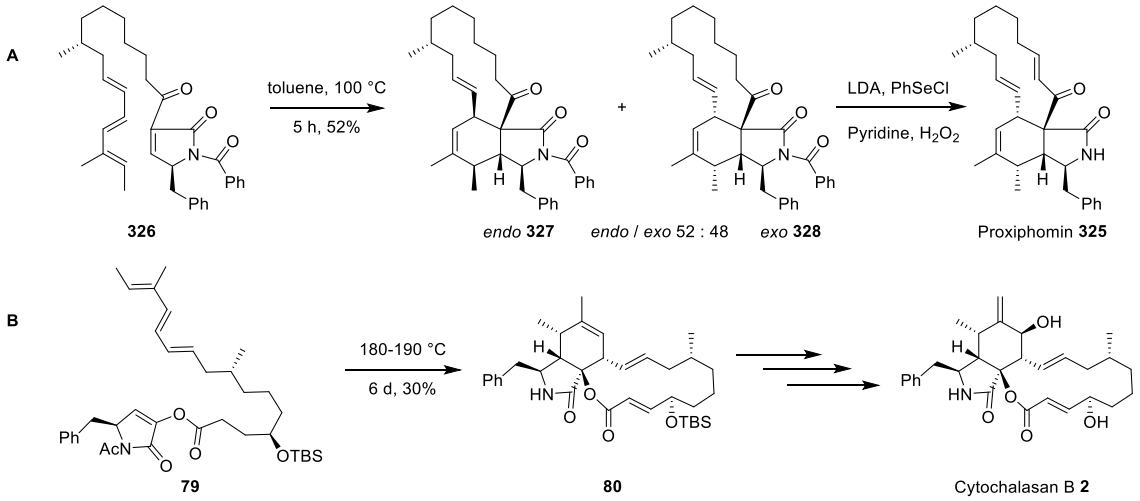

Scheme 4.11 IMDA reaction steps involved in the synthesis of proxiphomin **325** and cytochalasin B **2**.

In addition, as discussed in section 1.4.2, the pyrrolinones used as dienophile for DA reactions have been widely investigated. The parent compound **329** is thermally unstable.[147] Compound **330** tautomerises to its enol form irreversibly,[106] and compound **332** isomerizes to its 5-benzylidene isomer **333** (scheme 4.12A).[148] Thus these pyrrolinones are no longer directly competent for the DA cyclization in organic synthesis.[149] It has been found that an electron-withdrawing substituent, *e.g.* an acyl group on nitrogen, is particularly important to keep pyrrolinones active for the IMDA reactions (scheme 4.11). Introduction of the *N*-acyl group on the pyrrolinone can decrease the aromatic character of the heterocycle and prevent tautomerism (scheme 4.12B). An example is the synthesis of cytochalasin H **303** using *N*-benzoyl pyrrolinone **298** to construct the isoindolone core *via* IMDA reaction (scheme 4.12C).[133] But, in nature, the proposed pyrrolinone intermediate on the cytochalasin pathway does not bear an electron-withdrawing substituent, thus an enzyme must be needed.

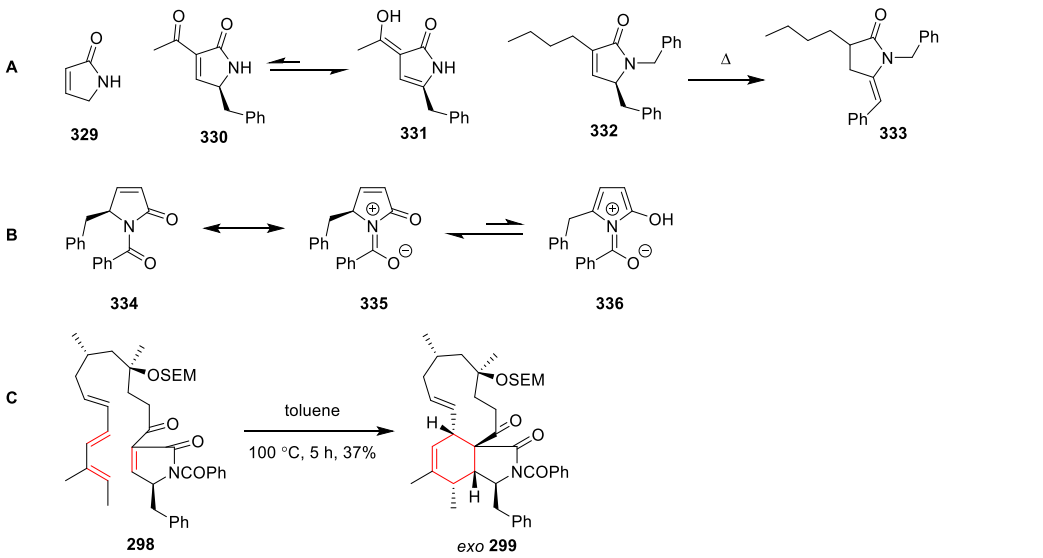

Scheme 4.12 A, Pyrrolinones are not suitable dienophiles; **B**, Introduction of acyl group decreases aromaticity; **C**, *N*-benzoyl pyrrolinone **298** used for synthesis of cytochalasin H **303**.[133]

However, a retro-Diels-Alder reaction of prochaetoglobosin I **22** produced equal amounts of prochaetoglobosin I **22** and its *exo* diastereomer **338** rather than the expected triene precursor **337** (scheme 4.13).[32] This demonstrates that the DA reaction actually occurs *via* pyrrolinone **337** to afford cyclization adducts without stereoselectivity although the *N*-acyl is absent. This provides indirect evidence for the involvement of DA reaction during the isoindolone core formation and also suggests a Diels-Alderase should be involved to favor the *endo*-transition state during biosynthesis at room temperature.

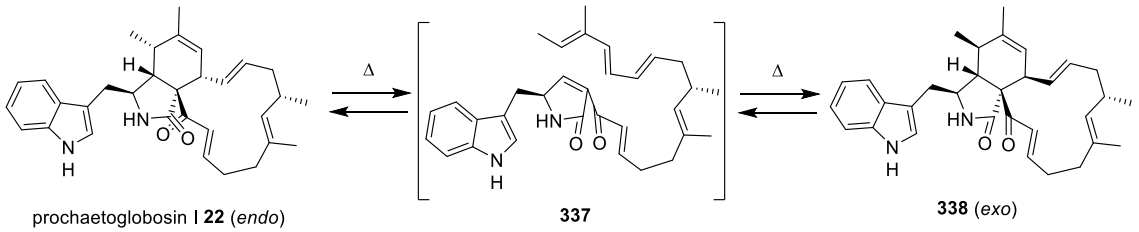

Scheme 4.13 Retro Diels-Alder reaction of the chaetoglobosin precursor **22**.

4.1.4.3 Indirect Biological Evidences of a Putative Diels-Alderase

Biologically, the heterologous expression of the cytochalasin E **5** gene cluster (*ccsC* and *ccsA*) from *A. clavatus* and PKS-NRPS gene cluster (*RAP2* and *SYN2*) from *P. oryzae*

in the host *A. nidulans* produced two decalin compounds niduclavin **39** and niduporthin **53** respectively.[44] The failure to observe the expected DA reaction adduct, *e.g.* the isoindolone core, demonstrates that the putative DAase is required to control the IMDA reaction regioselectively, otherwise the decalin will be formed possibly in a spontaneous way.

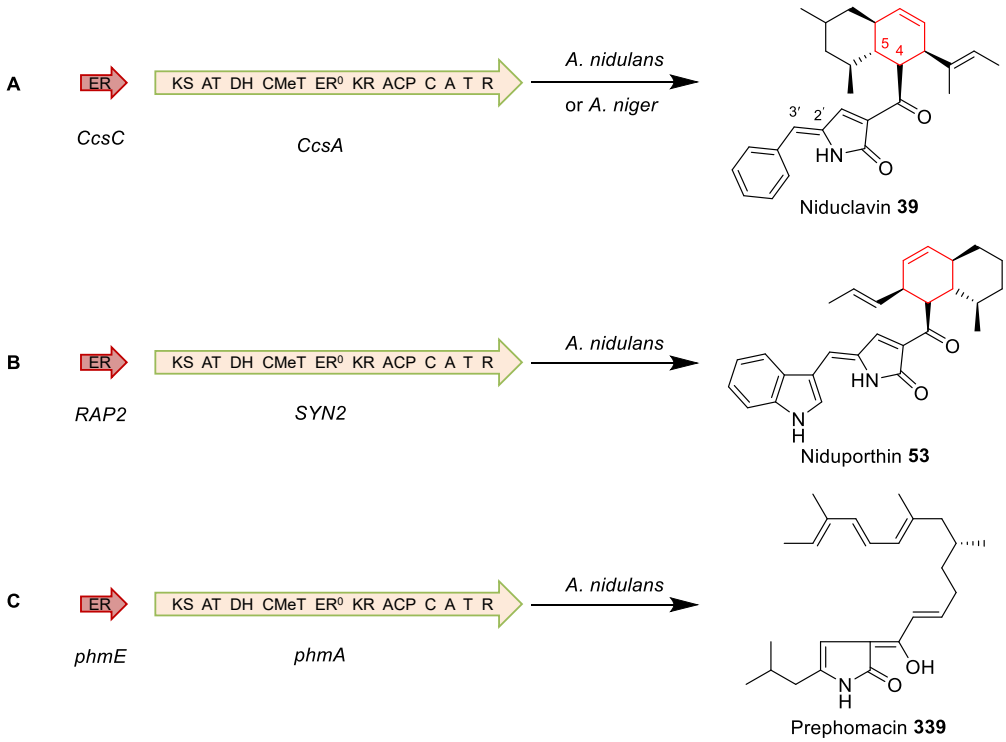

Sceheme 4.14 Heterologous expression of PKS-NRPS gene clusters in *A. nidulans*.

Recently, Chooi and co-workers reported the heterologous expression of the PKS-NRPS gene (*phmA*) and *trans*-ER (*phmE*) from *Parastogonospora nodorum* in *A. nidulans* (Scheme 4.14C).[150] Instead of the decalin compounds **39** and **53** (scheme 4.14), the Knoevenagel condensation product 2-pyrrolinone **339** was isolated and characterized. However, heterologous expression of the whole gene cluster in *A. nidulans* including the putative Diels-Alderase (*phmD*) still produced 2-pyrrolinone **339** rather than the expected isoindolone core, suggesting that the tautomeric pyrrolinone prephomacin **339** is not competent as a dienophile for the Diels-Alder reaction. This observation is consistent with what was observed during myceliothermophin E **60** biosynthesis that Diels-Alderase cannot catalyse cyclization with incorrect tautomeric pyrrolinone (section 1.4).[108]

Based on these indirect chemical and biological evidences, an IMDA reaction is speculated to be involved in the biosynthesis of the cytochalasan isoindolone core and a putative DAase must be needed to control the region- and stereo-selectivity. However, the DAase responsible for the isoindolone formation has not been identified yet.

4.2 Aims

From the first cytochalasan discovery in 1966, there have been approximately 400 cytochalasans reported.[151] However, the biosynthesis of this kind of bioactive and useful compound is still mysterious especially the formation of the isoindolone framework. The Diels-Alder reaction is proposed to occur to form the cytochalasan isoindolone core. But it is still not clear whether the Diels-Alder reaction is a spontaneous or an enzyme catalysed reaction. It is challenging to prove a putative Diels-Alderase partially because the natural [4+2] cyclization substrate is frequently complex and time-consuming to prepare for the testing of activity and mechanistic study of the candidate enzymes.[152]

In this section, we aim to verify the proposals of cytochalasan biosynthesis, especially Diels-Alder reaction through *in vitro* assays. The cryptic ACE1 metabolite is believed to be a member of the cytochalasan family even though the structure has not been elucidated yet.[47] As the ACE1 metabolite shows its potential application as an agrochemical for crop protection,[47] we expect to investigate cytochalasan biosynthesis with its DA precursor and find out its structure as well.

For the best case scenario, the substrate for the *in vitro* assays is the aldehyde **56b** after chain reductive release, which possesses the same backbone with ACE1 shunt product **52**. Considering that cytochalasin E **5** has the olefin at C-4/C-5, while the cytochalasin E **5** shunt metabolite C-4/C-5 is saturated during heterologous expression in *A. oryzae*, it is possible that the olefin at C-4/C-5 is reduced by an unknown enzyme in *A. oryzae* to saturated carbons (scheme 4.15A). Therefore, there is also a possible olefin at C-4/C-5 in the ACE1 shunt metabolite **52**, thus we would like to introduce the possible olefin at C-4/C-5 for the substrate. As the methyl groups on the alkyl chain may be not crucial for the enzyme activity, a model compound **116** is designed mimicking the ACE1 precursor **56b** for an initial attempt. As it is found out that *O*-methyl tyrosine is incorporated into the ACE1 metabolite backbone,[36] model C **116** is also designed with an *O*-methyl tyrosine (scheme 4.15B).

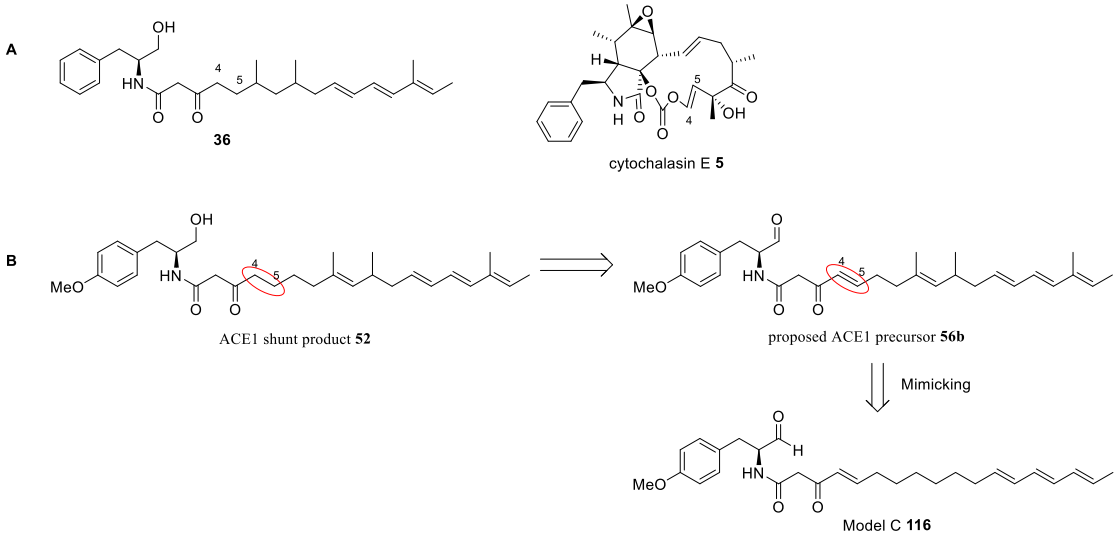

Scheme 4.15 A, possible reduction of cytochalasin E **5** backbone double bond at C-4/C-5 during heterologous expression in *A. oryzae*; **B**, design of model C **116** mimicking ACE1 shunt product **52**.

Model C **116** can be applied to both *in vivo* and *in vitro* assays. For *in vivo* assays, Model C **116** can be fed into *P. oryzae* cultures to study if it can be incorporated and modified to a new cytochalasan. For *in vitro* assays, firstly it will be used for Knoevenagel condensation tests to confirm if it is spontaneous. Afterwards, *in vitro* assays of Diels-Alder reaction would be performed using Knovenagel condensation product pyrrolinone as the substrate. The enzymes ORFZ and ORF3 would be expressed and purified from *E. coli* by Verena Hantke.

4.3 Results and Discussion

4.3.1 Model C Retrosynthetic Analysis

Model C **116** was designed to mimick the ACE1 shunt **52** for both Knovenagel condensation and Diels-Alder reaction tests. Therefore both β-keto amide and triene moieties have to be included in the model. We initially planned to make the aldehyde by deprotection of the corresponding cyclic acetal. At the start of this study, tyrosine, rather than *O*-methyl tyrosine, was believed to be the amino acid incorporated. We assumed that the methyl groups on the alkyl chain may be unimportant for the Knoevenagel and Diels-Alder reactions. This would greatly simplify the required synthesis. Therefore we

first planned to synthesize the model without the side-chain methyl groups (scheme 2.14).

The retrosynthetic analysis is shown in scheme 4.16. The amide bond is disconnected to fragment A **342** and fragment B **343**. The *β*-keto amide can be introduced through the thermolysis of dioxinone. Originally, fragment A **342** was a tyrosine derived cyclic acetal, while fragment B **343** can be further disconnected to fragment C **167** and fragment D **345** which can be assembled by a Horner-Wadsworth-Emmons reaction. Fragment C **167** is a known compound which was first prepared by Boeckman *et al*.[153] for the synthesis of tetramic acids, permitting Wadsworth-Emmons olefination under mild conditions. Fragment D **345** is long chain aldehyde with triene at the end of the chain.

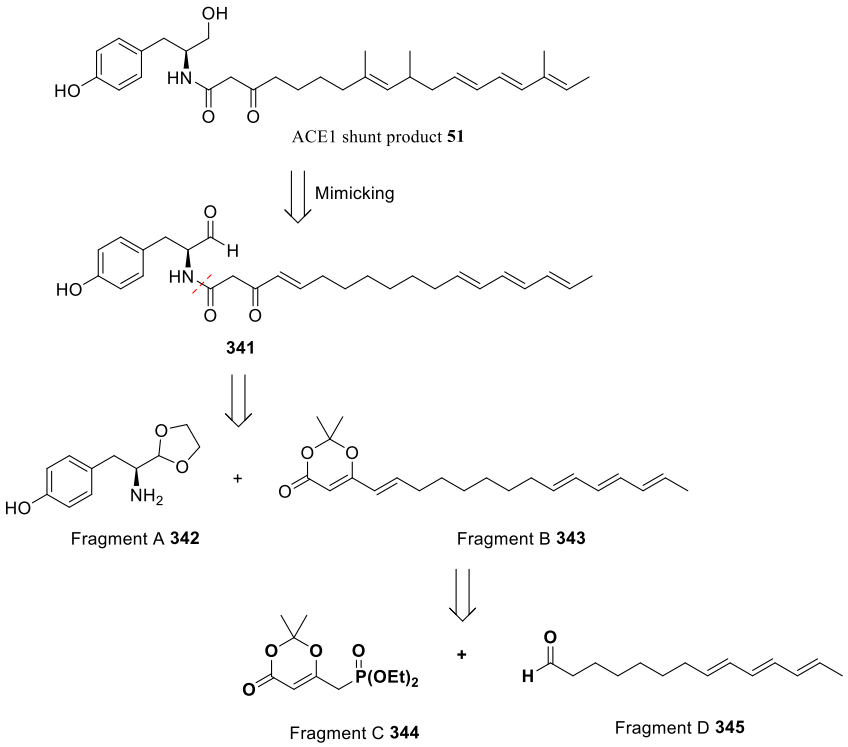

Scheme 4.16 Model design and retrosynthetic analysis.

Fragment A **342** is a known compound derived from methyl *L*-tyrosine **346** in 5 steps (Scheme 4.17).[154] Nakamura and co-workers protected the amino group with Cbz of *L*-tyrosine methyl ester **346**. The aldehyde **349** was prepared by oxidation of alcohol **348** following protection with ethylene glycol to afford the cyclic acetal **350**.

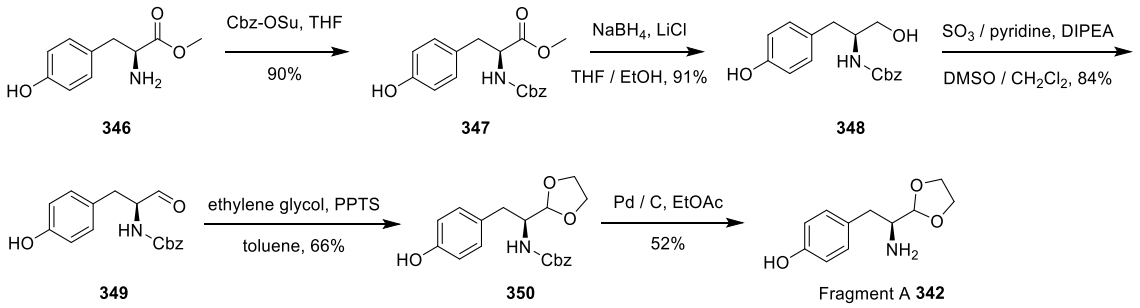

Scheme 4.17 Nakamura's synthetic route to fragment A **342**.

We chose a different synthetic route to provide fragment A **342** in 4 steps. Since different amino protected *L*-tyrosines are commercially available, we planned to start with Fmoc protected *L*-tyrosine because Fmoc is resistant to acid condition during cyclic acetal formation. However, Fmoc-tyrosine is very expensive as starting material (1 g, 75 €, Iris Biotech GmbH) while *bis*-protected compound **351** is much cheaper (25 g, 50 €, Iris Biotech GmbH) and the *tert*-Butyl group can be deprotected simultaneously during acetal formation under acid conditions. The aldehyde could be prepared by a reduction of ester, or Weinreb amide (scheme 4.18). Here we chose the latter method which is a reliable way to provide aldehydes in high yield. The aldehyde could be protected by ethylene glycol in the presence of acid. Organic base can be used to deprotect Fmoc easily to free amino group.

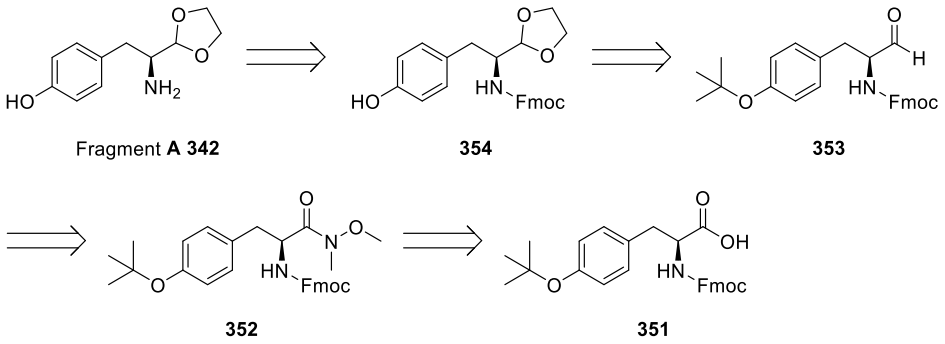

Scheme 4.18 Fragment A **342** retrosynthetic analysis.

Fragment D **345** is a new compound, but an analog **362** was prepared by Millar and co-workers in an efficient way (scheme 4.19).[155] In their synthesis, Wittig reaction was applied for the construction of the triene and the *ZEE* isomer was converted to *EEE* by

iodine under light. After release of alcohol and Swern oxidation, compound **362** was prepared in a short and effictive way.

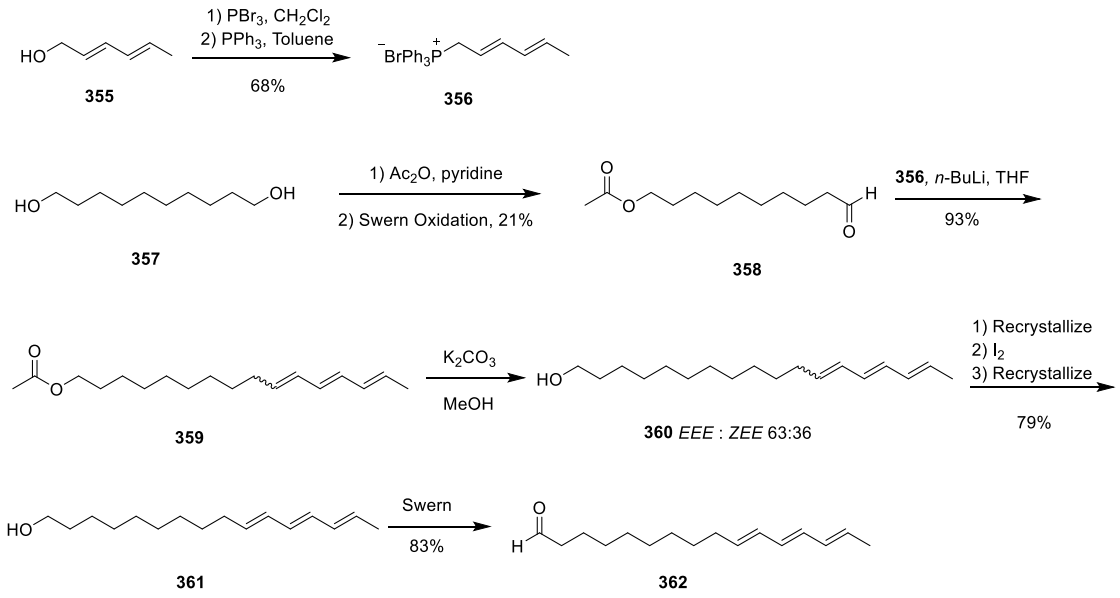

Scheme 4.19 Millar's strategy to prepare compound **362**.

Here we adopted their synthetic strategy to prepare fragment D **345**. Wittig reaction was applied to build the triene moiety between a diene **356** and aldehyde **365**. The diene compound **356** was known to be derived from commercially available dienol **355**.[155] The other reagent for the Wittig reaction is aldehyde **365** which could be prepared from mono protection of diol **363** and oxidation (Scheme 4.20).

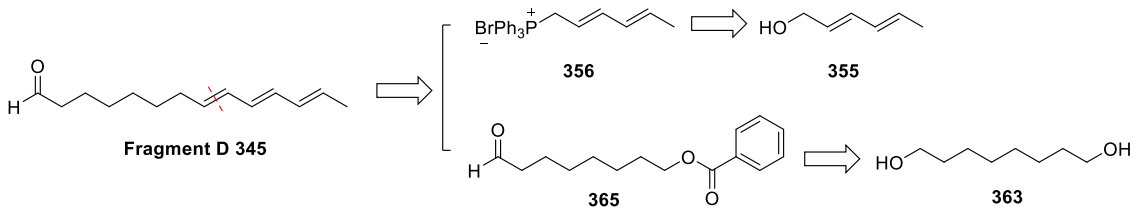

Scheme 4.20 Retrosynthetic analysis of fragment D **345**.

4.3.2 Model C Synthesis

4.3.2.1 Synthesis of Fragment A

The approach to the construction of modified tyrosine **342** began with commercially available Fmoc and *t*-Bu protected *L*-tyrosine **351**, which was employed to make Weinreb amide **352** in high yield. Weinreb amide **352** can be stored in -20 ^{o}C for long time until needed. Next, Weinreb amide **352** was selectively reduced with $LiAlH_4$ to aldehyde **353** at 0 °C for 1 h. The resulting aldehyde **353** was protected with ethylene glycol, catalysed by *p*-TsOH, in high yield. During the protection of the aldehyde **353**, the *tert*-butyl group on the phenol was simultaneously deprotected. Finally, diethylamine was used to remove the Fmoc group to afford fragment A **342** in good yield. All the compounds were prepared without optimisation (scheme 4.21).

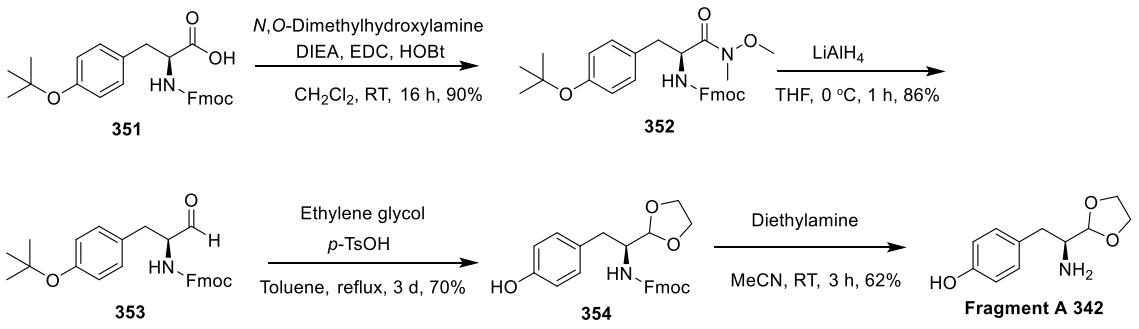

Scheme 4.21 Synthesis of fragment A **342**.

4.3.2.2 Synthesis of Fragment C

Fragment C **167** was prepared by lithiation of freshly distilled acetone diketene adduct **161** in THF at -50 °C, followed by quenching the resultant yellow precipitate with an excess of hexachloroethane (scheme 4.22).[153] The resultant chlorinated acetone diketene adduct **166** was treated with potassium diethylphosphite **367** in DMF to afford fragment C **167** *via* a nucleophilic substitution.

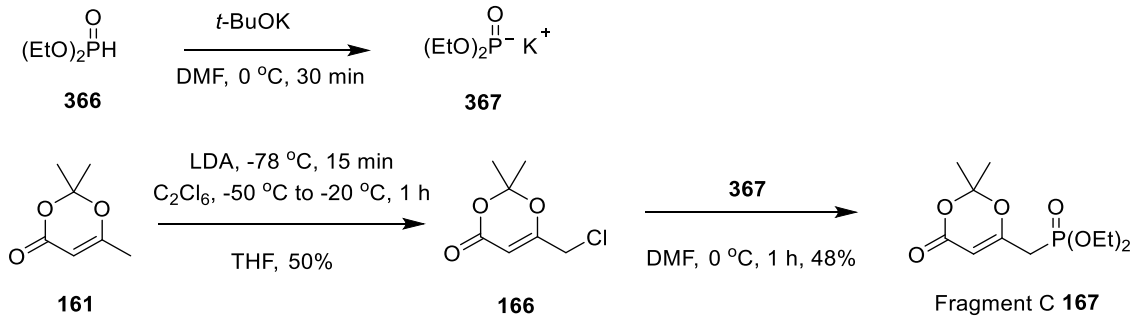

Scheme 4.22 Synthesis of Fragment C **167**.

4.3.2.3 Synthesis of Fragment D

The synthesis of fragment D **345** started from the preparation of Wittig reagent **356** and aldehyde **365**. Mono protection of octane-1,8-diol **363** with benzoyl chloride following by Swern oxidation afforded aldehyde **365**. Wittig reagent **356** was prepared by bromination of (2*E*,4*E*)-hexa-2,4-dien-1-ol **355** with phosphorus tribromide at -10 °C and treating with triphenylphosphine in toluene at room temperature for 3 d. Wittig reaction between **356** and aldehyde **365** with *n*-BuLi gave triene mixture **369** in moderate yield (*EEE*:*EEZ* = 64:36 from NMR). The mixture of *E* and *Z* isomers cannot be separated by flash chromatography, but the mixture was directly used for the hydrolysis of acetate **369** with anhydrous K_2CO_3 in MeOH. After hydrolysis, the *EEE*-isomer **370** can be obtained from recrystallization with *n*-hexane in 50% yield while the *EEZ*-isomer in mother liquor can be isomerized to the *EEE*-isomer **370** using a catalytic amount of iodine exposed to light for 10 min. After a second recrystallization, a further 15% *EEE*-isomer **370** was obtained and the combined trienol **370** was oxidized by Swern oxidation to give fragment D **345** (scheme 4.23). Fragment D **345** underwent rapid degradation during flash chromatography. Therefore it was used directly in the next step after drying, without further purification. Compounds containing the triene moiety are sensitive to light and undergo polymerization, so they should be kept in the dark.

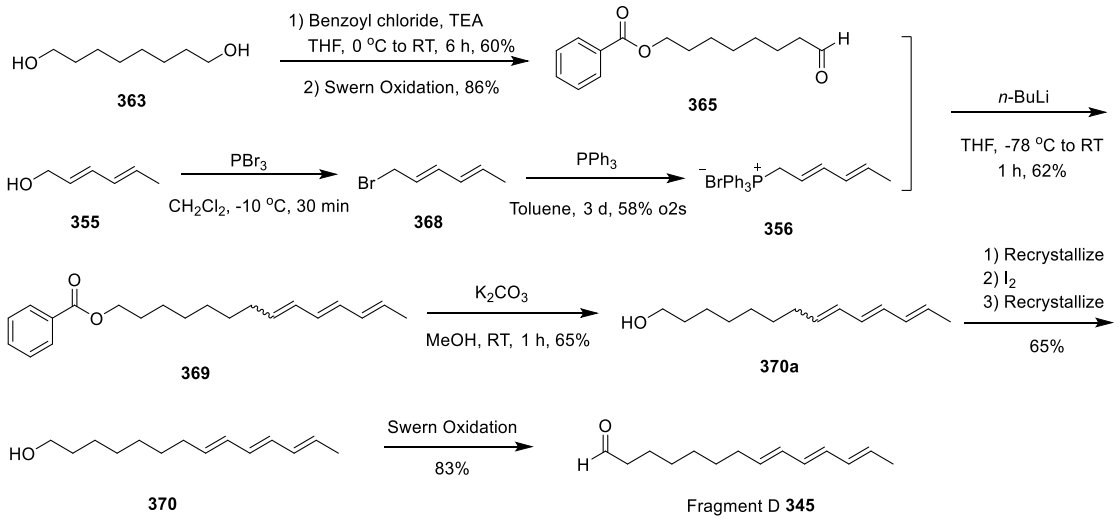

Scheme 4.23 Synthesis of Fragment D **345**.

4.3.2.4 Coupling of Fragment A, Fragment C and Fragment D

The coupling strategy is shown in scheme 4.24. Synthesis of fragment B **343** was achieved by a Horner-Wadsworth-Emmons (HWE) reaction between fragment C **167** and fragment D **345** with *n*-BuLi at -78 °C in low yield, possibly because of the triene degradation on the silica gel. After purification by flash chromatography, fragment B **343** underwent thermal decomposition above 100 °C in toluene in the presence of fragment A **342** to afford the corresponding *β*-keto amide **371**. But the deprotection of the cyclic acetal **371** proved to be more difficult than anticipated. Several attempts including HCl, AcOH, TFA, *p*-TsOH and several Lewis acids such as bis(acetonitrile)dichloropalladium(II), $FeCl_3$, $InCl_3$, $LiBF_4$, Ph_3BF_4, as well as netural catalysts pyridinium *p*-toluenesulfonate (PPTS) were made at room temperature overnight. All these attempts failed to deprotect **371** because either the triene degraded under the acidic conditions, or the cyclic acetal was resistant to the reaction conditions.

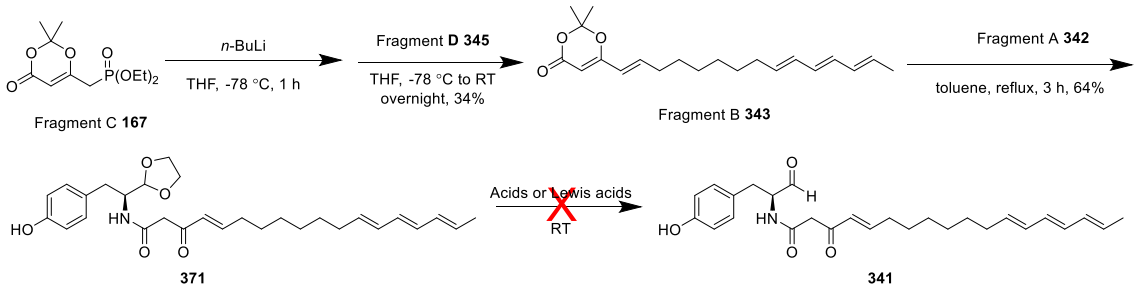

Scheme 4.24 Coupling of fragment A **342**, fragment C **167**, fragment D **345** and deprotection.

Finally, the deprotection was achieved using HCl in aqueous THF at 60 °C for 3 h. With lower concentration of acid and shorter reaction time, the triene can be kept intact. But the corresponding Knoevenagel condensation product pyrrolinone **372** was formed spontaneously under these conditions. As previously observed (chapter 3.3.3), the pyrrolinone **372** tautomerised to enol form **372b** (scheme 4.25).

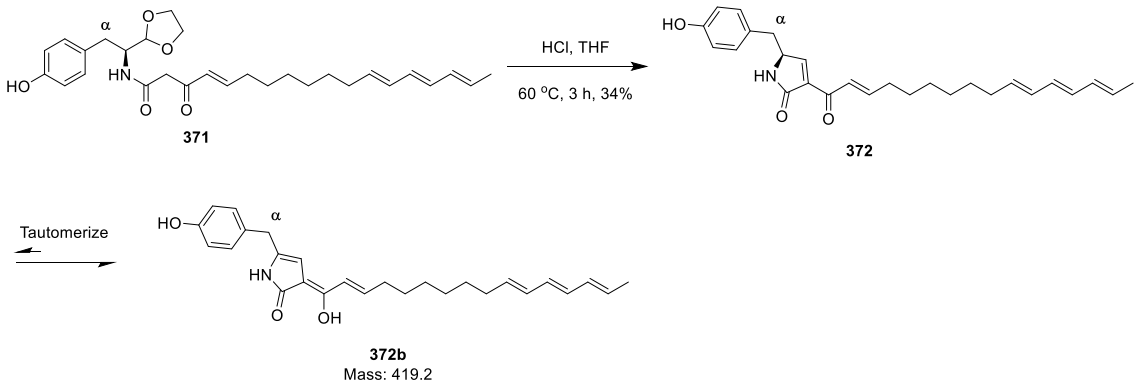

Scheme 4.25 Deprotection of **371** and tautomerism.

The LCMS data of pyrrolinone **372b** shows its UV absorbance at 398 nm, which is characteristic of pyrrolinone tautomerism absorbance and even longer because of the additional double bond conjugation (Figure 4.3). The characteristic trident triene UV is also observed around 266 nm. It is eluted quite late at 11.3 min in LCMS because of the high hydrophobicity of the molecule. The ES^+ (420.3) and ES^- (418.2) also fit the molecular mass (419.2). However, there is no DA adduct observed in LCMS.

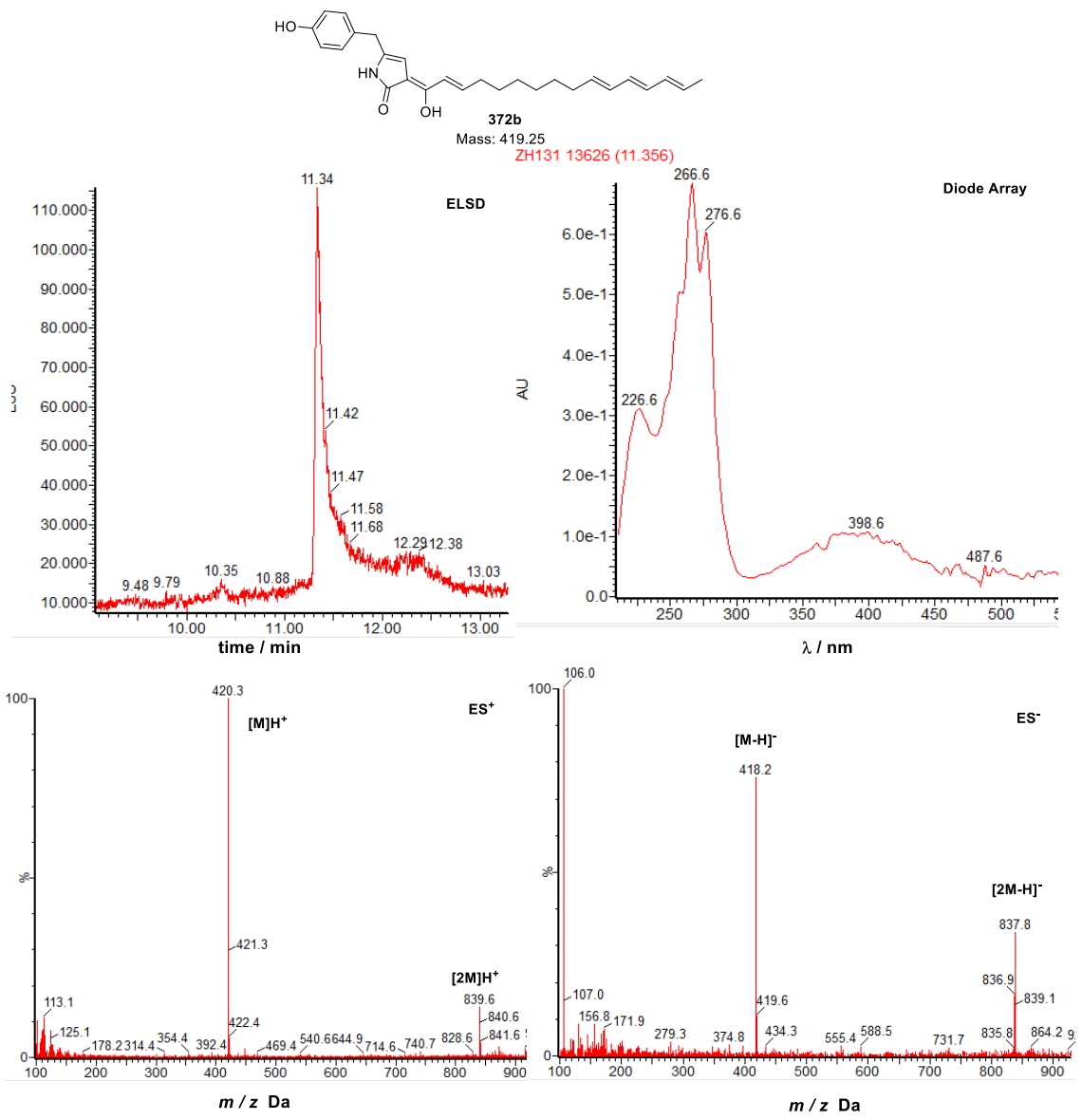

Figure 4.3 LCMS data of compound **372b**.

Pyrrolinone **372b** is relatively stable at -20 °C for several months, but it is unstable at room temperature and only ^{1}H NMR is available. From the ^{1}H NMR data shown in figure 4.4, we can see benzylic protons at 3.66 ppm are singlet rather than a doublet doublet because compound **372** rapidly tautomerised to **372b** and lost chiral center, which further confirms the pyrrolinone tautomerism. Also the ^{1}H chemical shift of H-4 at 5.6 ppm agrees with model B pyrrolinone **204b**.

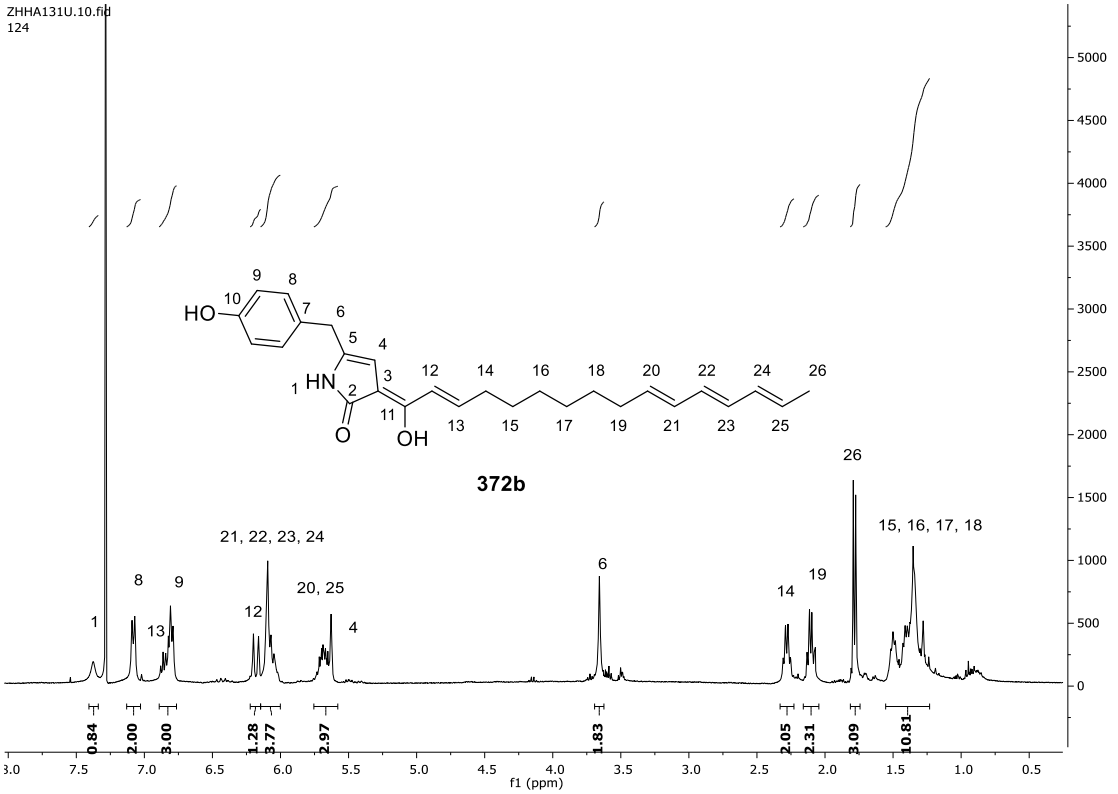

Figure 4.4 ^{1}H NMR of compound **372b** in $CDCl_3$.

Even though pyrrolinone **372b** was formed spontaneously at 60 °C under acidic conditions, it is hard to make a conclusion that the Knoevenagel condensation is a spontaneous reaction under biological conditions.

The inability to isolate the required aldehyde **341** meant that we had to redesign the synthesis to use a more easily deprotected aldehyde blocking group. Here we chose to use the diethyl acetal group which can be hydrolysed at 0 °C. Thus the synthetic route was modified as shown in scheme 4.26. Protected tyrosine *O*-methyl ether **212** was already available (section 3.3.2), and this coupled smoothly with fragment B **343** under standard conditions. This gave **374** which was then smoothly deprotected to the required aldehyde **116** at 0 °C in a mixture of aqueous HCl and THF. By this stage of the project we realized that *O*-methyl tyrosine was the correct substrate incorporated into ACE1 metabolite.

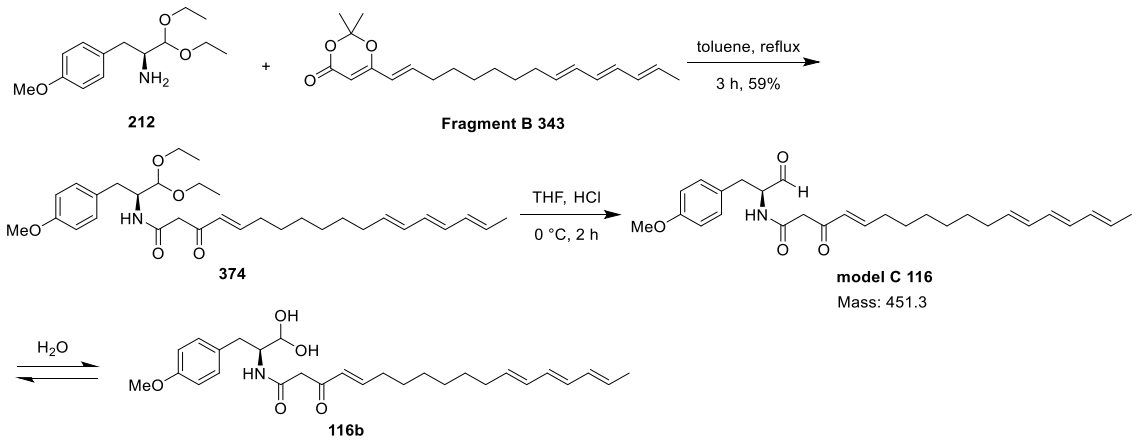

Scheme 4.26 Synthesis of model C **116** *via* hydrolysis.

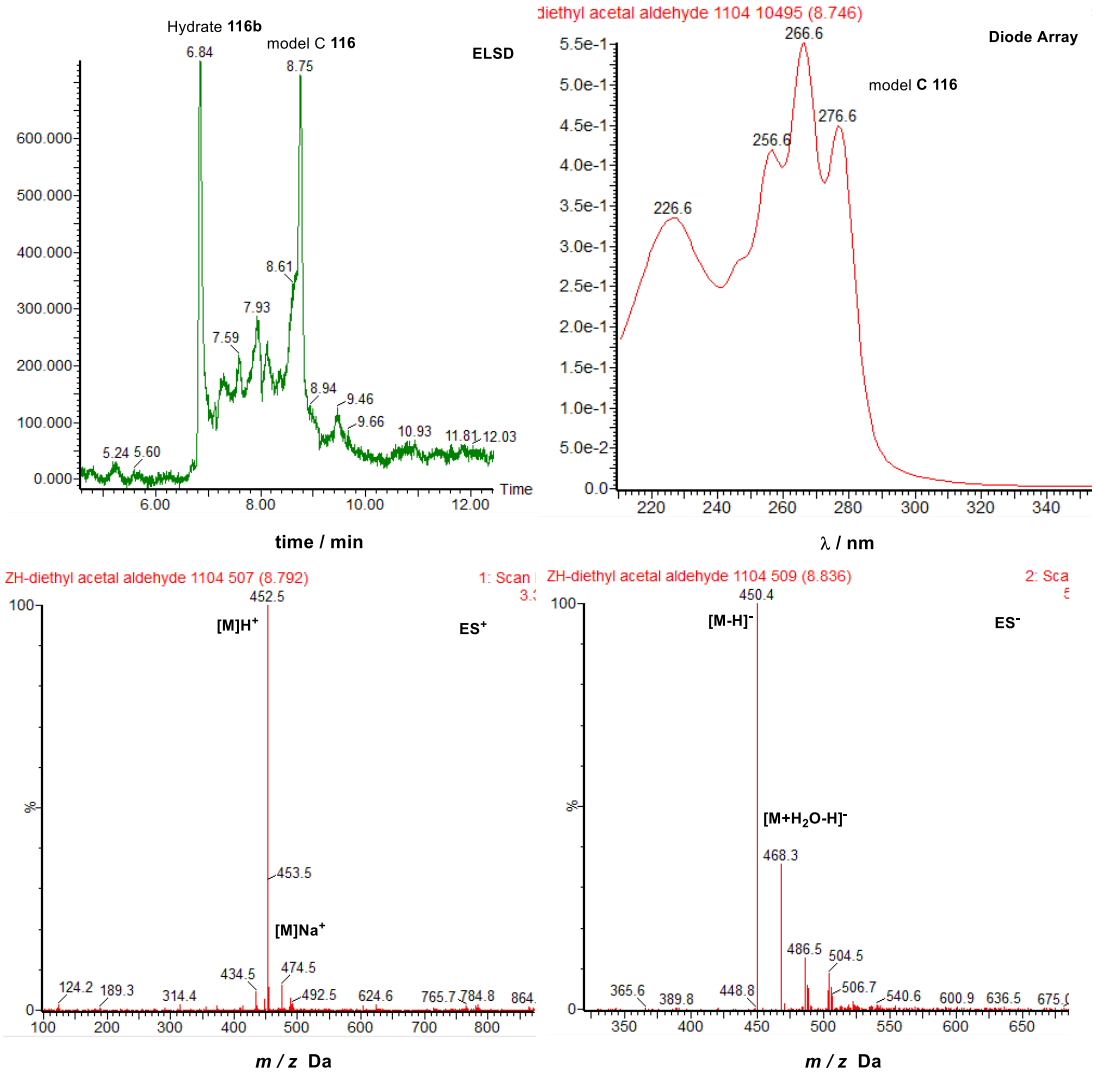

Figure 4.5 LCMS data of Model C **116**.

The LCMS data of model C **116** shows that it is eluted between 6.8 min to 8.8 min because the aldehyde is in equilibrium with hydrate in the presence of water (figure 4.5). The trident absorbance is the characteristic UV spectrum of the triene moiety around 266 nm. The molecular weight of model C **116** (451.3) can also be found in both ES^+ (452.5) and ES^- (450.6).

4.3.2.5 Model C Pyrrolinone Synthesis

Pyrrolinone **376b** was first synthesized by chemical methods to investigate its properties including retention time and UV spectrum before assays. The diethyl acetal **374** was treated with TFA in CH_2Cl_2 at room temperature for 3 h to provide **376** (Scheme 4.27). The UV absorbance at 387 nm indicates it tautomerises to **376b** (Figure 4.6). After tautomerism, it is no longer suitable for Diels-Alder reaction.[108] However, it is unstable to complete the NMR measurement, so only the LCMS data is available for the moment.

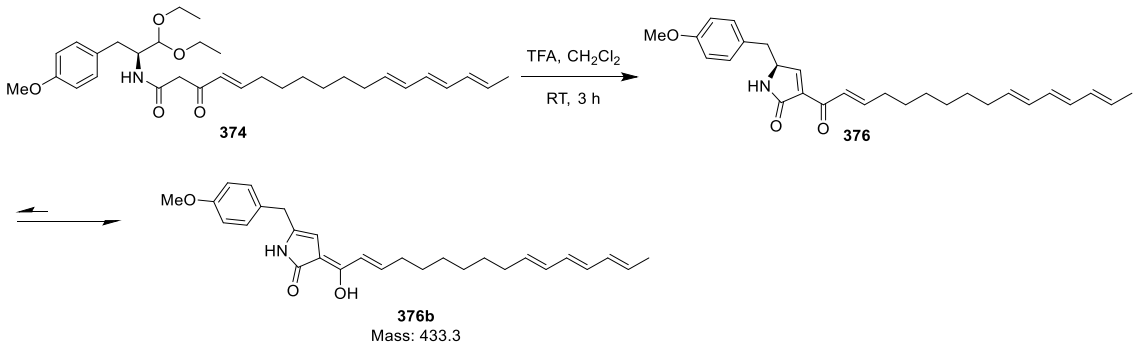

Scheme 4.27 Synthesis of pyrrolinone **376b**.

The LCMS data of pyrrolinone **376b** is shown in figure 4.6. A clear conversion of diethyl acetal **374** to pyrrolinone **376b** was observed after reaction and it was eluted quite late because of the hydrophobicity of the molecule. The UV showed the typical trident absorbance of the triene at 266 nm as well as the characteristic absorbance above 300 nm from the tautomerised pyrrolinone. The mass spectra ES^+ (434.5) and ES^- (432.3) also fit the pyrrolinone molecular weight (433.3).

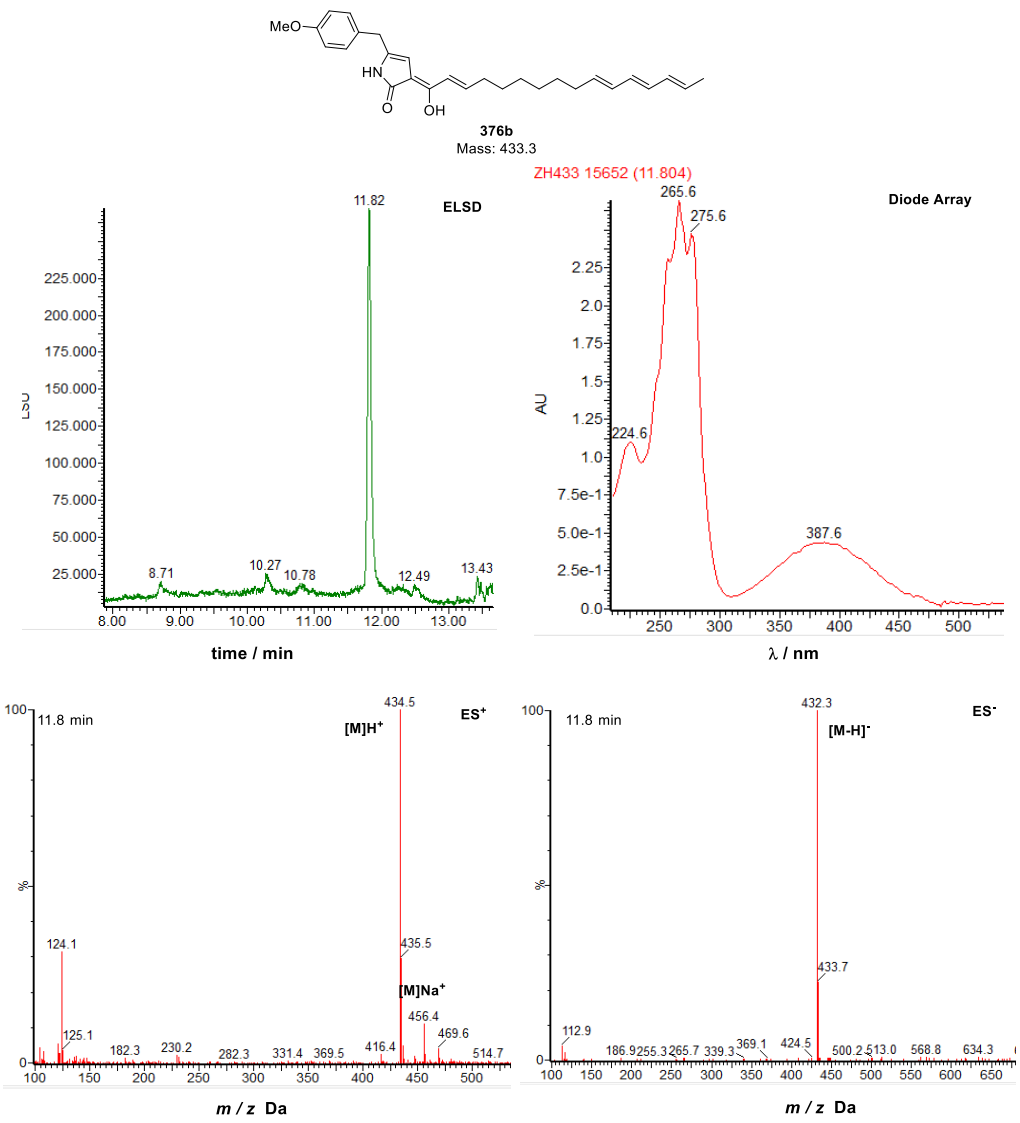

Figure 4.6 LCMS data of pyrrolinone **376b**.

4.3.3 Model C Bioassays

4.3.3.1 Preparation of Proteins and Cell Free Extract

The ORFZ and ORF3 proteins were prepared and partially purified from *E. coli* expression by Verena Hantke. In addition, cell free extract was prepared from *A. oryzae* NSAR1 cells expressing the *ACE1*, *RAP1* and *ORFZ* genes from the *ACE1* gene cluster. The cells were frozen in liquid nitrogen in mortar and ground to even powder. Then 2 mL potassium phosphate buffer (pH 7.0, 50 mM) was added and mixed with the cell

powder. After collection by centrifugation at 16000 × g for 30 min at 4 °C, the supernatant was collected and stored for further tests.

4.3.3.2 Model C Assays in Water and Buffers

As previously discussed in chapter 2, the Knoevenagel condensation involved in cytochalasan biosynthesis is probably a spontaneous reaction. Since model C **116** is similar to cytochalasin precursor, it was firstly used to test Knoevenagel condensation in water and potassium phosphate buffers to investigate its properties.

The assays were performed in 250 µl volume containing 4 mM model C **116** and 50 µl DMSO. The solvents used for assays were H_2O, 40 mM potassium phosphate buffer (pH 6.5, 7.0, 7.5, 8.0) and 80 mM potassium phosphate buffer (pH 8.0) respectively. After incubation at 30 °C over time (2 h, 4 h and 6 h), 50 µl reaction mixture was diluted with equal volume of acetonitrile before analysis by LCMS.

Figure 4.7 shows that model C **116** is stable in H_2O at 30 °C. After 6 h, there was still no pyrrolinone detected by LCMS. The peak at 10.3 min is diethyl acetal **374** due to the incomplete hydrolysis.

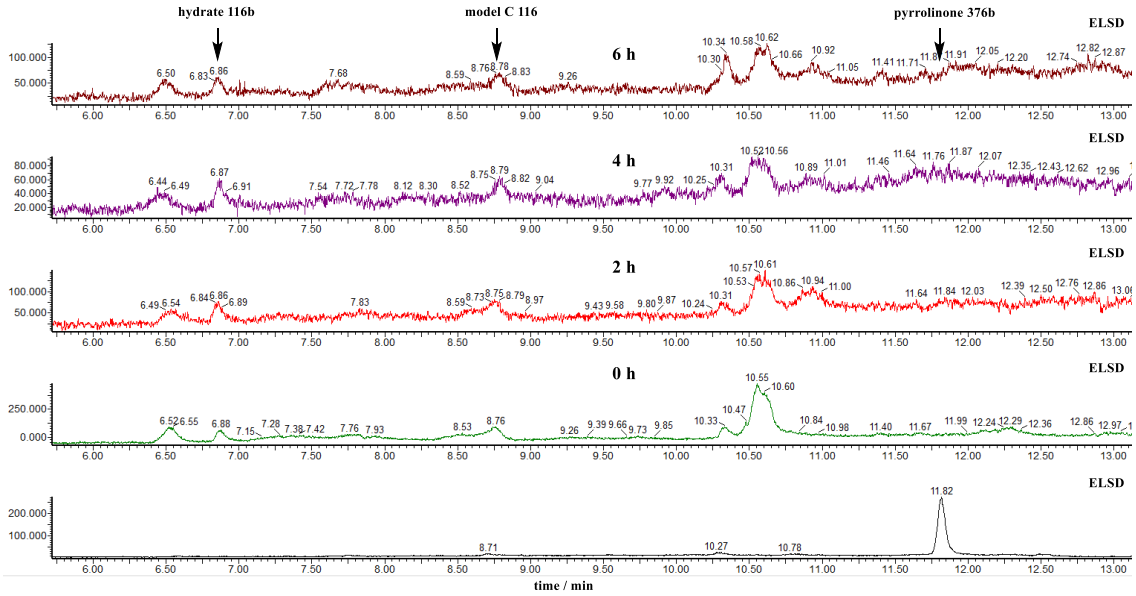

Figure 4.7 Model C **116** in H_2O over time at 30 °C.

However, model C **116** was converted to pyrrolinone **376b** at 11.8 min in 40 mM potassium phosphate buffer (pH 6.5) at 30 °C in 2 h (Figure 4.8). The peak at 8.7 min has the same molecular weight (433.3) as pyrrolinone **376b**, but its UV spectrum suggests that it is not pyrrolinone **376b** (Figure 4.9). Figure 4.10 shows the UV and mass at 7.7 min, which is possibly the hydrated pyrrolinone **378** based on the knowledge of model B **115** investigation.

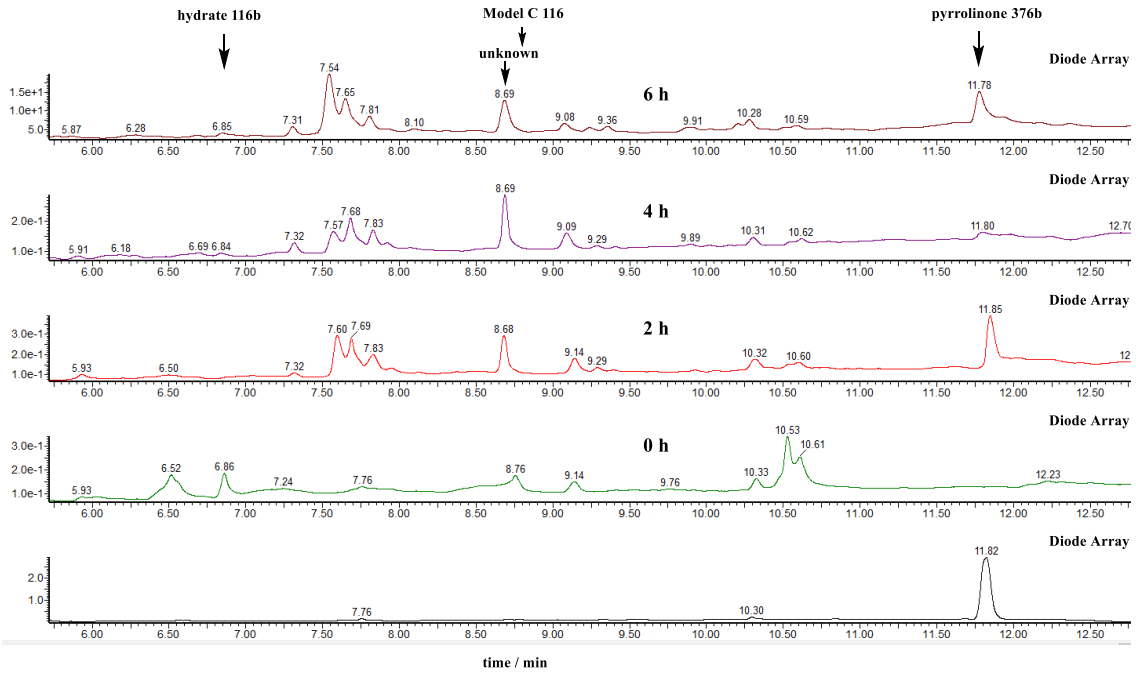

Figure 4.8 Model C **116** in 40 mM potassium phosphate buffer pH 6.5 over time at 30 °C.

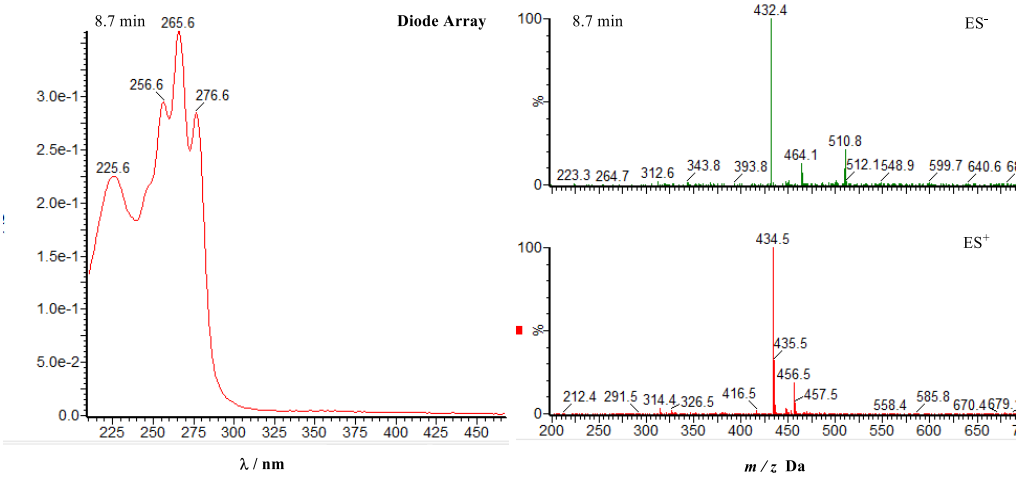

Figure 4.9 UV spectrum and molecular weight at 8.7 min.

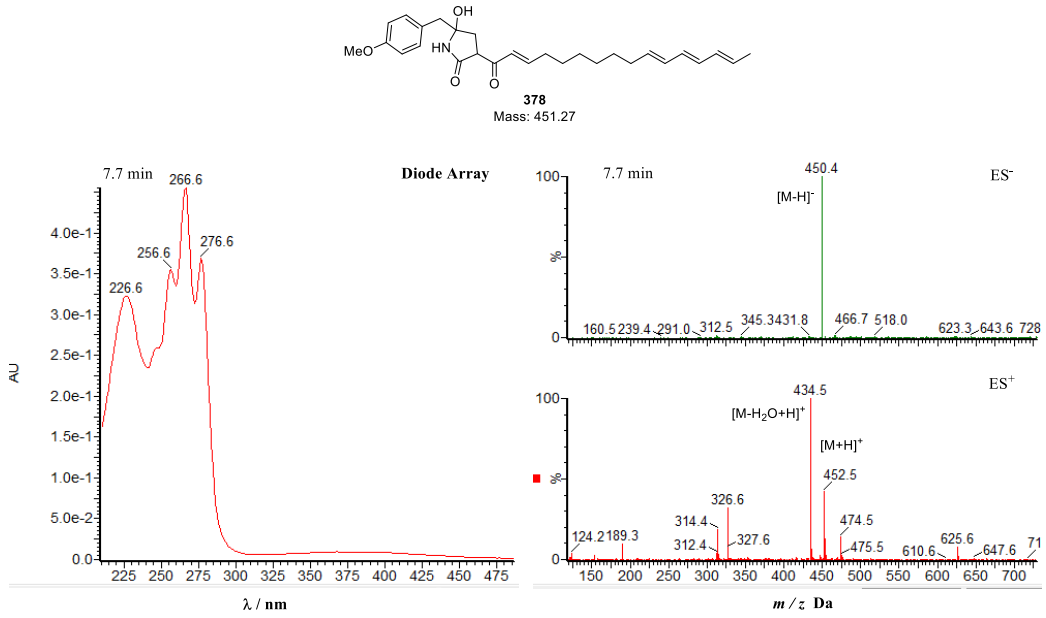

Figure 4.10 Possible structure, UV spectrum and molecular weight at 7.7 min.

Model C **116** showed similar performance in 40 mM phosphate buffer when pH value is 7.0 or 7.5 as shown in figure 4.11 and figure 4.12. Model C **116** disappeared and pyrrolinone **376b** was detected after 2 h at 30 °C. After 6 h, pyrrolinone **376b** was still detectable, suggesting that it is relatively stable in these conditions.

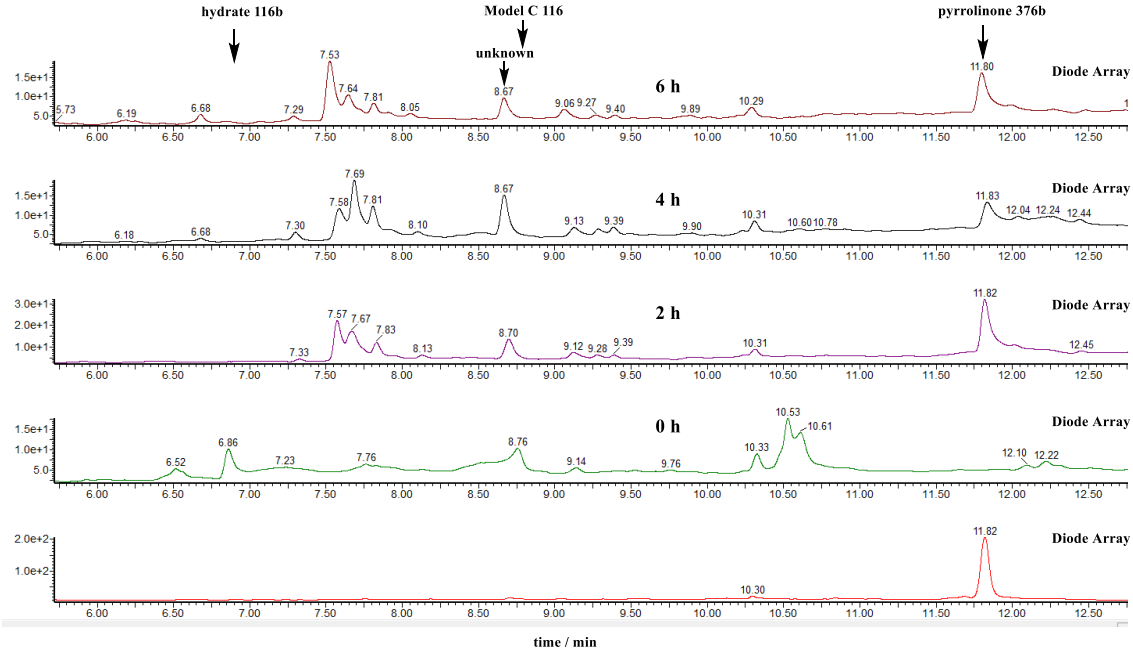

Figure 4.11 Model C **116** in 40 mM potassium phosphate buffer pH 7.0 over time at 30 °C.

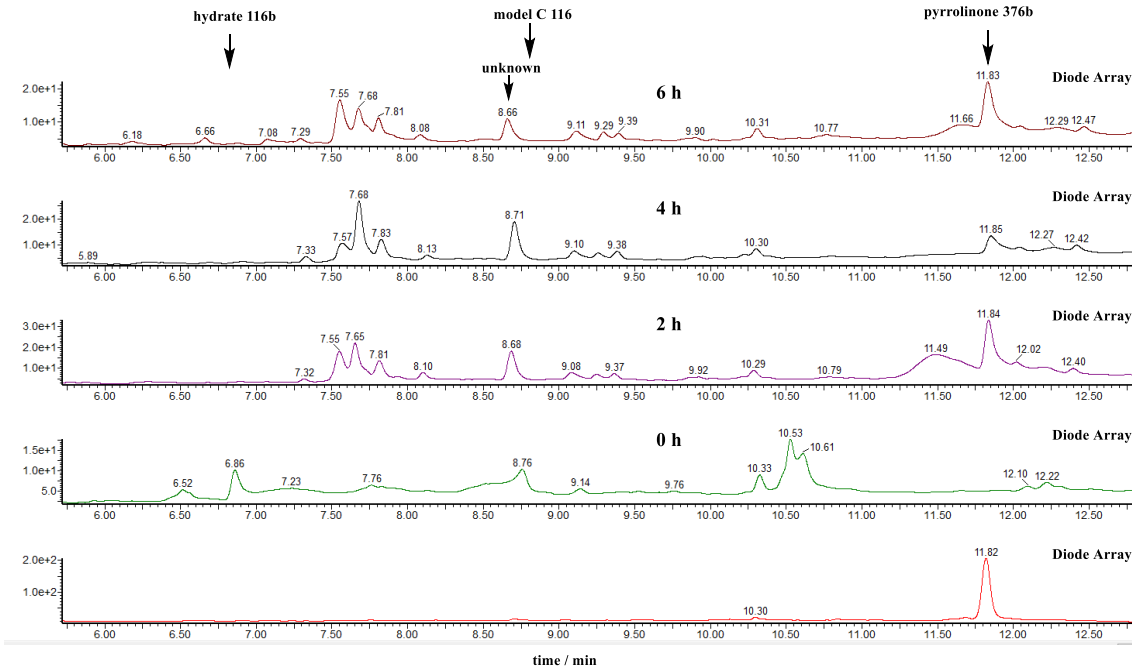

Figure 4.12 Model C **116** in 40 mM potassium phosphate buffer pH 7.5 over time at 30 °C.

Pyrrolinone **376b** was also formed in 40 mM potassium phosphate buffer (pH 8.0) after 2 h. However, it was converted after 4 h, indicating that pyrrolinone **376b** is less stable when the condition is more basic (Figure 4.13).

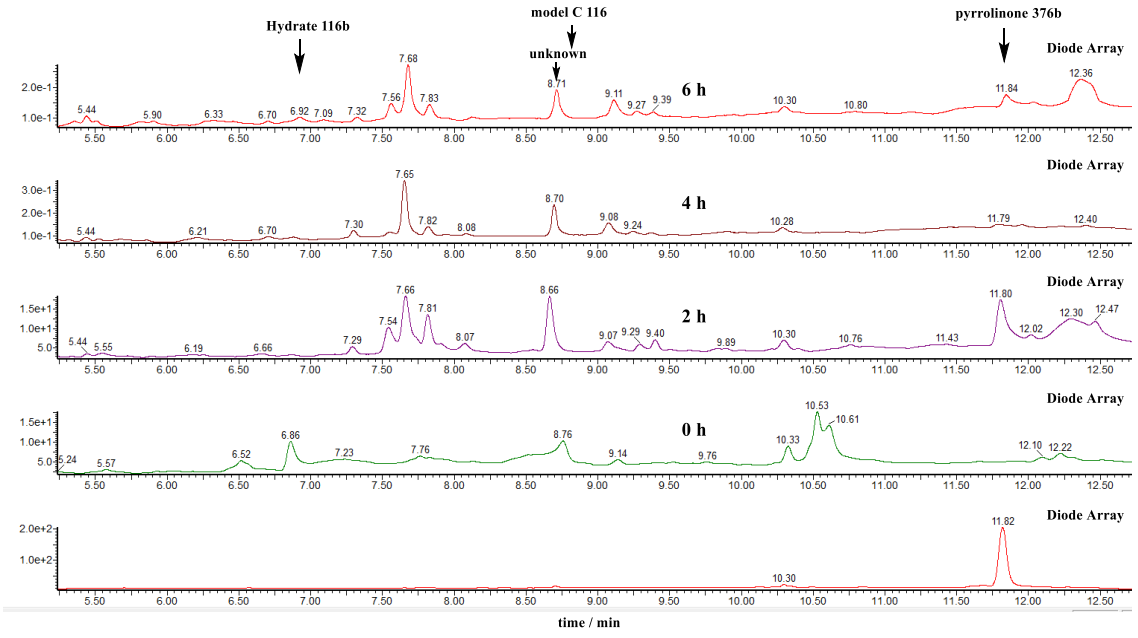

Figure 4.13 Model C **116** in 40 mM potassium phosphate buffer pH 8.0 over time at 30 °C.

When the concentration of phosphate buffer (pH 8.0) was 80 mM, there was no pyrrolinone **376b** detected after 2 h, possibly because it degraded in 2 h. Therefore it suggests phosphate ion has influence on the stability of pyrrolinone **376b** (Figure 4.14).

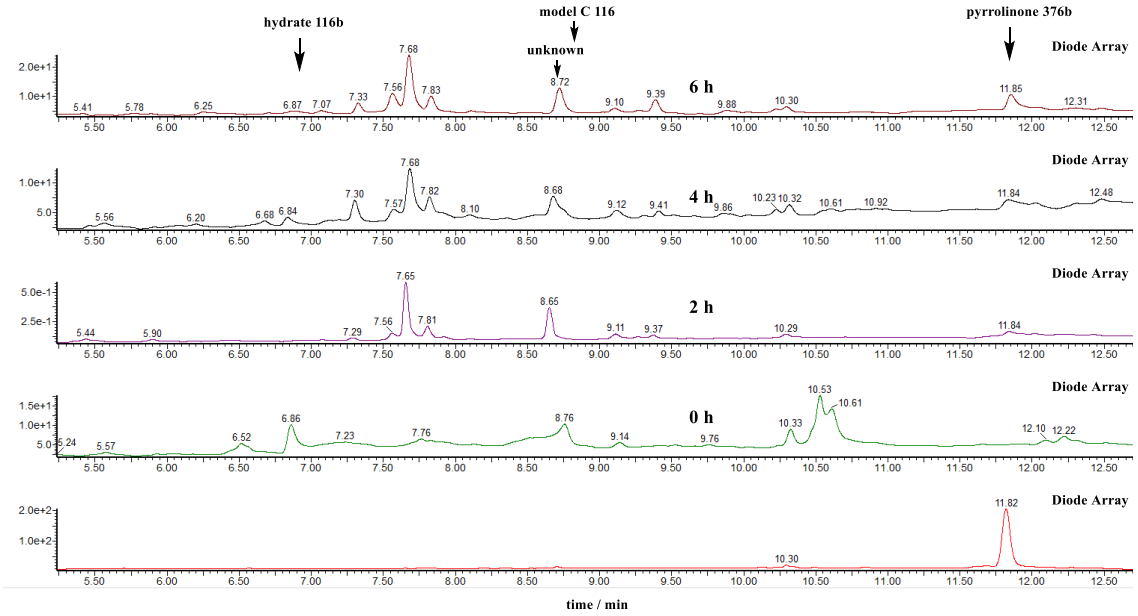

Figure 4.14 Model C **116** in 80 mM potassium phosphate buffer pH 8.0 over time at 30 °C.

4.4 Discussion and Future Work

4.4.1 Knoevenagel Condensation Tests

In this section, model C **116** mimicking shunt metabolite **52** was designed and prepared in a short and effective way. It was firstly used to test Knoevenagel condensation by *in vitro* assays. The assay results showed that Knoevenagel condensation was spontaneous in potassium phosphate buffer to give pyrrolinone **376b**, which was consistent with the assays with model B **115**. The recently reported cytochalasin heterologous expression in *A. nidulans* produced pyrrolinone **339**, which also suggests Knoevenagel condensation is spontaneous *in vivo* (scheme 4.28). Therefore we can make a conclusion that Knoevenagel condensation is a spontaneous reaction.

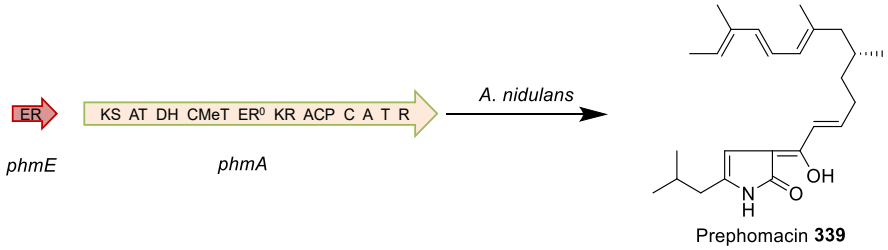

Scheme 4.28 Heterologous expression of cytochalasin genes in *A. nidulans* by Chooi and co-workers.[150]

But there is still minor possibility that α,β-hydrolase can accelerate pyrrolinone formation, even though the acceleration was not observed by *in vitro* assays with model B **115.** The enzyme activity has not been tested systematically with model C **116**.

4.4.2 Diels-Alder Reaction Investigations

The model C pyrrolinone **376b** was prepared under acidic condition which tautomerised to its enol form. There have been not much done with model C pyrrolinone **376b**, partially because all the chemical and biological evidences point to the fact that the enol form pyrrolinone cannot serve as dienophile for the Diels-Alder reaction.

Chemically, from the cytochalasan total synthesis (chapter one), it is known that tautomerised pyrrolinone is not suitable for Diels-Alder reaction any more in chemical conditions and an electron-withdrawing group has to be introduced to the pyrrolinone *N*-atom prior to Diels-Alder reaction.

Biologically, there has been no Diels-Alderase report regarding the isoindolone formation. However, the decalin ring formation catalyzed by Diels-Alderase MycB was reported by Tang group.[108] The non-tautomerised pyrrolinone **59** can form a decalin in the presence of MycB. But MycB cannot catalyse the decalin formation with tautomerised pyrrolinone **379** (scheme 4.29). This suggests that tautomerism of pyrrolinone can strongly influence the results of the *in vitro* assays even though the position of the dienophile did not change. Therefore it would be predictable the tautomerised pyrrolinone cannot form the isoindolone core of cytochalasan in biological condition since the position of the olefin in the dienophile shifts.

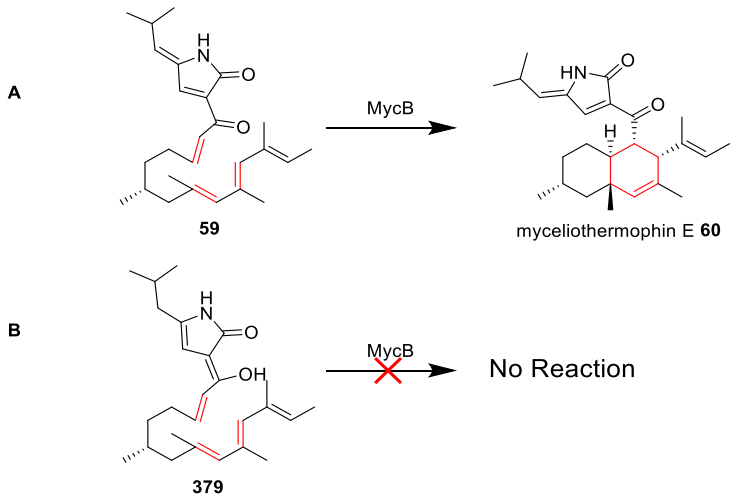

Scheme 4.29 Diels-Alderase cannot catalyze tautomerised pyrrolinone in the decalin formation.

Another biological evidence is heterologous expression of the full cytochalasin gene cluster including the gene encoding the putative Diels-Alderase in *A. nidulans* by Chooi and co-workers as shown in scheme 4.28.[150] However, instead of Diels-Alder adduct, pyrrolinone **339** was produced, suggesting the putative Diels-Alderase cannot catalyse the tautomerised pyrrolinone **339**.

4.4.3 Future Work

P. oryzae, which is the fungus for ACE1 metabolite production, can incorporate a variety of tyrosine derivatives to produce cytochalasan analogs. Therefore model C **116** feeding experiments in *P. oryzae* is ongoing to see if it can be incorporated and modified *in vivo*.

Besides, *in vitro* assays will be performed to investigate the ORFZ activity with model C **116** for catalysis of Knovenagel condensation. Moreover, model C pyrrolinone **376b** will be used for assays for Diels-Alder reaction. Though pyrrolinone tautomerism occurs, it might be still possible that Diels-Alderase can catalyse this reaction.

If ORF3 cannot catalyse the Diels-Alder cyclization of tautomerised pyrrolinone **376b**, it is worthwhile to have another try with non-tautomerised pyrrolinone, whose tautomerism is blocked by introducing a α-methyl group. Although the synthesis of compound **385** is not undertaken due to time constraints, a reasonable synthetic plan is drafted as shown in scheme 4.30. As α-methyl amino alcohol **228** and diketene

derivative **343** have already been prepared, so the synthesis can be achieved in 6 steps including protection of amino group, oxidation of alcohol, acetal formation, deprotection of carbamate, theromolysis and cyclization.

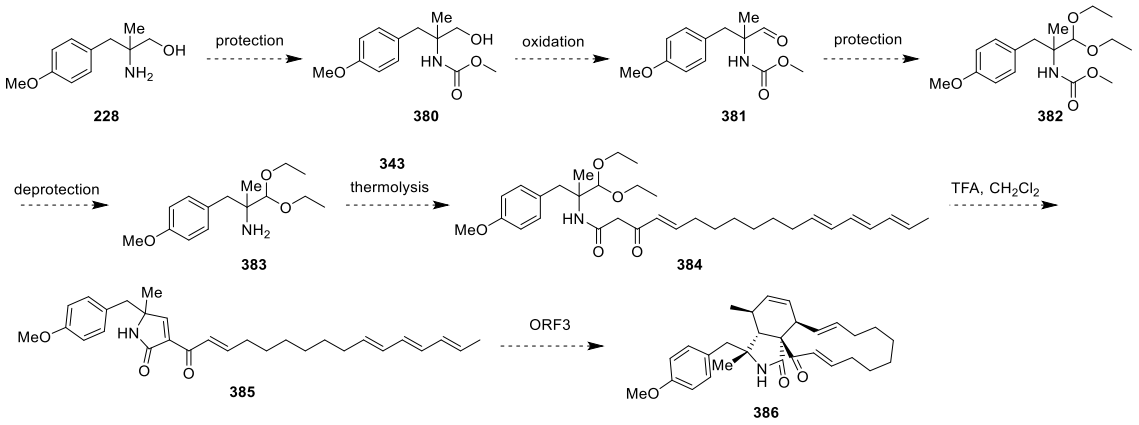

Scheme 4.30 Proposed synthetic plan for the compound **385**

5. ACE1 Metabolite Precursor Investigations

5.1 Introduction

All the compounds investigated in chapters 2-4 are only models mimicking the ACE1 shunt metabolite **52**. Since in some cases enzymes have strict substrate selectivity and the methyl groups on the polyketide chain might be necessary for the stereoselectivity of the Diels-Alder reaction, the correct ACE1 metabolite precursor **56** has to be synthesized and used for the *in vitro* assays. Heterologous expression and chemical synthesis are two applicable methods to produce the ACE1 metabolite precursor **56**.

Compared with chemical synthesis, heterologous expression is often more cost-effective in milligram scale synthesis. However, at the early stage, the fact that *OMET* is crucial for the correct biosynthesis of ACE1 metabolite had not been realized (section 1.3.2.3). Therefore only a minor alcohol compound **51** was produced by heterologous co-expression of *ACE1* and *RAP1* in *A. oryzae*. The alcohol compound **51** was not available in high enough titer to be extensively oxidized and studied for *in vitro* assays.

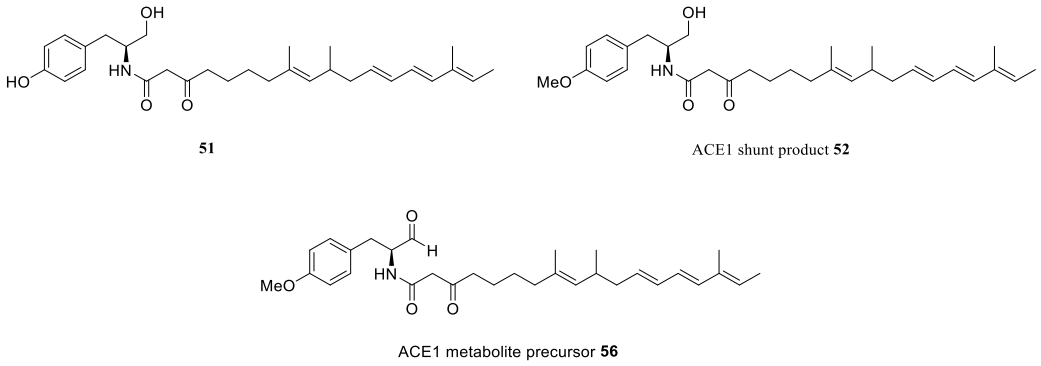

Figure 5.1 Structures of shunts **51** and **52** from heterologous expressions and proposed ACE1 metabolite precursor **56**.

In the middle of this project, it was found that *OMET* is involved in the early steps during pyrichalasin H **20** biosynthesis. Since pyrichalasin H **20** BGC shares high sequence similarities with ACE1 BGC and ACE1 BGC also contains *OMET* gene, it was deduced that OMET is also involved in ACE1 metabolite biosynthesis (section

1.3.2.3).[36] Feeding experiment with *O*-methyl tyrosine into *A. oryzae* expressing *ACE1*, *RAP1*, *ORF3* and *ORFZ* produced *O*-methyl tyrosine nonaketide **52** in much higher titer (2 mg/L) and abolished the production of **51**, suggesting *O*-methyl tyrosine is the correct amino acid moiety incorporated into ACE1 metabolite. Thus it makes heterologous expression possible and efficient for the production of ACE1 shunt metabolite **52**, which could be further oxidized by one step oxidation to provide ACE1 metabolite precursor **56**, if we think the double bond next to ketone is not crucial for the Diels-Alder reaction.

5.2 Aims

In this section, we aim to prepare the ACE1 metabolite precursor **56** for *in vitro* enzyme assays. Heterologous expression followed by oxidation will be the first priority for the preparation of **56** (scheme 5.1A). If possible, **56** will also be used for Knoevenagel condensation and Diels-Alder reaction tests. The loss of the olefin next to ketone should not have strong influence on Diels-Alder reaction.

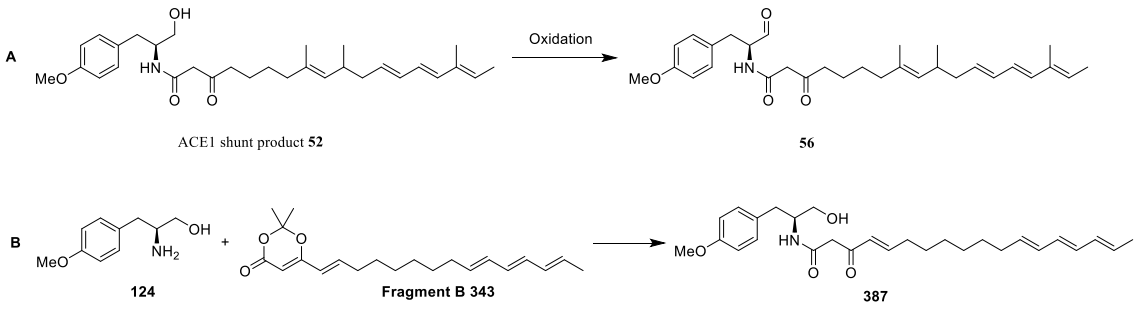

Scheme 5.1 A, proposed oxidation of alcohol **52** to **56**; **B**, synthesis of compound **387** for oxidation investigation.

Even though ACE1 shunt metabolite **52** can be extracted from fungi extracts in milligram scale, it is still too precious to investigate oxidation methods. Therefore we plan to make the alcohol **387** for the primary oxidation studies, which could be easily prepared from one step thermolysis of dioxinone **343** (scheme 5.1B). If succeeded, the method will be applied for the oxidation of **52**.

Chemical synthesis is an alternative way to provide ACE1 metabolite precursor **56** if the oxidation of alcohol **52** in the presence of triene is problematic.

5.3 Results and Discussion

5.3.1 Oxidation Attempts of Alcohol to Aldehyde

Compound **387** was easily prepared through thermolysis of fragment B **343** in the presence of amino alcohol **124** in toluene for 3 hours (scheme 5.2).

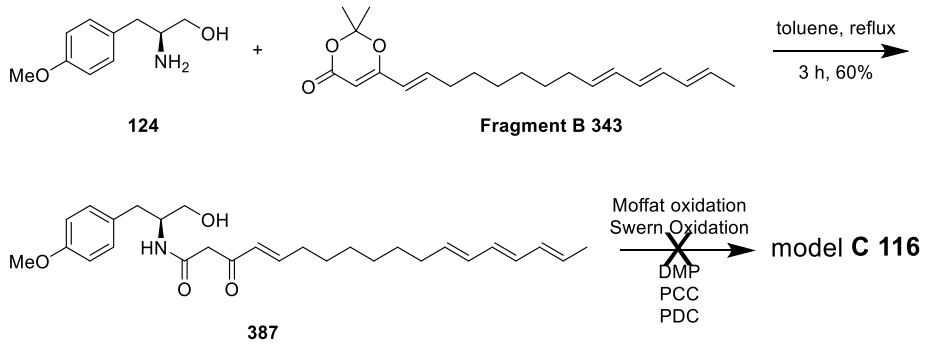

Scheme 5.2 Synthesis of compound **387** and failed attempts towards oxidation of **387**.

However, the oxidation of the primary alcohol **387** in the presence of the triene proved to be problematic because the conjugated trienes were sensitive to acid, heat, and electrophilic attack,[155] as well as the steric hindrance and possible hydrogen bond between the hydroxyl group and carbonyl group.

The first attempt to oxidize **387** was by Moffat oxidation because it worked very well for preparation of model B **115** (section 3.3.2). However, standard reaction conditions cannot oxidize compound **387** after overnight even with excess amount of oxidizing reagents. Detection by LCMS clearly showed no conversion of alcohol **387** to model C **116** even after 3 days. Moffat oxidation is not applicable to oxidation of compound **387**. The same story happened with Swern oxidation.

The third attempt was Dess-Martin periodinane in dichloromethane at room temperature without weak base. After reaction for 3 h, the reaction mixture was checked by LCMS and compound **387** had disappeared. But the new compounds were not aldehydes and the UV showed no triene absorbance any more. So DMP appeared to destroy the triene and it was not applicable for compound **387** oxidation.

A similar situation happened with PCC and PDC oxidation, which are stronger oxidizing reagents than DMP. The reactions were performed in CH_2Cl_2 at r.t. and compound **387** was totally degraded after 2 h. No further attempts were made towards this oxidation.

5.3.2 ACE1 Metabolite Precursor Retrosynthetic Analysis

Since the oxidation of alcohol in the presence of triene proved to be more difficult than anticipated, the organic synthesis of aldehyde *via* hydrolysis of diethyl acetal is more important.

ACE1 metabolite precursor **56** can be disconnected through the amide bond to two fragments: the amino acid fragment **212** and long alkyl chain fragment **388** (scheme 5.3). Compound **212** was prepared before for the synthesis of model B **115** and diethyl acetal can be hydrolysed with HCl in aqueous THF in the presence of triene. Compound **388** is supposed to be synthesized by the acylation of Meldrum's acid under basic condition. Construction of alkyl chain **390** is the major task including the conjugated triene and three methyl groups that will be discussed in scheme 5.4.

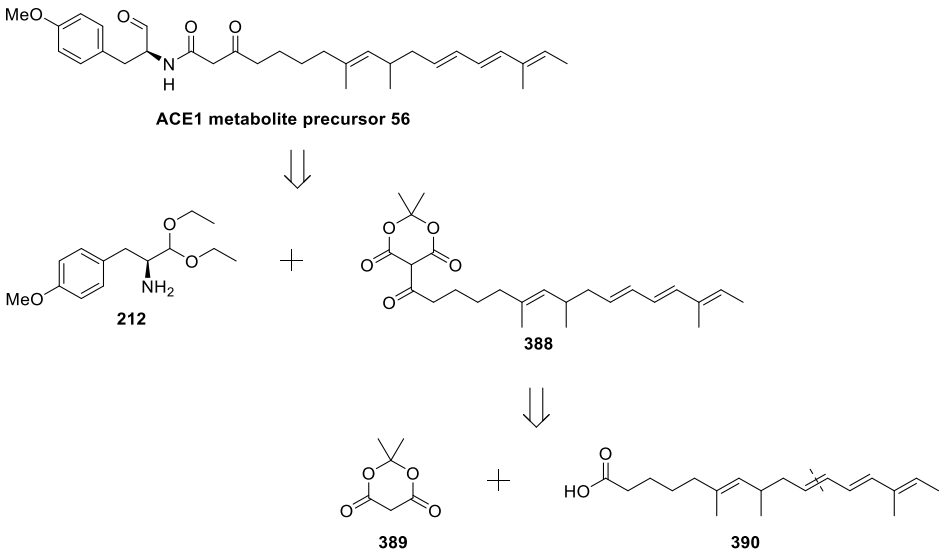

Scheme 5.3 Retrosynthetic analysis of cytochalasan precursor **56**.

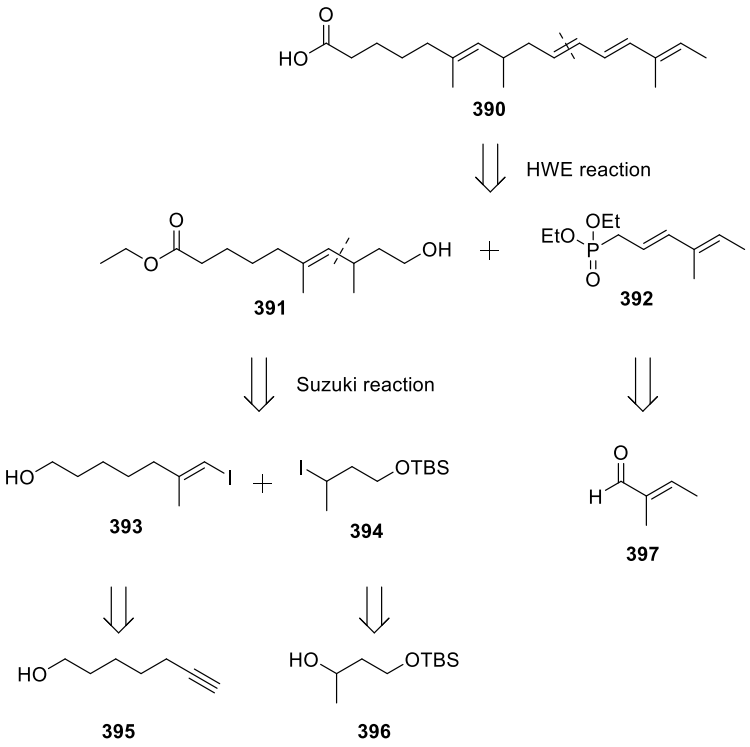

Scheme 5.4 Retrosynthetic analysis of compound **390**.

The triene can be constructed through Wittig reaction or Horner-Wadsworth-Emmons reaction. Here we can choose HWE reaction because phosphonate **392** is a known compound derived from tiglic aldehyde **397** through four steps.[156] Compound **391** can be further disconnected to compound **393** and **394**, which could link by a Suzuki reaction. Compound **393** and **394** are known and can be synthesized from commercially available compound **395** and TBS protected alcohol **396** respectively. Actually compound **392**, **393**, **394** have already been synthesized, but the Suzuki reaction did not work for the moment. The synthetic work paused because the shunt metabolite **5** can be obtained from fungal fermentation with milligram scale.

5.4 Discussion and Conclusion

In this section, attempts of alcohol oxidation towards aldehyde in the presence of triene have been made but all failed. The reasons behind was not investigated in detail. From the known knowledge, the conjugated trienes were sensitive to acid, heat, and electrophilic attack.[155] However, compound **361** can be oxidized by Swern oxidation efficiently (scheme 5.5). If it is because of the formation of possible hydrogen bond

between hydroxyl group and carbonyl group, Moffat oxidation can oxidize **210** to prepare model B **115**. Therefore it is hard to oxidize **387** possibly because of combination of several factors.

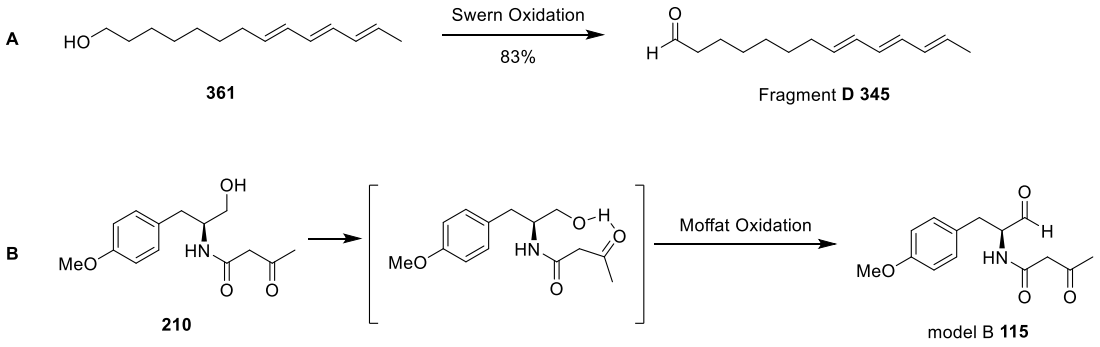

Scheme 5.5 Successful oxidation of alcohols.

In 2013, a PhD thesis towards total synthesis of cytochalasan (Hugh Allen Hoather, University of Manchester) reported a similar compound oxidation containing a tetraene.[157] Seven oxidizing reagents and different conditions were tried and failed to oxidize the secondary alcohol **398** to corresponding ketone **399** (scheme 5.6).

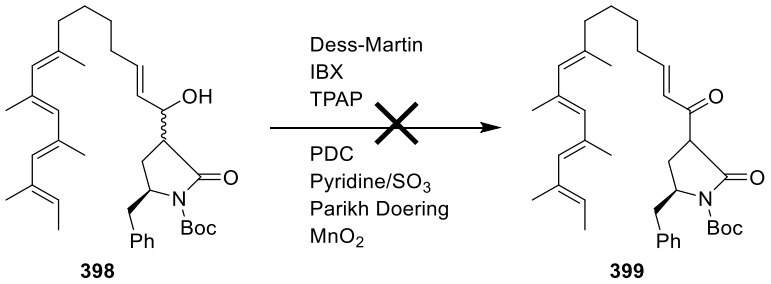

Scheme 5.6 Failed attempts of similar compound oxidation.

Since it is difficult to oxidize ACE1 metabolite **52**, it is meaningful to restart the synthesis of ACE1 metabolite precursor from hydrolysis of diethyl acetal. However, due to the problems met during model compounds studies and time constraints, this part of work has not been completed.

6. Conclusion and Outlook

The overall aim of the project was to investigate the biosynthesis of the cytochalasan backbone including reductive release, putative Knoevenagel condensation and Diels-Alder reactions. In order to achieve this, three model compounds were designed, prepared and applied for *in vitro* assays. The current findings include that:

A) *A. oryzae* is not a proper host for cytochalasin heterologous expression since the native alcohol dehydrogenase in *A. oryzae* can reduce aldehyde to alcohol shunt metabolite.

Model A **114** was designed and synthesized for over-reduction investigation. *In vitro* assays in phosphate buffer confirmed that model A **114** can be reduced to alcohol by alcohol hydrogenase in *A. oryzae*. This indicates that compound **52** is a shunt metabolite and *A. oryzae* is not a proper host for cytochalasan genes expression. However, if the genes responsible for the reductase could be knocked out, *A. oryzae* after deletion of reductase can be used for expression of cytochalasan BGC.

B) Pyrrolinones tautomerise to their enol form, which is no longer competent for the following Diels-Alder reaction. This has been already confirmed by both chemical and biological evidences.

Five pyrrolinones were prepared and the tautomerism was further confirmed by UV and NMR comparison of different pyrrolinones (Figure 6.1). After tautomerism, pyrrolinones have a characteristic UV absorbance above 300 nm and are no longer suitable for Diels-Alder reaction because the double bond shifts.

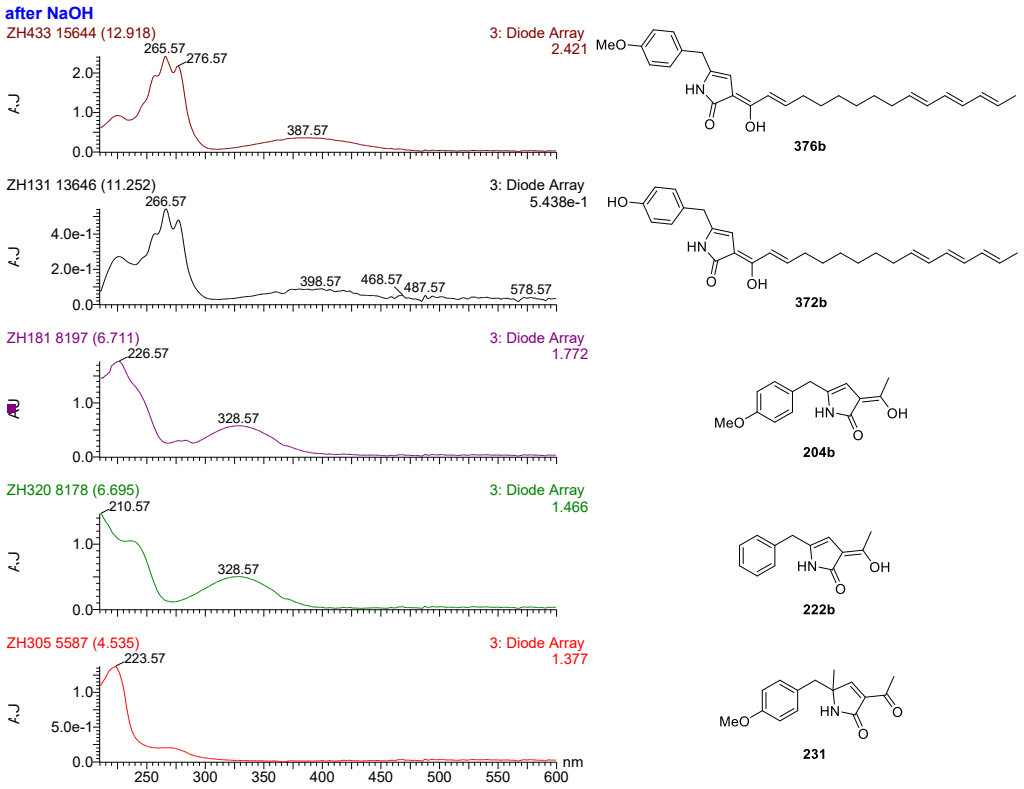

Figure 6.1 Comparison of UV spectra from different pyrrolinones.

C) The Knoevenagel condensation is a spontaneous reaction in potassium phosphate buffer, which is also proved by Chooi and co-workers by heterologous expression. But it is still mysterious if α,β-hydrolase could accelerate this reaction.

In vitro assays with model B **115** and model C **116** were performed. The results showed that Knoevenagel condensation is a spontaneous reaction in potassium phosphate buffer, which is consistent with the recent report by heterologous expression.[150] Though no enzyme activity was observed by *in vitro* assays with model B **115**, the possibility that ORFZ can accelerate the Knoevenagel condensation cannot be ruled out. There are several possible reasons accounting for this. Firstly and importantly, ORFZ is only a possible enzyme responsible for Knoevenagel condensation. Gene knock-out experiment performed by Verena Hantke showed that deletion of *orfz* abolished production of cytochalasin intermediate, suggesting that ORFZ must be involved in an early cytochalasin backbone assembly step, but lack of any intermediates precluded hard conclusions. Other possibilities include that the enzyme is inactive after *E.coli* expression or it has strict substrate selectivity.

Currently, model C **116** is applied for *in vivo* and *in vitro* assays. *In vivo* assays with model C **116** are ongoing by feeding experiments into *Pyricularia oryzae* to investigate if it can be incorporated and exploited as cytochalasin precursor. Moreover, *in vitro* assays with model C **116** will also be carried out to test ORFZ and ORF3 activities.

In future, if ORF3 cannot catalyse the Diels-Alder cyclization of tauromerised pyrrolinone, the non-tautomerised pyrrolinone **385** will be prepared and tested.

7. Experimental

7.1 General Experimental Details

All reactions in anhydrous solvents were conducted under an atmosphere of dry nitrogen in glassware that was flame-dried. All commercially available reagents and dry solvents were used directly without further purification unless otherwise stated.

***In vitro* assays:** Assay of ORFZ was performed in 200 µL volume containing 50 mM HEPES (pH 7.5), 0.5 mM model B **115**, 10 µL DMSO, and ORFZ. The reaction was incubated at 35 °C over time and monitored by LCMS. Before detection, reaction was quenched with the same amount of acetonitrile and protein was removed by centrifugation. The supernatant was analyzed directly by LCMS.

NMR analysis: ^{1}H-NMR data are reported in the following format: chemical shift (multiplicity, coupling constants, integration and assignment). Chemical shifts are reported in ppm with the residual solvent resonance as internal standard ($CDCl_3$: 7.26 ppm; CD_3CN: 1.94 ppm). Multiplicity is abbreviated as follows: s = singlet, d = doublet, t = triplet, q = quartet, m = multiplet, br = broad. ^{13}C NMR spectra were recorded at 100 or 125 MHz, with Bruker Avance 400, DPX 400, or DRX 500 instruments. Chemical shifts are reported in ppm with the solvent resonance as internal standard ($CDCl_3$: 77.2 ppm; CD_3CN: 116.0, 0.2 ppm). Some proton and carbon assignments were made with the aid of ^{1}H-^{1}H COSY, ^{1}H-^{13}C HSQC or ^{1}H-^{13}C HMBC experiments. All δ values are in ppm. All J values are in Hz.

Column Chromatography: For column chromatography silica 60 Å (particle size 35-70 micron, Sigma-Aldrich or 40-63 micron, Macherey-Nagel) was used. Columns were packed under N_2 pressure. Products were eluted with the indicated solvent mixtures. Purified fractions were analysed by TLC and combined if same R_f was observed. Final products were evaporated under vacuum.

TLC: TLC analysis was performed on TLC plates with a polyester backed 0.2 mm silica gel phase from Macherey and Nagel using the indicated solvent systems. Analysis

of the plates were performed by ultraviolet light (254 nm) or with potassium permanganate or 2,4-DNP solution.

Analytical LCMS: Analytical LC-MS data were obtained with a Waters LCMS system comprising of a Waters 2767 autosampler, Waters 2545 pump system, a Phenomenex Kinetex column (2.6 μ, C_{18}, 100 Å, 4.6 × 100 mm) equipped with a Phenomenex Security Guard precolumn (Luna C_5 300 Å) eluted at 1 mL/min. Detection was by Waters 2998 Diode Array detector between 200 and 600 nm; Waters 2424 ELSD and Waters SQD-2 mass detector operating simultaneously in ES^+ and ES^- modes between 100 *m/z* and 1000 *m/z*. Solvents were: **A**, HPLC grade H_2O containing 0.05% formic acid; **B**, HPLC grade MeOH containing 0.045% formic acid; and **C**, HPLC grade CH_3CN containing 0.045% formic acid. Gradients were as follows. Method 1. Kinetex/CH_3CN: 0 min, 10% **C**; 10 min, 90% **C**; 12 min, 90% **C**; 13 min, 10% **C**; 15 min, 10% **C**.

Preparative LCMS: Purification of compounds was generally achieved using a Waters mass-directed autopurification system comprising of a Waters 2767 autosampler, Waters 2545 pump system, a Phenomenex Kinetex Axia column (5 μ, C_{18}, 100 Å, 21.2 × 250 mm) equipped with a Phenomenex Security Guard precolumn (Luna C_5 300 Å) eluted at 20 mL/min at ambient temperature. Solvent **A**, HPLC grade H_2O + 0.05% formic acid; Solvent **B**, HPLC grade CH_3CN + 0.045% formic acid. The postcolumn flow was split (100:1) and the minority flow was made up with HPLC grade CH_3CN + 0.045% formic acid to 1 $mL \cdot min^{-1}$ for simultaneous analysis by diode array (Waters 2998), evaporative light scattering (Waters 2424) and ESI mass spectrometry in positive and negative modes (Waters SQD-2). Detected peaks were collected into glass test tubes. Acetonitrile in combined tubes were evaporated under vacuum, then water was evaporated using freeze dryer.

IR analysis: IR analysis was performed with the Fourier transform spectrophotometer IR Affinity-1S from the company Shimadzu.

HRMS: High-resolution mass spectra data were obtained on an electrospray ionization LC/MS equipped with a time-of-flight mass analyzer.

Optical rotation: Optical rotations were measured on a Perkin-Elmer polarimeter type 341 in a quartz glass cuvette (10 cm) with a Na lamp and are reported as: $[\alpha]_D^{T(°C)}$ = XX (c (g / 100 mL), solvent).

7.2 Synthesis of Intermediates and Model Compounds

(Methoxycarbonyl)-*L*-tyrosine 124.[73]

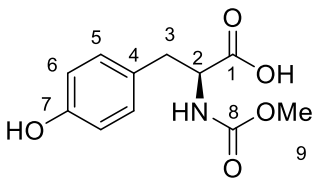

Methyl chloroformate (Sigma-Aldrich, 3.57 mL, 46.1 mmol) was added to a solution of *L*-tyrosine (8.30 g, 46.1 mmol) and $NaHCO_3$ (11.62 g, 138.3 mmol) in a mixture of H_2O/THF (200 mL/200 mL). After stirring at room temperature overnight, the mixture was diluted with H_2O (200 mL) and washed with Et_2O (200 mL). The aqueous layer was acidified and extracted with EtOAc (3 × 60 mL). The combined organic extracts were washed with H_2O, dried over $MgSO_4$ and concentrated under vacuum to give a white foam (8.8 g, 80%), which was used in the next step without further purification.

$[\alpha]_D^{23}$ = +19.2 (*c* = 0.25, MeOH) (lit. +21.5, *c* = 2.375, MeOH); **^{1}H NMR** (CD_3OD, 400 MHz): δ 7.03 (d, 2H, *J* = 8.4, 5-ArH), 6.68 (d, 2H, *J* = 8.4, 6-ArH), 4.30 (dd, 1H, *J* = 5.0, 8.7, 2-CH), 3.58 (s, 3H, 9-CH_3), 3.06 (dd, 1H, *J* = 5.0, 13.9, 3-CH_2), 2.82 (dd, 1H, *J* = 8.7, 13.9, 3-CH_2); **IR** (KBr) ν_{max} 3334, 2958, 2484, 1685, 1612, 1512, 1643, 1373, 1244, 1055 cm^{-1}; **ES-MS**: *m/z* (%): 194.1 [M-CO_2H] (100), 240.2 $[M]H^+$ (18), 262.2 $[M]Na^+$ (6).

Methyl-*S*-2-((methoxycarbonyl)amino)-3-(4-methoxyphenyl) propanoate 125.[73]

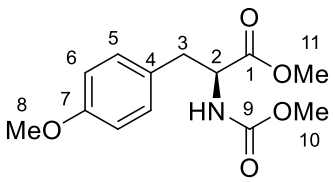

To a stirred solution of *N*-(methoxycarbonyl)-*L*-tyrosine **124** (8.8 g, 36.8 mmol) in DMF (90 mL) was added K_2CO_3 (18.9 g, 137 mmol) and iodimethane (7.4 mL, 115 mmol) at 0 °C. The solution was allowed to warm to room temperature. After overnight, the solution was filtrated and the filtrate was acidified with diluted aqeous HCl and extracted with EtOAc (3 × 50 mL). The extract was washed with sat. aqueous $NaHCO_3$ and NaCl, dried over $MgSO_4$, filtered and concentrated under vacuum to afford colourless oil (9.3 g, 95%).

$[\alpha]_D^{23}$ = +9.8 (*c* = 1.0, MeOH) (lit. +14.4, *c* = 1.11, EtOH); **^{1}H NMR** ($CDCl_3$, 400 MHz): δ 6.96 (d, 2H, *J* = 8.5, 5-ArH), 6.72 (d, 2H, *J* = 8.5, 6-ArH), 5.53 (d, 1H, *J* = 8.2, CONH), 4.49 (dd, 1H, *J* = 6.5, 14.3, 2-CH), 3.65 (s, 3H, 8-CH_3), 3.60 (s, 3H, 11-CH_3), 3.53 (s, 3H, 10-CH_3), 2.97 (dd, 1H, *J* = 5.8, 14.0, 3-CH_2), 2.89 (dd, 1H, *J* = 6.8, 14.0, 3-CH_2). **IR** (neat) ν_{max} 2953, 2839, 1720, 1666, 1612, 1512, 1438, 1244, 1176, 1058, 1031 cm^{-1}; **ES-MS**: *m/z* (%): 208.3 $[M\text{-}C_2H_3O_2]^+$ (74), 236.3 $[M\text{-}CH_3O]^+$ (40), 268.3 $[M]H^+$ (100), 290.3 $[M]Na^+$ (19).

Methyl-*S*-(1-hydroxy-3-(4-methoxyphenyl)propan-2-yl)carbamate 126.[73]

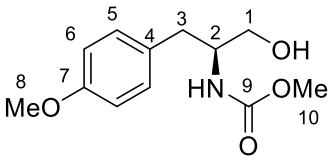

To a stirred suspension of $LiAlH_4$ (0.76 g, 20 mmol) in dry THF (20 mL) was slowly added the ester **125** (2.67 g, 10 mmol) in THF (10 mL) at 0 °C. After being stirred at the same temperature for 15 min, the mixture was allowed to warm to room temperature for 2 h. After complete reaction dectected by TLC, the mixture was cooled to 0 °C and acidified with 4N HCl. The mixture was extracted with EtOAc (3 × 30 mL), dried over $MgSO_4$, concentrated under vacuum and purified by flash chromatography (petroleum ether/EtOAc = 1:1) to give **126** as a colourless oil (1.88 g, 79%).

R_f = 0.2 (petroleum ether/EtOAc = 1:1); **$[\alpha]_D^{26}$** = -14.9 (*c* = 1.0, MeOH) (lit. -23.1, *c* = 1.95, EtOH); **^{1}H NMR** ($CDCl_3$, 400 MHz): δ 7.10 (d, 2H, *J* = 8.5, 5-ArH), 6.81 (d, 2H, *J* = 8.5, 6-ArH), 5.28 (s, 1H, CONH), 4.40 (s, 1H, OH), 3.90-3.80 (m, 1H, 2-CH), 3.75 (s, 3H, 8-CH_3), 3.64-3.56 (m, 4H, 1-CH_2 and 10-CH_3), 3.51 (dd, 1H, *J* = 5.2, 11.2, 1-CH_2), 2.78-2.73 (m, 2H, 4-CH_2); **IR** (neat) ν_{max} 3323, 2951, 1697, 1612, 1510, 1460, 1442, 1361, 1242, 1178, 1029 cm^{-1}; **ES-MS**: *m/z* (%): 208.1 $[M\text{-}H_2O\text{-}CH_2]^+$ (10), 222.0 $[M\text{-}H_2O]^+$ (19), 240.0 $[M]H^+$ (100).

***S*-2-Amino-3-(4-methoxyphenyl)propan-1-ol 127.**[73]

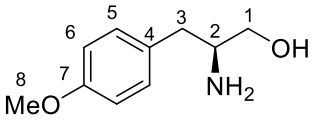

A solution of **126** (2.03 g, 8.5 mmol) in 25% aqueous KOH was stirred at 50 °C overnight. The mixture was then extracted with EtOAc (3 × 15 mL). The combined extracts were washed with H_2O, sat. aqueous NaCl and then concentrated under vacuum. Recrystallization from EtOAc and Et_2O afforded amino alcohol **127** as a white solid (1.32 g, 85%).

$[\alpha]_D^{25}$ = -17.3 (*c* = 1.0, MeOH) (lit. -21.5, *c* = 1.0, EtOH); m.p. 95 °C (lit. 94-96 °C); **^{1}H NMR** ($CDCl_3$, 400 MHz): δ 7.10 (d, 2H, *J* = 8.6, 5-ArH), 6.85 (d, 2H, *J* = 8.6, 6-ArH), 3.79 (s, 3H, 8-CH_3), 3.62 (dd, 1H, *J* = 3.9, 10.6 Hz, 1-CH), 3.37 (dd, 1H, *J* = 7.2, 10.6, 1-CH), 3.11-3.03 (m, 1H, 2-CH), 2.72 (dd, 1H, *J* = 5.2, 13.6, 3-CH), 2.46 (dd, 1H, *J* = 8.6, 13.6, 3-CH), 1.90 (br, 2H, NH_2); **IR**: (KBr) ν_{max} 3338, 3273, 3170, 2839, 1598, 1510, 1247, 1176, 1026 cm^{-1}; **ES-MS**: *m/z* (%): 121.1 $[C_8H_9O]^+$ (100), 182.2 $[M]H^+$ (22).

_S_-2-Acetamido-3-(4-methoxyphenyl)propyl acetate 128.

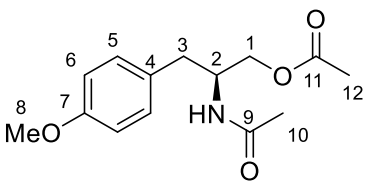

Amino alcohol **127** (50 mg, 0.27 mmol) was dissolved in pyridine (10 mL) and excess acetic anhydride was added dropwise. After reaction at room temperature for 2 h, the solvent was evaporated and the residue was dissolved in EtOAc (20 mL). The solution was washed with H_2O, sat. aqueous NaCl, dried over $MgSO_4$ and evaporated under vacuum to afford **128** as a colourless oil (65 mg, 99%).

$[\alpha]_D^{23}$ = -4.9 (*c* = 0.3, MeOH); **^{1}H NMR** ($CDCl_3$, 400 MHz): δ 7.09 (d, 2H, *J* = 8.6, 5-ArH), 6.83 (d, 2H, *J* = 8.6, 6-ArH), 5.82 (s, 1H, CONH), 4.42-4.32 (m, 1H, 2-CH), 4.10-4.00 (m, 2H, 1-CH_2), 3.78 (s, 3H, 8-CH_3), 2.83 (dd, 1H, *J* = 6.3, 13.9, 3-CH), 2.74 (dd, 1H, *J* = 7.8, 13.9, 3-CH), 2.08 (s, 3H, 12-CH_3), 1.96 (s, 3H, 10-CH_3); **^{13}C NMR** ($CDCl_3$, 101 MHz) δ 171.0 (11-C), 170.4 (9-C), 158.5 (7-C), 130.2 (5-C), 128.7 (4-C), 114.1 (6-C), 64.6 (1-C), 55.2 (8-C), 50.1 (2-C), 36.4 (3-C), 23.0 (12-C), 20.9 (10-C); **IR**: (KBr) ν_{max} 3286, 1720, 1643, 1556, 1514, 1469, 1458, 1390, 1246, 1033 cm^{-1}; **HRMS** calcd for $C_{14}H_{19}NO_4$ $[M+Na]^+$ *m/z* = 288.1212, found 288.1212.

_S_-_N_-(1-Hydroxy-3-(4-methoxyphenyl)propan-2-yl)acetamide 129.[158]

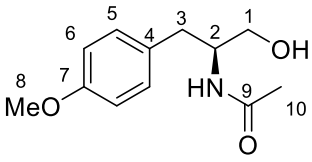

K_2CO_3 (180 mg, 1.3 mmol) was added to a solution of ester **128** in CH_3OH (15 mL). After reaction at room temperature overnight, the solvent was evaporated under vacuum and the residue was dissolved in EtOAc. After washing with H_2O, sat. aqueous NaCl and dried over $MgSO_4$, organic solvent was evaporated under reduced pressure to afford the target compound **129** as white solid (52 mg, 90%).

$[\alpha]_D^{26}$ = -10.5 (*c* = 0.4, MeOH) (lit. -28.8, *c* = 1, MeOH); **^{1}H NMR** ($CDCl_3$, 400 MHz): δ 7.12 (d, 2H, *J* = 8.6, 5-ArH), 6.83 (d, 2H, *J* = 8.6, 6-ArH), 5.89 (d, 1H, *J* = 7.2, CONH), 4.15-4.06 (m, 1H, 2-CH), 3.78 (s, 3H, 8-CH_3), 3.65 (dd, 1H, *J* = 3.6, 11.1, 1-CH), 3.55 (dd, 1H, *J* = 5.2, 11.1, 1-CH), 2.86-2.73 (m, 2H, 3-CH), 1.95 (s, 3H, 10-CH_3); **IR**: (KBr) ν_{max} 3317, 2956, 2931, 1645, 1612, 1552, 1512, 1438, 1300, 1247, 1047, 1026 cm^{-1}; **ES-MS**: *m/z* (%): 224.3 $[M]H^+$ (100), 206.3 $[M\text{-}H_2O]H^+$ (40), 182.3 $[M\text{-}43]H^+$ (16), 147.2 $[M\text{-}H_2O\text{-}NH_3]H^+$ (15), 121.2 $[C_8H_9O]^+$ (39).

_S_-_N_-(1-(4-Methoxyphenyl)-3-oxopropan-2-yl)acetamide 114.

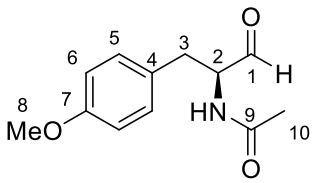

Modified Moffat oxidation was applied for the preparation of model A **114**. EDC·HCl (42.8 mg, 0.22 mmol) and dichloroacetic acid (11.6 mg, 0.09 mmol) were added to a solution of alcohol **129** (10 mg, 0.045 mmol) in toluene (1 mL) and DMSO (1 mL). The reaction was stirred at 25 °C for 16 h and then H_2O was added. The mixture was extracted with EtOAc (3 × 2 mL), washed with sat. aqueous NaCl, dried over $MgSO_4$ and evaporated under vacuum to give a crude aldehyde which was purified by preparative LCMS to afford model A **114** as a colourless oil (4.6 mg, 46%).

$[\alpha]_D^{30}$ = -1.0 (*c* = 2.8, CH_2Cl_2); **^{1}H NMR** ($CDCl_3$, 400 MHz): δ 9.63 (s, 1H, 1-CHO), 7.06 (d, 2H, *J* = 8.6, 5-ArH), 6.84 (d, 2H, *J* = 8.6, 6-ArH), 5.96 (s, 1H, CONH), 4.71 (dd, 1H, *J* = 6.6, 12.7, 2-CH), 3.79 (s, 3H, 8-CH_3), 3.16 (dd, 1H, *J* = 5.7, 14.3, 3-CH_2), 3.08 (dd, 1H, *J* = 7.0, 14.3, 3-CH_2), 2.02 (s, 3H, 10-CH_3); **^{13}C NMR** (CD_3CN, 101 MHz) δ 200.1 (1-C), 170.3 (9-C), 158.5 (7-C), 130.3 (5-C), 129.1 (4-C), 113.8 (6-C), 60.3 (2-C), 54.8 (8-C), 32.9 (3-C), 21.7 (10-C); **IR**: (KBr) ν_{max} 3280, 1732, 1637, 1610, 1510, 1440, 1373, 1300, 1244, 1176, 1029 cm^{-1}; **HRMS** calcd for $C_{12}H_{15}NO_3$ $[M+Na]^+$ *m/z* = 244.0950, found 244.0950.

_S_-_N_-(1-Hydroxy-3-(4-methoxyphenyl)propan-2-yl)-3-oxobutanamide 210.

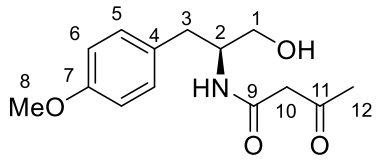

To a stirred solution of amino alcohol **127** (100 mg, 0.55 mmol) in anhydrous toluene (10 mL) was added a solution of dioxinone (78 mg, 0.55 mmol). The reaction was heated to 105 °C for 3 h. The mixture was concentrated under vacuum and the residue was purified by flash chromatography (CH_2Cl_2/MeOH = 20:1) to give **210** as a yellow solid (78 mg, 53%).

R_f = 0.6 (CH_2Cl_2/MeOH = 40:1); **$[\alpha]_D^{25}$** = -2.7 (*c* = 1.0, MeOH); m.p. 62-63 °C; **^{1}H NMR** ($CDCl_3$, 400 MHz): δ 7.24-7.18 (m, 1H, CONH), 7.12 (d, 2H, *J* = 8.1, 5-ArH), 6.81 (d, 2H, *J* = 8.1, 6-ArH), 4.19-4.09 (m, 1H, 2-CH), 3.76 (s, 3H, 8-CH_3), 3.69-3.62 (m, 1H, 1-CH_2), 3.57-3.50 (m, 1H, 1-CH_2), 3.42-3.29 (m, 2H, 10-CH_2), 2.85-2.71 (m, 2H, 3-CH_2), 2.19 (d, 3H, *J* = 2.1, 12-CH_3); **^{13}C NMR** ($CDCl_3$, 101 MHz) δ 204.6 (11-C), 166.3 (9-C), 158.3 (7-C), 130.2 (5-C), 129.6 (4-C), 114.0 (6-C), 63.8 (1-C), 55.2 (8-C), 53.3 (2-C), 49.9 (10-C), 36.1 (3-C), 30.8 (12-C); **IR** (KBr) ν_{max} 3383, 3319, 2927, 2837, 1710, 1639, 1614, 1529, 1514, 1442, 1359, 1325, 1290, 1246, 1222, 1176, 1026 cm^{-1}; **HRMS** calcd for $C_{14}H_{19}NO_4$ $[M+Na]^+$ *m/z* = 288.1212, found 288.1212.

Methyl-*S*-(1,1-diethoxy-3-(4-methoxyphenyl)propan-2-yl)carbamate 211.

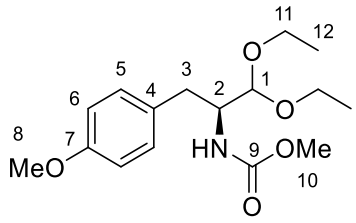

EDC·HCl (25 g, 130.5 mmol) and dichloroacetic acid (6.78 g, 52.2 mmol) were added to a solution of alcohol **126** (6.24 g, 26.1 mmol) in toluene (30 mL) and DMSO (30 mL). The reaction was stirred at 25 °C for 16 h and then H_2O was added. The aqueous layer was extracted with EtOAc (3 × 100 mL), washed with sat. NaCl, dried over $MgSO_4$ and evaporated under vacuum to give a crude aldehyde which was used for next step without purification. The crude aldehyde (6.18 g, 26.1 mmol) and catalytic amount of *p*-TsOH were added to a solution of triethyl orthoformate (19.3 g, 130 mmol) in dry EtOH (50 mL). After reaction at 50 °C overnight, EtOH was removed under reduced pressure. The crude oil was diluted with EtOAc and washed with H_2O, sat. aqueous NaCl solution. After drying over $MgSO_4$, EtOAc was removed and the crude product was purified by flash chromatography (petroleum ether/EtOAc = 8:1) to give **211** as an oil (6.5 g, 80%).

R_f = 0.3 (petroleum ether/EtOAc = 4:1); **$[\alpha]_D^{25}$** = -16.8 (*c* = 1.0, MeOH); **^{1}H NMR** ($CDCl_3$, 400 MHz): δ 7.11 (d, *J* = 8.4, 2H, 5-ArH), 6.82 (d, 2H, *J* = 8.4, 6-ArH), 4.91 (d, *J* = 8.5, 1H, 12-NH), 4.30 (d, *J* = 3.1, 1H, 1-CH), 4.04-3.94 (m, 1H, 2-CH), 3.80-3.69 (m, 4H, 8-CH_3 and 11-CH_2), 3.64-3.55 (m, 4H, 10-CH_3 and 11-CH_2), 3.54-3.44 (m, 2H, 11-CH_2), 2.86 (dd, 1H, *J* = 6.4, 14.1, 3-CH_2), 2.73 (dd, 1H, *J* = 7.8, 14.1, 3-CH_2), 1.25-1.15 (m, 6H, 12-CH_3); **^{13}C NMR** ($CDCl_3$, 101 MHz) δ 158.1 (7-C), 156.8 (9-C), 130.3 (5-C), 130.1 (4-C),113.8 (6-C), 102.2 (1-C), 63.7 (11-C), 55.2 (8-C), 54.2 (10-C), 52.0 (2-C), 35.2 (3-C), 15.3 (12-C); **IR** (neat) ν_{max} 2976, 1708, 1504, 1234, 1159, 894, 758, 738 cm^{-1}; **HRMS** calcd for $C_{16}H_{25}NO_5$ $[M+Na]^+$ *m/z* = 334.1630, found 334.1631.

_S_-1,1-Diethoxy-3-(4-methoxyphenyl)propan-2-amine 212.

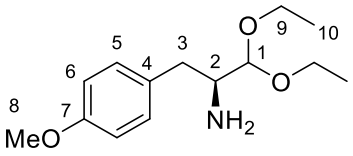

To a solution of compound **211** (2.0 g, 6.1 mmol) in MeOH and H_2O 60 mL (1:1) was added KOH (7.2 g, 12.2 mmol) and stirred at 50 °C overnight. The mixture was then extracted with EtOAc (3 × 15 mL). The combined extracts were washed with H_2O, sat. aqueous NaCl and concentrated under vacuum. Purification by flash chromatography (CH_2Cl_2/MeOH = 30:1, TEA was added) afforded **212** as a white solid (1.3 g, 85%).

R_f = 0.35 (CH_2Cl_2/MeOH = 15:1); **$[\alpha]_D^{23}$** = -13.2 (*c* = 0.67, MeOH); **^{1}H NMR** ($CDCl_3$, 400 MHz): δ 7.11 (d, 2H, *J* = 8.6, 5-ArH), 6.85 (d, 2H, *J* = 8.6, 6-ArH), 4.20 (d, 1H, *J* = 5.6, 1-CH), 3.79-3.65 (m, 5H, 8-CH_3 and 9-CH_2), 3.59-3.49 (m, 2H, 9-CH_2), 3.07-3.00 (m, 1H, 2-CH), 2.90 (dd, 1H, *J* = 4.1, 13.6, 3-CH_2), 2.44 (dd, 1H, *J* = 9.4, 13.6, 3-CH_2), 1.46 (br, 2H, NH_2), 1.25-1.18 (m, 6H, 10-CH_3); **^{13}C NMR** ($CDCl_3$, 101 MHz) δ 158.1 (7-C), 131.0 (5-C), 130.2 (4-C), 113.9 (6-C), 105.7 (1-C), 63.5 (9-C), 63.1 (9-C), 55.2 (8-C), 54.9 (2-C), 37.7 (3-C), 15.4 (10-C), 15.4 (10-C); **IR** (KBr) ν_{max} 2974, 2900, 1610, 1583, 1510, 1442, 1300, 1244, 1176, 1107, 1056, 1033, 808 cm^{-1}; **HRMS** calcd for $C_{14}H_{23}NO_3$ $[M+H]^+$ *m/z* = 254.1756, found 254.1758.

_S-N_-(1,1-Diethoxy-3-(4-methoxyphenyl)propan-2-yl)-3- oxobutanamide 213.

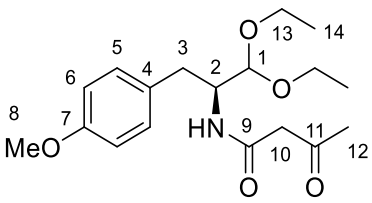

161 (35.0 mg, 0.25 mmol) was added to a solution of **212** (63.0 mg, 0.25 mmol) in anhydrous toluene (10 mL). The solution was heated at 105 °C for 3 h. The reaction

mixture was concentrated under vacuum and the residue was purified by flash chromatography (CH_2Cl_2/MeOH = 100:1) to give **213** as a yellow solid (72.0 mg, 86%).

R_f = 0.3 (CH_2Cl_2/MeOH = 30:1); **$[\alpha]_D^{25}$** = -16.9 (*c* = 0.3, MeOH); **^{1}H NMR** ($CDCl_3$, 400 MHz): δ 7.06 (d, 2H, *J* = 8.6, 5-ArH), 6.80 (d, 1H, *J* = 8.9, CONH), 6.75 (d, 2H, *J* = 8.6, 6-ArH), 4.33-4.23 (m, 2H, 1-CH and 2-CH), 3.76-3.66 (m, 4H, 8-CH_3 and 13-CH_2), 3.61-3.40 (m, 3H, 13-CH_2), 3.25 (s, 2H, 10-CH_2), 2.85 (dd, 1H, *J* = 6.0, 14.3, 3-CH_2), 2.68 (dd, 1H, *J* = 8.3, 14.3, 3-CH_2), 2.11 (s, 3H, 12-CH_3), 1.22-1.09 (m, 6H, 14-CH_3); **^{13}C NMR** ($CDCl_3$, 101 MHz) δ 203.8 (11-C), 165.3 (9-C), 158.1 (7-C), 130.1 (5-C), 129.9 (4-C), 113.7 (6-C), 102.1 (1-C), 63.7 (13-C), 63.6 (13-C), 55.1 (8-C), 52.6 (2-C), 50.5 (10-C), 34.8 (3-C), 30.5 (12-C), 15.3 (14-C), 15.2 (14-C); **IR** (KBr) ν_{max} 3282, 2976, 2931, 1716, 1641, 1610, 1583, 1550, 1510, 1415, 1244, 1060, 1031, 954 cm^{-1}; **HRMS** calcd for $C_{18}H_{27}NO_5$ $[M+Na]^+$ *m/z* = 360.1787, found 360.1782.

***S*-*N*-(1-(4-Methoxyphenyl)-3-oxopropan-2-yl)-3-oxobutanamide 115.**

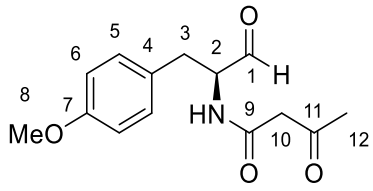

Diethyl acetal **213** (30.0 mg, 89.0 mmol) was dissolved in THF (2 mL) mixed with H_2O (0.5 mL). After cooling to 0 °C, concentrated HCl (37%, 1.0 mL) was added and the reaction was stirred for 3 h. After complete reaction checked by LCMS, the solution was neutralized with NaOH solution and extracted with EtOAc (3 × 2 mL). The organic solvents were combined and evaporated under vacuum to afford **115** as a yellow oil (21.0 mg, 90%). The aldehyde is unstable because of possible polymerization and cannot be purified by flash chromatography. But it can be purified by preparative LCMS to afford yellow solid after freeze drying.

$[\alpha]_D^{30}$ = -12.0 (*c* = 0.9, CH_2Cl_2). **^{1}H NMR** (CD_3CN, 400 MHz): δ 9.57 (s, 1H, 1-CHO), 7.17 (d, 2H, *J* = 8.6, 5-ArH), 6.88 (d, 1H, *J* = 8.6, 6-ArH), 4.51-4.44 (m, 1H, 2-CH), 3.79 (s, 3H, 8-CH_3), 3.39 (s, 2H, 10-CH_2), 3.15 (dd, 2H, *J* = 5.3, 14.3, 3-CH_2), 2.91 (dd, 2H, *J* = 8.5, 14.3, 3-CH_2), 2.15 (s, 3H, 12-CH_3); **^{13}C NMR** (CD_3CN, 101 MHz) δ 203.0 (11-C), 199.7 (1-C), 166.7 (9-C), 158.5 (7-C), 130.4 (5-C), 128.8 (4-C), 113.8 (6-C), 60.3 (2-C), 54.8 (8-C), 50.2 (10-C), 33.0 (3-C), 29.5 (12-C); **IR** (KBr) ν_{max} 3250, 1647, 1610, 1510, 1300, 1244, 1176, 1110, 1031, 819 cm^{-1}; **HRMS** calcd for $C_{14}H_{17}NO_4$ $[M+Na]^+$ *m/z* = 286.1055, found 286.1053.

_S_-_N_-(1-Hydroxy-3-phenylpropan-2-yl)-3-oxobutanamide 209.[107]

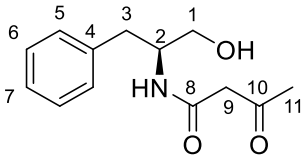

A mixture of amino alcohol **208** (Sigma-Aldrich, 200 mg, 1.32 mmol) and dioxinone **161** (188 mg, 1.32 mmol) in anhydrous toluene (10 mL) was heated to 103 °C for 3 h. The reaction mixture was concentrated under vacuum and the residue was purified by flash chromatography (CH_2Cl_2:MeOH = 20:1) to give **209** as a white solid (180 mg, 58%).

R_f = 0.3 (CH_2Cl_2/MeOH = 20:1); **$[\alpha]_D^{23}$** = -20.6 (*c* = 0.5, MeOH); **^{1}H NMR** ($CDCl_3$, 400 MHz): δ 7.33-7.21 (m, 5H, 5,6,7-ArH), 7.14-7.07 (br, 1H, CONH), 4.26-4.17 (m, 1H, 2-CH), 3.71 (dd, 1H, *J* = 3.7, 11.2, 1-CH), 3.59 (dd, 1H, *J* = 5.4, 11.2, 1-CH), 3.37 (q, 2H, *J* = 17.3, 21.5, 9-CH_2), 2.91 (dd, 1H, *J* = 7.1, 13.9, 3-CH), 2.84 (dd, 1H, *J* = 7.7, 13.7, 3-CH), 2.21 (s, 3H, 11-CH_3); **IR** (KBr) ν_{max} 3292, 3084, 2924, 1712, 1641, 1543, 1357, 1159, 1039 cm^{-1}; **ES-MS**: *m/z* (%): 218.2 [M-H_2O] (76), 236.2 $[M]H^+$ (100).

_Z_-5-Benzyl-3-(1-hydroxyethylidene)-1,3-dihydro-2H-pyrrol-2-one 222b.

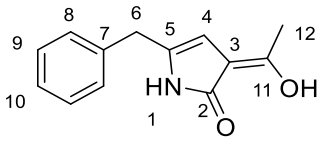

EDC·HCl (40.8 mg, 0.21 mmol) and dichloroacetic acid (10.9 mg, 0.08 mmol) were added to a solution of **209** (10 mg, 0.04 mmol) in toluene (1 mL) and DMSO (1 mL). The reaction was stirred at 25 °C for 16 h and then H_2O was added. The aqueous layer was extracted with EtOAc (3 × 5 mL), and the organic solvents combined to give a solution of aldehyde, which was treated with 1 M NaOH solution (10 mL) for 5 min at 0 °C. The organic phase was separated and the aqueous phase was extracted with EtOAc. The combined organic solvents were washed with sat. aqueous NaCl, dried over $MgSO_4$ and evaporated under vacuum. Purification by preparative LCMS gave **222b** as a white solid (5.5 mg, 60%).

$[\alpha]_D^{23}$ = 0 (*c* = 0.3, MeOH); **^{1}H NMR** ($CDCl_3$, 400 MHz): δ 7.35-7.19 (m, 5H, 8, 9, 10-ArH), 5.54 (s, 1H, 4-CH), 3.70 (s, 2H, 6-CH_2), 2.15 (s, 3H, 12-CH_3); **IR** (KBr) ν_{max} 3153, 3026, 1668, 1626, 1494, 1452, 1436, 1419, 1357, 1263, 1070, 966 cm^{-1}; **ES-MS**: *m/z* (%): 216.1 $[M]H^+$ (100).

4-Methoxybenzenediazonium tetrafluoroborate 225.[159]

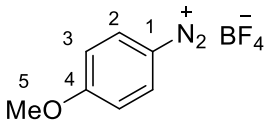

To an ice-salt-cooled solution of the 4-methoxyaniline (4.92 g, 40.0 mmol) in HBF_4 (50%, 14 mL) and H_2O (15 mL) was added dropwise a precooled solution of $NaNO_2$ (2.90 g, 42.0 mmol) in H_2O (6.5 mL). During the addition, the temperature was carefully kept below 5 °C and the resulting mixture was left to stir at 0 °C for 30 min. The diazonium salt was collected by filtration, washed with Et_2O, and extensively dried under vacuum to afford **225** as a purple solid (7.50 g, 85%). (Caution: Diazonium salts may decompose violently upon heating.)

^{1}H NMR (d_6-DMSO, 400 MHz): δ 8.59 (d, 2H, *J* = 9.4, 2-ArH), 7.47 (d, 2H, *J* = 9.4, 3-ArH), 4.03 (s, 3H, 5-CH_3); **^{13}C NMR** (d_6-DMSO, 101 MHz) δ 169.3, 136.5, 117.7, 103.7, 57.9; **IR** (KBr) ν_{max} 3118, 2250, 1581, 1568, 1512, 1492, 1465, 1440, 1342, 1286, 1195, 1029, 997, 839 cm^{-1}; **ES-MS**: *m/z* (%): 107.1 $[C_7H_7O]^+$ (100), 135.2 $[C_7H_7N_2O]^+$ (17).

***E*-3-(4-Methoxyphenyl)-2-((4-methoxyphenyl)diazenyl)-2-methylpropan-1-ol 227.**[160]

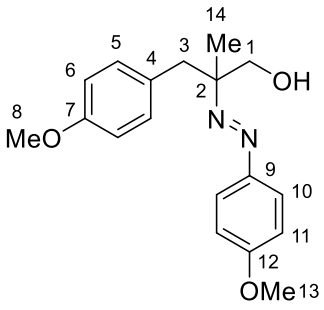

To a mixture of DMSO/H_2O (6 mL, 5:2, *v*/*v*, previously degassed with N_2) were added $FeSO_4 \cdot 7H_2O$ (1.67 g, 6.00 mmol) and 2-methallyl alcohol (1.0 mL, 0.87 g, 12.0 mmol) under an N_2 atmosphere. A solution of diazonium tetrafluoroborate (2.0 mmol) in a mixture of DMSO/H_2O (3.0 mL, 5:2, *v*/*v*, previously degassed with N_2) was added dropwise. The reaction mixture was stirred for an additional 15 min, then diluted with H_2O (50 mL) and extracted with diethyl ether (3 × 50 mL). The combined organic phases were washed with sat. aqueous NaCl (50 mL), then dried over Na_2SO_4. The solvent was evaporated under high vacuum to afford **227** as a yellow oil (376 mg, 60%).

^{1}H NMR ($CDCl_3$, 400 MHz): δ 7.65 (d, 2H, *J* = 8.9, 10-ArH), 7.10 (d, 2H, *J* = 8.6, 5-ArH), 6.92 (d, 2H, *J* = 8.9, 11-ArH), 6.76 (d, 2H, *J* = 8.6, 6-ArH), 3.81 (s, 3H, 13-CH_3),

3.73 (s, 3H, 8-CH_3), 3.70 (d, 2H, J = 2.2, 1-CH_2), 3.04 (d, 1H, J = 13.4, 3-CH_2), 2.92 (d, 1H, J = 13.4, 3-CH_2), 1.17 (s, 3H, 14-CH_3); **IR** (KBr) ν_{max} 3415, 2933, 2835, 1722, 1602, 1585, 1510, 1462, 1440, 1419, 1369, 1300, 1244, 1176, 1143, 1103, 1029, 835 cm^{-1}; **ES-MS**: *m/z* (%): 194.0 $[C_{11}H_{15}]H^+$ (17), 243.0 [2 × $C_7H_7NO]H^+$ (100), 315.0 $[M]H^+$ (66).

2-Amino-3-(4-methoxyphenyl)-2-methylpropan-1-ol 228.[160]

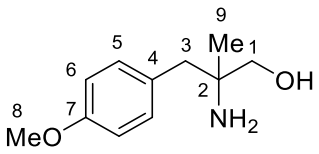

Alcohol **227** (12.0 mg, 0.05 mmol) was dissolved in MeOH (2 mL) and zinc dust (300 mg, 4.59 mmol) and HCl (6 M, 5 mL) were added. After reaction overnight at room temperature, the pH was adjusted with aqueous NaOH (20%) to pH > 12 and the aqueous solution extracted with EtOAc (3 × 20 mL). The combined organic phases were dried over Na_2SO_4 and the solvent was evaporated. The residue was purified by flash chromatography (CH_2Cl_2/MeOH = 20:1) to give **228** as a yellow oil (8.0 mg, 82%).

R_f = 0.3 (CH_2Cl_2/MeOH = 20:1); **^{1}H NMR** ($CDCl_3$, 400 MHz): δ 7.08 (d, 2H, J = 8.5, 5-ArH), 6.80 (d, 2H, J = 8.5, 6-ArH), 3.75 (s, 3H, 8-CH_3), 3.32 (dd, J = 10.7, 14.7, 2H, 1-CH_2), 2.74 (s, 3H, OH and NH_2), 2.62 (s, 2H, 3-CH_2), 0.98 (s, 3H, 9-CH_3); **^{13}C NMR** ($CDCl_3$, 101 MHz) δ 158.2 (7-C), 131.4 (5-C), 129.4 (4-C), 113.6 (6-C), 69.3 (1-C), 55.2 (8-C), 53.6 (2-C), 44.5 (3-C), 24.4 (9-C); **IR** (KBr) ν_{max} 3228, 2910, 2814, 2736, 1610, 1570, 1535, 1508, 1465, 1246, 1031, 763 cm^{-1}; **ES-MS**: *m/z* (%): 196.1 $[M]H^+$ (100), 391.1 $[2M]H^+$ (6.2).

***N*-(1-Hydroxy-3-(4-methoxyphenyl)-2-methylpropan-2-yl)-3- oxobutanamide 229.**

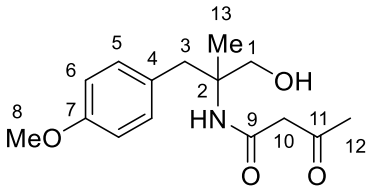

A mixture of amino alcohol **228** (180 mg, 0.92 mmol) and dioxinone **161** (130 mg, 0.92 mmol) in anhydrous toluene (15 mL) was heated to 103 °C for 3 h. The reaction mixture was concentrated under vacuum and the residue was purified by flash chromatography (CH_2Cl_2/MeOH = 20:1) to give **229** as a colourless oil (148 mg, 58%).

R_f = 0.5 (CH_2Cl_2/MeOH = 20:1); **^{1}H NMR** ($CDCl_3$, 400 MHz): δ 7.12 (d, 2H, J = 8.5, 5-ArH), 6.93 (s, 1H, CONH), 6.83 (d, 2H, J = 8.5, 6-ArH), 3.79 (s, 3H, 8-CH_3), 3.70-3.60

(m, 2H, 1-CH_2), 3.39 (s, 2H, 10-CH_2), 3.01 (d, 1H, J = 13.6, 3-CH), 2.86 (d, 1H, J = 13.6, 3-CH), 2.26 (s, 3H, 12-CH_3), 1.16 (s, 3H, 13-CH_3); **^{13}C NMR** ($CDCl_3$, 101 MHz) δ 204.6 (11-C), 166.3 (9-C), 158.5 (7-C), 131.5 (5-C), 128.3 (4-C), 113.7 (6-C), 68.8 (1-C), 59.6 (2-C), 55.2 (8-C), 49.8 (10-C), 40.7 (3-C), 31.1 (12-C), 22.6 (13-C); **IR** (KBr) ν_{max} 3305, 3078, 2933, 1712, 1647, 1610, 1550, 1463, 1244, 1161, 1031, 883 cm^{-1}; **HRMS** calcd for $C_{15}H_{21}NO_4$ $[M+Na]^+$ m/z = 302.1368, found 302.1367.

3-Acetyl-5-(4-methoxybenzyl)-5-methyl-1,5-dihydro-2H-pyrrol-2-one 231.

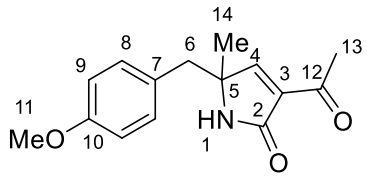

EDC·HCl (17.2 mg, 0.09 mmol) and dichloroacetic acid (4.6 mg, 0.04 mmol) were added to a solution of **229** (5.0 mg, 0.02 mmol) in toluene (0.5 mL) and DMSO (0.5 mL). The reaction was stirred at 25 °C for 16 h and then H_2O was added. The aqueous layer was extracted with EtOAc (3 × 2 mL), and the organic solvents combined to give a solution of aldehyde, which was treated with 1 M NaOH solution (5 mL) for 5 min at 0 °C to afford pyrrolinone **231**. The organic phase was separated and the aqueous phase was extracted with EtOAc. The combined organic solvents were washed with sat. aqueous NaCl, dried over $MgSO_4$ and evaporated under vacuum. Purification by preparative LCMS gave **231** as a yellow solid (2.6 mg, 56%).

^{1}H NMR ($CDCl_3$, 400 MHz): δ 7.72 (d, 1H, J = 2.0, 4-CH), 7.05 (d, 2H, J = 8.6, 8-ArH), 6.84 (d, 2H, J = 8.6, 9-ArH), 6.26 (s, 1H, 1-CONH), 3.79 (s, 3H, 11-CH_3), 2.90 (d, 1H, J = 13.6, 6-CH_2), 2.83 (d, 1H, J = 13.6, 6-CH_2), 2.51 (s, 3H, 13-CH_3), 1.35 (s, 3H, 14-CH_3); **^{13}C NMR** ($CDCl_3$, 101 MHz) δ 194.3 (12-C), 168.6 (2-C), 160.6 (4-C), 158.9 (10-C), 135.2 (3-C), 131.1 (8-C), 126.9 (7-C), 114.0 (9-C), 61.7 (5-C), 55.3 (11-C), 44.1 (6-C), 29.2 (13-C), 23.0 (14-C); **IR** (KBr) ν_{max} 3261, 2920, 1697, 1512, 1246, 1031, 819 cm^{-1}; **HRMS** calcd for $C_{15}H_{17}NO_3$ $[M+Na]^+$ m/z = 282.1106, found 282.1106.

(9H-Fluoren-9-yl)methyl-*S*-(3-(4-(*tert*-butoxy)phenyl)-1-(methoxy(methyl)amino)-1-oxopropan-2-yl)carbamate 352.[161]

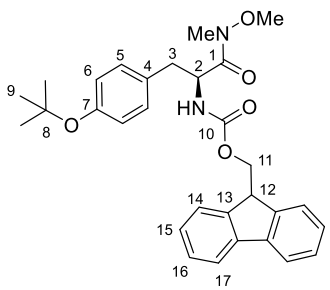

Fmoc-protected amino acid (Iris Biotech GmbH, 2.5 mmol, 1.15 g) was added to a dry 100 mL round bottom flask equipped with a magnetic stir bar, dissolved in dry CH_2Cl_2

(10 mL) with DIEA (0.4 mL) and cooled to 0 ºC. After stirring for 10 min at 0 ºC, EDC·HCl (575 mg, 3.0 mmol) and HOBt (400 mg, 3.0 mmol) were added as solids. The mixture was stirred at 0 ºC for another 10 min, then *N*,*O*-dimethylhydroxylamine (300 mg, 3 mmol) and DIEA (0.5 mL) were added. The mixture was allowed to stir at 0 ºC for an additional hour, then allowed to warm to room temperature. The mixture was stirred for another 16 h. The reaction mixture was transferred with CH_2Cl_2 rinses (50 mL) to a separatory funnel, then washed with aqueous HCl (2 N, 3 × 30 mL), sat. aqueous $NaHCO_3$ solution (2 × 30 mL) and sat. aqueous NaCl solution (2 × 30 mL). The organic layer was dried over anhydrous Na_2SO_4, concentrated on a rotary evaporator, dried under vacuum and the residue was purified by flash chromatography (petroleum ether/EtOAc = 2:1) to give a white crystalline solid (1.12 g, 90%).

R_f = 0.2 (petroleum ether/EtOAc = 4:1); **$[\alpha]_D^{23}$** = -4.7 (*c* = 0.3, MeOH; lit. no report); **^{1}H NMR** ($CDCl_3$, 400 MHz): δ 7.76 (d, *J* = 7.6, 2H, 17-CH), 7.57 (t, *J* = 6.8, 2H, 14-CH), 7.40 (t, *J* = 7.6, 2H, 16-CH), 7.33-7.28 (m, 2H, 15-CH), 7.07 (d, *J* = 8.1, 2H, 5-CH), 6.90 (d, *J* = 8.1, 2H, 6-CH), 5.48 (d, *J* = 8.5, 1H, CONH), 5.05-4.95 (m, 1H, 2-CH), 4.39-4.24 (m, 2H, 11-CH_2), 4.18 (t, *J* = 7.2, 1H, 12-CH), 3.62 (s, 3H, OCH_3), 3.16 (s, 3H, NCH_3), 3.08-3.00 (m, 1H, 3-CH), 2.95-2.86 (m, 1H, 3-CH), 1.30 (s, 9H, 9-$C(CH_3)_3$); **IR** (KBr) ν_{max} 3300, 2974, 1716, 1654, 1504, 1448, 1284, 1159, 1105, 1043, 897, 738 cm^{-1}; **ES-MS**: *m/z* (%): 503.3 $[M]H^+$ (100), 525.3 $[M]Na^+$ (64.5).

(9H-Fluoren-9-yl)methyl-*S*-(1-(4-(*tert*-butoxy)phenyl)-3-oxopropan-2-yl)carbamate 353.[161]

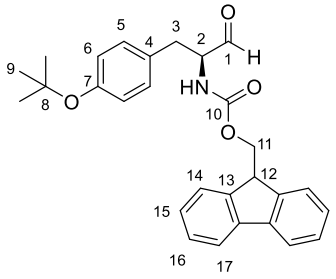

Fmoc-Weinreb amide **352** (12.0 mmol, 6.0 g) was dissolved in dry THF (100 mL) in an oven dry 250 mL round bottom flask equipped with stir bar. The solution was cooled to 0 °C, then $LiAlH_4$ (550 mg, 0.15 mmol) was added in portions as a solid. The mixture was stirred at 0 ºC for 1 h. After this time the reaction mixture was quenched with a solution of $NaHSO_4$ (7.0 g, 50.0 mmol) in H_2O (200 mL), which was added dropwise. The mixture was stirred for an additional 10 min before being transferred to a separatory funnel. The reaction flask was washed with sat. aqueous NaCl solution (30 mL) and EtOAc (30 mL). The layers were separated and the aqueous layer extracted with EtOAc (100 mL). The organic layers were combined and washed with aqueous HCl (1.5 N, 3 × 100 mL), sat.

aqueous $NaHCO_3$ solution (2 × 10 mL) and sat. aqueous NaCl solution (2 × 100 mL). The organic layer was dried over Na_2SO_4, concentrated on a rotary evaporator, dried under vacuum and purified by flash chromatography (petroleum ether/EtOAc = 4:1) to give the aldehyde as a white solid (4.6 g, 86%).

R_f = 0.6 (petroleum ether/EtOAc = 2:1); **$[\alpha]_D^{23}$** = -9.9 (*c* = 0.14, MeOH; lit. no report); **^{1}H NMR** ($CDCl_3$, 400 MHz): δ 9.63 (s, 1H, 1-CHO), 7.77 (d, *J* = 7.5, 2H, 17-CH), 7.58 (d, 2H, *J* = 7.8, 14-CH), 7.41 (t, *J* = 7.5, 2H, 16-CH), 7.32 (t, *J* = 7.4, 2H, 15-CH), 7.02 (d, *J* = 8.2, 2H, 5-CH), 6.91 (d, *J* = 8.2, 2H, 6-CH), 5.32 (d, *J* = 6.9, 1H, CONH), 4.54-4.37 (m, 3H, 2-CH and 11-CH_2), 4.22 (t, *J* = 6.8, 1H, 12-CH), 3.14-3.07 (m, 2H, 3-CH_2), 1.33 (s, 9H, 9-$C(CH_3)_3$); **IR** (KBr) ν_{max} 2976, 1708, 1504, 1234, 1159, 894, 758, 738 cm^{-1}; **ES-MS**: *m/z* (%): 466.3 $[M]Na^+$ (100), 444.2 $[M]H^+$ (38), 484.3 $[M+H_2O]Na^+$ (17), 210.2 $[M-C_{18}H_{20}O+H_2O]^+$ (68).

(9H-Fluoren-9-yl)methyl-*S*-(1-(1,3-dioxolan-2-yl)-2-(4-hydroxyphenyl)ethyl)carba mate 354.

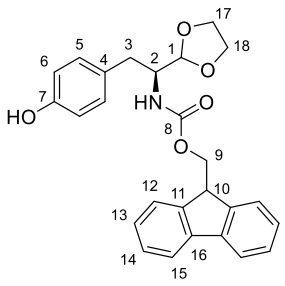

Fmoc-protected aldehyde **353** (13.5 mmol, 6.0 g), a catalytic amount of *p*-TsOH (1.35 mmol, 0.26 g), and toluene (50 mL) were introduced into a 100 mL flask equipped with a Dean-Stark apparatus. After refluxing for 3 days, the solution was allowed to cool to room temperature and the product was precipitated as yellow solid. The solid was collected by filtration and washed with toluene. The filtrate was washed with sat. $NaHCO_3$, NaCl and dried with anhydrous Na_2SO_4, evaporated under vacuum to give the yellow compound, which was recrystallized with toluene. The yellow solid was combined to give the target compound (4.1 g, 70%).

$[\alpha]_D^{23}$ = -38.7 (*c* = 0.4, MeOH); **^{1}H NMR** (DMSO, 400 MHz): δ 9.08 (s, 1H, OH), 7.81 (d, *J* = 7.5, 2H, 15-CH), 7.58 (dd, 2H, *J* = 7.4, 10.8, 12-CH), 7.38-7.21 (m, 5H, CONH and 13, 14-CH), 6.96 (d, *J* = 8.4, 2H, 5-CH), 6.56 (d, *J* = 8.4, 2H, 6-CH), 4.74 (d, *J* = 3.7, 1H, 1-CH), 4.13-4.02 (m, 3H, 9-CH and 10-CH_2), 3.90-3.83 (m, 2H, 17-CH_2), 3.79-3.72 (m, 2H, 18-CH_2), 3.69-3.61 (m, 1H, 2-CH); 2.70-2.63 (m, 1H, 3-CH_2), 2.53-2.47 (m, 1H, 3-CH_2); **^{13}C NMR** (DMSO, 101 MHz): δ 156.3 (8-CO), 155.9 (7-C), 144.3 (11-C), 141.1 (16-C), 130.4 (4-C), 129.1 (5-C), 128.0 (14-C), 127.5 (13-C), 125.9 (12-C), 120.5 (15-C),

115.3 (6-C), 104.2 (1-C), 65.8 (9-C), 65.3 (17-C), 65.0 (18-C), 55.3 (2-C), 47.1 (10-C), 34.1 (3-C); **IR** (KBr) ν_{max} 3307, 1695, 1614, 1514, 1448, 1328, 1228 cm^{-1}; **HRMS** calcd for $C_{26}H_{25}NO_5$ $[M+Na]^+$ *m/z* = 454.1630 found 454.1630.

_S_-4-(2-Amino-2-(1,3-dioxolan-2-yl)ethyl)phenol 342.

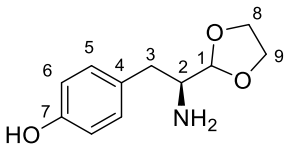

Fmoc-protected acetal **354** (1.0 g, 2.32 mmol) was dissolved in acetonitrile (10 mL). Diethylamine (10 mL) was added and the mixture was stirred at room temperature for 3 h. After completed reaction, the solution was concentrated under vacuum and purified by flash chromatography (CH_2Cl_2/MeOH = 30:1, additional TEA was added) to give **342** as a yellow solid (0.33 g, 62%).

R_f = 0.15 (petroleum ether/EtOAc = 2:1); **$[\alpha]_D^{23}$** = -15.2 (*c* = 0.7, MeOH). **^{1}H NMR** ($CDCl_3$, 400 MHz): δ 7.02 (d, 2H, *J* = 8.5, 5-CH), 6.66 (d, *J* = 8.5, 2H, 6-CH), 4.75 (d, 1H, *J* = 3.6, 1-CH), 4.05-4.98 (m, 2H, 8-CH_2), 3.94-3.89 (m, 2H, 9-CH_2), 3.35 (s, 2H, NH_2), 3.12-3.06 (m, 1H, 2-CH), 2.87 (dd, 1H, *J* = 4.8, 13.8, 3-CH_2), 2.55 (dd, 1H, *J* = 9.3, 13.8, 3-CH_2); **^{13}C NMR** ($CDCl_3$, 101 MHz): δ 155.3 (7-C), 130.3 (4-C), 128.9 (5-C), 115.8 (6-C), 105.1 (1-C), 65.4 (8-C), 65.3 (9-C), 54.9 (2-C), 37.5 (3-C); **IR** (KBr) ν_{max} 3346, 2887, 1612, 1591, 1514, 1247, 1128, 1097 cm^{-1}; **HRMS** calcd for $C_{11}H_{16}NO_3$ $[M+H]^+$ *m/z* = 210.1131 found 210.1131.

6-(Chloromethyl)-2,2-dimethyl-4H-1,3-dioxin-4-one 166.[162]

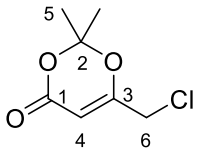

2,2-Dimethyl-(4H)-1,3-dioxin-4-one **161** (Sigma-Aldrich, 4.60 mL, 5.00 g, 35.0 mmol) was added dropwise to a solution of LDA (47.3 mmol, 1.35 eq.) in dry THF (100 mL) within 5 min at -78 °C. The resulting mixture was stirred for another 5 min. The temperature was gradually raised to -48 °C. A solution of C_2Cl_6 (14.6 g, 61.6 mmol, 1.76 eq.) in THF (40 mL) was added dropwise within 50 min. After stirring for another 10 min, the red solution was quenched by the addition of ice cold diluted aqueous HCl. The layers were separated and the aqueous layer was extracted with Et_2O (3 × 50 mL). The combined organic extracts were washed with H_2O (15 mL) and dried over anhydrous $MgSO_4$. The solvent was removed under vacuum and the residue purified by flash chromatography (petroleum ether/EtOAc = 4:1) to give **166** as a yellow liquid (3.1 g, 50%).

R_f = 0.5 (petroleum ether/EtOAc = 4:1); **^{1}H NMR** ($CDCl_3$, 400 MHz): δ 5.57 (s, 1H, 4-CH), 4.04 (s, 2H, 6-CH_2), 1.74 (s, 6H, 5-$(CH_3)_2$); **IR** (neat) ν_{max} 2999, 1718, 1637, 1388, 1271, 1199, 1029 cm^{-1}; **ES-MS**: *m/z* (%): 118.94 $[C_4H_3{}^{35}ClO_2]H^+$ (100), 121.0 $[C_4H_3{}^{37}ClO_2]H^+$ (25), 177.0 $[M]H^+$ (98), 179.1 $[M]H^+$ (77).

Diethyl((2,2-dimethyl-4-oxo-4H-1,3-dioxin-6-yl)methyl)phosphonate 167.[162]

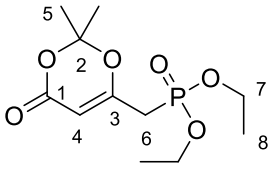

Diethyl phosphite (Sigma-Aldrich, 8.74 g, 63.4 mmol) was added dropwise to a solution of potassium *tert*-butoxide (7.09 g, 63.4 mmol) in DMF (30 mL), cooled to 0 °C. After 30 min, **166** (3.73 g, 21.1 mmol) in DMF (10 mL) was added dropwise over 20 min and the deep purple solution generated was stirred at 0 °C for a further 60 min. Dropwise addition of concentrated aqueous HCl discharged the colour and the pale brown mixture was filtrated through silica gel, and the silica gel washed with diethyl ether. The combined solvents were washed with H_2O (3 × 30 mL) and the organic phase was washed with sat. NaCl, dried over $MgSO_4$, concentrated under vacuum, purified by flash chromatography (petroleum ether/EtOAc = 1:2) to give **167** as a yellow oil (4.74 g, 48%).

R_f = 0.4 (pure EtOAc); **^{1}H NMR** ($CDCl_3$, 400 MHz): δ 5.34 (d, 1H, *J* = 3.7, 4-CH), 4.14-4.06 (m, 4H, 7-CH_2), 2.76 (d, *J* = 22.2, 6-CH_2), 1.65 (s, 6H, 5-$(CH_3)_2$), 1.29 (t, *J* = 7.1, 6H, 8-CH_3); **IR** (neat) ν_{max} 2981, 1726, 1666, 1633, 1384, 1253 cm^{-1}; **ES-MS**: *m/z* (%): 221.2 $[C_8H_{13}O_5P]H^+$ (100), 239.3 $[C_8H_{13}O_5P+H_2O]H^+$ (27), 557.4 $[2M]H^+$ (14), 499.4 $[M+ C_8H_{13}O_5P]H^+$ (14).

(2*E*,4*E*-Hexa-2,4-dien-1-yl)triphenylphosphonium bromide 356.[155]

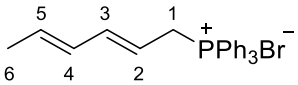

To a stirred solution of 2*E*,4*E*-hexadien-l-ol (abcr GmbH, 9.8 g, 100 mmol) of in 20 mL of CH_2Cl_2 under nitrogen atmosphere at -10 °C was slowly added a solution of 9.20 g (34 mmol) of $PhBr_3$ in 20 mL of CH_2Cl_2. After all the phosphorous tribromide was added, the reaction mixture was stirred for an additional 15-20 min before it was quenched with an ice-cold sat. aqueous solution of $NaHCO_3$ (30 mL). The resulting mixture was extracted with pentane (350 mL), the organic phase was washed with sat. aqueous NaCl (2 × 50 mL), and dried over Na_2SO_4. After removal of the pentane and CH_2Cl_2 by rotary evaporation at room temperature, the crude bromide was transferred to a wide-mouth brown glass bottle

containing triphenylphosphine (Sigma-Aldrich, 28 g, 108 mmol) and dry toluene (160 mL). The mixture was kept at room temperature for 3 days, and the resulting crystalline product was collected by suction filtration, rinsing the solids with a small amount of toluene. After pumping under vacuum at room temperature for 6 h to remove traces of toluene, 24.0 g of the crystalline phosphonium salt **356** was obtained (58%);

^{1}H NMR ($CDCl_3$, 400 MHz): δ 7.83-7.62 (m, 15H, ArH), 6.38-6.28 (m, 1H, 3-CH), 5.93-5.82 (m, 1H, 4-CH), 5.69-5.58 (m, 1H, 5-CH), 5.33-5.22 (m, 1H, 2-CH), 4.74 (dd, 2H, J = 7.6, 15.4, 1-CH_2), 1.66 (d, J = 6.3, 3H, 6-CH_3); **IR** (neat) ν_{max} 2858, 1587, 1435, 1109, 995, 931, 873 cm^{-1}; **ES-MS**: *m/z* (%): 343.0 [M-Br^-] (100).

8-Hydroxyoctyl benzoate 364.[163]

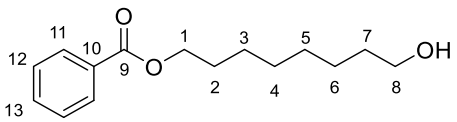

Benzoyl chloride (Sigma-Aldrich, 12.6 g, 89.5 mmol) was added dropwise to a mixture of octane-1,8-diol (abcr GmbH, 19.6 g, 134 mmol) and TEA (9.0 g, 89.5 mmol) in dry THF (100 mL) at 0 °C. The mixture was allowed to warm to room temperature and stirred for 6 h. After reaction, the solution was filtrated and the filtrate was washed with sat. $NaHCO_3$ and NaCl, dried over $MgSO_4$, concentrated under vacuum and purified by flash chromatography (petroleum ether/EtOAc = 4:1) to give **364** as a colourless oil (7.8 g, 60%).

R_f = 0.3 (PE/EA = 2:1); **^{1}H NMR** ($CDCl_3$, 400 MHz): δ 8.04 (d, 2H, J = 8.1, 11-CH), 7.57-7.54 (m, 1H, 13-CH), 7.46-7.41 (m, 2H, 12-CH), 4.31 (t, 2H, J = 6.7, 1-CH_2), 3.63 (t, 2H, J = 6.6, 8-CH_2), 1.81-1.72 (m, 2H, 2-CH_2), 1.59-1.52 (m, 2H, 7-CH_2), 1.51-1.32 (m, 8H, 3, 4, 5, 6-CH_2); **IR** (neat) ν_{max} 2928, 2854, 1716, 1450, 1284, 1159, 1271, 1109, 707 cm^{-1}; **ES-MS**: *m/z* (%): 105.0 $[C_7H_5O]^+$ (62), 111.1 $[C_8H_{14}]H^+$ (65), 123.0 $[C_7H_6O_2]H^+$ (62), 129.1 $[C_8H_{16}O]H^+$ (55), 233.2 [M-H_2O]H^+ (22), 251.2 [M]H^+ (100), 273.2 [M]Na^+ (25).

8-Oxooctyl benzoate 365.[164]

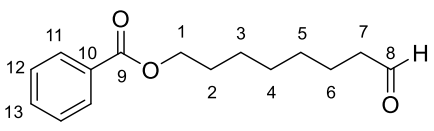

To a cold (-78 °C), stirred solution of oxalyl chloride (Sigma-Aldrich, 4.82 g, 38 mmol) in dry CH_2Cl_2 (40 mL) was added a solution of DMSO (4.45 g, 57

mmol) dropwise in dry CH_2Cl_2 (30 mL) under N_2. After 30 min of stirring, a solution of the monobenzoate of 1,8-octanediol **364** (4.8 g, 19 mmol) in dry CH_2Cl_2 (30 mL) was added over 30 min at -78 °C. The resulting cloudy solution was stirred at -78 °C for 1 h before TEA (9.6 g, 95 mmol) was introduced. The cold bath was removed and the mixture was allowed to warm to 0 °C before being quenched with a sat. aqueous solution of NH_4Cl (50 mL). The separated aqueous phase was extracted with CH_2Cl_2 (3 × 50 mL). The organic layers were combined, dried over $MgSO_4$, and concentrated under vacuum and purified by flash chromatography (petroleum ether/EtOAc = 15:1) to give **365** as a colourless oil (4.2 g, 86%).

R_f = 0.5 (petroleum ether/EtOAc = 8:1); **^{1}H NMR** ($CDCl_3$, 400 MHz): δ 9.74 (t, 1H, *J* = 1.5, 8-CHO), 8.03 (d, 2H, *J* = 7.4, 11-CH), 7.57-7.51 (m, 1H, 13-CH), 7.42 (t, 2H, *J* = 7.8, 12-CH), 4.30 (t, 2H, *J* = 6.7, 1-CH_2), 2.46-2.41 (dt, 2H, *J* = 7.4, 1.5, 7-CH_2), 1.80-1.71 (m, 2H, 2-CH_2), 1.67-1.58 (m, 2H, 6-CH_2), 1.47-1.31 (m, 6H, 3, 4, 5-CH_2); **IR** (neat) ν_{max} 2931, 2856, 1714, 1452, 1388, 1313, 1273, 1109 cm^{-1}; **ES-MS**: *m/z* (%): 249.1 $[M]H^+$ (48), 271.1 $[M]Na^+$ (100), 289.0 $[M+H_2O]Na^+$ (72).

8*E*,10*E*,12*E*-Tetradeca-8,10,12-trien-1-yl benzoate 369.

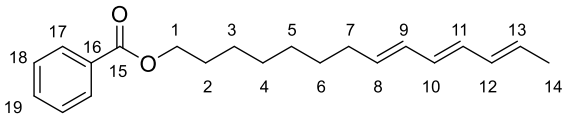

Phosphonium salt **356** (2.15 g, 5.1 mmol) in dry THF (20 mL) was cooled with a dry ice-acetone bath. BuLi (2.5 M in hexanes, 2.04 mL, 5.1 mmol) was added dropwise, and the mixture was stirred at -78 ºC for 1 h. Then aldehyde (1.04 g, 4.2 mmol) in THF (5 mL) was added dropwise. After the addition was complete, the mixture was warmed to room temperature over 1 h, then quenched with ice-water (25 mL), and extracted with hexane (80 mL). The hexane extract was washed with H_2O (2 × 10 mL), sat. aqueous NaCl (2 × 10 mL), dried and concentrated. Flash chromatography (petroleum ether/EtOAc = 30:1) of the residue gave mixture of the title compound as colourless oil (0.81 g, 62%, *EEE*: *ZEE*, 62:38 by crude NMR).

^{1}H NMR ($CDCl_3$, 400 MHz): δ 8.05 (d, 2H, *J* = 7.6, 17-ArH), 7.58-7.53 (m, 1H, 19-ArH), 7.47-7.41 (m, 2H, 18-ArH), 6.12-5.99 (m, 4H, 9,10,11,12-CH), 5.74-5.59 (m, 2H, 8,13-CH), 4.32 (t, 2H, *J* = 6.7, 1-CH_2), 2.13-2.05 (m, 2H, 7-CH), 1.82-1.72 (m, 5H, 2-CH_2 and 14-CH_3), 1.49-1.29 (m, 8H, 3,4,5,6-CH_2); **^{13}C NMR** ($CDCl_3$, 101 MHz): δ 166.7 (15-C), 134.3 (8-C), 132.8 (19-C), 131.8 (10-C), 130.8 (11-C), 130.6 (12-C), 130.5

(9-C), 129.5 (16-C), 128.8 (13-C), 128.7 (16-C), 125.8 (17-C), 65.1 (1-C), 32.8 (7-C), 29.6 (2-C), 29.3 (6-C), 29.2 (4-C), 29.0 (5-C), 28.7 (3-C), 18.3 (14-C); **IR** (neat) ν_{max} 2928, 2854, 1716, 1450, 1313, 1269, 1174, 1111, 707 cm^{-1}; **HRMS**: calcd for $C_{21}H_{28}O_2$ $[M+Na]^+$ *m/z* = 335.1987, found 335.1986.

8*E*,10*E*,12*E*-Tetradeca-8,10,12-trien-1-ol 370.

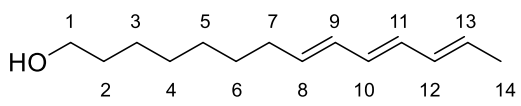

Dry K_2CO_3 (8.72 g, 63.2 mmol) was added to an ice-cold solution of the acetates **369** (9.86 g, 31.6 mmol) in MeOH (100 mL). The mixture was stirred at room temperature for 1 h, then quenched with ice-cold H_2O (100 mL) and extracted with hexane (3 × 100 mL). The organic phase was washed with sat. aqueous NaCl, dried, concentrated. The residue was recrystallized with hexane to give the target compound as white solid (3.35 g, 16.1 mmol, 50%). The mother liquor was evaporated and dissolved in 1:1 hexane-Et_2O (1 L) containing a few crystals I_2 (~ 5 mg), and kept in laboratory light for 10 min. The solution was washed with sat. $Na_2S_2O_3$ (30 mL), sat. aqueous NaCl (2 × 100 mL) and dried over $MgSO_4$. After concentration and recrystallization as before, a further 1.05 g (15%) of pure *EEE* **370** was obtained.

^{1}H NMR ($CDCl_3$, 400 MHz): δ 6.12-6.00 (m, 4H, 9,10,11,12-CH), 5.73-5.62 (m, 2H, 8,13-CH), 3.65 (t, 2H, *J* = 6.6, 1-CH_2), 2.13-2.06 (m, 2H, 7-CH_2), 1.78 (d, 3H, *J* = 6.6, 14-CH_3), 1.62-1.53 (m, 2H, 2-CH_2), 1.45 (s, 1H, OH), 1.43-1.29 (m, 8H, 3,4,5,6-CH_2); **^{13}C NMR** ($CDCl_3$, 101 MHz): δ 134.3 (8-C), 131.8 (10-C), 130.7 (11-C), 130.6 (12-C), 130.5 (9-C), 128.8 (13-C), 63.0 (1-C), 32.8 (7-C), 29.3 (2-C), 29.3 (6-C), 29.1 (4-C), 25.7 (3-C), 18.3 (14-C); **IR** (neat) ν_{max} 3373, 2926, 2848, 1465, 1371, 1062, 993, 976, 764 cm^{-1}; **HRMS** calcd for $C_{14}H_{24}O$ $[M+Na]^+$ *m/z* = 231.1725 found 231.1727.

8*E*,10*E*,12*E*-Tetradeca-8,10,12-trienal 345.

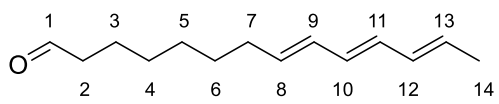

To a cold (-78 °C), stirred solution of oxalyl chloride (1.2 g, 9.4 mmol) in dry CH_2Cl_2 (10 mL) was added a solution of DMSO (1.1 g, 14.1 mmol) dropwise in dry CH_2Cl_2 (10 mL) under N_2. After 30 min of stirring, a solution of the 8*E*,10*E*,12*E*-tetradeca-8,10,12-trien-1-ol **370** (0.99 g, 4.7 mmol) in dry CH_2Cl_2 (10 mL) was added over 30 min at -78 °C. The resulting cloudy solution was stirred at -78 °C

for 1 h before Et_3N (2.4 g, 23.5 mmol) was introduced. The cold bath was removed and the mixture was allowed to warm to 0 °C before being quenched with a sat. solution of NH_4Cl (20 mL). The separated aqueous phase was extracted with CH_2Cl_2 (3 × 20 mL). The organic layers were combined, dried over $MgSO_4$, and concentrated under vacuum to afford **345** as a white solid (0.81 g, 83%). The residue was applied to freeze dryer to remove tiny amount of H_2O inside and used for next step without further purification.

^{1}H NMR (CD_3CN, 400 MHz): δ 9.68 (t, 1H, *J* = 1.7, 1-CHO), 6.13-6.00 (m, 4H, 9,10,11,12-CH), 5.73-5.62 (m, 2H, 8,13-CH), 2.38 (dt, 2H, *J* = 1.7, 7.3, 2-CH_2), 2.11-2.03 (m, 2H, 7-CH_2), 1.74 (d, 3H, *J* = 6.6, 14-CH_3), 1.60-1.53 (m, 2H, 3-CH_2), 1.41-1.29 (m, 6H, 4,5,6-CH_2); **^{13}C NMR** ($CDCl_3$, 101 MHz): δ 204.1 (1-CHO), 135.3 (8-C), 132.7 (10-C), 131.8 (11-C), 131.6 (12-C), 131.5 (9-C), 129.7 (13-C), 44.3 (2-C), 33.3 (7-C), 29.9 (6-C), 29.6 (4-C), 29.6 (5-C), 22.7 (3-C), 18.4 (14-C); **IR** (neat) ν_{max} 2926, 1718, 995 cm^{-1}; **HRMS** calcd for $C_{14}H_{22}O$ $[M+Na]^+$ *m/z* = 229.1568 found 229.1567.

2,2-Dimethyl-6-(1*E*,9*E*,11*E*,13*E*-pentadeca-1,9,11,13-tetraen-1-yl)-4H-1,3-dioxin-4-one 343.

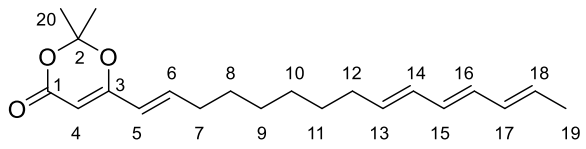

In a flame-dried round bottom flask under nitrogen atmosphere, phosphonate **167** (0.88 g, 3.2 mmol) in anhydrous THF (15 mL) was added dropwise *n*-BuLi (2.4 mL, 1.6 M in hexane) at -78 °C and was allowed to stir for 1 h. To this stirred solution, crude aldehyde **345** (0.96 g, 4.7 mmol) in THF (10 mL) was added at -78 °C. The resulting mixture was allowed to warm to room temperature and stirred overnight. The reaction was quenched with diluted HCl and extracted with hexane (3 × 20 mL). The organic phases were combined, washed with sat. $NaHCO_3$, sat. aqueous NaCl, dried over $MgSO_4$, concentrated under vacuum and purified by flash chromatography (petroleum ether/EtOAc = 15:1) to give **343** as a white solid (0.36 g, 34%).

R_f = 0.3 (petroleum ether/EtOAc = 9:1); **^{1}H NMR** ($CDCl_3$, 400 MHz): δ 6.54 (dt, 1H, *J* = 6.9, 15.5, 5-CH), 6.12-6.00 (m, 4H, 14,15,16,17-CH), 5.88 (dt, *J* = 1.5, 15.5, 1H, 6-CH), 5.73-5.60 (m, 2H, 13,18-CH), 5.22 (s, 1H, 4-CH), 2.22-2.15 (m, 2H, 7-CH_2), 2.11-2.03 (m, 2H, 12-CH_2), 1.75 (d, 3H, *J* = 6.6, 19-CH_3), 1.70 (s, 6H, 20-$(CH_3)_2$), 1.50-1.28 (m, 8H,

8,9,10,11-CH_2); **^{13}C NMR** ($CDCl_3$, 101 MHz): δ 163.4 (3-C), 162.1 (1-C), 142.6 (6-C), 134.1 (13-C), 131.7 (15-C), 130.8 (16-C), 130.6 (17-C), 130.5 (14-C), 128.9 (18-C), 122.4 (5-C), 106.2 (2-C), 93.2 (4-C), 32.7 (7-C), 29.2 (12-C), 29.0 (8-C), 28.9 (11-C), 28.3 (9-C), 25.0 (20-C), 18.3 (19-C); **IR** (neat) ν_{max} 2922, 2850, 1709, 1653, 1593, 1391, 1375, 1271, 1250, 1202, 1016, 999, 972, 905, 816 cm^{-1}; **HRMS** calcd for $C_{21}H_{30}O_3$ $[M+Na]^+$ *m/z* = 353.2093 found 353.2093.

4*E*,12*E*,14*E*,16*E*-*N*-(*S*-1-(1,3-Dioxolan-2-yl)-2-(4-hydroxyphenyl)ethyl)-3-oxooctadeca-4,12,14,16-tetraenamide 371.

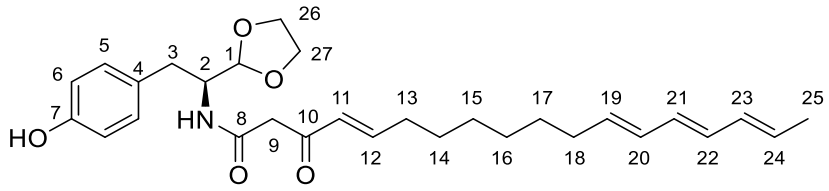

343 (0.33 g, 1.0 mmol) was added to a solution of **342** (0.21 g, 1.0 mmol) in anhydrous toluene (20 mL). The solution was refluxed for 2 h. After complete reaction, reaction mixture was concentrated under vacuum and purified by flash chromatography (petroleum ether/EtOAc = 2:1) to afford **371** as a white solid (0.31 g, 64%).

R_f = 0.4 (petroleum ether/EtOAc = 1:1); **$[\alpha]_D^{23}$** = -10.3 (*c* = 0.4, MeOH); **^{1}H NMR** ($CDCl_3$, 400 MHz): δ 7.44 (d, 1H, *J* = 9.5, CONH), 7.03 (d, 2H, *J* = 8.5, 5-ArH), 6.91 (dt, 1H, *J* = 6.8, 15.8, 12-CH), 6.67 (d, 2H, *J* = 8.5, 6-ArH), 6.11-5.97 (m, 5H, 11,20,21,22,23-CH), 5.74-5.60 (m, 2H, 19,24-CH), 4.91 (d, 1H, *J* = 2.2, 1-CH), 4.57-4.48 (m, 1H, 2-CH), 4.09-3.84 (m, 4H, 26,27-CH_2), 3.50 (d, 1H, *J* = 17.0, 9-CH_2), 3.41 (d, 1H, *J* = 17.0, 9-CH_2), 2.88 (dd, 1H, *J* = 2.9, 14.1, 3-CH_2), 2.68 (dd, 1H, *J* = 9.5, 14.1, 3-CH_2), 2.23-2.15 (m, 2H, 13-CH_2), 2.11-2.03 (m, 2H, 18-CH_2), 1.76 (d, 3H, *J* = 7.1, 25-CH_3), 1.47-1.24 (m, 8H, 14,15,16,17-CH_2); **^{13}C NMR** ($CDCl_3$, 101 MHz): δ 195.7 (10-C), 166.4 (8-C), 155.1 (7-C), 151.4 (12-C), 134.1 (19-C), 131.8 (21-C), 130.8 (22-C), 130.6 (23-C), 130.5 (20-C), 130.1 (5-C), 129.8 (11-C), 128.9 (24-C), 128.4 (4-C), 115.4 (6-C), 103.2 (1-C), 65.5 (26-C), 65.5 (27-C), 52.4 (2-C), 45.6 (9-C), 35.5 (3-C), 32.7 (13-C), 32.6 (18-C), 29.2 (17-C), 29.0 (16-C), 28.9 (15-C), 27.8 (14-C), 18.3 (25-C); **IR** (neat) ν_{max} 3363, 2922, 2852, 1659, 1607, 1545, 1514, 1441, 1261, 1229, 1146, 993, 970, 943, 791, 727, 542 cm^{-1}; **HRMS** calcd for $C_{29}H_{39}NO_5$ $[M+Na]^+$ *m/z* = 504.2726 found 504.2724.

***Z*-5-(4-Hydroxybenzyl)-3-(2*E*,10*E*,12*E*,14*E*-1-hydroxyhexadeca-2,10,12,14-tetraen-1-ylidene)-1,3-dihydro-2H-pyrrol-2-one 372b.**

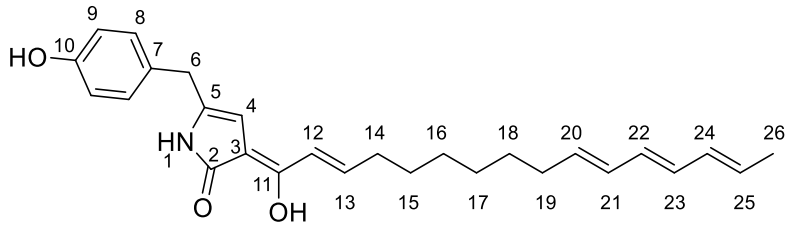

Cyclic acetal **371** (17.0 mg) was dissolved in THF (5 mL) and 5 M HCl (2 mL) was added. The reaction mixture was heated at 60 °C for 3 h. After completion of reaction, the mixture was diluted with EtOAc and washed with H_2O, sat. $NaHCO_3$, saturated aqueous NaCl, dried over $MgSO_4$, concentrated under vacuum and purified by flash chromatography (petroleum ether/EtOAc = 3:1) to afford **372b** as a yellow solid (5 mg, 34%). The compound is not stable during NMR measurement, so only the ^{1}H NMR is available.

R_f = 0.5 (petroleum ether/EtOAc = 2:1); **^{1}H NMR** ($CDCl_3$, 400 MHz): δ 7.35 (s, 1H, CONH), 7.04 (d, 2H, *J* = 8.4, 8-ArH), 6.87-6.76 (m, 3H, 13-CH and 9-ArH), 6.16 (d, 1H, *J* = 15.5, 12-CH), 6.10-6.00 (m, 4H, 21,22,23, 24-CH), 5.72-5.60 (m, 2H, 20,25-CH), 5.60 (s, 1H, 4-CH), 3.62 (s, 2H, 6-CH_2), 2.26 (dd, 1H, *J* = 6.4, 14.0, 14-CH_2), 2.08 (dd, 1H, *J* = 7.0, 14.0, 19-CH_2), 1.76 (d, 3H, *J* = 7.1, 26-CH_3), 1.47-1.28 (m, 8H, 15,16,17,18-CH_2); **HRMS** calcd for $C_{27}H_{33}NO_3$ $[M+Na]^+$ 442.2358 found 442.2356.

4*E*,12*E*,14*E*,16*E*-*N*-(*S*-1,1-Diethoxy-3-(4-methoxyphenyl)propan-2-yl)-3-oxooctadeca-4,12,14,16-tetraenamide 374.

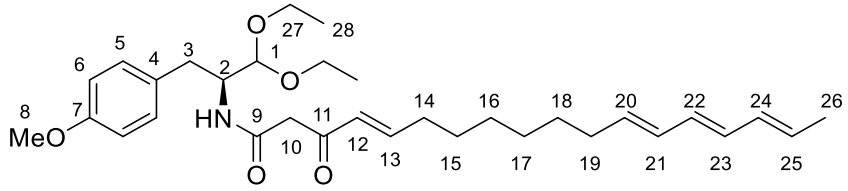

343 (82.0 mg, 0.25 mmol) was added to a solution of **212** (63.0 mg, 0.25 mmol) in anhydrous toluene (10 mL). The solution was heated at 105 °C for 3 h. The reaction

mixture was concentrated under vacuum and the residue was purified by flash chromatography (petroleum ether/EtOAc = 4:1) to give **374** as a yellow solid (78.0 mg, 59%).

R_f = 0.4 (petroleum ether/EtOAc = 4:1); **$[\alpha]_D^{26}$** = -5.3 (*c* = 0.2, MeOH); **^{1}H NMR** ($CDCl_3$, 400 MHz): δ 7.09 (d, 2H, *J* = 8.6, 5-ArH), 7.00-6.86 (m, 2H, 13-CH and CONH), 6.78 (d, 2H, *J* = 8.6, 6-ArH), 6.12-5.98 (m, 5H, 12, 21, 22, 23, 24-CH), 5.70-5.57 (m, 2H, 20, 25-CH), 4.35-4.27 (m, 2H, 2-CH and 1-CH), 3.79-3.70 (m, 4H, 8-CH_3 and 27-CH_2), 3.63-3.47 (m, 3H, 27-CH_2), 3.43 (s, 2H, 10-CH_2), 2.89 (dd, 2H, *J* = 5.9, 14.1, 3-CH_2), 2.72 (dd, 2H, *J* = 8.1, 14.1, 3-CH_2), 2.23-2.16 (m, 2H, 14-CH_2), 2.08-2.02 (m, 2H, 19-CH_2), 1.74 (d, 3H, *J* = 6.8, 26-CH_3), 1.42-1.16 (m, 14H, 28-CH_3 and 15, 16, 17, 18-CH_2); **^{13}C NMR** ($CDCl_3$, 101 MHz): δ 195.2 (11-C), 165.5 (9-C), 158.0 (7-C), 150.7 (13-C), 134.1 (20-C), 131.8 (22-C), 130.8 (23-C), 130.6 (24-C), 130.5 (21-C), 130.2 (5-C), 130.1 (4-C), 129.9 (12-C), 128.8 (25-C), 113.7 (6-C), 102.1 (1-C), 55.1 (8-C), 52.7 (2-C), 46.9 (10-C), 34.7 (14-C), 32.7 (3-C), 32.6 (19-C), 29.2 (18-C), 29.0 (17-C), 28.9 (16-C), 27.9 (15-C), 18.3 (26-C), 15.3 (28-C), 15.2 (28-C); **IR** (KBr) ν_{max} 3288, 3008, 2972, 2924, 2852, 1610, 1548, 1512, 1246, 1060, 993 cm^{-1}; **HRMS** calcd for $C_{32}H_{47}NO_5$ $[M+Na]^+$ *m/z* = 548.3352, found 548.3353.

4*E*,12*E*,14*E*,16*E*-*N*-(*S*-1-Hydroxy-3-(4-methoxyphenyl)propan-2-yl)-3-oxooctadeca -4,12,14,16-tetraenamide 387.

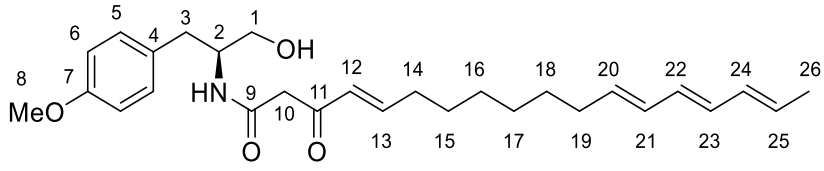

343 (82 mg, 0.25 mmol) was added to a solution of **127** (45 mg, 0.25 mmol) in anhydrous toluene (10 mL). The solution was heated at 105 °C for 3 h. The reaction mixture was concentrated under vacuum and the residue was purified by flash chromatography (CH_2Cl_2/MeOH = 20:1) to give **387** as a yellow solid (68 mg, 60%).

R_f = 0.3 (CH_2Cl_2/MeOH = 20:1); **$[\alpha]_D^{23}$** = -20.4 (*c* = 0.3, MeOH); **^{1}H NMR** ($CDCl_3$, 400 MHz): δ 7.29-7.26 (m, 1H, CONH), 7.13 (d, 2H, *J* = 8.6, 5-ArH), 6.94 (dt, 1H, *J* = 6.8, 15.8, 13-CH), 6.83 (d, 2H, *J* = 8.6, 6-ArH), 6.15-5.96 (m, 5H, 12,21,22,23,24-CH),

5.72-5.58 (m, 2H, 20,25-CH), 4.19-4.09 (m, 1H, 2-CH), 3.78 (s, 3H, 8-CH_3), 3.69 (dd, 1H, *J* = 3.6, 11.2, 1-CH), 3.57 (dd, 1H, *J* = 5.5, 11.2, 1-CH), 3.54-3.44 (m, 2H, 10-CH_2), 2.89-2.73 (m, 2H, 3-CH_2), 2.27-2.19 (m, 2H, 14-CH_2), 2.11-2.02 (m, 2H, 19-CH_2), 1.76 (d, 3H, *J* = 6.6, 26-CH_3), 1.50-1.26 (m, 8H, 15,16,17,18-CH_2); **^{13}C NMR** ($CDCl_3$, 101 MHz): δ 195.7 (11-C), 166.6 (9-C), 158.3 (7-C), 151.3 (13-C), 134.1 (20-C), 131.7 (22-C), 130.8 (23-C), 130.6 (24-C), 130.5 (21-C), 130.2 (5-C), 129.9 (4-C), 129.5 (12-C), 128.9 (25-C), 114.0 (6-C), 64.3 (1-C), 55.2 (8-C), 53.5 (2-C), 46.2 (10-C), 36.2 (14-C), 32.7 (3-C), 32.6 (19-C), 29.2 (18-C), 29.0 (17-C), 28.9 (16-C), 27.8 (15-C), 18.3 (26-C); **IR** (KBr) ν_{max} 3292, 2926, 2852, 1610, 1510, 1300, 1244, 1176, 1033 cm^{-1}; **HRMS** calcd for $C_{28}H_{39}NO_4$ $[M+Na]^+$ *m/z* = 476.2777, found 476.2779.

4*E*,12*E*,14*E*,16*E*-*N*-(*S*-1-(4-Methoxyphenyl)-3-oxopropan-2-yl)-3-oxooctadeca-4,12,14,16-tetraenamide 116.

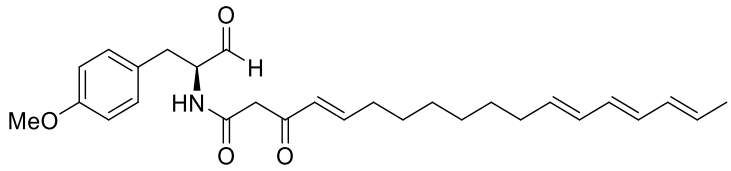

Diethyl acetal **374** (20.0 mg, 0.04 mmol) was dissolved in aqueous THF (2 mL). After cooling to 0 °C, concentrated HCl (37%, 1.5 mL) was added and the reaction was stirred for 1.5 h. After complete reaction checked by LCMS, the solution was diluted with H_2O and extracted with EtOAc (3 × 2 mL). The organic solvents were combined and evaporated under vacuum to afford yellow oil (12 mg, 70%). But the compound is not stable during NMR measurement, thus only the LCMS and HRMS are available.

HRMS calcd for $C_{28}H_{37}NO_4$ $[M+Na]^+$ *m/z* = 474.2620, found 474.2620.

References

1. W. Rothweiler and C. Tamm, *Experientia.*, **1966**, 22, 750–752.
2. D. C. Aldridge, J. J. Armstrong, R. N. Speake and W. B. Turner, *Chem. Commun.*, **1967**, 12, 26.
3. D. C. Aldridge and W. B. Turner, *J. Chem. Soc. C*, **1969**, 923–928.
4. S. Hayakawa, T. Matsushima, T. Kimura, H. Minato and K. Katagiri, *J. Antibiot.*, **1968**, 21, 523–524.
5. D. C. Aldridge and W. B. Turner, *J. Antibiot.*, **1969**, 22, 170–170.
6. D. C. Aldridge, B. F. Burrows and W. B. Turner, *J. Chem. Soc. Chem. Commun.*, **1972**, 1765, 148.
7. Z. Wu, Q. Tong, X. Zhang, P. Zhou, C. Dai, J. Wang, C. Chen, H. Zhu and Y. Zhang, *Org. Lett.*, **2019**, 21, 1026–1030.
8. B. C. Yan, W. G. Wang, D. B. Hu, X. Sun, L. M. Kong, X. N. Li, X. Du, S. H. Luo, Y. Liu, Y. Li, H. D. Sun and J. X. Pu, *Org. Lett.*, **2016**, 18, 1108–1111.
9. C. Chen, Q. Tong, H. Zhu, D. Tan, J. Zhang, Y. Xue, G. Yao, Z. Luo, J. Wang, Y. Wang and Y. Zhang, *Sci. Rep.*, **2016**, 6, 18711.
10. C. J. Zheng, C. L. Shao, L. Y. Wu, M. Chen, K. L. Wang, D. L. Zhao, X. P. Sun, G. Y. Chen and C. Y. Wang, *Mar. Drugs*, **2013**, 11, 2054–2068.
11. Z. Zhang, X. Min, J. Huang, Y. Zhong, Y. Wu, X. Li, Y. Deng, Z. Jiang, Z. Shao, L. Zhang and F. He, *Mar. Drugs*, **2016**, 14, 233.
12. E. La Kim, H. Wang, J. H. Park, J. Hong, J. S. Choi, D. S. Im, H. Y. Chung and J. H. Jung, *Bioorganic Med. Chem. Lett.*, **2015**, 25, 2096–2099.
13. A. Probst and C. Tamm, *Helv. Chim. Acta*, **1981**, 64, 2065–2077.
14. G. Biichi, Y. Kitaura, S. S. Yuan, H. E. Wright, J. Clardy, A. L. Demain, T. Glinsukon, N. Hunt and G. N. Wogan, *J. Am. Chem. Soc.*, **1973**, 95, 5423–5425.
15. H. Tomoda, I. Namatame, S. Si, K. Kawaguchi, R. Masuma, M. Namikoshi and S. Omura, *J. Antibiot.*, **1999**, 52, 851–856.
16. M. Zaghouani, C. Kunz, L. Guédon, F. Blanchard and B. Nay, *Chem. Eur. J.*, **2016**, 22, 15257–15260.
17. G. Ding, H.-L. Wang, L. Chen, A.-J. Chen, J. Lan, X.-D. Chen, H.-W. Zhang, H. Chen, X.-Z. Liu and Z.-M. Zou, *J. Antibiot.*, **2012**, 65, 143–145.
18. Y. Zhang, R. Tian, S. Liu, X. Chen, X. Liu and Y. Che, *Bioorganic Med. Chem.*, **2008**, 16, 2627–2634.
19. K. Scherlach, D. Boettger, N. Remme and C. Hertweck, *Nat. Prod. Rep.*, **2010**, 27, 869.
20. A. M. Haidle and A. G. Myers, *Proc. Natl. Acad. Sci.*, **2004**, 101, 12048–12053.

21. M. Binder, J. -R Kiechel and C. Tamm, *Helv. Chim. Acta*, **1970**, 53, 1797–1812.
22. M. Binder and C. Tamm, *Angew. Chem Int. Ed. Eng.*, **1973**, 12, 370–380.
23. W. Graf, J.-L. Robert, J. C. Vederas, C. Tamm, P. H. Solomon, I. Miura and K. Nakanishi, *Helv. Chim. Acta*, **1974**, 57, 1801–1815.
24. J.-L. Robert and C. Tamm, *Helv. Chim. Acta*, **1975**, 58, 2501–2504.
25. M. Binder and C. Tamm, *Helv. Chim. Acta*, **1973**, 56, 966–976.
26. Y. Hu, D. Dietrich, W. Xu, A. Patel, J. A. J. J. Thuss, J. Wang, W. B. Yin, K. Qiao, K. N. Houk, J. C. Vederas and Y. Tang, *Nat. Chem. Biol.*, **2014**, 10, 552–554.
27. C. Lebet and C. Tamm, *Helv. Chim. Acta*, **1974**, 57, 1785–1801.
28. J. C. Vederas, W. Graf, L. David and C. Tamm, *Helv. Chim. Acta*, **1975**, 58, 1886–1898.
29. J. C. Vederas and C. Tamm, *Helv. Chim. Acta*, **1976**, 59, 558–566.
30. R. Wyss, C. Tamm and J. C. Vederas, *Helv. Chim. Acta*, **1980**, 63, 1538–1541.
31. S. Sekita, K. Yoshihira, S. Natori and H. Kuwano, *Tetrahedron Lett.*, **1973**, 14, 2109–2112.
32. H. Oikawa, Y. Murakami and A. Ichihara, *J. Chem. Soc., Perkin Trans. 1*, **1992**, 2955–2959.
33. L. Du, C. Sánchez, M. Chen, D. J. Edwards and B. Shen, *Chem. Biol.*, **2000**, 7, 623–642.
34. Z. Song, R. J. Cox, C. M. Lazarus and T. J. Simpson, *ChemBioChem*, **2004**, 5, 1196–1203.
35. V. Hantke, C. Wang, E. J. Skellam and R. J. Cox, *RSC Adv.*, **2019**, 9, 35797–35802.
36. C. Wang, V. Hantke, R. J. Cox and E. Skellam, *Org. Lett.*, **2019**, 21, 4163–4167.
37. J. Schümann and C. Hertweck, *J. Am. Chem. Soc.*, **2007**, 129, 9564–9565.
38. A.-R. Ballester, C. Selma-Lázaro, L. Carmona, L. González-Candelas, M. Marcet-Houben, T. Gabaldón, E. Levin, N. Sela, S. Droby and M. Wisniewski, *Mol. Plant-Microbe Interact.*, **2015**, 28, 232–248.
39. E. Skellam, *Nat. Prod. Rep.*, **2017**, 34, 1252–1263.
40. K. Ishiuchi, T. Nakazawa, F. Yagishita, T. Mino, H. Noguchi, K. Hotta and K. Watanabe, *J. Am. Chem. Soc.*, **2013**, 135, 7371–7377.
41. K. Qiao, Y. H. Chooi and Y. Tang, *Metab. Eng.*, **2011**, 13, 723–732.
42. R. Fujii, A. Minami, K. Gomi and H. Oikawa, *Tetrahedron Lett.*, **2013**, 54, 2999–3002.
43. R. Fujii, T. Ugai, H. Ichinose, M. Hatakeyama, T. Kosaki, K. Gomi, I. Fujii, A. Minami and H. Oikawa, *Biosci. Biotechnol. Biochem.*, **2016**, 80, 426–431.
44. M. L. Nielsen, T. Isbrandt, L. M. Petersen, U. H. Mortensen, M. R. Andersen, J. B. Hoof and T. O. Ostenfeld, *PLoS One*, **2016**, 11, No. e0161199.
45. Z. J. Lin, G. J. Zhang, T. J. Zhu, R. Liu, H. J. Wei and Q. Q. Gu, *Helv. Chim. Acta*, **2009**, 92, 1538–1544.
46. P. Skamnioti and S. J. Gurr, *Trends Biotechnol.,* **2009**, 27, 141–150.
47. Z. Song, W. Bakeer, J. W. Marshall, A. A. Yakasai, R. M. Khalid, J. Collemare, E. Skellam, D. Tharreau, M. H. Lebrun, C. M. Lazarus, A. M. Bailey, T. J. Simpson and R. J. Cox, *Chem. Sci.*, **2015**,

6, 4837–4845.

48. I. Fudal, J. Collemare, H. U. Böhnert, D. Melayah and M. H. Lebrun, *Eukaryot. Cell.*, **2007**, 6, 546–554.
49. J. Collemare, M. Pianfetti, A. E. Houlle, D. Morin, L. Camborde, M. J. Gagey, C. Barbisan, I. Fudal, M. H. Lebrun and H. U. Böhnert, *New Phytol.*, **2008**, 179, 196–208.
50. R. J. Cox, *Org. Biomol. Chem.*, **2007**, 5, 2010–2026.
51. H. U. Böhnert, I. Fudal, W. Dioh, D. Tharreau, J.-L. Notteghem and M.-H. Lebrun, *Plant Cell*, **2004**, 16, 2499–2513.
52. N. Khaldi, J. Collemare, M. H. Lebrun and K. H. Wolfe, *Genome Biol.*, **2008**, 9, 1–10.
53. N. Kato, T. Nogawa, H. Hirota, J. H. Jang, S. Takahashi, J. S. Ahn and H. Osada, *Biochem. Biophys. Res. Commun.*, **2015**, 460, 210–215.
54. G. Stork, Y. Nakahara, Y. Nakahara and W. J. Greenlee, *J. Am. Chem. Soc.*, **1978**, 100, 7775–7777.
55. S. Masamune, Y. Hayase, W. S. W. K. Chan and G. S. Bates, *J. Am. Chem. Soc.*, **1977**, 99, 6756–6758.
56. G. Stork and E. Nakamura, *J. Am. Chem. Soc.*, **1983**, 105, 5510–5512.
57. E. Vedejs and J. G. Reid, *J. Am. Chem. Soc.*, **1984**, 106, 4617–4618.
58. E. Vedejs and R. C. Gadwood, *J. Org. Chem.*, **1978**, 43, 376–378.
59. R. Mondelli, V. Bocchi, G. P. Gardini and L. Chierici, *Org. Magn. Reson.*, **1970**, 3, 7–22.
60. J. H. Atkinson, R. S. Atkinson and A. W. Johnson, *J. Chem. Soc.*, **1964**, I, 5999.
61. A. R. Katritzky and J. M. Lagowski, *Adv. Heterocycl. Chem.*, **1963**, 1, 1–26.
62. E. Vedejs, J. B. Campbell, R. C. Gadwood, J. D. Rodgers, K. L. Spear and Y. Watanabe, *J. Org. Chem.*, **1982**, 47, 1534–1546.
63. E. Merifield and E. J. Thomas, *J. Chem. Soc. Chem. Commun.*, **1990**, 464–466.
64. K. Sakai, H. Kinoshita and T. Nihira, *Appl. Microbiol. Biotechnol.*, **2012**, 93, 2011–2022.
65. J. Marui, S. Ohashi-Kunihiro, T. Ando, M. Nishimura, H. Koike and M. Machida, *J. Biosci. Bioeng.*, **2010**, 110, 8–11.
66. L. M. Halo, J. W. Marshall, A. A. Yakasai, Z. Song, C. P. Butts, M. P. Crump, M. Heneghan, A. M. Bailey, T. J. Simpson, C. M. Lazarus and R. J. Cox, *ChemBioChem*, **2008**, 9, 585–594.
67. R. Fujii, A. Minami, T. Tsukagoshi, N. Sato, T. Sahara, S. Ohgiya, K. Gomi and H. Oikawa, *Biosci. Biotechnol. Biochem.*, **2011**, 75, 1813–1817.
68. K. Tagami, C. Liu, A. Minami, M. Noike, T. Isaka, S. Fueki, Y. Shichijo, H. Toshima, K. Gomi, T. Dairi and H. Oikawa, *J. Am. Chem. Soc.*, **2013**, 135, 1260–1263.
69. K. Sakai, H. Kinoshita, T. Shimizu and T. Nihira, *J. Biosci. Bioeng.*, **2008**, 106, 466–472.
70. A. Yoshimi, S. Yamaguchi, T. Fujioka, K. Kawai, K. Gomi, M. Machida and K. Abe, *Front. Microbiol.*, **2018**, 9, 1–12.
71. K. A. K. Pahirulzaman, K. Williams and C. M. Lazarus, *Methods Enzymol.*, **2012**, 517, 241–260.

72. T. Ugai, A. Minami, R. Fujii, M. Tanaka, H. Oguri, K. Gomi and H. Oikawa, *Chem. Commun.*, **2015**, 51, 1878–1881.
73. M. Ousmer, N. A. Braun, C. Bavoux, M. Perrin and M. A. Ciufolini, *J. Am. Chem. Soc.*, **2001**, 123, 7534–7538.
74. E. Knoevenagel, *Berichte Chem.*, **1898**, 31, 2596–2619.
75. R. H. Vekariya and H. D. Patel, *Synth. Commun.*, **2014**, 44, 2756–2788.
76. H. M. Mohamed, A. H. F. Abd El-Wahab, K. A. Ahmed, A. M. El-Agrody, A. H. Bedair, F. A. Eid and M. M. Khafagy, *Molecules*, **2012**, 17, 971–988.
77. A. Al Fahad, A. Abood, K. M. Fisch, A. Osipow, J. Davison, M. Avramović, C. P. Butts, J. Piel, T. J. Simpson and R. J. Cox, *Chem. Sci.*, **2014**, 5, 523–527.
78. M. Sato, J. E. Dander, C. Sato, Y. S. Hung, S. S. Gao, M. C. Tang, L. Hang, J. M. Winter, N. K. Garg, K. Watanabe and Y. Tang, *J. Am. Chem. Soc.*, **2017**, 139, 5317–5320.
79. L. Li, M. C. Tang, S. Tang, S. Gao, S. Soliman, L. Hang, W. Xu, T. Ye, K. Watanabe and Y. Tang, *J. Am. Chem. Soc.*, **2018**, 140, 2067–2071.
80. J. M. Gao, S. X. Yang and J. C. Qin, *Chem. Rev.*, **2013**, 113, 4755–4811.
81. B. Balakrishnan, C. C. Chen, T. M. Pan and H. J. Kwon, *Tetrahedron Lett.*, **2014**, 55, 1640–1643.
82. A. W. Trautwein, R. D. Süßmuth and G. Jung, *Bioorganic Med. Chem. Lett.*, **1998**, 8, 2381–2384.
83. R. R. Amaresh and P. T. Perumal, *Tetrahedron*, **1999**, 55, 8083–8094.
84. D. M. Ketcha, L. J. Wilson and D. E. Portlock, *Tetrahedron Lett.*, **2000**, 41, 6253–6257.
85. G. M. Abou-Elenien, B. E. El-Anadouli and R. M. Baraka, *J. Chem. Soc. Perkin Trans. 2*, **1991**, 1377–1380.
86. C. O. Kappe, *Acc. Chem. Res.*, **2000**, 33, 879–888.
87. B. Zaleska and L. Sławomir, *Synthesis*, **2001**, 811–827.
88. M. Dekhane, K. T. Douglas and P. Gilbert, *Tetrahedron Lett.*, **1996**, 37, 1883–1884.
89. J. S. Witzeman and W. D. Nottingham, *J. Org. Chem.*, **1991**, 56, 1713–1718.
90. H. ok Kim, R. K. Olser and O. soon Choi, *J. Org. Chem.*, **1987**, 52, 4531–4536.
91. K. Sung and S. Y. Wu, *Synth. Commun.*, **2001**, 31, 3069–3074.
92. R. J. Clemens and J. A. Hyatt, *J. Org. Chem.*, **1985**, 50, 2431–2435.
93. U. S. Sørensen, E. Falch and P. Krogsgaard-Larsen, *J. Org. Chem.*, **2000**, 65, 1003–1007.
94. F. Calo, J. Richardson and A. G. M. Barrett, *Org. Lett.*, **2009**, 11, 4910–4913.
95. R. L. Danheiser, R. F. Miller and R. G. Brisbois, *Org. Synth.*, **1988**, 66, 194.
96. K. Jomon, Y. Kuroda, M. Ajisaka and H. Sakai, *J. Antibiot.*, **1972**, 25, 271–280.
97. R. K. Boeckman, C. H. Weidner, R. B. Perni and J. J. Napier, *J. Am. Chem. Soc.*, **1989**, 111, 8036–8037.
98. R. K. Boeckman, J. J. Napier, E. W. Thomas and R. I. Sato, *J. Org. Chem.*, **1983**, 48, 4152–4154.
99. F. Rübsam, A. M. Evers, C. Michel and A. Giannis, *Tetrahedron*, **1997**, 53, 1707–1714.

100. D. S. Dalisay, B. I. Morinaka, C. K. Skepper and T. F. Molinski, *J. Am. Chem. Soc.*, **2009**, 131, 7552–7553.
101. F. Liu and E. I. Negishi, *J. Org. Chem.*, **1997**, 62, 8591–8594.
102. S. B. Hendi, M. S. Hendi and J. F. Wolfe, *Synth. Commun.*, **1987**, 17, 13–18.
103. A. G. Groß, H. Deppe and A. Schober, *Tetrahedron Lett.*, **2003**, 44, 3939–3942.
104. Y. Chen and S. M. N. Sieburth, *Synthesis*, **2002**, 2191–2194.
105. V. Gotor, R. Liz and A. M. Testera, *Tetrahedron*, **2004**, 60, 607–618.
106. T. Schmidlin and C. Tamm, *Helv. Chim. Acta*, **1980**, 63, 121–131.
107. B. B. Snider and B. J. Neubert, *J. Org. Chem.*, **2004**, 69, 8952–8955.
108. L. Li, P. Yu, M. C. Tang, Y. Zou, S. S. Gao, Y. S. Hung, M. Zhao, K. Watanabe, K. N. Houk and Y. Tang, *J. Am. Chem. Soc.*, **2016**, 138, 15837–15840.
109. M. R. Heinrich, O. Blank and A. Wetzel, *J. Org. Chem.*, **2007**, 72, 476–484.
110. E. Vedejs, J. G. Reid, J. D. Rodgers and S. J. Wittenberger, *J. Am. Chem. Soc.*, **1990**, 112, 4351–4357.
111. H. He, H. Y. Yang, R. Bigelis, E. H. Solum, M. Greenstein and G. T. Carter, *Tetrahedron Lett.*, **2002**, 43, 1633–1636.
112. Y. Shiono, K. Shimanuki, F. Hiramatsu, T. Koseki, M. Tetsuya, N. Fujisawa and K. ichi Kimura, *Bioorganic Med. Chem. Lett.*, **2008**, 18, 6050–6053.
113. X.-W. Li, A. Ear and B. Nay, *Nat. Prod. Rep.*, **2013**, 30, 765–782.
114. S. B. Singh, M. A. Goetz, E. T. Jones, G. F. Bills, R. A. Giacobbe, L. Herranz, S. Stevens-Miles and D. L. Williams, *J. Org. Chem.*, **1995**, 60, 7040–7042.
115. B. Clark, R. J. Capon, E. Lacey, S. Tennant and J. H. Gill, *Org. Biomol. Chem.*, **2006**, 4, 1512–1519.
116. O. Diels and H. Kech, *Justus Liebigs Ann. Chem.*, **1935**, 519, 140–146.
117. W. E. Bachmann and N. C. Deno, *J. Am. Chem. Soc.*, **1949**, 71, 3062–3072.
118. N. K. Devaraj, R. Weissleder and S. A. Hilderbrand, *Bioconjug. Chem.*, **2008**, 19, 2297–2299.
119. M. L. Blackman, M. Royzen and J. M. Fox, *J. Am. Chem. Soc.*, **2008**, 130, 13518–13519.
120. D. S. Liu, A. Tangpeerachaikul, R. Selvaraj, M. T. Taylor, J. M. Fox and A. Y. Ting, *J. Am. Chem. Soc.*, **2012**, 134, 792–795.
121. A. K. Späte, H. Bußkamp, A. Niederwieser, V. F. Schart, A. Marx and V. Wittmann, *Bioconjug. Chem.*, **2014**, 25, 147–154.
122. J. Schoch, M. Wiessler and A. Jäschke, *J. Am. Chem. Soc.*, **2010**, 132, 8846–8847.
123. F. Emmetiere, C. Irwin, N. T. Viola-Villegas, V. Longo, S. M. Cheal, P. Zanzonico, N. V. K. Pillarsetty, W. A. Weber, J. S. Lewis and T. Reiner, *Bioconjug. Chem.*, **2013**, 24, 1784–1789.
124. K. C. Nicolaou, S. A. Snyder, T. Montagnon and G. Vassilikogiannakis, *Angew. Chem. Int. Ed.*, **2002**, 41, 1668–1698.
125. L. T. Burke, D. J. Dixon, S. V. Ley and F. Rodríguez, *Org. Biomol. Chem.*, **2005**, 3, 274–280.

126. A. Ichihara, S. Miki, H. Kawagishi and S. Sakamura, *Tetrahedron Lett.*, **1989**, 30, 4551–4554.
127. R. B. Woodward, F. E. Bader, H. Bickel, A. J. Frey and R. W. Kierstead, *J. Am. Chem. Soc.*, **1956**, 78, 2023–2025.
128. H. Uchiro, N. Shionozaki, R. Tanaka, H. Kitano, N. Iwamura and K. Makino, *Tetrahedron Lett.*, **2013**, 54, 506–511.
129. N. Shionozaki, N. Iwamura, R. Tanaka, K. Makino and H. Uchiro, *Chem. Asian J.*, **2013**, 8, 1243–1252.
130. S. B. Singh, D. L. Zink, M. A. Goetz, A. W. Dombrowski, J. D. Polishook and D. J. Hazuda, *Tetrahedron Lett.*, **1998**, 39, 2243–2246.
131. J. M. Müller, E. Schlittler and H. J. Bein, *Experientia.*, **1952**, 8, 338–338.
132. S. Pornpakakul, S. Roengsumran, S. Deechangvipart, A. Petsom, N. Muangsin, N. Ngamrojnavanich, N. Sriubolmas, N. Chaichit and T. Ohta, *Tetrahedron Lett.*, **2007**, 48, 651–655.
133. E. J. Thomas and J. W. F. Whitehead, *J. Chem. Soc. Perkin Trans. 1*, **1989**, 507–518.
134. K. Auclair, A. Sutherland, J. Kennedy, D. J. Witter, J. P. Van den Heever, C. R. Hutchinson and J. C. Vederas, *J. Am. Chem. Soc.*, **2000**, 122, 11519–11520.
135. H. Oikawa, K. Katayama, Y. Suzuki and A. Ichihara, *J. Chem. Soc. Chem. Commun.*, **1995**, 1321–1322.
136. R. Daduang, S. Kitani, J. Hashimoto, A. Thamchaipenet, Y. Igarashi, K. Shin-ya, H. Ikeda and T. Nihira, *Microbiol. Res.*, **2015**, 180, 30–39.
137. A. Minami and H. Oikawa, *J. Antibiot.*, **2016**, 69, 500–506.
138. H. Oikawa, Y. Suzuki, A. Naya, K. Katayama and A. Ichihara, *J. Am. Chem. Soc.*, **1994**, 116, 3605–3606.
139. R. N. Moore, G. Bigam, J. K. Chan, A. M. Hogg, T. T. Nakashima and J. C. Vederas, *J. Am. Chem. Soc.*, **1985**, 107, 3694–3701.
140. H. J. Kim, M. W. Ruszczycky, S. H. Choi, Y. N. Liu and H. W. Liu, *Nature*, **2011**, 473, 109–112.
141. D. Tan, C. S. Jamieson, M. Ohashi, M. C. Tang, K. N. Houk and Y. Tang, *J. Am. Chem. Soc.*, **2019**, 141, 769–773.
142. Z. Tian, P. Sun, Y. Yan, Z. Wu, Q. Zheng, S. Zhou, H. Zhang, F. Yu, X. Jia, D. Chen, A. Mándi, T. Kurtán and W. Liu, *Nat. Chem. Biol.*, **2015**, 11, 259–265.
143. M. Binder and C. Tamm, *Helv. Chim. Acta*, **1973**, 56, 2387–2396.
144. H. Oikawa, Y. Murakami and A. Ichihara, *Tetrahedron Lett.*, **1991**, 32, 4533–4536.
145. E. M. Stocking and R. M. Williams, *Angew. Chem. Int. Ed.*, **2003**, 42, 3078–3115.
146. E. J. Thomas and J. W. F. Whitehead, *J. Chem. Soc. Perkin Trans. 1*, **1989**, 0, 499–505.
147. V. Bocchi, L. Chierici, G. P. Gardini and R. Mondelli, *Tetrahedron*, **1970**, 26, 4073–4082.
148. S. A. Harkin, O. Singh and E. J. Thomas, *J. Chem. Soc., Perkin Trans. 1*, **1984**, 0, 1489–1499.
149. E. J. Thomas, *Acc. Chem. Res.*, **1991**, 24, 229–235.

150. H. Li, H. Wei, J. Hu, E. Lacey, A. N. Sobolev, K. A. Stubbs, P. S. Solomon and Y. Chooi, *ACS Chem. Biol.*, **2019**, acschembio.9b00791.

151. X. Zhang, L. Yang, W. Wang, Z. Wu, J. Wang, W. Sun, X. Li, C. Chen, H. Zhu and Y. Zhang, *J. Nat. Prod.*, **2019**, 82, 2994–3001.

152. B. S. Jeon, S. A. Wang, M. W. Ruszczycky and H. W. Liu, *Chem. Rev.*, **2017**, 117, 5367–5388.

153. R. K. Boeckman and A. J. Thomas, *J. Org. Chem.*, **1982**, 47, 2823–2824.

154. M. Nakamura, H. Miyashita, M. Yamaguchi, Y. Shirasaki, Y. Nakamura and J. Inoue, *Bioorganic Med. Chem.*, **2003**, 11, 5449–5460.

155. X. Chen and J. G. Millar, *Synthesis*, **2000**, 2000, 113–118.

156. D. Enders, G. Geibel and S. Osborne, *Chem. Eur. J.*, **2000**, 6, 1302–1309.

157. H. A. Hoather (**2013)**. Towards the total synthesis of Diaporthichalasin (Doctoral Dissertation).

158. Dambrin, Valéry; Lenoir, Jean-Yves; Schneider, Jean-Marie. Novel intermediates for the synthesis of (R)-Tamsulosin and its pharmaceutically acceptable salts and process for their preparation. **2003**.WO 2005/058810 A1.

159. M. R. Heinrich, O. Blank, D. Ullrich and M. Kirschstein, *J. Org. Chem.*, **2007**, 72, 9609–9616.

160. F. R. Dietz, A. Prechter, H. Gröger and M. R. Heinrich, *Tetrahedron Lett.*, **2011**, 52, 655–657.

161. G. R. Lawton and D. H. Appella, *J. Am. Chem. Soc.*, **2004**, 126, 12762–12763.

162. D. Petrović and R. Brückner, *Org. Lett.*, **2011**, 13, 6524–6527.

163. H. Sharghi and M. H. Sarvari, *Tetrahedron*, **2003**, 59, 3627–3633.

164. S. Pichlmair, M. de Lera Ruiz, K. Basu and L. A. Paquette, *Tetrahedron*, **2006**, 62, 5178–5194.

Appendix

S-*N*-(1-(4-Methoxyphenyl)-3-oxopropan-2-yl)acetamide **114**.

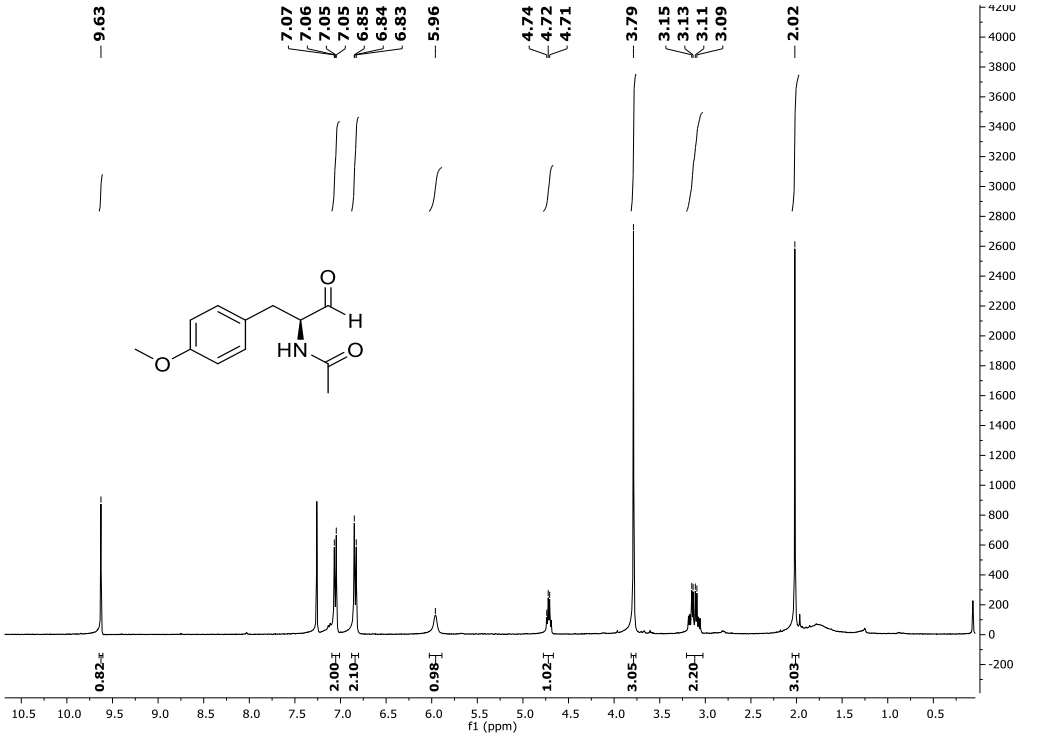

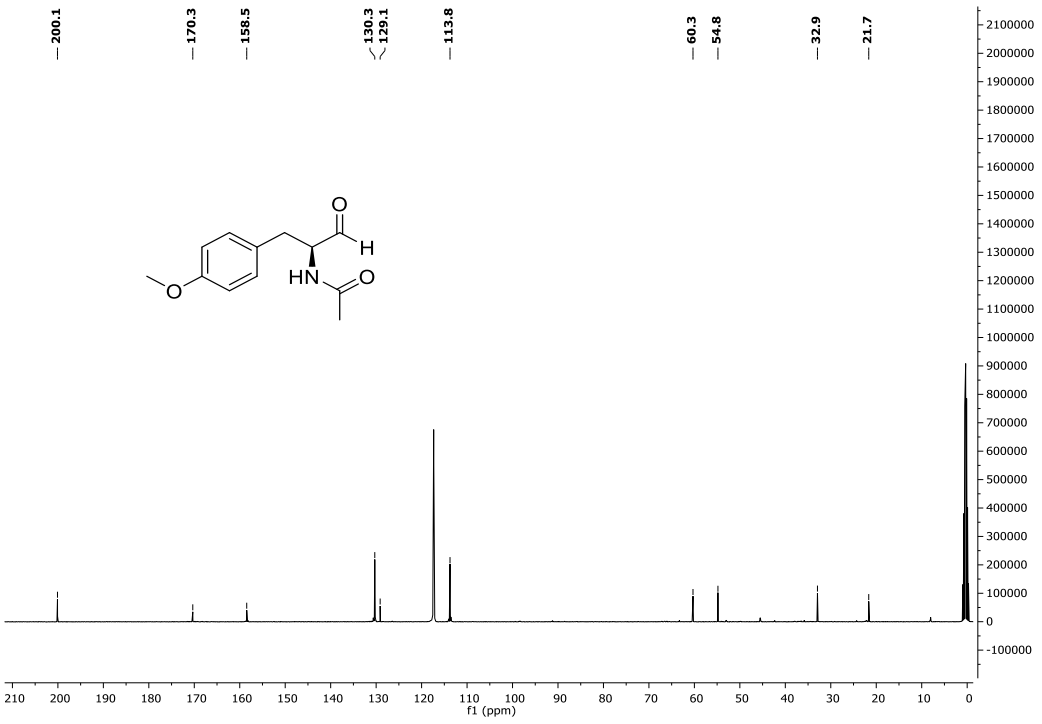

S-*N*-(1-(4-Methoxyphenyl)-3-oxopropan-2-yl)-3-oxobutanamide **115**.

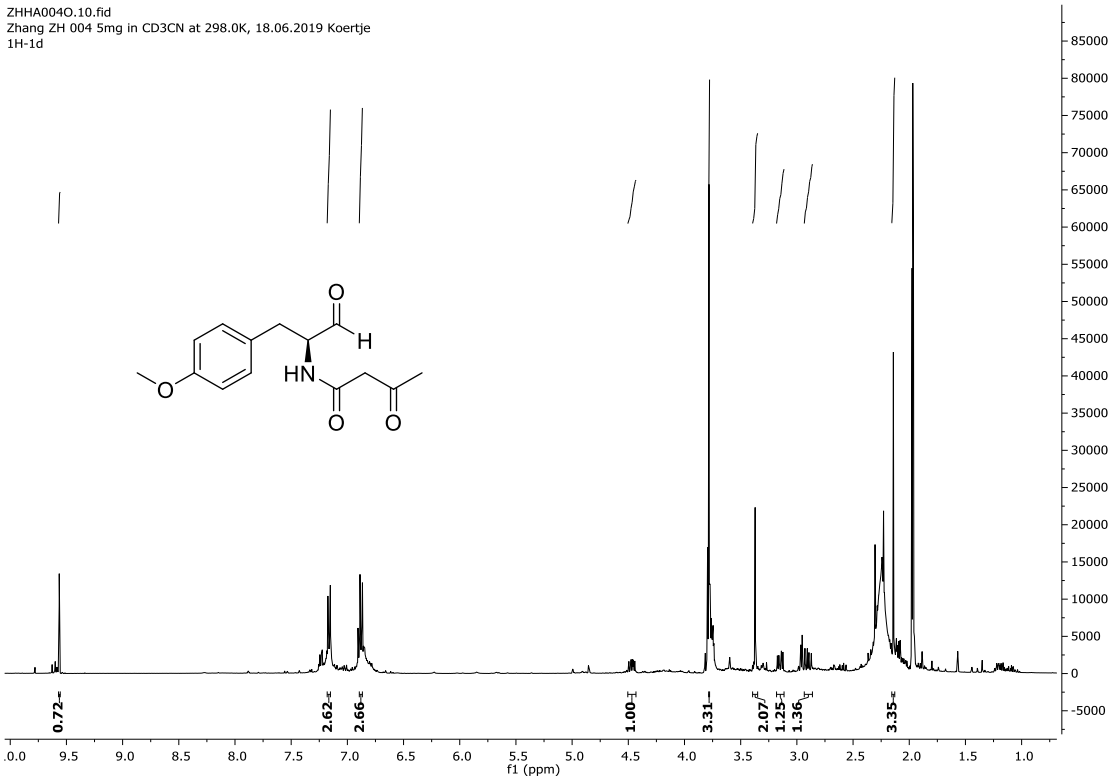

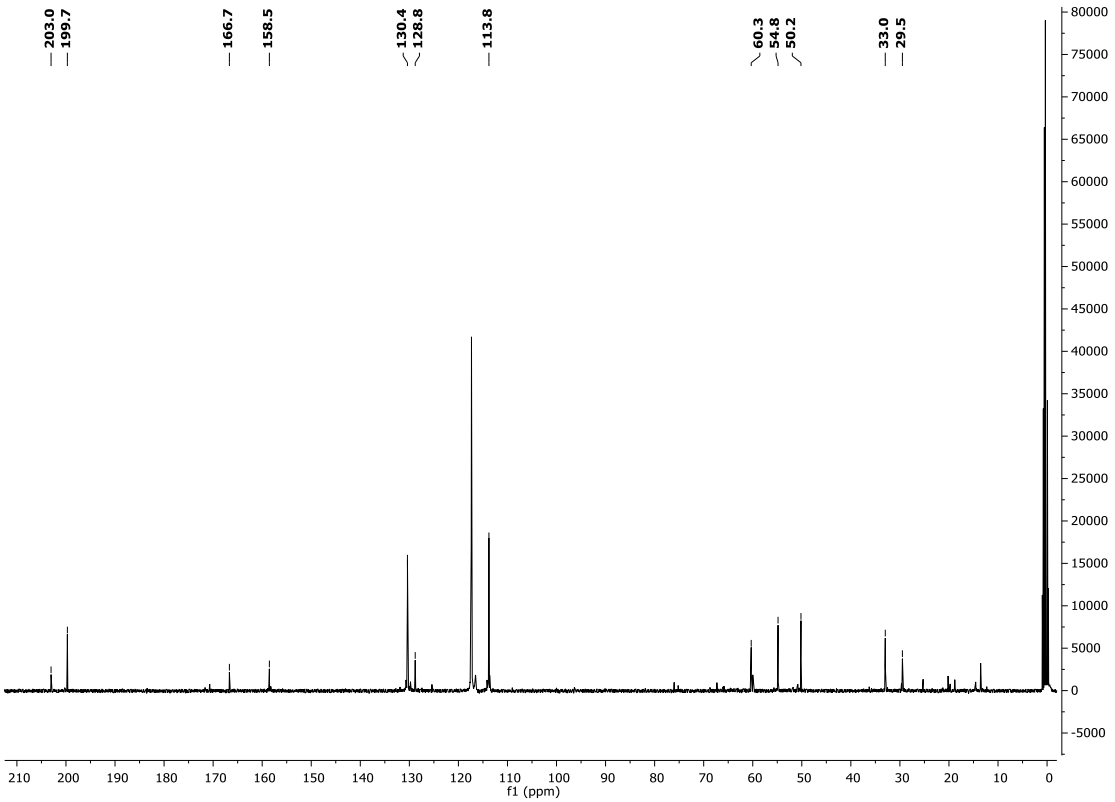

N-(1-Hydroxy-3-(4-methoxyphenyl)propan-2-yl)-3-oxobutanamide **210**.

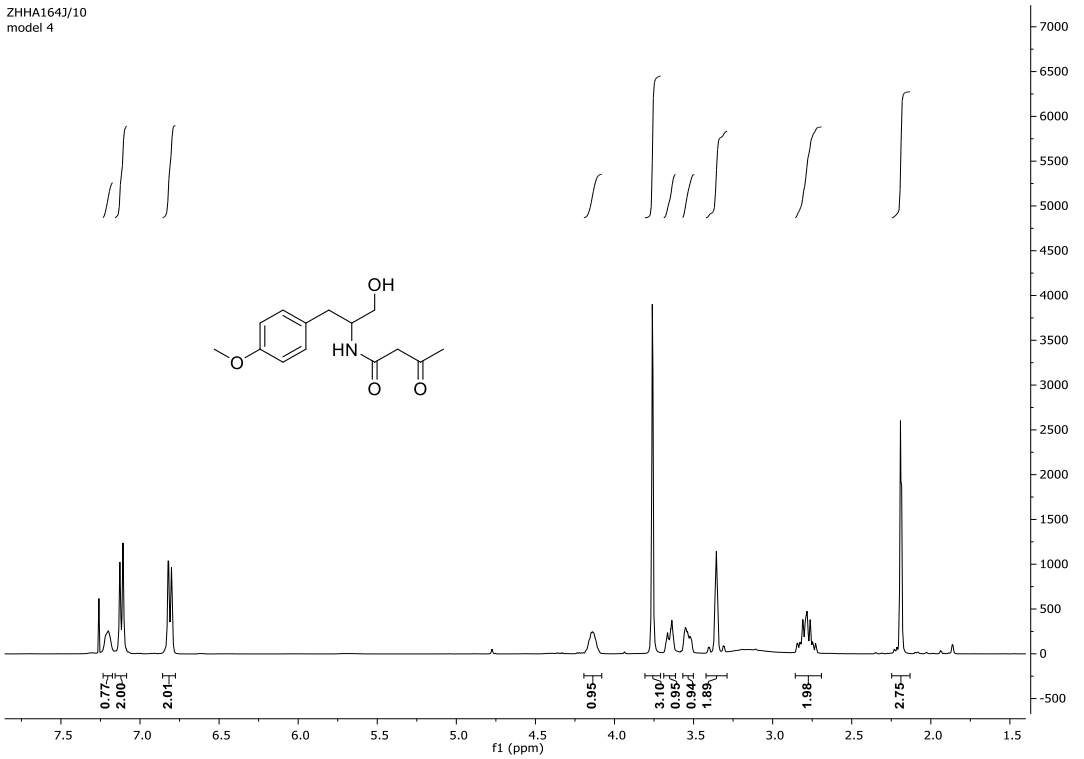

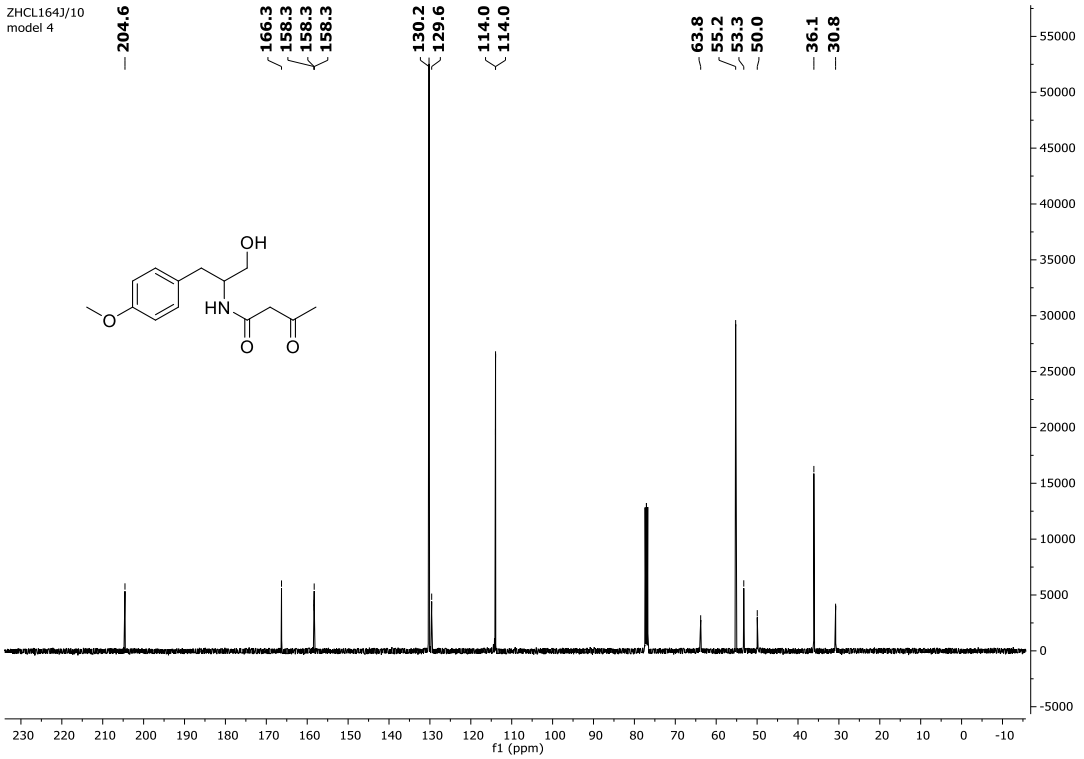

Methyl-*S*-(1,1-diethoxy-3-(4-methoxyphenyl)propan-2-yl)carbamate **211**.

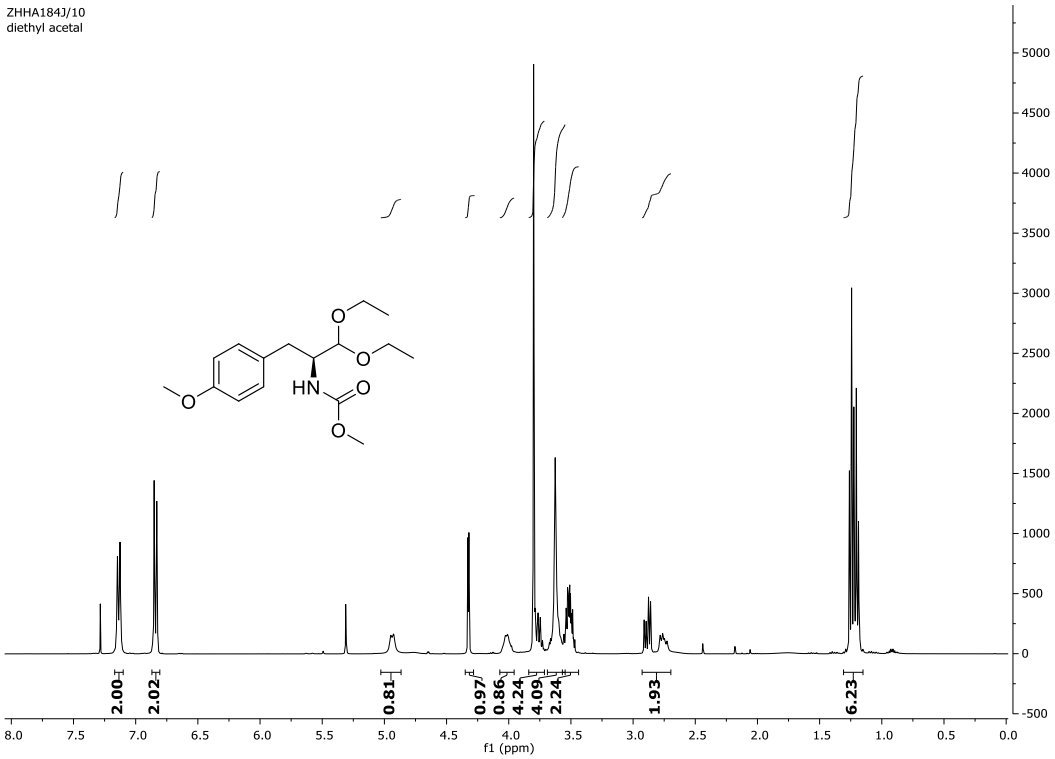

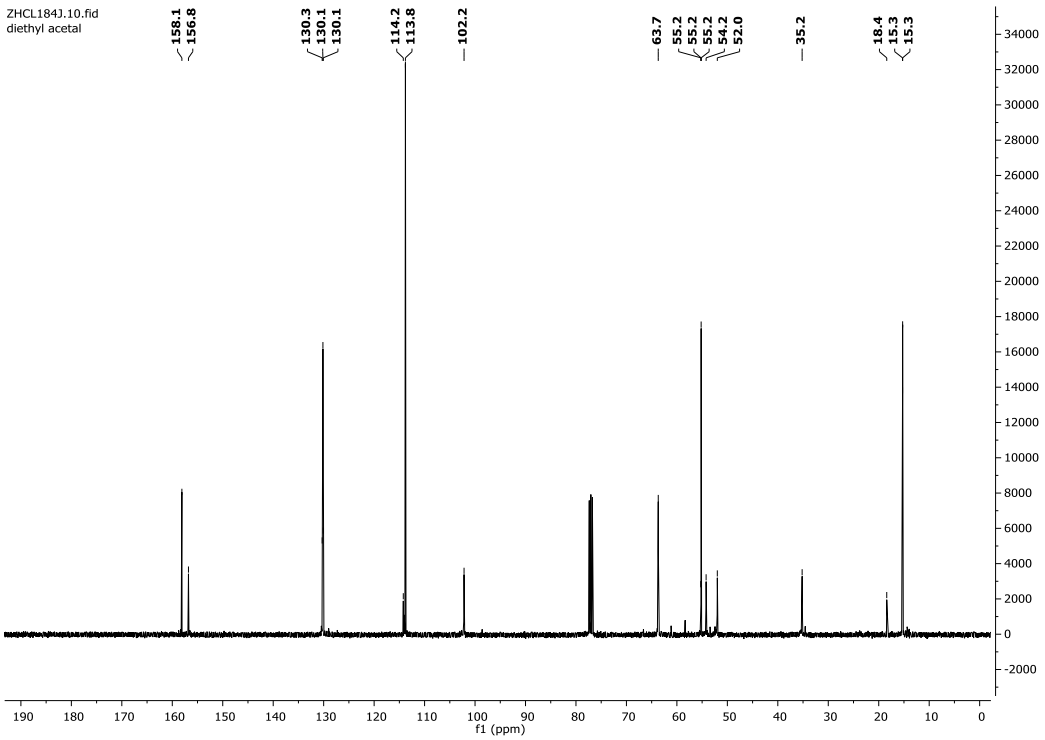

S-1,1-Diethoxy-3-(4-methoxyphenyl)propan-2-amine **212**.

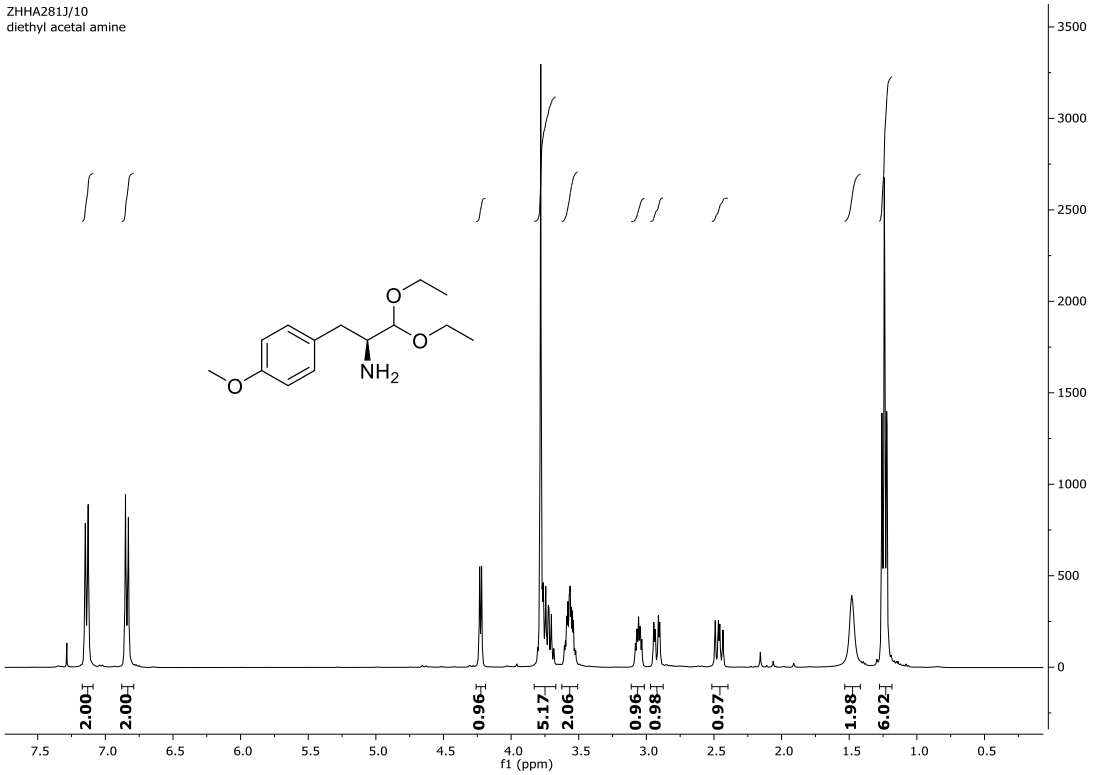

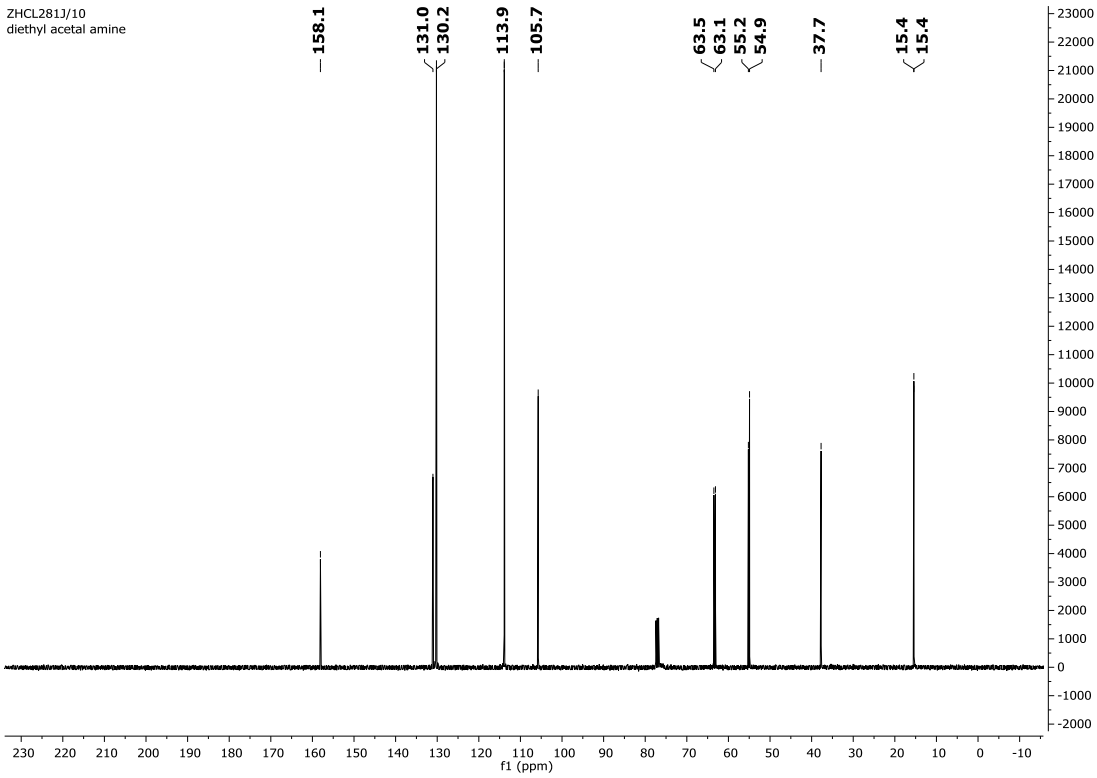

S-*N*-(1,1-Diethoxy-3-(4-methoxyphenyl)propan-2-yl)-3-oxobutanamide **213**.

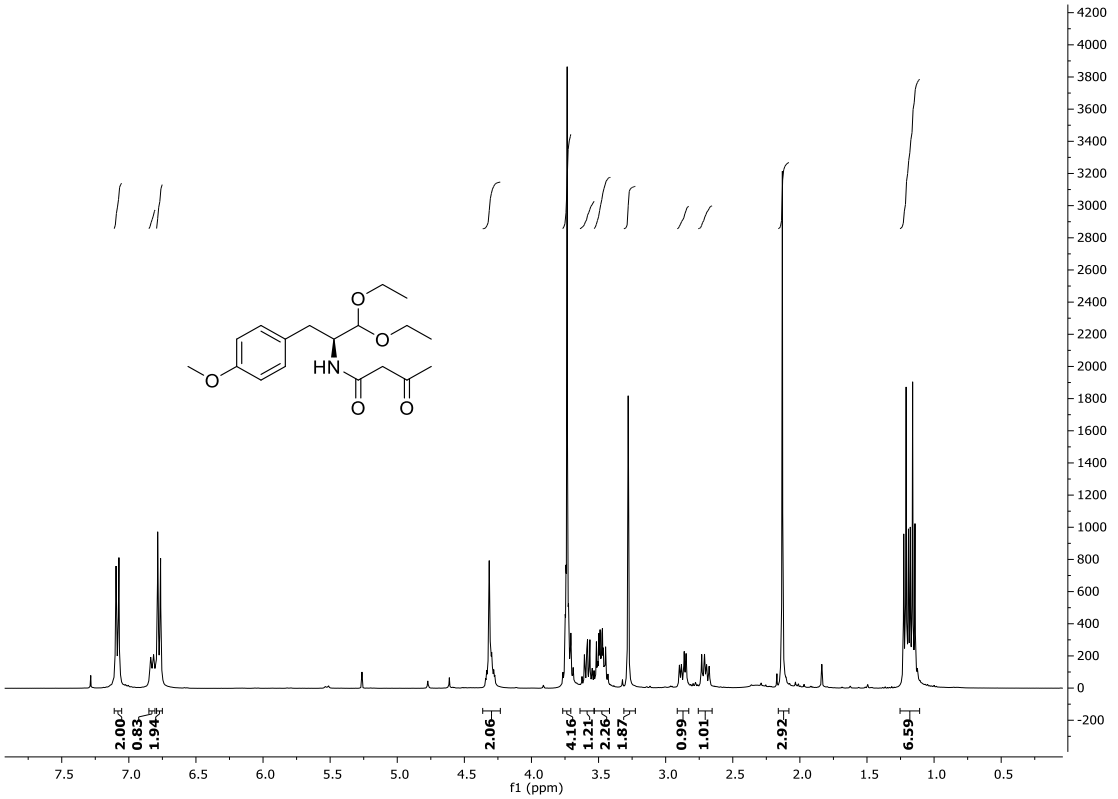

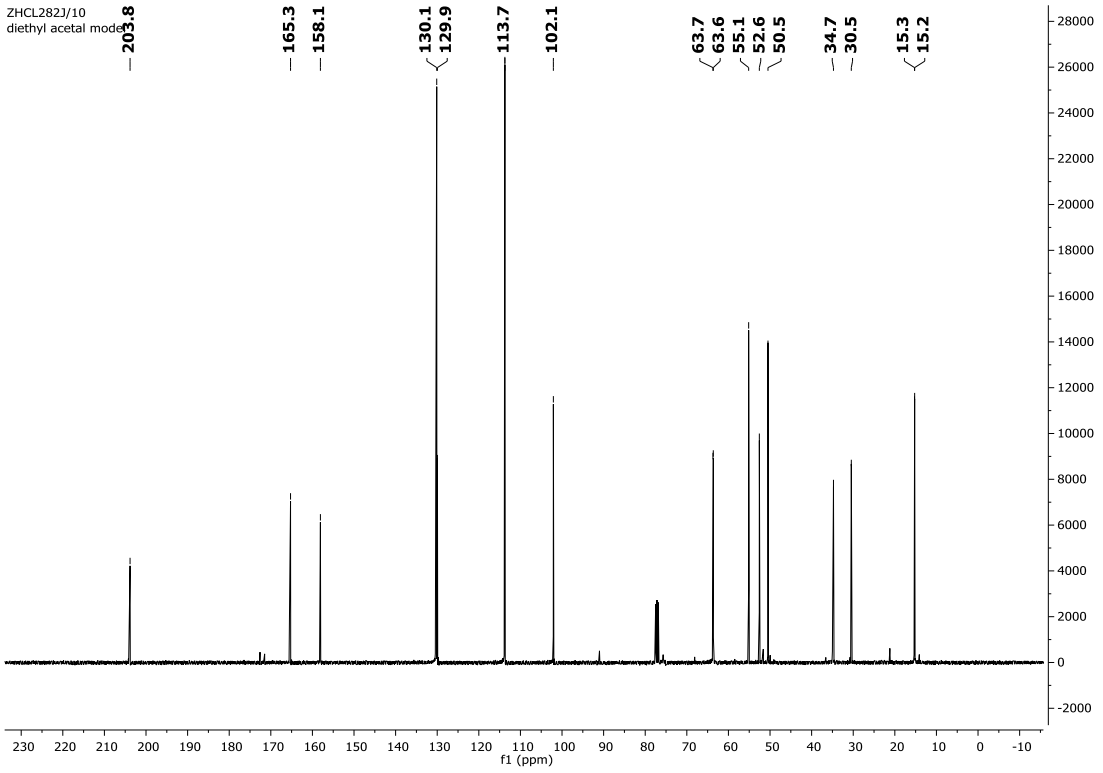

3-Acetyl-4-hydroxy-5-(4-methoxybenzyl)pyrrolidin-2-one **216**.

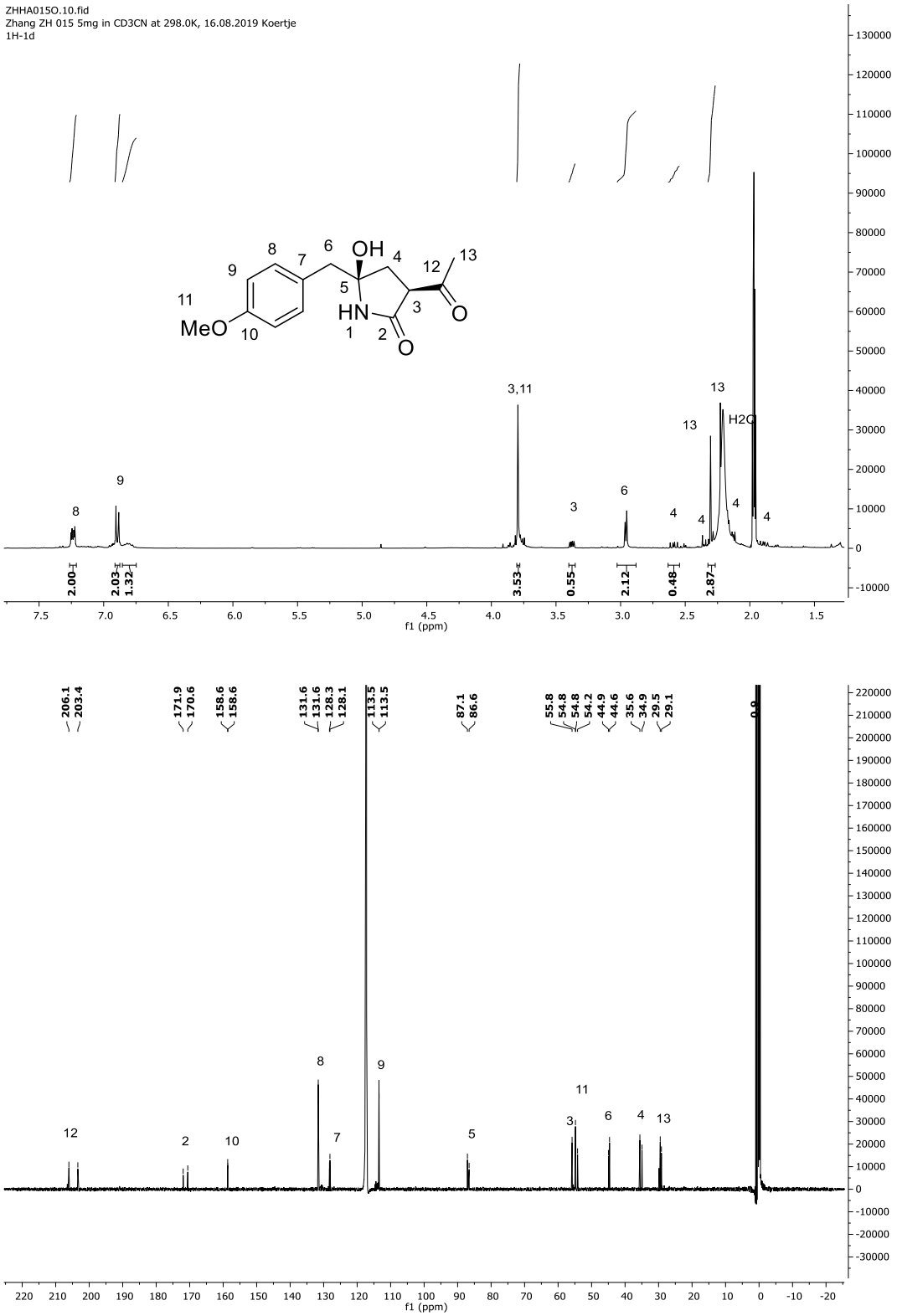

Z-5-Benzyl-3-(1-hydroxyethylidene)-1,3-dihydro-2H-pyrrol-2-one **222b**.

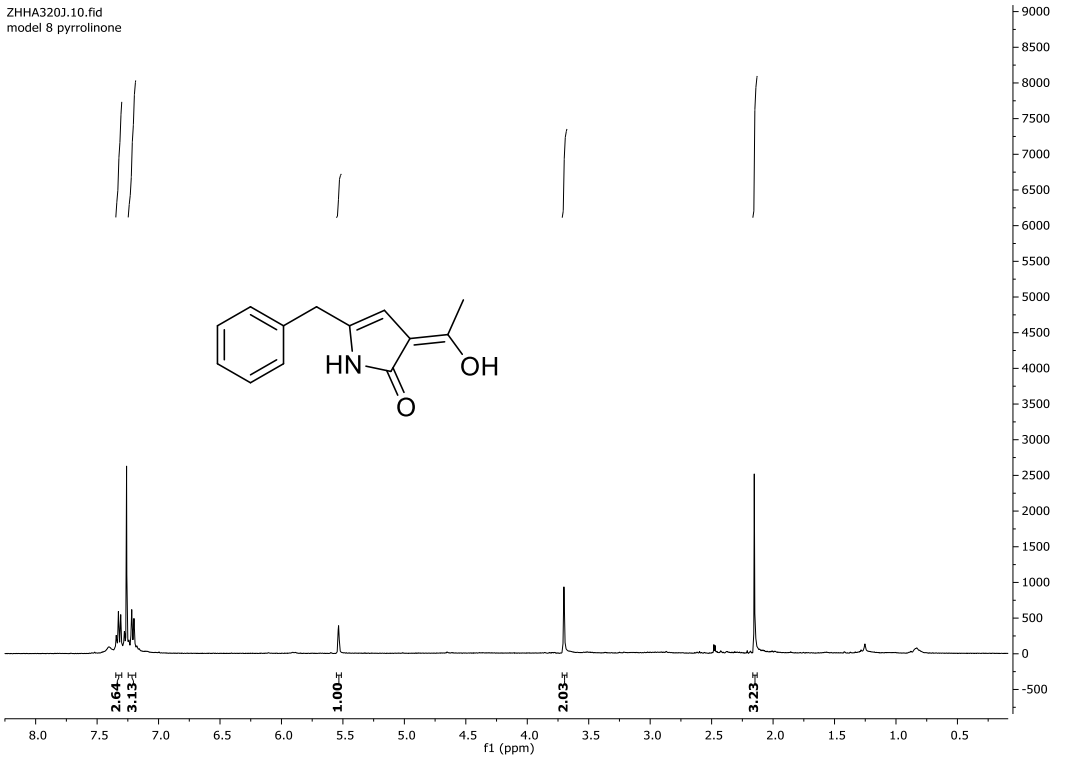

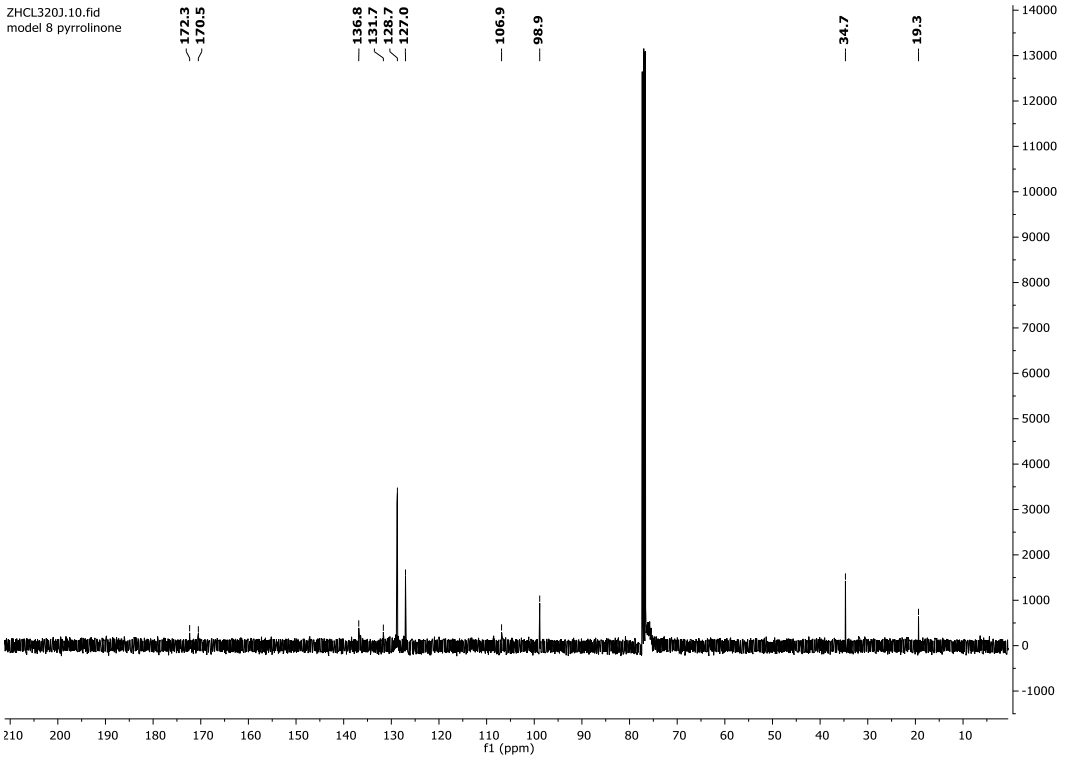

2-Amino-3-(4-methoxyphenyl)-2-methylpropan-1-ol **228**.

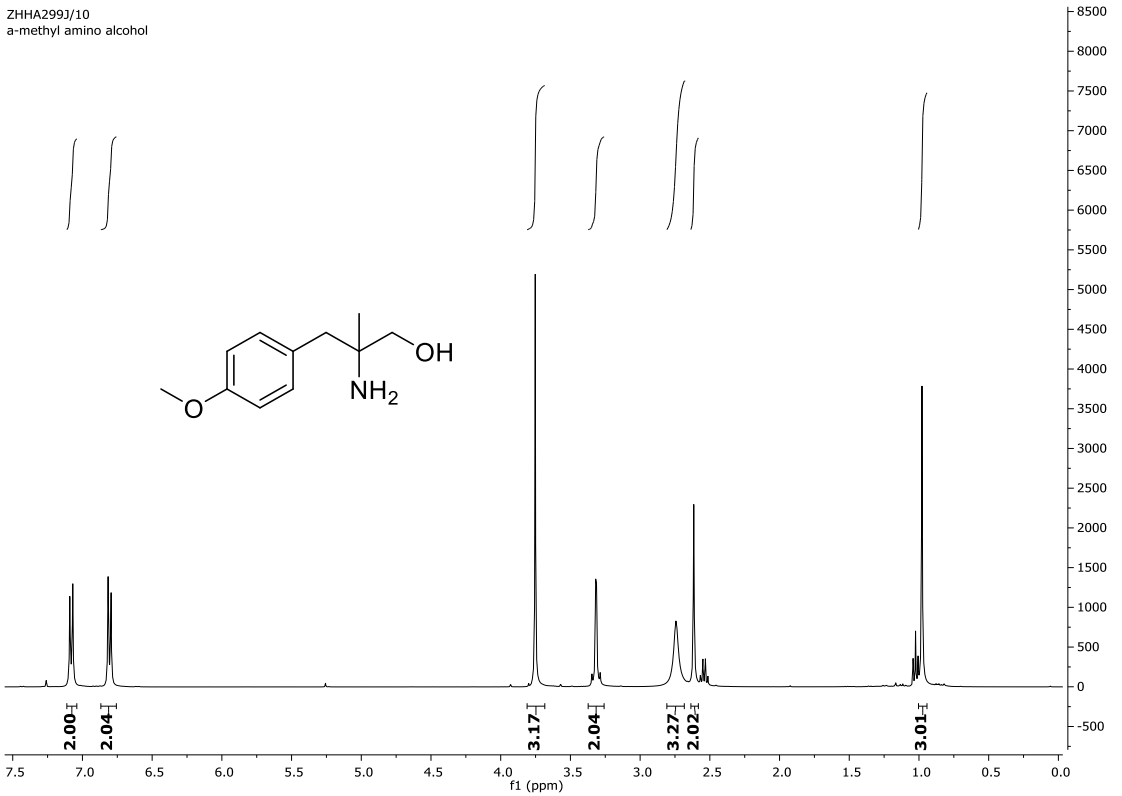

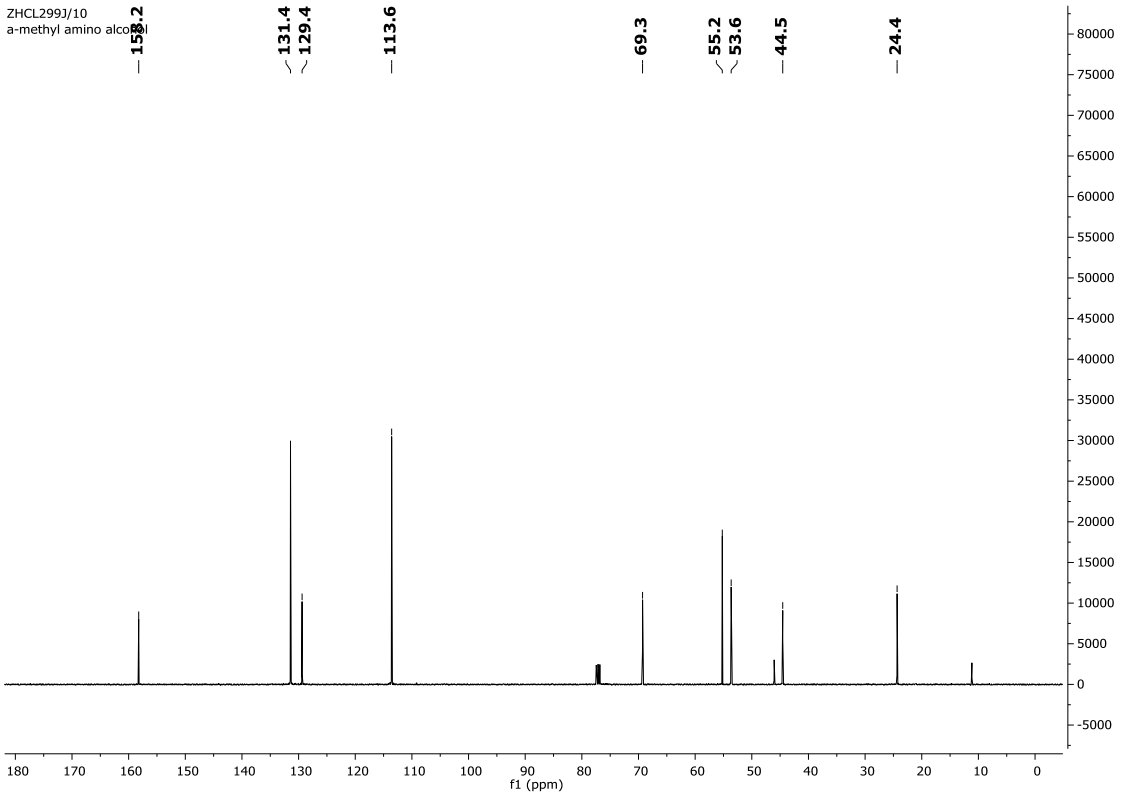

N-(1-Hydroxy-3-(4-methoxyphenyl)-2-methylpropan-2-yl)-3-oxobutanamide **229**.

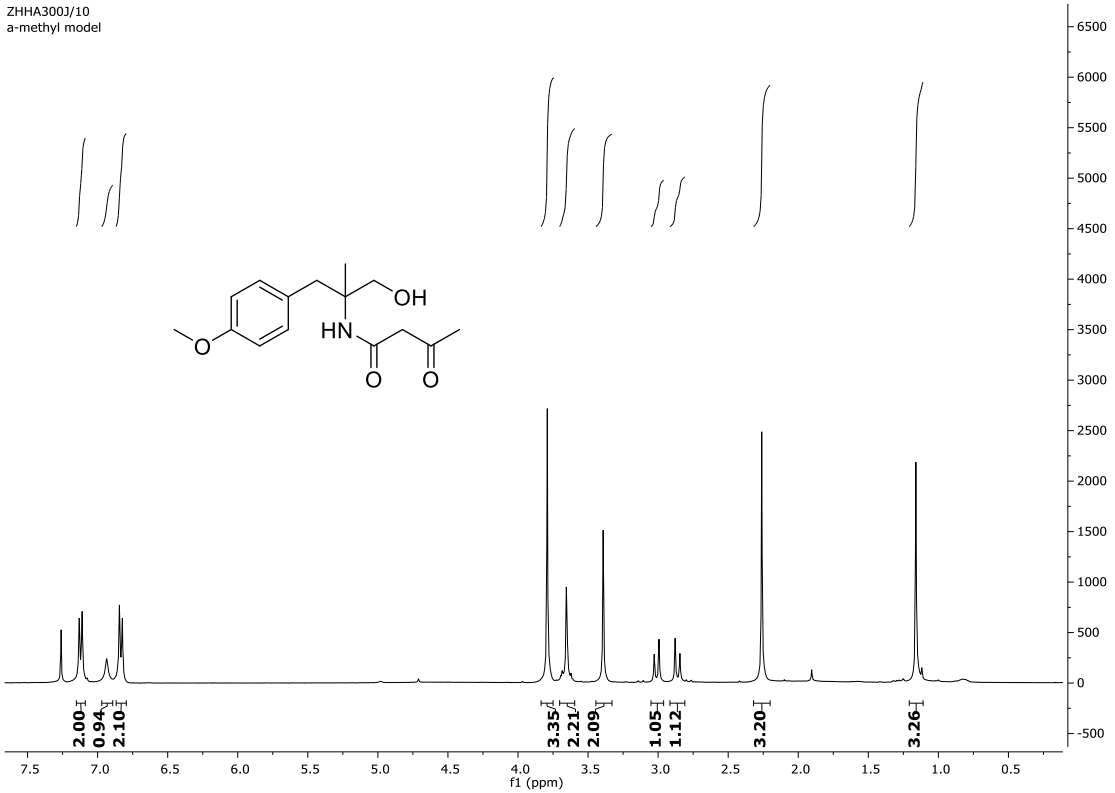

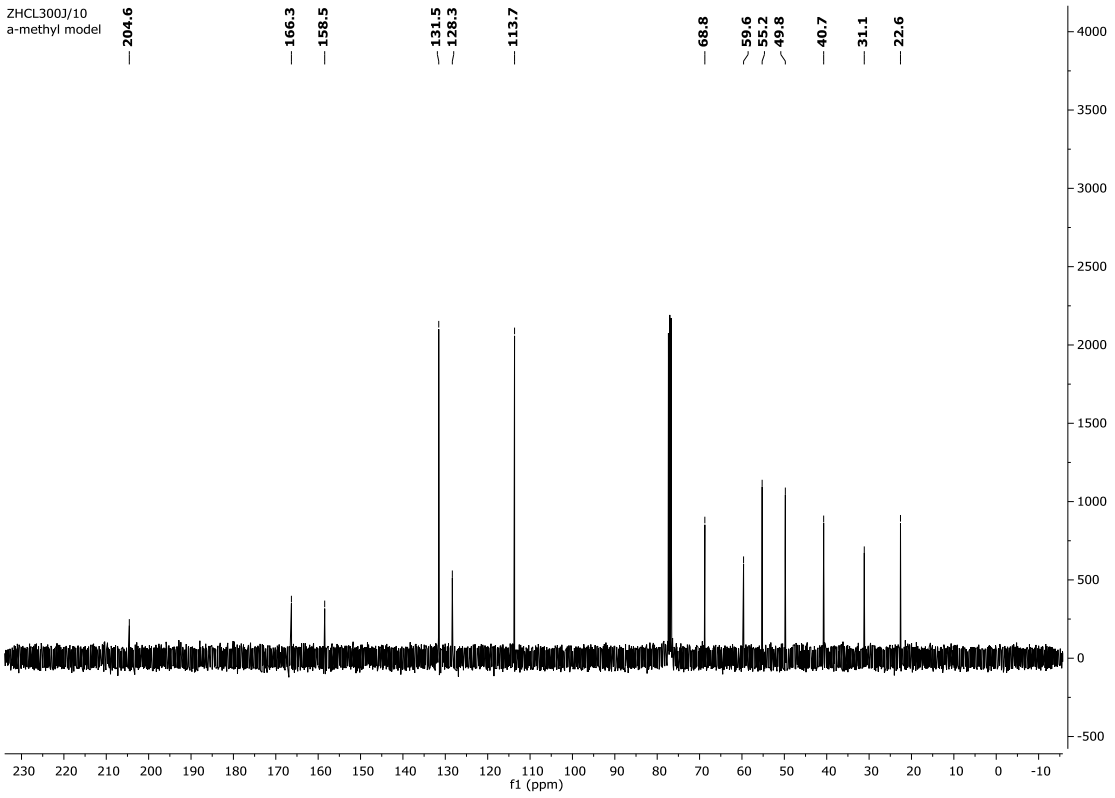

3-Acetyl-5-(4-methoxybenzyl)-5-methyl-1,5-dihydro-2H-pyrrol-2-one **231**.

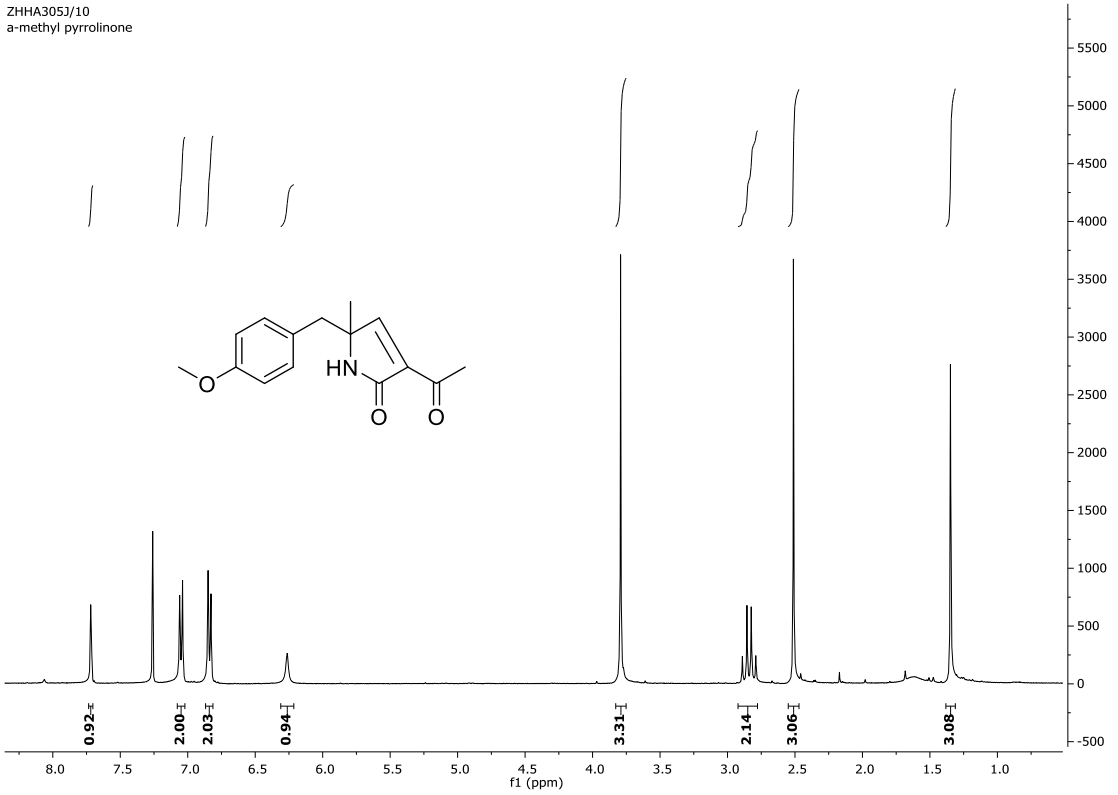

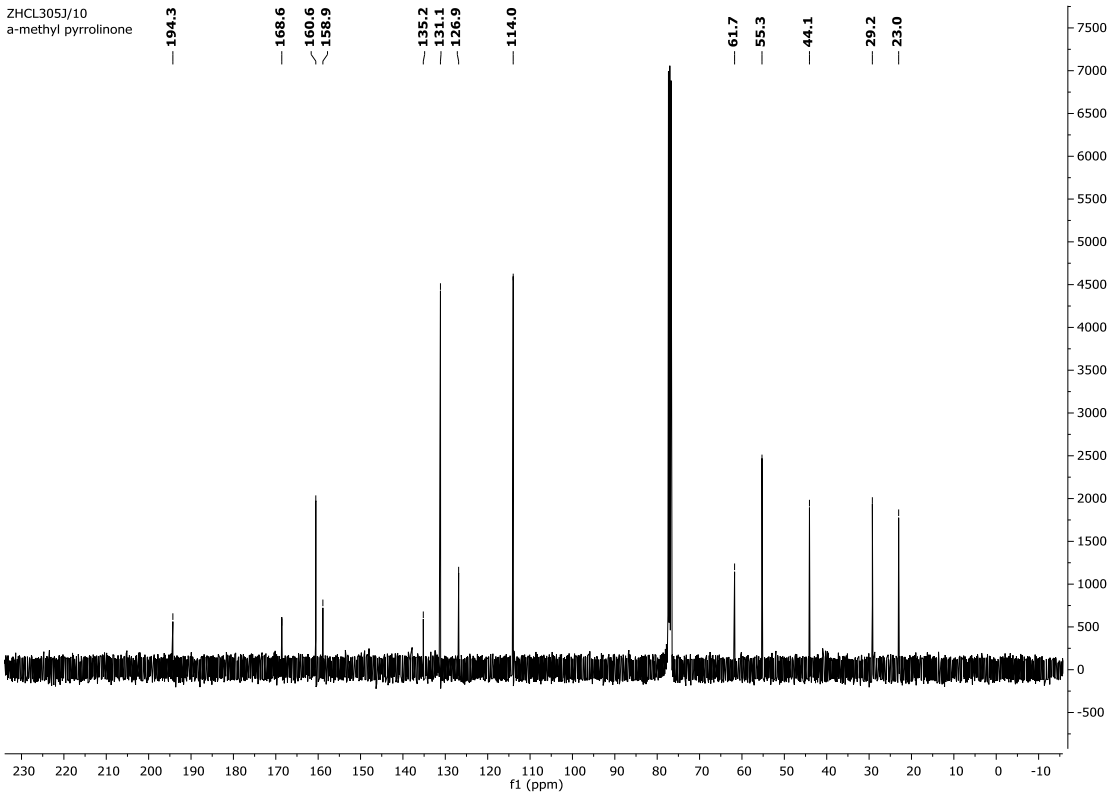

S-4-(2-Amino-2-(1,3-dioxolan-2-yl)ethyl)phenol **342**.

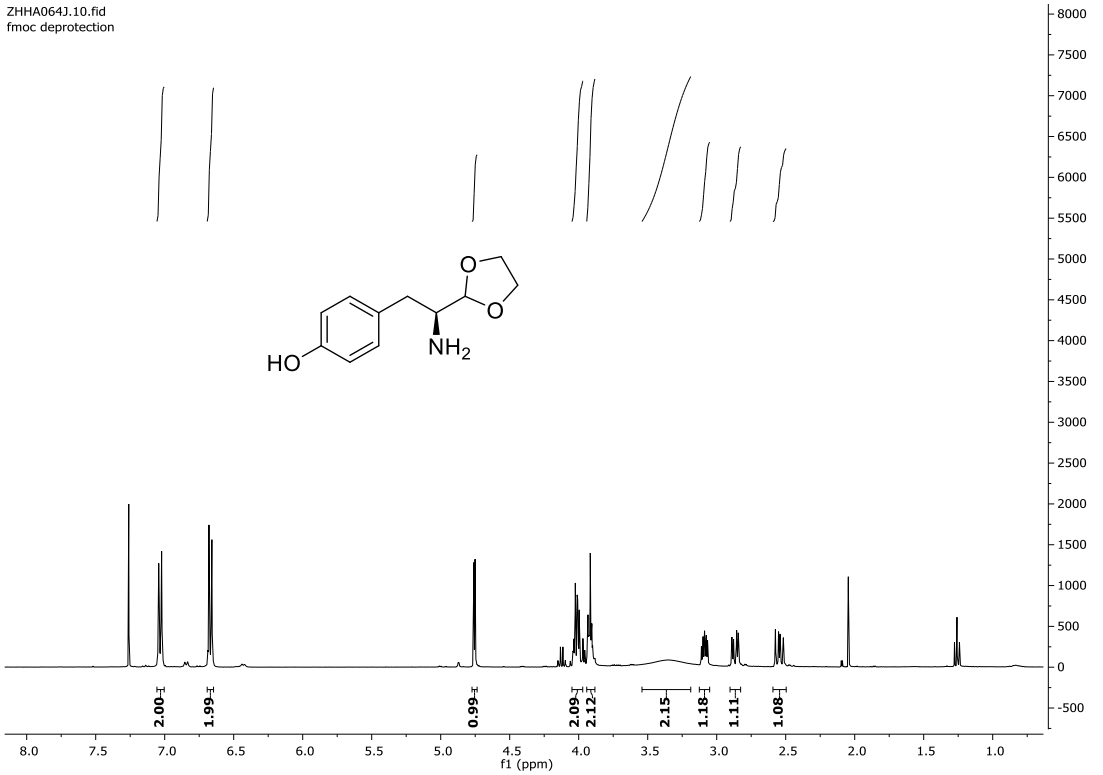

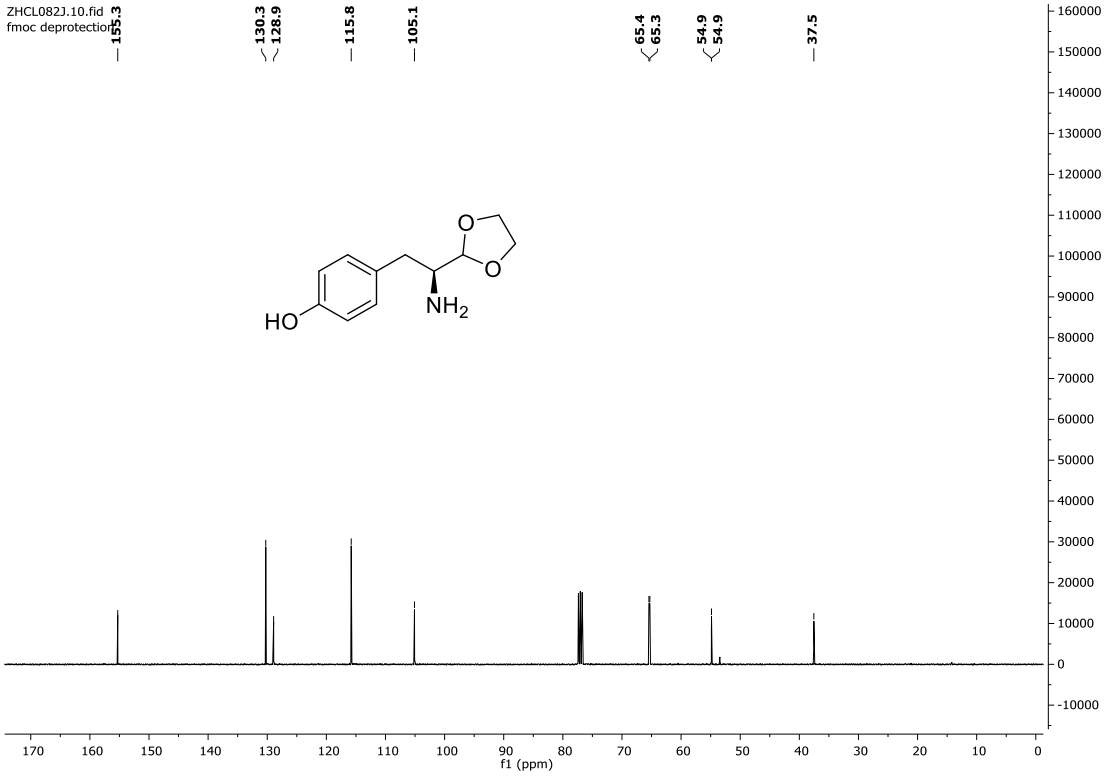

2,2-Dimethyl-6-(1*E*,9*E*,11*E*,13*E*-pentadeca-1,9,11,13-tetraen-1-yl)-4H-1,3-dioxin-4-one **343**.

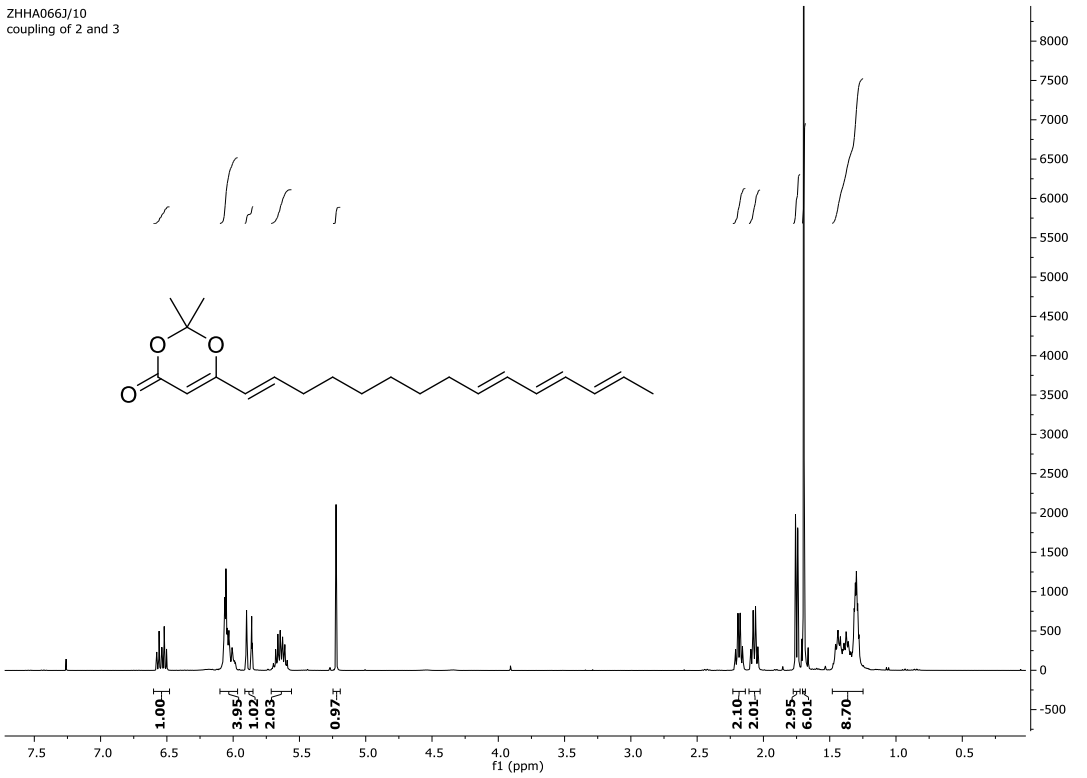

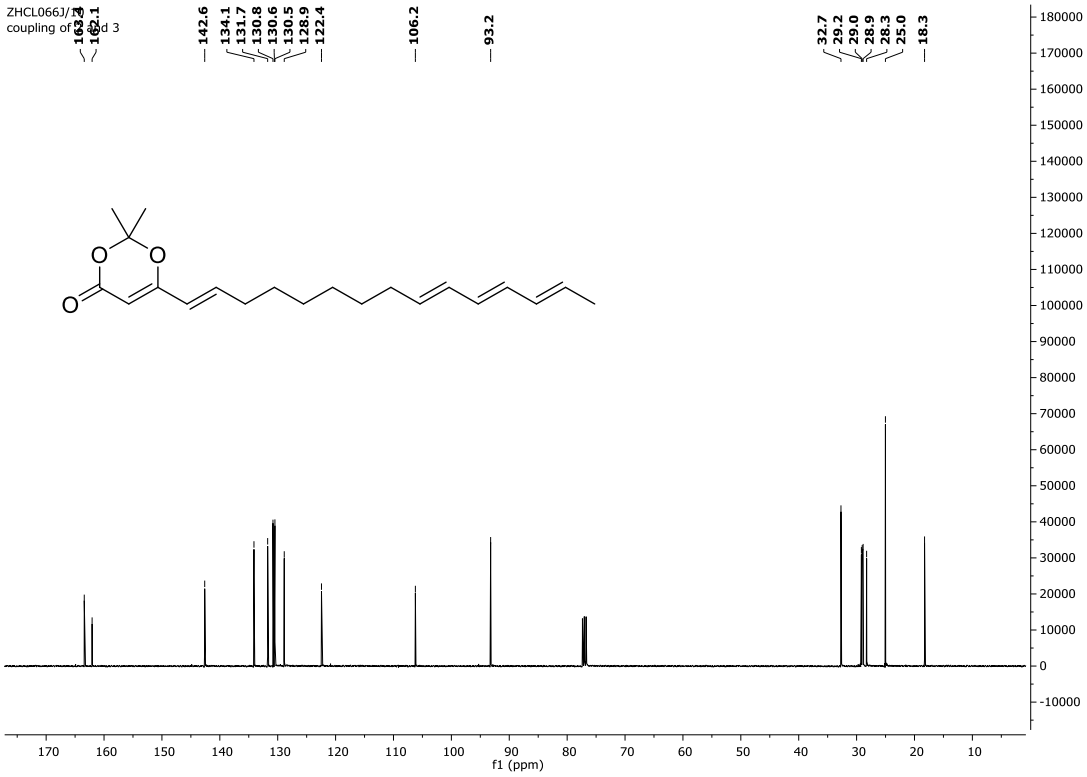

8*E*,10*E*,12*E*-Tetradeca-8,10,12-trienal **345**.

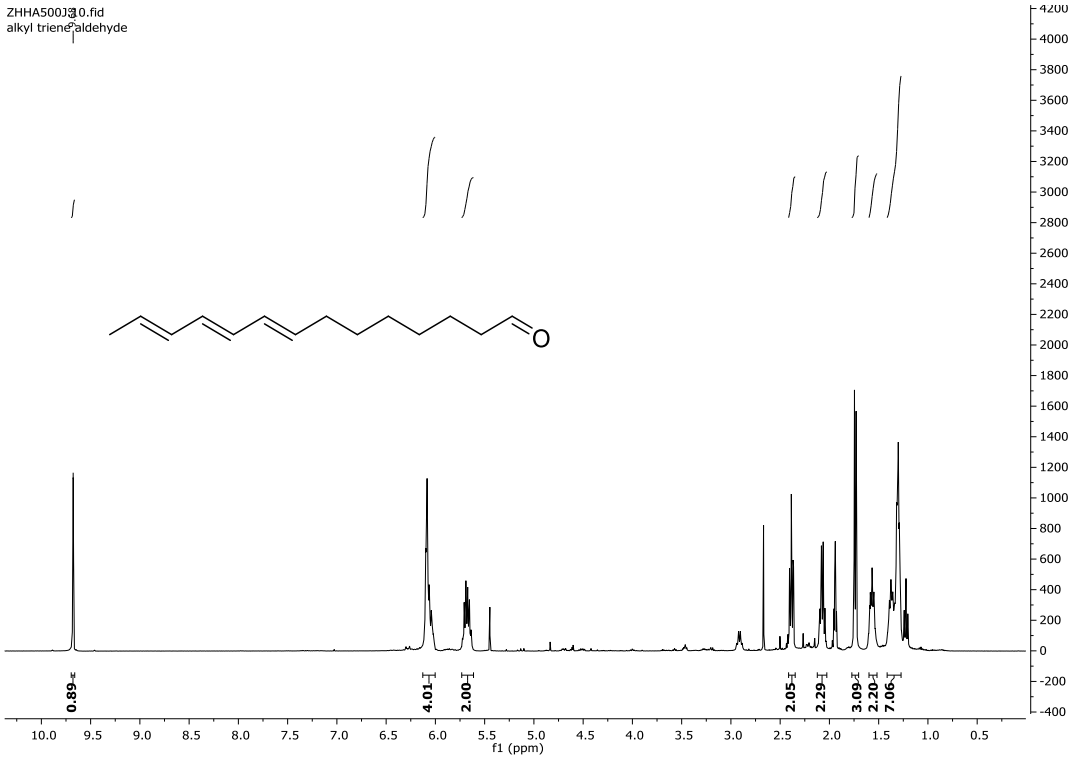

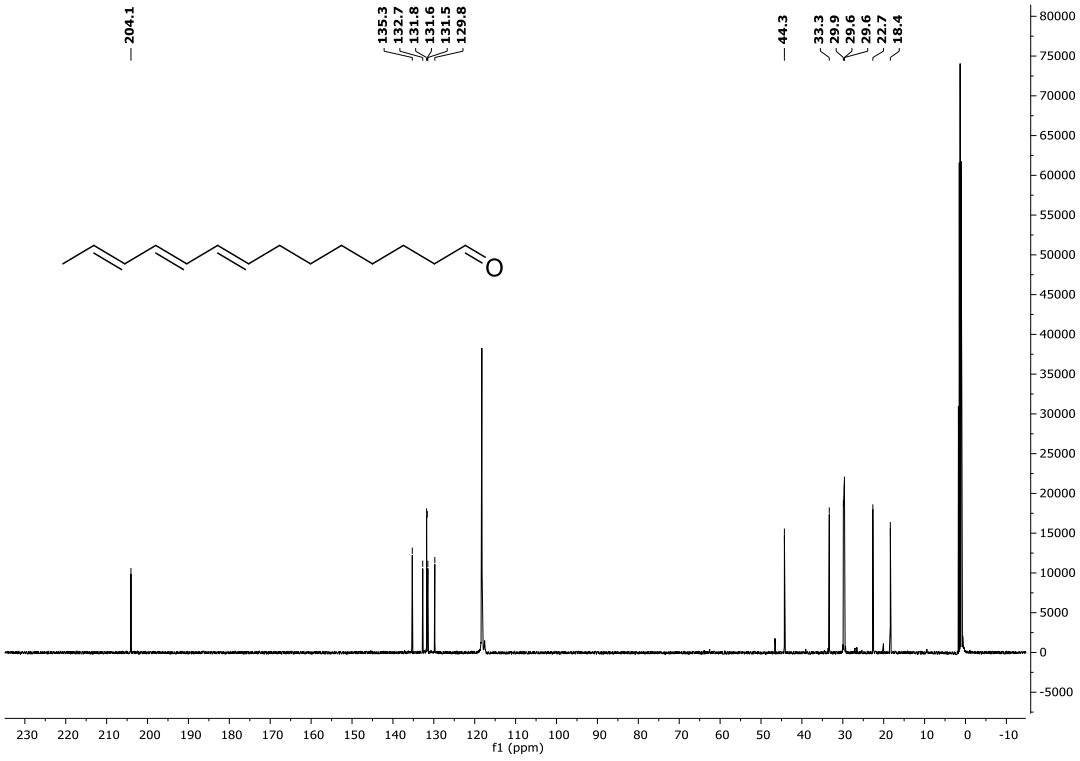

(9H-Fluoren-9-yl)methyl-*S*-(1-(1,3-dioxolan-2-yl)-2-(4-hydroxyphenyl)ethyl)carbamate **354**.

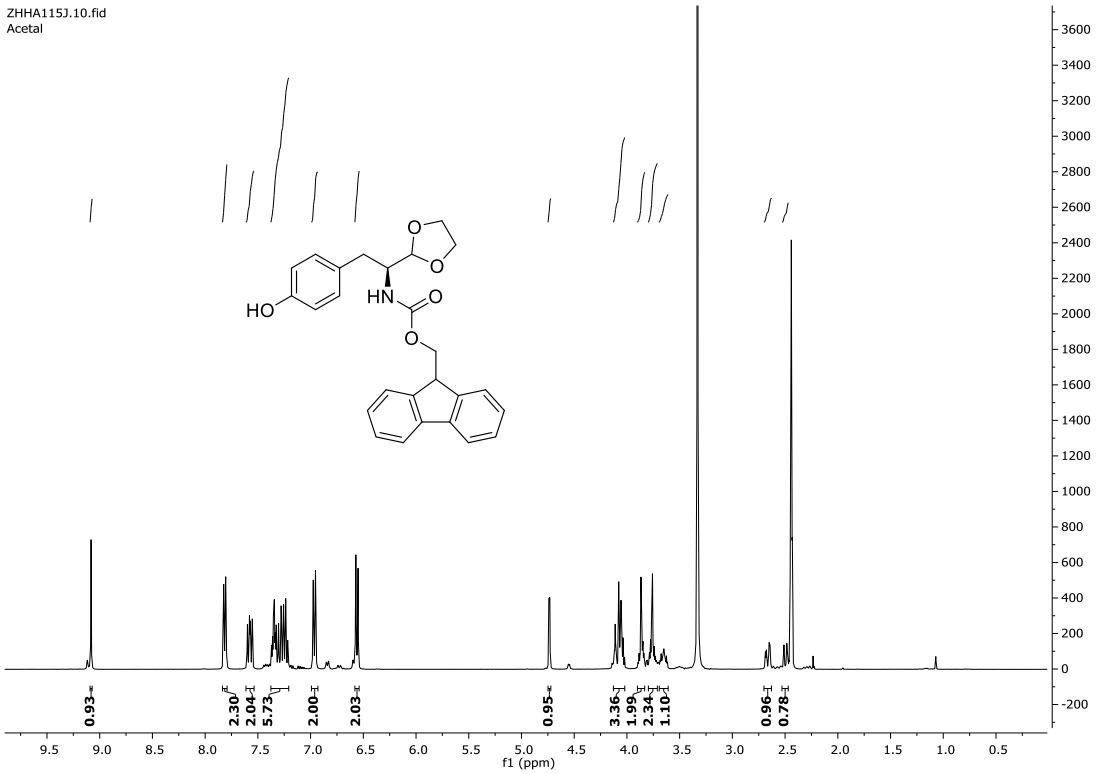

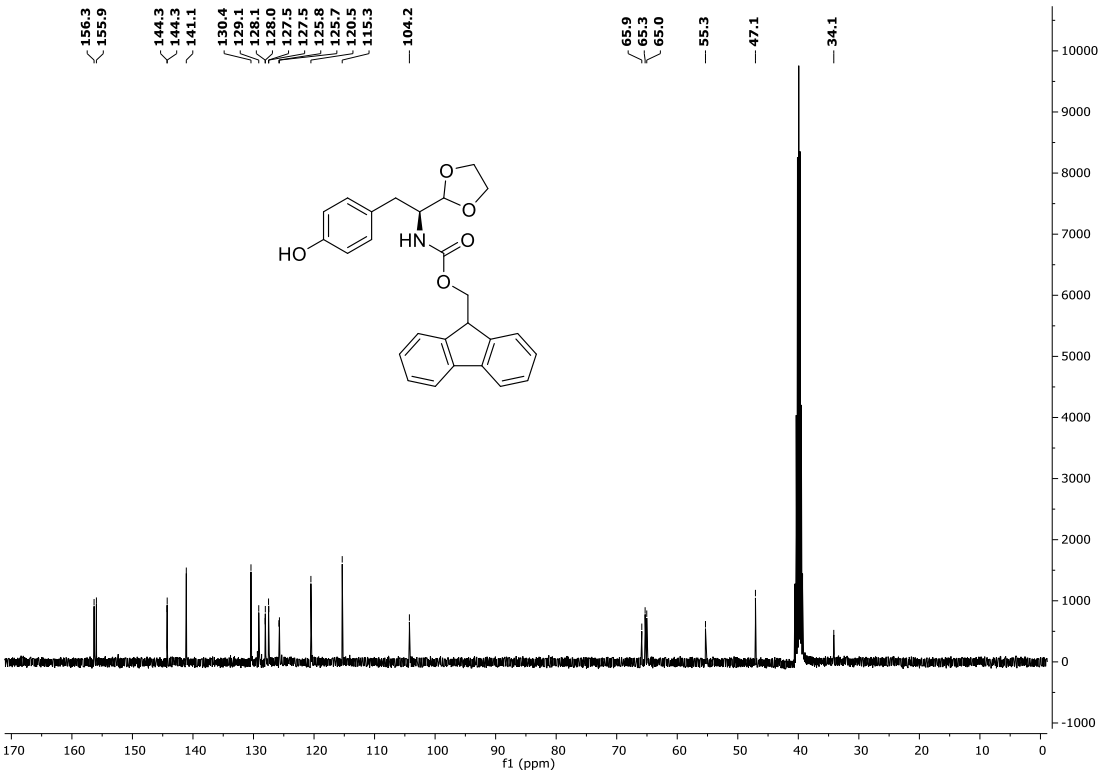

8-Oxooctyl benzoate **365**.

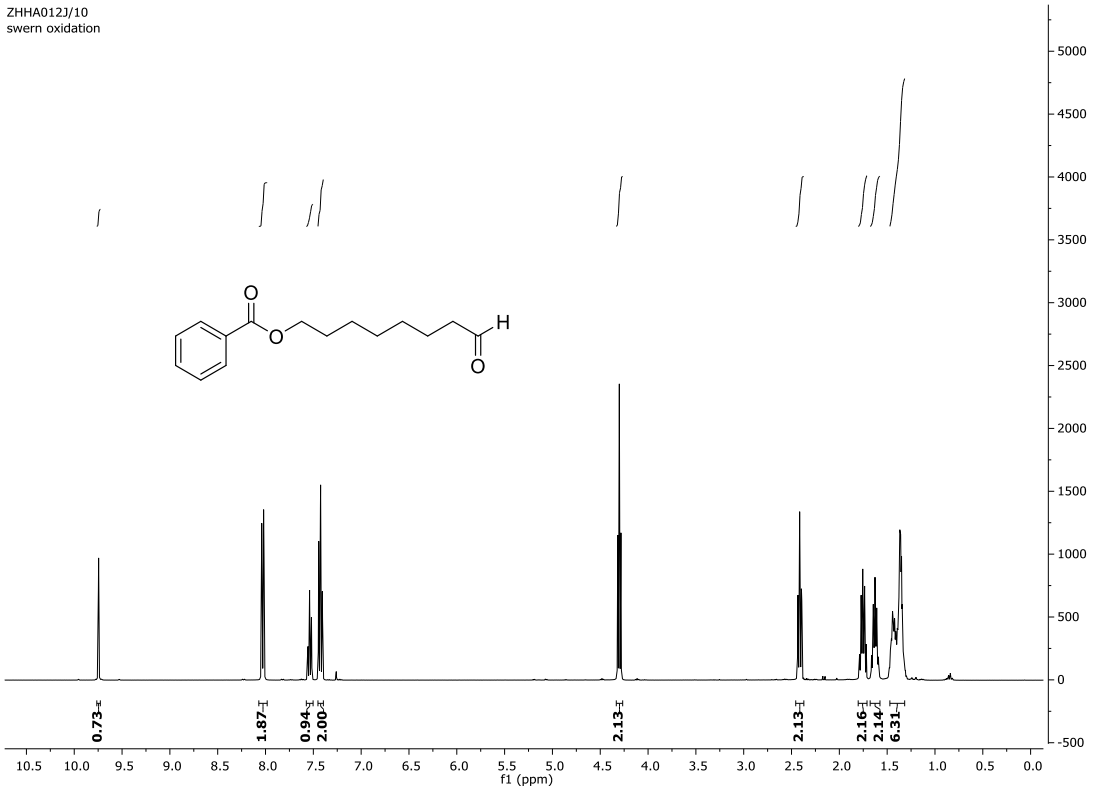

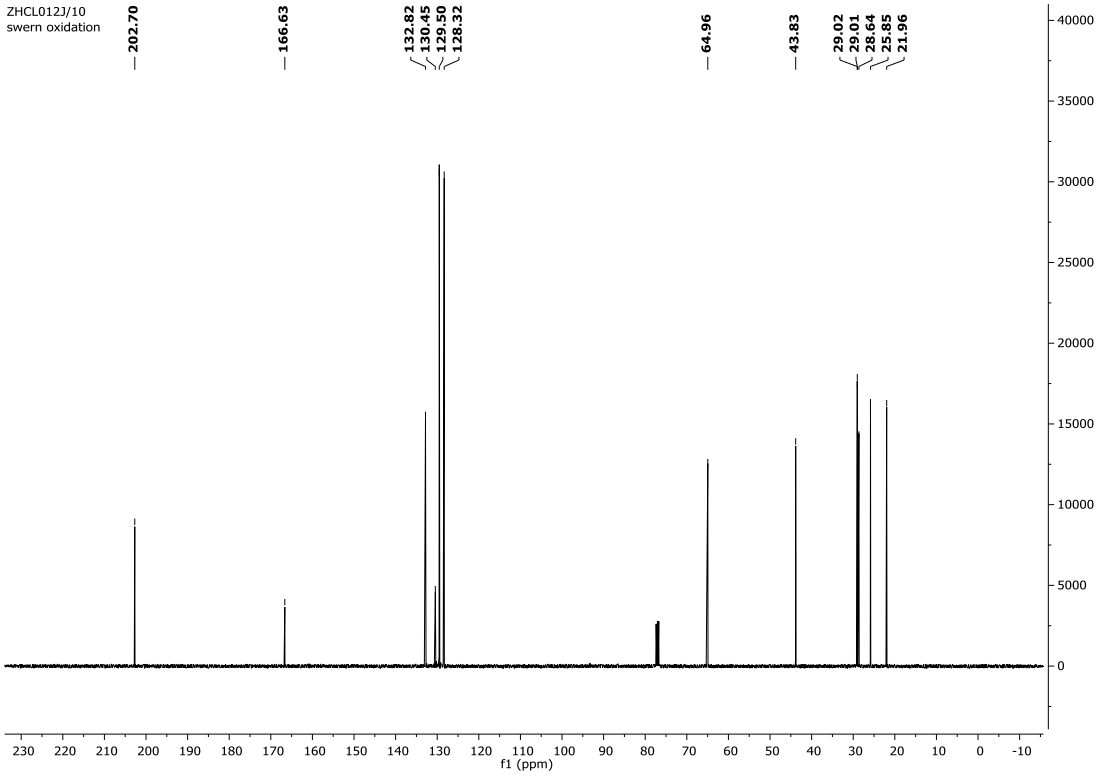

8*E*,10*E*,12*E*-Tetradeca-8,10,12-trien-1-yl benzoate **369**.

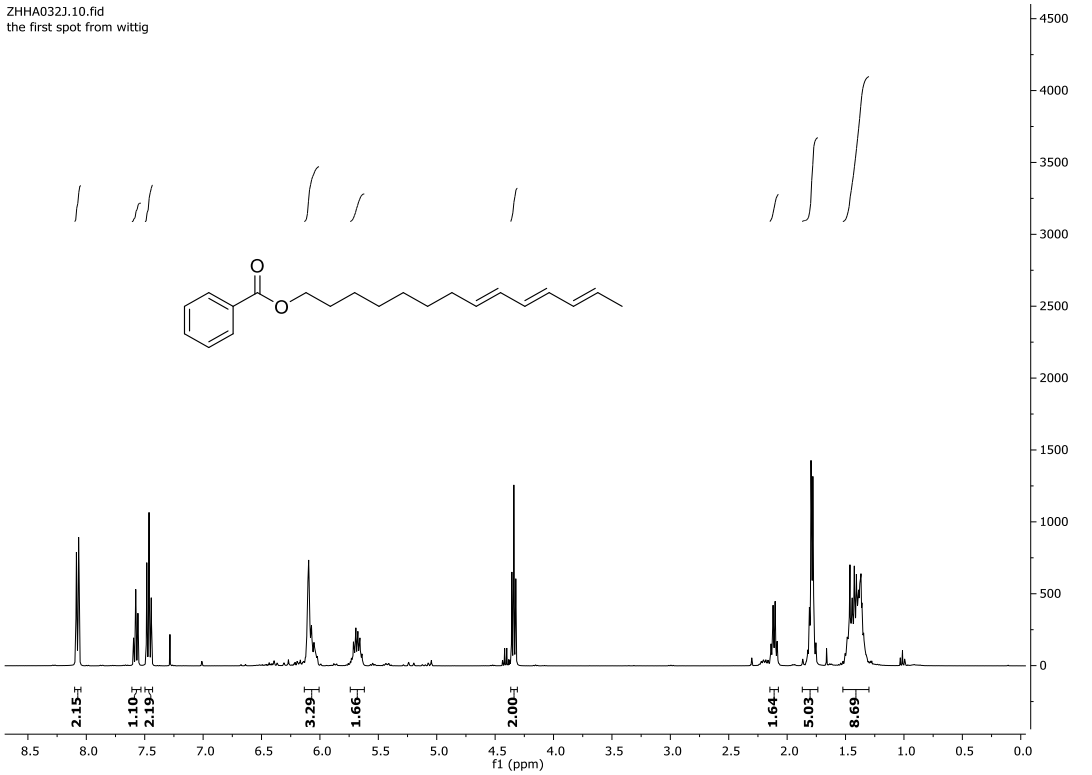

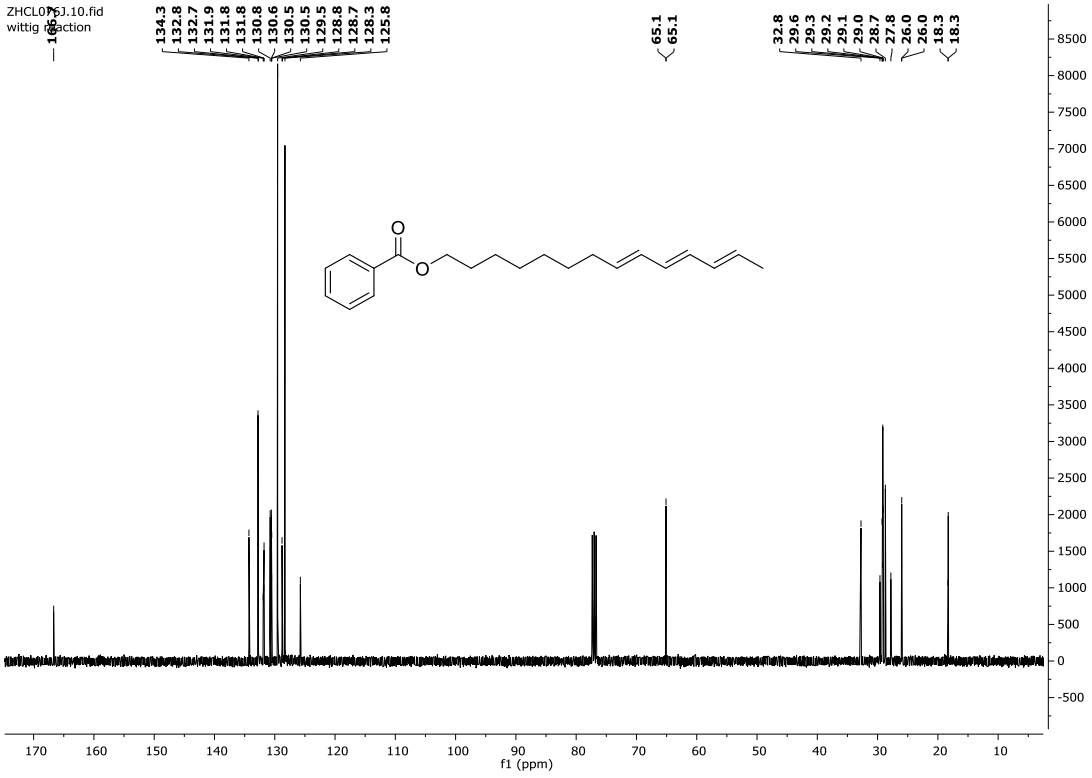

8*E*,10*E*,12*E*-Tetradeca-8,10,12-trien-1-ol **370**.

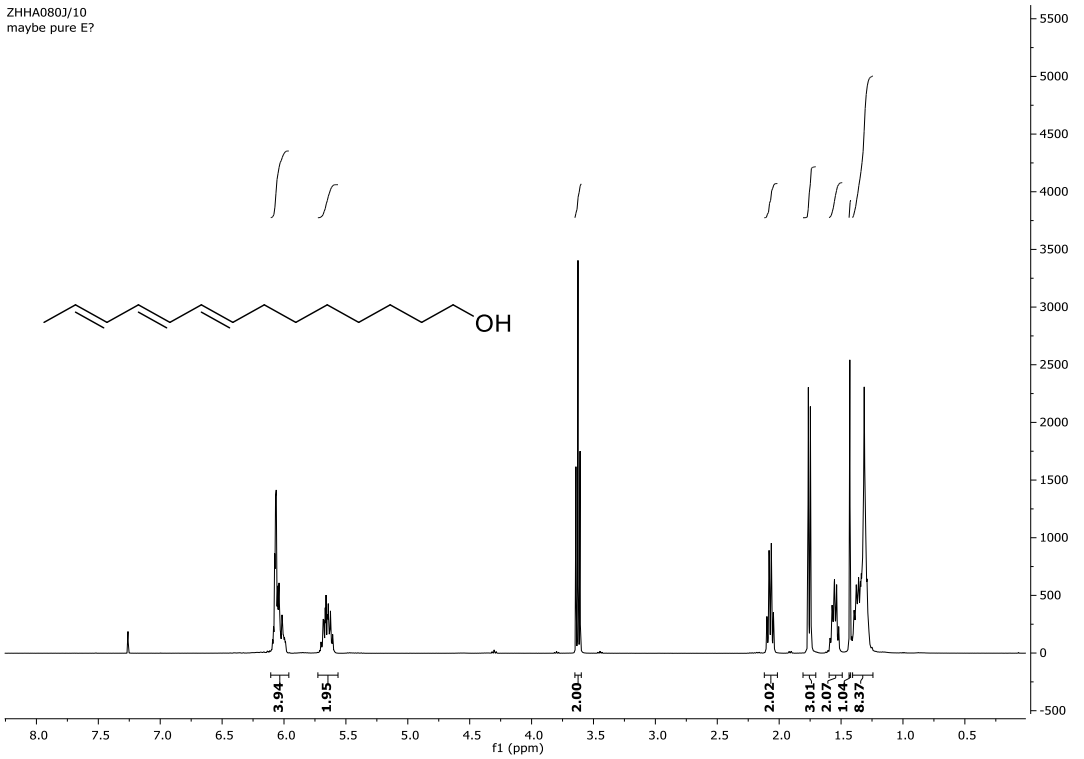

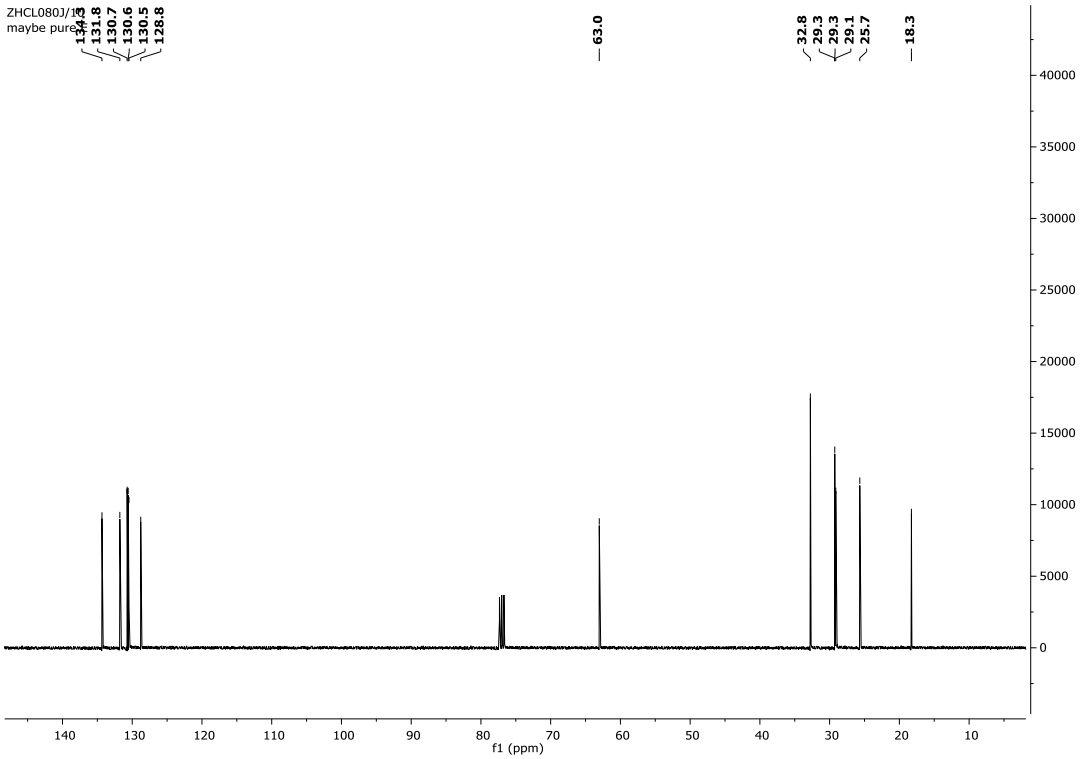

4*E*,12*E*,14*E*,16*E*-*N*-(*S*-1-(1,3-Dioxolan-2-yl)-2-(4-hydroxyphenyl)ethyl)-3-oxooctadeca-4,12,14,16-tetraenamide **371**.

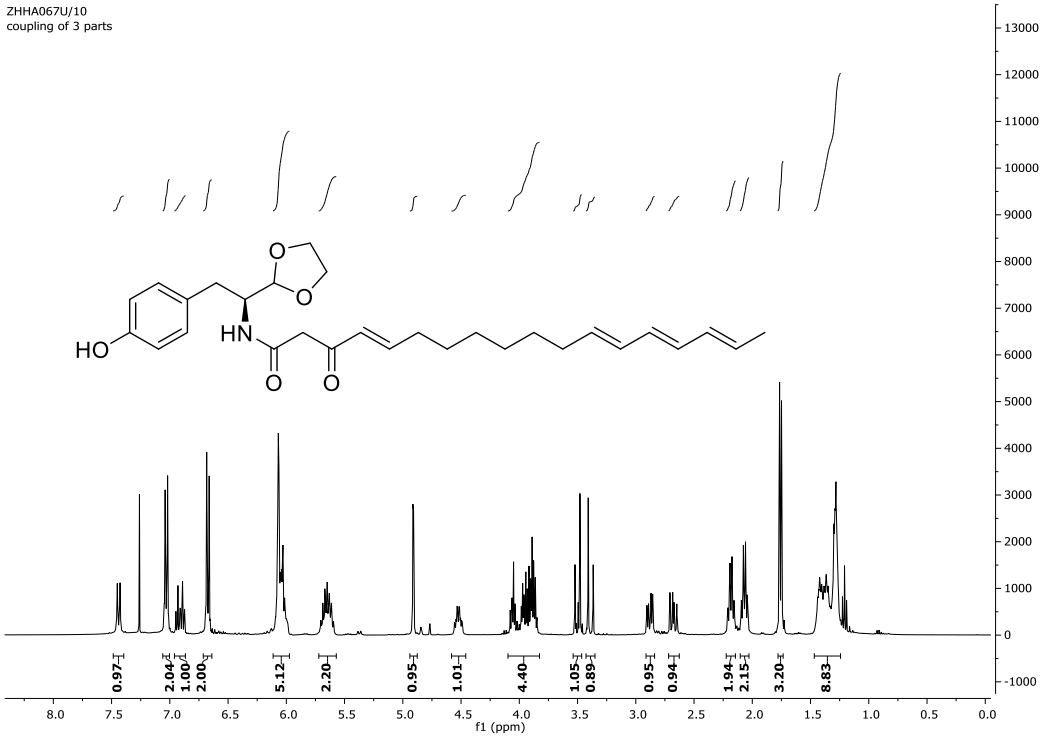

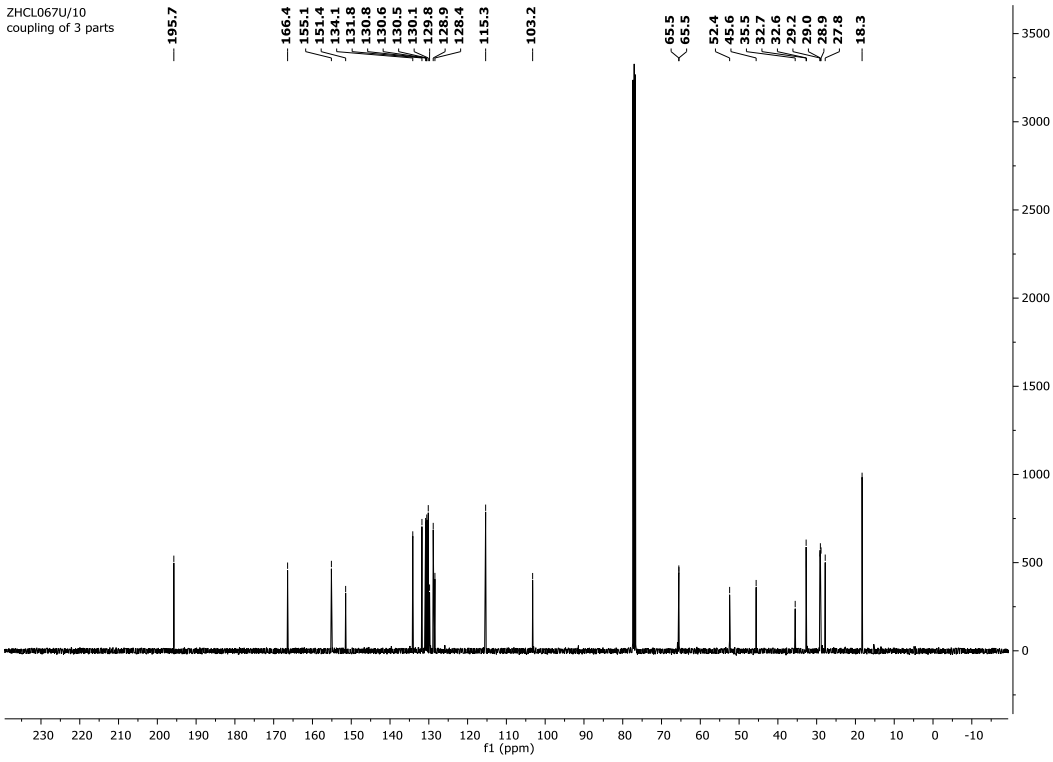

Z-5-(4-Hydroxybenzyl)-3-(*2E,10E,12E,14E*-1-hydroxyhexadeca-2,10,12,14-tetraen-1-ylidene)-1,3-dihydro-2H-pyrrol-2-one **372b**.

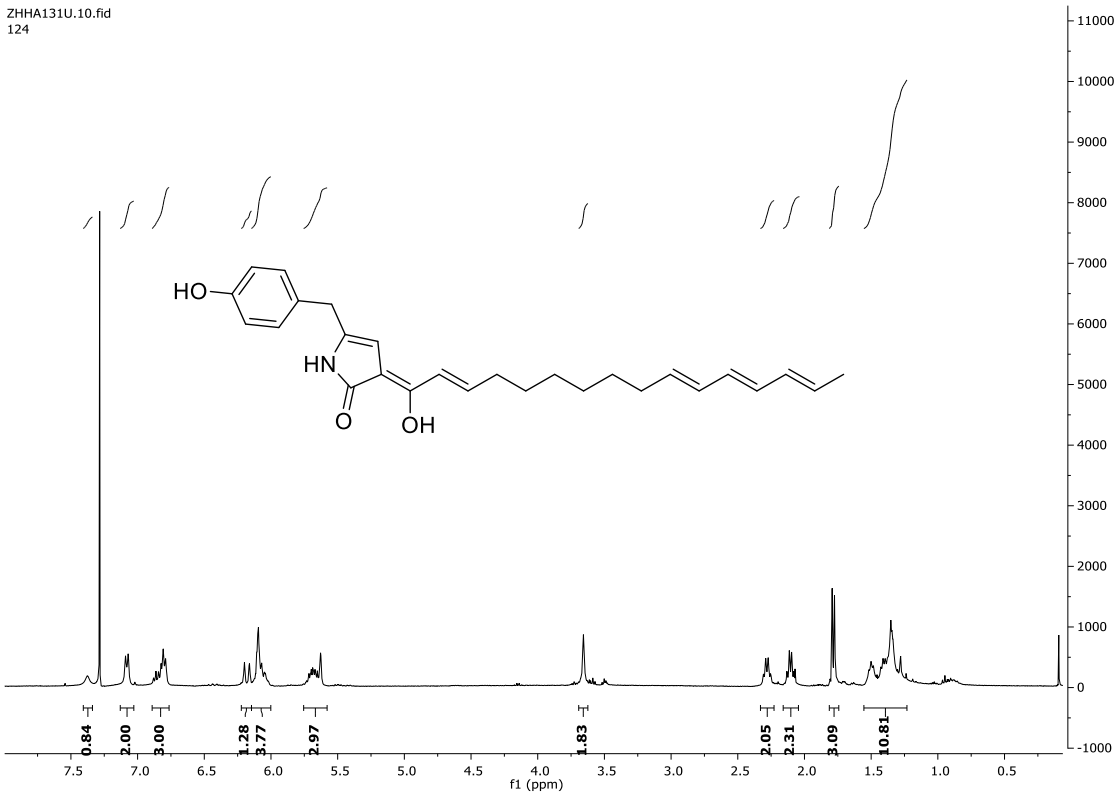

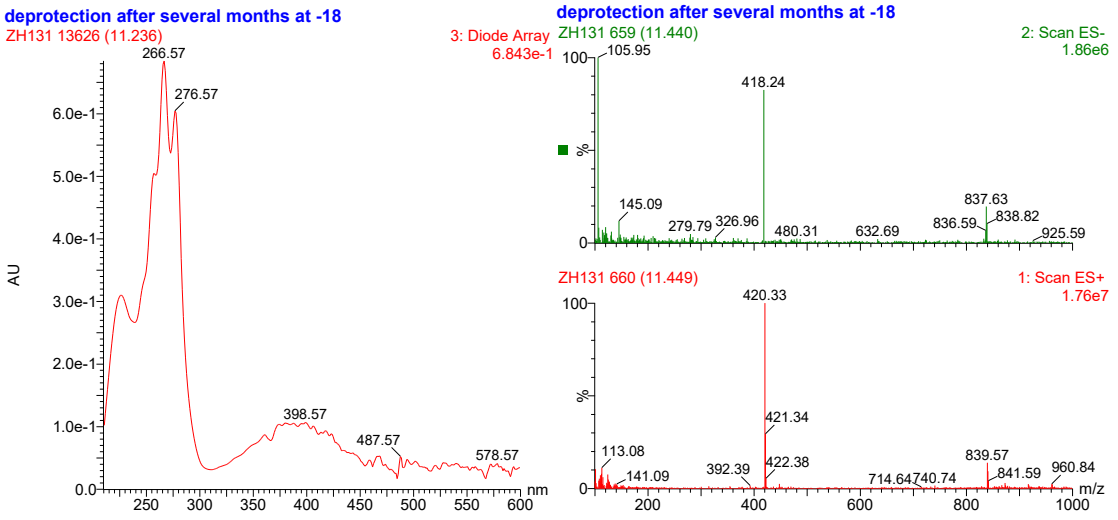

4*E*,12*E*,14*E*,16*E*-*N*-(*S*-1,1-Diethoxy-3-(4-methoxyphenyl)propan-2-yl)-3-oxooctadeca-4,12,14,16-tetraenamide **374**.

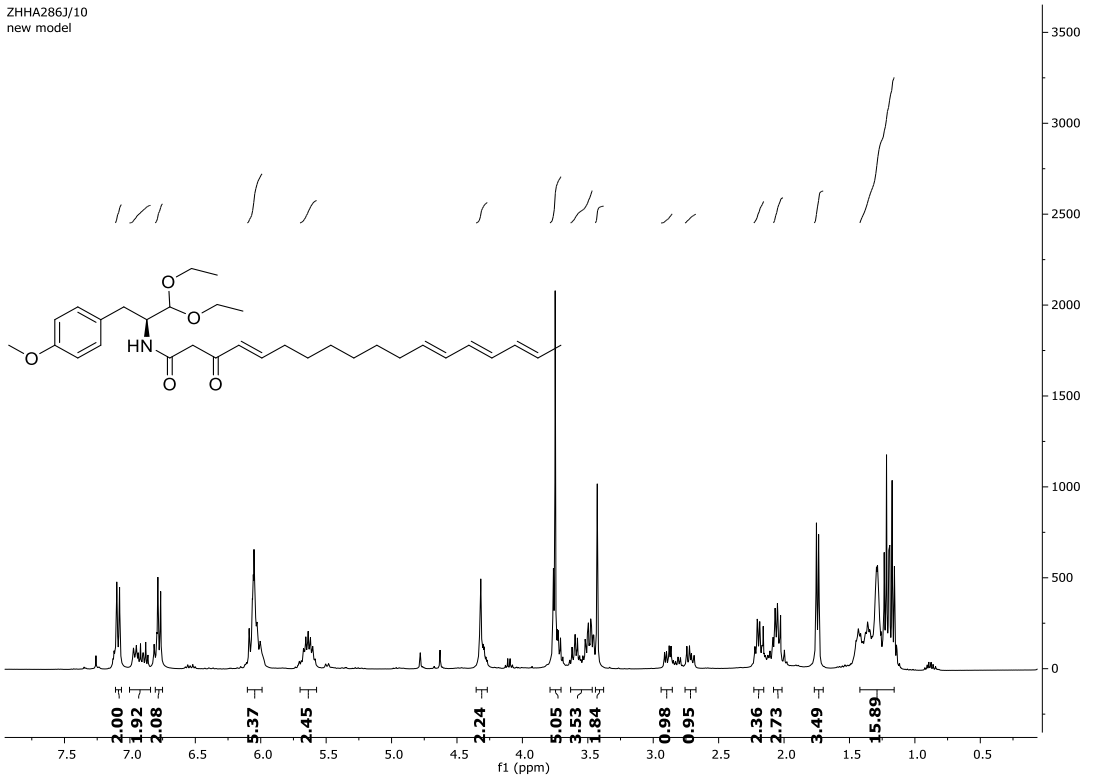

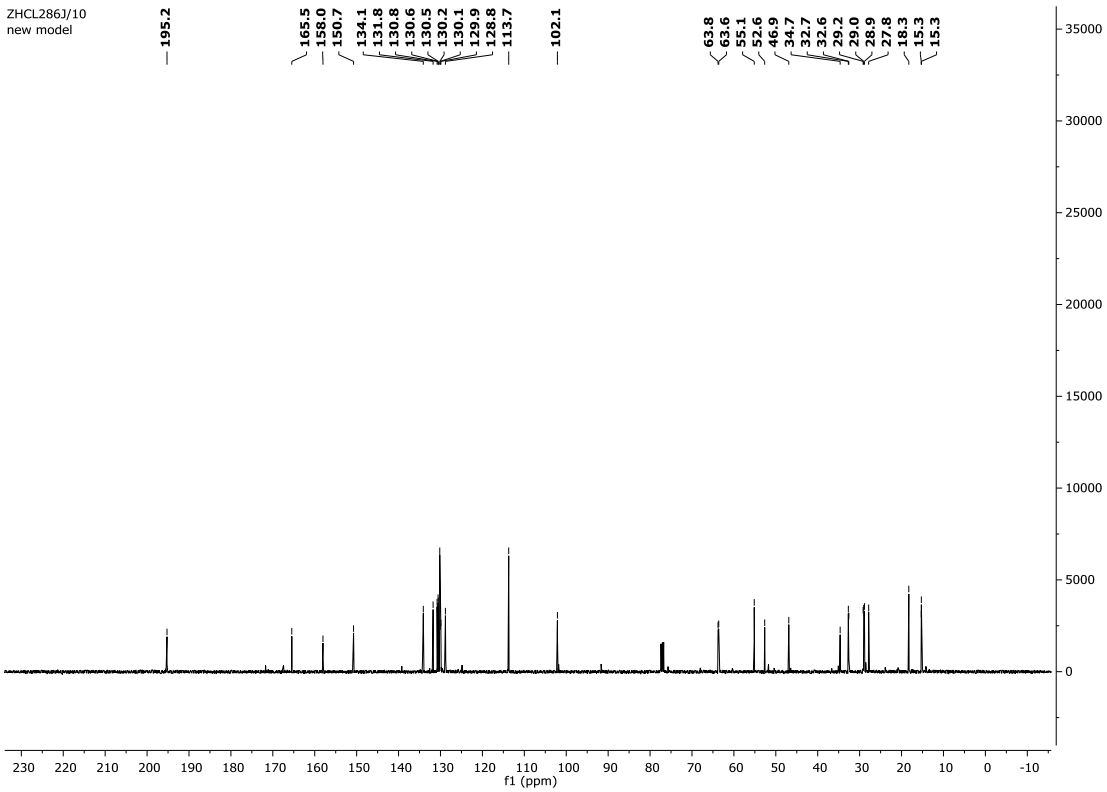

4*E*,12*E*,14*E*,16*E*-*N*-(*S*-1-Hydroxy-3-(4-methoxyphenyl)propan-2-yl)-3-oxooctadeca-4,12,14,16-tetraenamide **387**.

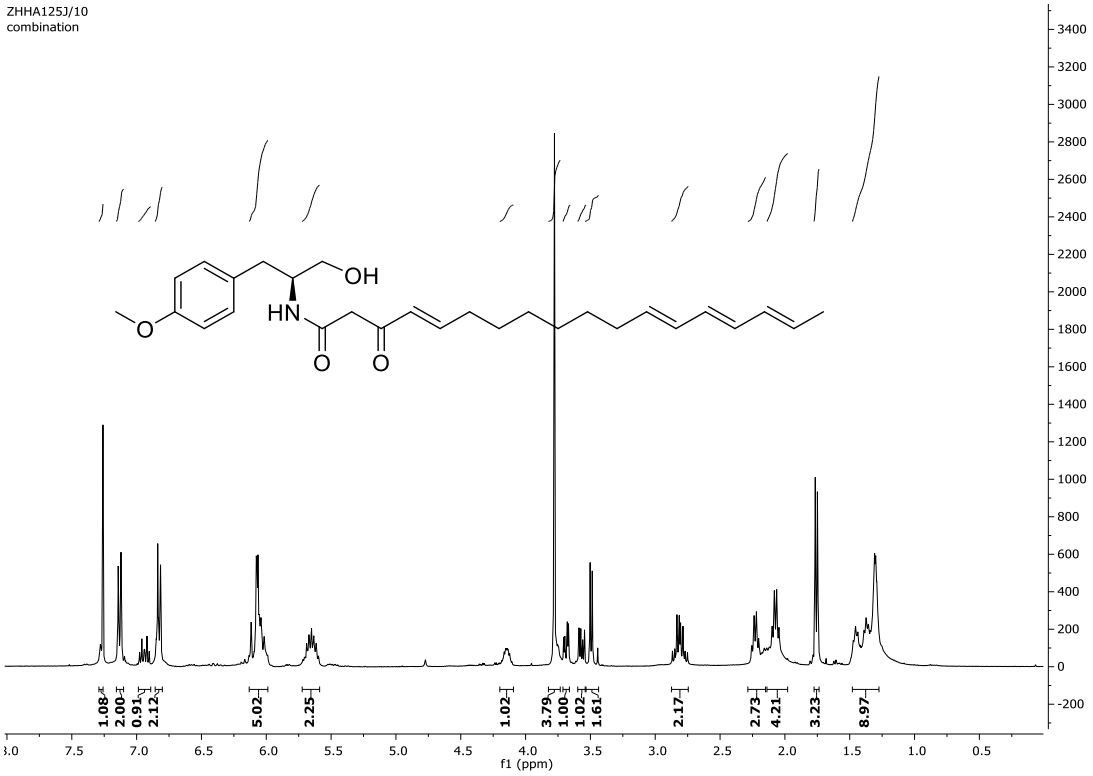

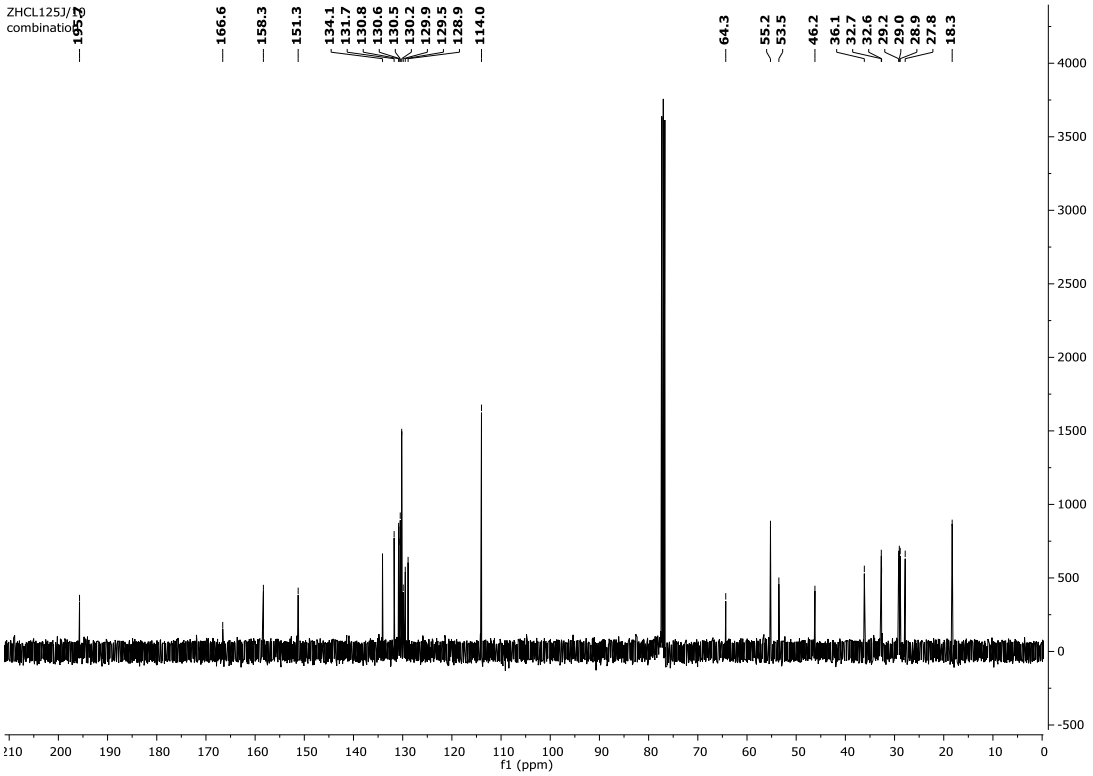

Curriculum Vitae

Personal Details

Name:	Haili Zhang	Gender:	Male
Date of Birth:	1988.02.23	Nationality:	Chinese
Place of Birth:	Shandong (China)	Email:	haili.zhang@oci.uni-hannover.de

Education Background

Jul 2016 - Nov 2019	**PhD student** in Organic Chemistry, Gottfried Wilhelm Leibniz Universität Hannover, Germany
Sep 2012 - Jun 2015	**Master degree** in Pesticide Science, Nankai University, China
Sep 2008 - Jun 2012	**Bachelor degree** in Pharmaceutical Engineering, Shandong Agricultural University, China
Sep 2005 – Jun 2008	Anqiu Experimental High School

List of Publications

1. Youquan Zhu, **Haili Zhang**, Danyang Wang, Lei Li, Han Xu, Huabin Li, and Yuan Ma. De sign, Synthesis and Biological Evaluation of Novel N-(4-([2,2':5',2"-terthiophen]-5-yl)-2-methyl but-3-yn-2-yl) Benzamide Derivatives. *Chin. J. Chem*. 2015, 33, 268-276.
2. XU Hai-Zhen, XIE Li-Fen, **ZHANG Hai-Li**, LI Lei, MA Yuan, ZHU You-Quan. Synthesis, Dimer Crystal Structure and Herbicidal Activity of 2-(4-Ethoxybenzoyl) cyclopentane-1,3-dione. *Chinese J. Struct. Chem*. 2014, 33, 1451-1454.
3. Zhu, Youquan; **Zhang, Haili**; Wang, Danyang; Li, Lei. Preparation of N-(4-(2,2':5',2"-terthien yl- 5-yl)-2-methylbut-3-yn-2-yl) benzamide compounds for inhibiting tobacco mosaic virus. Pat ent No. CN104045622 A; Date: July, 2014.
4. Zhu, Youquan; **Zhang, Haili**; Li, Lei; Li, Junxian. Herbicidal activity of 2-(2,2-dimethyl-7-flu oro-2H-benzoxazin-3(4H)-on-6-yl)tetrazolone. Patent No. CN 104610246 A; Date: May, 2015.